4-26-2022 2:00 PM

The Streptococcus pyogenes hyaluronic acid capsule prevents neutrophil clearance, and greater insights into the streptococcal M protein as a vaccine candidate and driver of heart dysfunction

Jacklyn Hurst, *The University of Western Ontario*

Supervisor: McCormick, John K., *The University of Western Ontario*
A thesis submitted in partial fulfillment of the requirements for the Doctor of Philosophy degree in Microbiology and Immunology
© Jacklyn Hurst 2022

Abstract

Streptococcus pyogenes is a human-specific opportunistic pathogen that exploits an assortment of surface molecules to overcome host clearing mechanisms and cause a substantial burden of acute and chronic diseases worldwide. In the present work we utilize the M18 serotype *S. pyogenes* strain MGAS8232 to demonstrate that genomic deletion of the hyaluronic acid capsule significantly reduces bacterial densities in murine models of experimental nasopharyngeal and skin infections. We show that α-Ly6G administration recovers the deteriorated burden by unencapsulated bacteria at both infection sites, indicating that capsule expression promotes resistance to neutrophil-mediated clearance during acute infections. We also evaluated the efficacy of serotype-specific immunity against the surface M protein and show that induction of serum M protein-specific IgG levels by monovalent M protein immunizations is not sufficient by itself to protect mice from acute nasopharyngeal or skin challenges. Lastly, we implemented a recurring infection model to evaluate whether M protein expression is a possible driver of long-term cardiac complications. Multiple homologous infections with *S. pyogenes* MGAS8232 altered left ventricle filling dynamics and weakened ejection fractions by echocardiography compared to control inoculations with PBS or infection with *S. pyogenes* lacking its M protein, suggesting that M protein expression is directly associated with cardiac alterations. Together, this work provides deeper understandings on how *S. pyogenes* avoids innate clearance to establish superficial infections and reveals physiological insights on the development of cardiac impediments following multiple acute infections. This work has also provided valuable insights that will help guide future vaccine development strategies against this globally prominent pathogen.

Keywords

Summary for Lay Audience

Streptococcus pyogenes is a human-specific bacterium responsible for an enormous amount of disease worldwide. Pharyngitis, more commonly known as 'strep throat,' is reported in over 600 million people each year, and impetigo, a benign skin infection, affects more than 100 million people annually. Since there is currently no licensed vaccine available it is critical to understand bacterial factors that promote initial stages of infection and induce severe diseases. In this study we examined how the *S. pyogenes* capsule helps support bacterial infection and found that removal of the capsule dramatically weakened the ability to cause nasal and skin infections in mice. We discovered that the capsule specifically protected bacteria from killing by a key immune cell, the neutrophil. We also evaluated the efficacy of a *S. pyogenes* vaccine against the surface M protein and found that vaccination against the M protein triggers antibody production but does not provide any protection from nasal or skin infections. Lastly, we performed multiple *S. pyogenes* nasal infections in mice and assessed the impact on heart function using echocardiograms. Interestingly, we demonstrate that multiple *S. pyogenes* infections results in reduced left ventricle function only when the M protein is expressed by the bacteria. Overall, this work reveals how *S. pyogenes* overcomes the human immune system to establish infection and demonstrates that the M protein is an ineffective vaccine target that may contribute to heart defects.

Co-Authorship Statement

All studies presented in this thesis were completed by Jacklyn Hurst with the assistance of past and present members in the laboratory of Dr. John McCormick as listed:

Chapter 2: Stephen Tuffs performed bioinformatic analyses of *S. pyogenes* MGAS8232 wildtype and Δ*hasA* genome sequences, including whole genome alignment, assembly, annotation, and detection of SNPs from the reference *S. pyogenes* MGAS8232 genome. Blake Shannon assisted with animal infections, monitoring animals, euthanizing animals, processing tissues, and recording data.

Chapter 3: Katherine Kasper performed the nasopharyngeal infections with *S. pyogenes* MGAS315, HKU16, MGAS8232, and NGAS979 in conventional C57Bl/6 mice purchased from the Jackson Laboratory. Construction of the M12:pET28 and M74:pET28 recombinant plasmids was generated by Aanchal Rishi. Blake Shannon assisted with animal infections, monitoring animals, euthanizing animals, processing tissues, and recording data.

Chapter 4: Sections from the discussion have been previously published in a review coauthored by Katherine Kasper, Akshay Sule, and John McCormick:

Hurst, J.R., Kasper, K.J., Sule, A.N., and McCormick, J.K. (2018). Streptococcal pharyngitis and rheumatic heart disease: the superantigen hypothesis revisited. Infection, Genetics and Evolution. 61:160-175

Acknowledgements

Table of Contents

List of Tables

List of Figures

Chapter 4: Repeated nasal exposure to *S. pyogenes* MGAS8232 impairs left ventricle function in HLA-transgenic mice

List of Appendices

List of Abbreviations

°C	degrees Celsius
$\times g$	times gravity
μg	microgram
μl	microliter
μm	micrometer
A wave	atrial transmitral velocity
Ab	antibody
ACK	ammonium-chloride-potassium
AET	aortic ejection time
Amp	ampicillin
Ao	aorta
APCs	antigen presenting cells
APS	ammonium persulfate
APSGN	acute post-streptococcal glomerulonephritis
ARF	acute rheumatic fever
AUP	animal use protocol
B6 mice	conventional C57BL/6 mice
B6$_{HLA}$ mice	human MHC class II transgenic B6 mice
BCA	bicinchoninic acid
bp	base pair
BHI	brain heart infusion
BSA	bovine serum albumin
C4BP	C4b binding protein
CFA	complete Freund's adjuvant
CFU	colony forming unit
cNT	complete nasal turbinate
cRPMI	complete RPMI-1640
cTnT	cardiac troponin T
cTnI	cardiac troponin I
Da	daltons
DMEM	Dulbecco's modified eagle medium
DNA	deoxyribonucleic acid
DNase	deoxyribonuclease
dNTP	deoxyribonucleotide triphosphate
EAM	experimental autoimmune myocarditis
ECM	extracellular matrix
EDTA	ethylenediaminetetraacetic acid
ELISA	enzyme-linked immunosorbent assay
E wave	early transmitral velocity
FBS	fetal bovine serum
FBP	fibronectin binding protein
FCT	fibronectin- and collagen-binding proteins and T-antigen
FH	factor H
FHL-1	factor H-like protein 1

For	forward
g	gram
GAC	group A carbohydrate
GlcNAc	*N*-acetylglucosamine
h	hour
HA	hyaluronic acid
HBSS	Hank's balanced saline solution
HLA	human leukocyte antigen
HR	heart rate
HRP	horseradish peroxidase
Hu-C4BP	human C4b binding protein
Hu-CD46	human CD46
Hu-FH	human factor H
ICE	integrative conjugative element
IdeS	Ig degrading enzyme of *Streptococcus pyogenes*
IFA	incomplete Freund's adjuvant
Ig	immunoglobulin
IP	intraperitoneal injection
IPTG	isopropyl-β-D-1-thiogalactopyranoside
IRDye	infrared dye
IVCT	isovolumetric contraction time
IVIG	intravenous immunoglobulins
IVRT	isovolumetric relaxation time
kb	kilobase
kDa	kilodalton
LA	left atrium
LB	Luria-Bertani broth
LTA	lipoteichoic acid
LV	left ventricle
LVAW;d	left ventricle anterior wall in diastole
LVAW;s	left ventricle anterior wall in systole
LVID;d	left ventricle internal diameter in diastole
LVID;s	left ventricle internal diameter in systole
LVPW;d	left ventricle posterior wall in diastole
LVPW;s	left ventricle posterior wall in systole
M	molar
mAb	monoclonal antibody
MAC	membrane attack complex
MEM	minimal essential medium
MIP	macrophage inflammatory protein
MHC	major histocompatibility complex
min	minute
mL	milliliter
mm	millimeter
mM	millimolar
MOI	multiplicity of infection
MS	maxillary sinuses

ms	millisecond
MWL	molecular weight ladder
MV	mitral valve
MV decel	MV deceleration
NALT	nasal associated lymphoid tissue
NETs	neutrophil extracellular traps
NFT	non-flow time
NHP	non-human primate
ng	nanogram
nM	nanomolar
NT	nasal turbines
OD	optical density
O/N	overnight
PAGE	polyacrylamide gel electrophoresis
PANDAS	pediatric autoimmune neuropsychiatric disorders
PBS	phosphate buffered saline
PBS-T	PBS with 0.1% (v/v) Tween-20
PCR	polymerase chain reaction
pg	picogram
PMN	polymorphonuclear cell
PSAX	parasternal short axis
PSLAX	parasternal long axis
PTS	phosphoenolpyruvate phosphotransferase system
PW Doppler	pulsed-wave Doppler
PVDF	polyvinylidene difluoride
RA	right atrium
Rev	reverse
RHD	rheumatic heart disease
RNA	ribonucleic acid
RPMI-1640	Roswell Park Memorial Institute medium
RPMI-HSA	RPMI containing 0.05% human serum albumin
RV	right ventricle
ScpA	streptococcal C5a peptidase
SDS	sodium dodecyl sulphate
SDS-PAGE	sodium dodecyl sulfate polyacrylamide gel electrophoresis
sec	second
SIC	streptococcal inhibitor of complement-mediated lysis
SLO	streptolysin O
SLS	streptolysin S
SmeZ	streptococcal mitogenic exotoxin Z
SNP	single nucleotide polymorphism
Spe	streptococcal pyrogenic exotoxin
SpeA	streptococcal pyrogenic exotoxin A
SpeB	streptococcal pyrogenic exotoxin B
SpnA	streptococcal cell wall-anchored nuclease A
SpyAD	*Streptococcus pyogenes* adhesion and division protein

SpyCEP	*Streptococcus pyogenes* cell envelope protease
STSS	streptococcal toxic shock syndrome
TBS	tris-buffered saline
TBS-T	TBS with 0.1% (v/v) Tween-20
TC	tissue culture
TCR	T cell receptor
TEMED	tetramethylethylenediamine
TEV	tobacco etch virus
THY	Todd Hewitt media broth plus 1% (w/v) yeast extract
TMB	tetramethylbenzidine
TNF	tumour necrosis factor
Treg	regulatory T cell
TSA	tryptic soy agar
TSB	tryptic soy broth
TSS	toxic shock syndrome
U	unit
v/v	volume per volume
Vβ	variable beta chain
VEGF	vascular endothelial growth factor
w/v	weight per volume
WHO	World Health Organization
WT	wildtype

Chapter 1: Introduction

Introduction

The introduction of this thesis will summarize relevant and current literature on *Streptococcus pyogenes*. The various topics presented here outline several clinical disease manifestations followed by descriptions underlying important molecular mechanisms of disease by this globally prominent pathogen. Applicable transgenic animal infection models will be reviewed, concluding with current vaccine approaches that elicit protective immunity against this bacterium.

1.1   *Streptococcus pyogenes*

Streptococcus pyogenes, also referred to as Group A *Streptococcus* (GAS), is a Gram-positive extracellular aerotolerant anaerobe with human-specific tropism. This bacterium typically grows in pairs or chains of varying length with each coccus approximately 0.5 to 1 μm in diameter, with a genome composed of a single ~1.8 Mbp circular chromosome with a G+C content of ~39%. Much of the genetic variability between strains can be attributed to the inclusions of mobile (or putatively mobile) genetic elements, such as integrative conjugative elements (ICEs) and phage or phage-like insertional sequences that can harbour several virulence determinants [1–3]. When grown on blood agar, *S. pyogenes* is often identified by its unique mucoid, white-greyish colonies with β-hemolytic zones of clearance due to the complete lysis of red blood cells [4]. Laboratory diagnosis of *S. pyogenes* is largely based on expression of the Lancefield group A carbohydrate, a major cell wall polysaccharide. *S. pyogenes* remains as the only species under the Group A *Streptococcus* classification [5]. While some individuals can carry the bacterium asymptomatically [6], clinical manifestations of *S. pyogenes* are among the most diverse of any human pathogen. Varied presentation can range from self-limiting pharyngitis and skin infections to more devastating illnesses such as necrotizing fasciitis and streptococcal toxic shock syndrome (STSS) [4,7]. Some diseases may occur as a complication from previous streptococcal infection and can result in potential long-term disability in susceptible individuals, including glomerulonephritis, acute rheumatic fever (ARF), and rheumatic heart disease (RHD) [4,7,8]. Although *S. pyogenes* remains vulnerable to β-

lactam antibiotics, it represents a significant burden on human health and no human-approved vaccine is currently available.

1.2   Global burden of *S. pyogenes* diseases

Systematic reviews generally use population-based analyses to estimate the global burden of *S. pyogenes*, however, absolute disease burdens are widely underestimated due to inadequacy of comprehensive disease registries, a lack of infrastructure for disease surveillance, and inaccessible diagnostic facilities. Consequently, acute and chronic illnesses by *S. pyogenes* are severely underreported in resource-poor regions, where diseases occur most frequently [9]. In a landmark 2005 publication, in-depth evaluations of disease burdens using conservative methodologies provided the most comprehensive estimates of *S. pyogenes* morbidity and mortality to date. Approximately 15% of schoolchildren and up to 10% of adults may suffer from streptococcal pharyngitis each year, and in some resource-poor settings, these rates may be 5-10 times higher [10]. It is estimated that at least 616 million annual cases of acute pharyngitis and 140 million cases of superficial skin infections occur each year globally [10,11]. These relatively benign infections are typically self-limiting and can be effectively treated with β-lactam antibiotics [7], however, more severe manifestations may occur if *S. pyogenes* breaches the epithelial barrier or if acute infections are left untreated.

Invasive streptococcal diseases are defined by *S. pyogenes* invading normally sterile sites, including deep tissues such as fascia (necrotizing fasciitis), muscle (myositis), or blood (bacteremia and STSS). Over 660,000 invasive infections by *S. pyogenes* occur each year and result in 163,000 deaths [10]. Invasive infections are often life-threatening with high mortality rates (<50%) in both the developed and developing world. Despite the steady decline in developed countries [11], data from recent decades suggest that the prevalence of invasive diseases have increased in resource-limited countries and account for nearly all 163,000 deaths globally [10–12]. A study of young infants in Papua New Guinea, Ethiopia, the Gambia, and the Philippines determined that *S. pyogenes* accounted for ~29% of all bacteremia isolates in children under 90 days of age [11].

The persistence or recurrence of untreated *S. pyogenes* acute infections can also result in autoimmune post-infection sequalae, including ARF and RHD. ARF continues to be the leading cause of acquired heart disease in children and remains the greatest contributor to streptococcal-associated morbidity and mortality worldwide. With at least 18.1 million cases of severe *S. pyogenes* infections worldwide and 517,000 resulting deaths [10,11], approximately 350,000 deaths each year are due to either ARF or RHD, and almost all cases and deaths occur in developing countries or indigenous populations [10,11]. More recently, the Global Burden of Disease study estimated that there are 33.4 million prevalent cases of RHD, causing more than 9 million disability-adjusted life years lost each year [13], which represents the sum of years of life lost due to premature mortality and/or years lived with disability from RHD. With ~60% of ARF cases leading to RHD [10], RHD is recognized as a prominent global health concern. According to the 2008 Population Reference Bureau (PRB), 80–85% of children younger than 15 years of age live in areas where ARF and RHD is endemic [14]. The predominant association between low-resources and mortality is similar to other *S. pyogenes* manifestations such as glomerulonephritis with 97% of deaths occurring in developing countries [10]. Due to the prominent global disease burden reported, the World Health Organization (WHO) ranks *S. pyogenes* as the ninth leading cause of human mortality by an infectious agent worldwide [15], which emphasizes the significance of understanding pathogenic mechanisms by this organism. Through improved living conditions and preventative measures by prophylactic treatments, 20% of the world's population living in industrialized regions have witnessed dramatic declines in the prevalence of *S. pyogenes*, yet disease burdens continue to manifest for the economically disadvantaged [16]. Without sufficient prevention and treatment of primary infections, combined with inefficient data managing systems and epidemiological models, we are unable to reduce the global burden of human illness caused by *S. pyogenes.*

1.3   Asymptomatic carriage

S. pyogenes causes a significant global burden of disease yet the predominant form of interaction between this pathogen and its human host is asymptomatic carriage. This carrier state can be described as a prolonged presence of *S. pyogenes* in absence of symptoms of infection. Persistence within the human nasopharynx is considered a primary reservoir for

many *S. pyogenes* strains [17] and individuals with positive pharyngeal and/or serological test without clinical signs of sore throat, inflamed tonsils, or fever are described as asymptomatic carriers [18,19]. Asymptomatic carriage rate of *S. pyogenes* is high among school age children and more prevalent among females than males [20]. High-income regions report around 12% of school-aged children as asymptomatic carriers [18,21,22], and close environmental exposures increase associated risks. Approximately 25% of household cohabitants of children with streptococcal pharyngitis test asymptomatically positive for *S. pyogenes* [23] and household contacts were almost twice as likely to acquire secondary *S. pyogenes* infections [24].

While asymptomatic carriers are unaffected by *S. pyogenes,* a long-recognized limitation to effective prevention of autoimmune sequelae is the absence of respiratory symptoms in the months prior to infection. During an outbreak of ARF in Salt Lake City, Utah, as many as 76% of ARF patients do not recall a symptomatic pharyngeal infection within the preceding 3 months [25,26]. In a study of 17 patients with invasive infection in Quebec, Canada, 27% of patient close contacts harbored the same *S. pyogenes* serotype in their pharynx [27], suggesting that carriers may act as reservoirs for bacterial transmission. Transmission from carriers, however, is substantially less likely than from those with active respiratory secretions from symptomatic infections [28,29]. Despite decades of research, the carrier state for *S. pyogenes* is complex and underlying molecular mechanisms driving this dominant state remain unclear, however, eradicating carriage could substantially reduce closely spaced recurrent episodes of streptococcal pharyngitis in susceptible individuals.

1.4   Superficial streptococcal infections

Most infections caused by *S. pyogenes* are superficial infections of the throat and skin resulting in pharyngitis and impetigo, respectively. Streptococcal pharyngitis is often observed as a sudden-onset fever accompanied by a sore throat with inflammation of the pharynx and tonsils often with patchy exudates and swollen cervical lymph nodes. Transmission occurs by direct contact presumably through nasal secretions or saliva droplets from those harboring the bacteria. *S. pyogenes* is diagnosed in 15 to 35% of

children and in 5 to 15% of adults with sore throats [22,30]. Uncomplicated *S. pyogenes* pharyngitis is generally self-limiting however, the cost of diagnosing, treating, and caring for children with strep throat costs up to $539 million per year in the United States [31].

Impetigo, also referred to as school sores or skin sores, is a contagious skin infection that presents as purulent lesions that enlarge and rupture to form characteristic thick crusts [32]. The disease is spread through direct skin contact and frequently appears on exposed areas of the body including lower extremities or the face. Lesions remain well localized though transfer from lesions on the skin to the upper respiratory tract is common and can occur within 2-3 weeks [33]. The greatest disease burden affects economically disadvantaged children in tropical or subtropical climates, or indigenous populations in developed countries, in areas with poor hygiene, and crowded living conditions [34].

1.5   Invasive streptococcal disease

S. pyogenes has the capacity to breach epithelial cell barriers and invade normally sterile sites such as the bloodstream, lungs, fascia, or muscles. Invasive infections include bacteremia, pneumonia, necrotizing fasciitis, myositis, and STSS. While less common than superficial infections and immune-mediated sequelae, invasive infections are often associated with shock and multiple organ failure and carry a high mortality rate in both the developed and developing world [4,7]. Approximately 8-23% of patients with invasive *S. pyogenes* disease die within 7 days of infection, and if complicated by the development of STSS, 23-81% of patients die within 7 days post-infection [35–37]. STSS is a toxin-mediated systemic disease and is the most dangerous form of invasive streptococcal diseases. STSS is induced by potent immunostimulatory streptococcal superantigens that trigger massive proliferation of T cells and production of proinflammatory cytokines (cytokine storm) that mediate shock and organ failure [38,39]. The rapid onset of STSS includes flu-like symptoms with fever, swollen lymph nodes, vomiting, diarrhea, rash, hypotension, skin peeling, and muscle and joint pain [38]. Severe localized pain disproportionate to the injury is a hallmark of these infections and the primary reason patients seek medical attention. Multi-organ failure and tachycardia may occur as well as fasciitis and myositis [38].

Necrotizing fasciitis, otherwise known as "flesh-eating disease" is an infection of the subcutaneous tissue and fascia that results in severe inflammation, tissue necrosis, and mortality [40,41]. Trauma is the most common identifiable etiology with most patients having a history of minor or major injuries involving external injuries and surgical wounds. Early clinical manifestations begin with swelling, tenderness, erythema, and local warmth, but as the infection develops the pain becomes more intense and symptoms present as general toxicity including fever, dehydration, confusion, dizziness, diarrhea, nausea, vomiting, weakness, and malaise [41]. The cutaneous symptoms may progress to blisters and bullae, ultimately leading to extensive necrosis of soft tissue and the potential to become hemorrhagic. Necrotizing fasciitis can affect an entire extremity within 24 hours, but it can also display slow progression over a period of several weeks [42]. A septic condition and hypotension at admission are significant predictors of poor outcome and mortality. Treatment of NF is similar to STSS with evidence that administration of intravenous immunoglobulins (IVIG) may help reduce mortality by toxin neutralization [43].

1.6   Post-infection sequelae

Streptococcal infections are typically acute and superficial, but the greatest burden of morbidity and mortality arise from important postinfectious sequelae including ARF, RHD, APSGN, and, debatably, pediatric autoimmune neuropsychiatric disorders (PANDAS). Post-infection sequelae can result from prior and untreated *S. pyogenes* infections whereby the host generates an immune response against invading bacterial factors that cross-reacts with similar epitopes on host molecules, referred to as molecular mimicry.

ARF is a delayed autoimmune consequence that appears approximately 2-4 weeks after pharyngeal infection by *S. pyogenes* [44]. This disease is a multifocal inflammatory disorder that can affect the skin, joints, brain, and heart, and diagnosis consists of fulfilling a certain number of major and minor disease criteria such as two major manifestations, one major and two minor manifestations, or three minor manifestations. In addition, evidence of preceding infection with *S. pyogenes* must be shown. Major and minor clinical

manifestations for ARF diagnosis are outlined in the recently updated Jones Criteria (**Table 1**) and include erythema marginatum (rash), subcutaneous nodules, polyarthritis, chorea, and carditis [44–46]. Patients experiencing these clinical features may be hospitalized for 2-3 weeks during which symptoms usually resolve [46]. Persistent cardiac damage caused by repeated episodes of streptococcal pharyngitis and exacerbation of ARF, however, can lead to RHD [8,47]. Carditis occurs in over 50% of patients with ARF and is predominantly characterized by inflammation of the mitral valve, which can lead to stenosis and regurgitation [26,48]. RHD is a particular serious problem in resource-poor regions where patients may present with established late-stage RHD rather than ARF due to insufficient diagnosis and treatment of primary *S. pyogenes* infections. Many patients with ARF progress to RHD and consequently, the importance of secondary prophylaxis with antibiotics for prevention of recurrent ARF, to reduce the risk of RHD in ARF patients, or to slow the progression and severity of disease in patients with established RHD cannot be overemphasized [46]. Surgical intervention of patients with progressed RHD may be required to prevent sudden cardiac death, likely as a result of cardiac arrhythmia [49]. Several factors affect the prevalence of ARF and RHD through increased exposure to *S. pyogenes* infections, including sex, socioeconomic status, household overcrowding, access to primary and secondary prevention regimes, and genetic susceptibility [46,50].

Acute post streptococcal glomerulonephritis (APSGN) is an immune complex-mediated disorder that remains the most common cause of acute nephritis in children worldwide. APSGN typically occurs 1-2 weeks following exposure to streptococcal pharyngitis or 3-6 weeks following impetigo [51]. The exact mechanism by which APSGN occurs is not fully defined, but it is understood that exposure to "nephritogenic" strains of *S. pyogenes* stimulates immune complexes comprised of IgG antibodies with streptococcal nephritogenic antigens and complement proteins within the kidney glomeruli. Glomerular trapping of circulating immune complexes and *in situ* immune complex formation in the glomerulus are two proposed mechanisms [51,52]. The presence of immune complexes activates the complement pathway and leads to infiltration of immune cells to the kidney

Table 1. Modified Jones criteria for diagnosis of acute rheumatic fever

For patients with evidence of preceding Group A *Streptococcus* infection	
Initial ARF	**2 major** manifestations OR
	1 major plus **2 minor** manifestations
Recurrent ARF	**2 major** manifestations OR
	1 major plus **2 minor** manifestations OR
	3 minor manifestations

Major Criteria	
Low risk	Moderate and high risk
Carditis (clinical and/or subclinical)	Carditis (clinical and/or subclinical)
Arthritis (polyarthritis only)	Arthritis (monoarthritis, polyarthritis, or
Chorea	polyarthralgia)
Erythema marginatum	Chorea
Subcutaneous nodules	Erythema marginatum
	Subcutaneous nodules

Minor Criteria	
Low risk	Moderate and high risk
Polyarthalgia	Monoarthalgia
Fever (($\geq$ 38.5 °C)	Fever ($\geq$ 38 °C)
ESR of $\geq$60 mm/hr and/or CRP of $\geq$3.0 mg/dL	ESR of $\geq$30 mm/hr and/or CRP of $\geq$3.0 mg/dL
Prolonged PR interval, after accounting for age variability (unless carditis is a major criterion)	Prolonged PR interval, after accounting for age variability (unless carditis is a major criterion)

and inflammation of the glomerulus, which impairs capillary perfusion and glomerular filtration rate. Reduction in serum complement (C3) levels (hypocomplementemia) are key markers of acute disease development due to its consumption during the inflammatory response, though they return to normal levels within 6 weeks [52]. When symptomatic, clinical manifestations include hematuria (discolored urine), edema, fatigue, hypertension, and proteinuria, which can result in renal failure [4], however, many patients develop APSGN without experiencing symptoms of a prior streptococcal infection.

The onset of obsessive-compulsive disorder and Tourette's syndrome has been associated with prior infections by *S. pyogenes* and is defined as pediatric autoimmune neuropsychiatric disorders associated with streptococcal infections (PANDAS). The relationship of *S. pyogenes* to these behavioral disorders is highly controversial and the long latency period between the detection of PANDAS and streptococcal infections has made the association more difficult to assess. The pathogenesis of PANDAS remains unknown, and it is unclear whether antineuronal antibodies have a role in disease development. It is believed that antibodies against the streptococcal associated epitope *N*-acetyl-β-D-glucosamine (GlcNAc) may disrupt neuronal cell function and lead to disease [53,54]. Symptoms of the disorder can include unusual movements, obsessive compulsive and repetitive behaviours, separation anxiety disorder, incessant screaming and frequent mood changes, deterioration of small motor skills, and poor handwriting [55].

1.7   Serological typing of *S. pyogenes* strains

Serological typing of *S. pyogenes* has generated key insights on the association between certain strains with specific diseases, helping elucidate population genetics, molecular epidemiology, and tissue-tropism characteristics of emerging strains. Most commonly, *S. pyogenes* strains are differentiated through serological analysis of the surface M protein as it displays high levels of antigenic heterogeneity. Early studies revealed that M protein antibodies were protective against strains sharing the same serotype [56], and thus, M-typing raised important biological implications beyond the identification of strains. Serotyping was more recently replaced by sequence analysis of the hypervariable N-terminal region of the M protein, encoded by the *emm* gene, known as *emm*-typing.

Extensive reference databases of *emm* sequences have allowed for the rapid translation of *emm* sequence data into M-type designation and has revealed a deeper genetic diversity of M proteins along with the identification and description of novel strains. At present, there are 234 distinct *emm*-types defined [57]. Although historically it was accepted that M protein-specific antibodies provide type-specific immunity to individual M proteins, it is now apparent that M protein-specific antibodies may allow for cross-reactivity within 'clusters' of homologous M proteins [58,59]. Researchers have divided serotypes into 16 phylogenetically supported *emm*-clusters that evolved from distinct selective pressures and are found with similar host factor binding properties and function [59]. These clusters are further classified into an *emm* pattern-typing scheme, denoted by patterns A through E. Strains with patterns B and C are rare and are grouped with *emm* pattern A strains (patterns A-C strains) [60]. Patterns A-C strains are overwhelmingly recovered from pharyngeal isolates, while strains with pattern D are often obtained from skin infections. Unlike patterns A to D, strains with pattern E are not associated with a specific tissue site and have been isolated from both the skin and pharynx [17,60]. Importantly, different "throat" and "skin" isolates do not appear to have specific preferences to bind skin or oropharyngeal immortalized cells in *in vitro* cell adhesion assays [61].

A supplemental serotyping system for *S. pyogenes* is based on the T antigen found within the Fibronectin- and Collagen-binding proteins and T-antigen (FCT) genomic region [62]. T antigens encode the major pilus backbone subunits that polymerize to form the elongated pilus shaft. While strains that encode distinct pilus backbone variants can exhibit antigenically diverse pili [63], FCT regions are found exclusively in one locus, and thus, only one pilus variant can be expressed in a given strain. Sequence analysis of approximately 100 isolates revealed that there are 18 distinct *tee*-types and 3 sub-types with little to no variation within each *tee*-type [63,64]. In many cases, *tee*-types can be inferred from *emm*-types with multiple isolates belonging to one *emm*-type having a strong tendency to harbor almost identical pilus proteins [57,65]; however, more than one *emm*-type can be associated with a specific *tee*-type. The strong linkage between FCT regions and *emm*-types also supports that FCT gene products may play an adaptive role in establishing tissue tropisms. Interestingly, *emm* pattern D "skin" isolates preferentially encode the FCT-4 region (~80% of strains), whereas <15% of *emm* pattern A–C "throat"

isolates encode FCT-4, indicating a potential role for tissue specific adhesion [17]. Yet, inferring tissue tropisms is complicated when considering that FCT region genes are subject to global regulators that alter their transcriptional expression during different environmental scenarios [66]. Depending on strain, the regulation for expression of pilin genes can be positive or negative [67,68], therefore, not all *S. pyogenes* strains express pili and those with a negative regulator may be T non-typable organisms.

1.8   Mechanisms of colonization and disease

The principal sites of *S. pyogenes* colonization are the nasopharynx and skin that serve as primary reservoirs for the maintenance and transmission of *S. pyogenes* to a new host. *S. pyogenes* expresses an arsenal of virulent molecules and, while not ubiquitously expressed by all strains, are highly regulated and exhibit functionally reductant tactics to help overcome physical barriers, evade host immune responses, and adapt to different tissue environments encountered during infection [69]. Improved understanding of these host-pathogen interactions has led to the formulation of models that investigate the coordinated expression of multiple virulence determinants and their diverse mechanisms of disease progression.

1.8.1   Mechanisms of adhesion

Attachment to nasopharyngeal and skin epithelial cell surfaces represent an important critical step in establishing *S. pyogenes* colonization and subsequent infection. Although the presence and expression of individual surface adhesins differ across various serotypes and infection models, adherence is widely accepted to involve a two-step process. Initial interactions overcome electrostatic repulsion between *S. pyogenes* and host cells and are mediated by weak hydrophobic interactions from the highly conserved and vital cell wall component lipoteichoic acid (LTA) [70,71]. LTA must be in the proper orientation with its fatty acid moieties exposed to contribute to adhesion and biofilm formation [70,72]. Most epithelial or endothelial cell surfaces are covered by a layer of extracellular matrix (ECM) proteins and many *S. pyogenes* adhesins function to specifically bind various ECM components throughout an infection, including collagen, fibrinogen, laminin, or

fibronectin [73]. Fibronectin functions as a ligand for LTA-mediated cell adhesion to numerous cell types, including buccal epithelial cells [74], HEp-2 laryngeal cells [75], and pharyngeal epithelial cells [76]. Many *S. pyogenes* strains non-selectively bind host cells through LTA, however, more secure attachments are facilitated by simultaneous or subsequent high-affinity tissue-specific interactions formed by other adhesins and their cognate receptors.

S. pyogenes is encased with a polysaccharide capsule consisting of hyaluronic acid (HA) with alternating monosaccharide units of GlcNAc and glucuronic acid [77]. The HA capsule has been shown to support adherence by binding to the HA receptor CD44 on keratinocytes [78–81]. Once bound to CD44, cytoskeletal rearrangements are triggered and intracellular junctions in human epithelial cells are disrupted and bacteria infiltrate into deeper tissue [82]. While HA capsule expression has been shown to support nasopharyngeal persistence in infection models [83,84], it has also been demonstrated that HA encapsulation reduces cellular attachment by physically obstructing access of other adhesin molecules to their host ligands [80,85].

Other high-affinity *S. pyogenes* adhesins include cell wall-anchored proteins such as the M protein. The role of M proteins in streptococcal adherence is controversial, but it remains as one of the best studied surface molecules and can bind to several host molecules. Early work supported an important role in M protein-mediated adherence to human buccal cells [86], yet M1, M5, M6, and M24 serotypes do not bind buccal cells and are essential for HEp-2 and Detroit 562 cell adherence [75,87–89]. Furthermore, M proteins have been shown to bind sialic acid on mucin that coats the pharyngeal epithelium [88], fibronectin on oropharyngeal cells [90], and fucose-containing oligosaccharides on HEp-2 cells [91]. Attachment to keratinocytes by membrane cofactor protein CD46 has been also been demonstrated, though serotypes M6, M12, and M18 present weak or no binding to CD46 [92–94]. Together, various M protein serotypes express dramatically different binding properties and may play a role in strain-specific tissue tropism [17,65]. It was recently noted, however, that *emm* pattern-inferred tropisms were not reflected by their preferred adhesion to skin versus throat cell lines, highlighting limitations to tissue-specific implications from *in vitro* immortalized cell culture observations [61].

The FCT region of *S. pyogenes* also expresses important binding properties to ECM proteins and various epithelial cells [71]. The FCT region contains fibronectin-binding proteins (FBPs) that facilitate adhesion to fibronectin and internalization via the integrin $\alpha_5\beta_1$ [95–97]. To date, nine different FCT pathogenicity islands have been identified [17], with the pilus as the most notable component encoded. The streptococcal pilus is a polymer composed of a pilus subunit with up to two ancillary proteins that mediate attachment to collagen (ancillary protein 1, AP1) and anchors the pilus to the cell wall peptidoglycan (AP2) [62,98,99]. AP1, otherwise referred to as collagen-binding protein Cpa, can bind collagen type I and type IV and provide collagen-mediated adhesion to lung and pharyngeal cells [17,87,100]. Generally, pili can bind to a broad range of host epithelial cells, including cells from the nasopharynx, tonsils, lung, and intestine [87,101], with removal of the pilus significantly reducing attachment to pharyngeal cells compared to parental strains [102]. Furthermore, thermal stable isopeptide bonds within the pilus subunit help withstand mechanical clearance forces such as coughing [103,104].

1.8.2   Mechanisms of immune evasion

The expression of virulence factors can vary across *S. pyogenes* serotypes, but a cooperative feature exhibited by all strains is the ability to avoid host innate immune defenses that promote bacterial survival. Following initial attachment and colonization of host cells, *S. pyogenes* employs an arsenal of evasion strategies that act synergistically to overcome and escape host clearing mechanisms, including resisting complement deposition, antibody opsonization, phagocytosis, antimicrobial peptides, neutrophil-mediated killing, and accelerating phagocytic death.

Once physical epithelial barriers of the body are breached, the complement system participates in the rapid labeling of bacteria with opsonins and recruitment of phagocytes to sites of infection through the production of chemoattractants. Although Gram-positive cell walls deflect membrane perturbations and direct bacterial killing by the membrane attack complex (MAC), they remain vulnerable to C3b opsonization and phagocyte infiltration via the leukocyte chemotactic factor C5a. *S. pyogenes* counteracts these responses by secreting ScpA (streptococcal C5a peptidase) that cleaves and inactivates

C5a, anaphylatoxin C3a, and the central complement protein C3, which dampens amplification of the complement system and reduces cellular activation and recruitment at the site of infection [105,106]. Similarly, the cysteine protease Streptococcal pyrogenic exotoxin B (SpeB) also degrades C3b to resist opsonization and detection [107], while the streptococcal cell envelope protease (SpyCEP) cleaves the chemoattractant IL-8 and prevents neutrophil infiltration and ingestion [108–110]. The surface M protein impedes complement deposition by binding soluble complement regulatory proteins such as C4b binding protein (C4BP) [111–114], CD46 [92], Factor H [114–118], fibrinogen [119,120], and plasminogen [116,121]. Likewise, FBPs are reported to bind factor H and factor H-like protein 1 (FHL-1) and prevent C3b deposition [110,122]. Through binding and sequestering soluble complement regulators on the bacterial surface, *S. pyogenes* accelerates the inactivation and decay of C3b and limits complement activation, thereby promoting bacterial survival [123,124]. The HA capsule has also been shown to act as a barrier that inhibits complement deposition [125] and blocks antibody access to surface epitopes [126] to prevent phagocytic uptake.

Phagocytosis of bacteria is prominently enhanced upon binding surface-bound Igs to allow for Fc receptor–mediated recognition and uptake. To avoid antibody-mediated opsonophagocytosis, *S. pyogenes* expresses surface-associated Ig binding proteins that bind the Fc region of human IgA and IgG to inhibit downstream Fc effector functions. M proteins and fibronectin binding repeats of FBPs are reported to bind to the Fc regions of IgA and IgG respectively [113,127] and thwart complement activation on the bacterial surface. *S. pyogenes* can also cleave the Fc region of surface-bound IgG via the Ig degrading enzyme of *S. pyogenes* (IdeS) [128], hydrolyze glycans on the heavy chain of IgG via EndoS to prevent antibody interaction with Fc receptors [129–132], or degrade IgG, IgA, IgM, IgG, and IgE directly via SpeB [129,132].

Resistance to phagocytic killing is also enhanced by SLS and SLO toxin activity, which help prevent acidification of the phagolysosome to escape bacterial killing and trigger phagocytic cell death. These pore-forming cytolysins directly kill phagocytic cells by disrupting the integrity of cell membranes to induce osmotic lysis [133–140]. Distinct from phagocytic engulfment, neutrophils can capture and kill *S. pyogenes* extracellularly

through the release of DNA rich neutrophil extracellular traps (NETs), which captures bacteria and subjects them to antimicrobial effectors. Bacteriophage-encoded DNases, such as Sda1 and Spd1, and cell wall-anchored nuclease A (SpnA), protect against neutrophil-mediated killing by degrading NETs to liberate entrapped bacteria [141–144]. HA capsule expression has also been shown to enhance survival within NETs by increasing resistance to the antimicrobial peptide cathelicidin LL-37 [145]. LL-37 forms membrane pores that would otherwise destabilize bacterial cells. *S. pyogenes* also encodes a streptococcal inhibitor of complement-mediated lysis (SIC) that binds and inactivates LL-37 [146]. Similarly, M1 protein was shown to bind and sequester LL-37, preventing access to the bacterial membrane [147], while SpeB cleaves and inactivates LL-37 directly [148,149]. Given the key role of complement-mediated opsonophagocytic killing in orchestrating host-protective immune responses, it is not surprising that *S. pyogenes* has evolved several virulent mechanisms to target and subvert innate immune defenses during infection.

1.9   Transgenic murine models of *S. pyogenes* infection

One of the many barriers in revealing the complexities of host-pathogen interactions on a molecular level stem from the challenge that *S. pyogenes* has strict human tropism and many central virulence factors are only active against human immune components. Various genetic tools exist and support the use of murine models to study *S. pyogenes* pathogenesis as mice can be bred to select for desired traits and can be genetically altered to express functional human genes [150,151]. Nevertheless, it is unlikely that any one transgenic model will represent an accurate interaction of all bacterial and host factors during murine infection as there are many *S. pyogenes* molecules described to interact with human components.

1.9.1   HLA-transgenic murine models

It has long been recognized that different HLA types can render humans either more susceptible or protected from *S. pyogenes* infections. The role of specific MHC class II molecules in *S. pyogenes* pathogenesis may be driven entirely by their ability to present

particular peptides, yet the ability of MHC class II molecules to serve as receptors for streptococcal superantigens has been widely shown to magnify host inflammatory responses and promote infection. Indeed, differential superantigen inflammatory responses driven by HLA allele expression increases risk of severe streptococcal disease [152–154] and may advance autoimmune responses (reviewed in [50]), increasing the relevance of this human component in *S. pyogenes* pathogenesis. Therefore, it is of great interest to evaluate animal models that permit superantigen activity to account for susceptibility to disease.

The tonsils remain as one of the most common sites of infection and carriage of *S. pyogenes* in the human pharynx. While mice lack tonsils, all rodents have a functionally homologous tissue known as the complete nasal turbinates (cNT) that contains the nasal-associated lymphoid tissue (NALT), and *S. pyogenes* resides in both the cNT and airway mucosa following nasopharyngeal infection [155]. In conventional C57Bl/6 mice, superantigen-dependent T cell responses are not induced and *S. pyogenes* fails to infect the cNT, yet infection is significantly enhanced with transgenic expression of HLA and the presence of T cells [156,157]. Superantigens mediate specific reactivity with variable-beta (Vβ) chains on T cell receptors (TCRs) and induce profound Vβ-specific T cell activation and proinflammatory cytokine responses that simultaneously recruit and then subvert the activity of effector cells to promote high bacterial loads in the nasopharynx [156,157]. Furthermore, superantigen-sensitive HLA-transgenic mice were also shown to be more susceptible to both skin infection and toxic shock-like syndrome [154,158]. These studies outline the importance in utilizing HLA-transgenic mice to retain human-specific tropism and more accurately model inflammation induced by streptococcal-host interactions. Although HLA-transgenic mice are receptive to superantigen-mediated activity, a limited number of *S. pyogenes* strains have demonstrated the ability to infect these mice, and many other virulence determinants promote pathogenesis *in vivo* by binding other distinct human-specific immune factors, including complement inhibitors.

1.9.2 Human complement-transgenic murine models

Host cells are typically protected from the complement system by membrane-bound or soluble regulator proteins that interfere with and prevent complement activation. In order to survive within its host, *S. pyogenes* has evolved to express several virulence factors that recruit and bind human complement inhibitors to help escape complement-mediated opsonophagocytosis and reduce bacterial killing. While mice do not adequately express human complement regulators, transgenic expression of human C4BP, factor H, or CD46 may present an acceptable model to study these host-pathogen interactions in mice.

C4BP and factor H are two major soluble negative complement regulators that, once bound, serve as cofactors for the plasma serine protease, factor I, which binds and inactivates deposited C4b and C3b, respectively [124]. By targeting C4b and C3b, C4BP and factor H accelerate decay of the classical pathway and alternative pathway convertases accordingly. Studies have shown that many M protein serotypes can bind and recruit C4BP [111–114] and factor H [114–118] to the bacterial surface to inhibit complement activation. The fibronectin-binding protein FbaA [110,122] and collagen-like protein 1 [159] also mediate recruitment of factor H. Transgenic mouse models that express human C4BP (hu-C4BP) and human Factor H (hu-FH) demonstrate reduced neutrophil recruitment and bacterial uptake with greater bacterial burden and dissemination compared to wildtype mice following invasive *S. pyogenes* infection [160,161]. In another study, however, binding factor H had no effect on the virulence of *S. pyogenes* in hu-FH transgenic mice compared to conventional mice [162].

In addition, CD46 is an abundant membrane-bound complement regulator that also acts as a cofactor for factor I-mediated proteolytic inactivation of deposited C3b and C4b [124]. Certain M protein serotypes can interact with CD46 to promote bacterial adhesion on keratinocytes [92,163], and this interaction may also protect cells from complement-mediated lysis. Intravenous injection of *S. pyogenes* in transgenic mice expressing human CD46 (hu-CD46) exhibited higher bacteremia levels and mortality rates, supporting that CD46 interactions enhance *S. pyogenes* survival in the blood and accelerates severe disease [164]. Hu-CD46 expression was also associated with more severe necrotic dermal lesions

following subcutaneous inoculations of footpads, which increased bacterial burden and mortality compared to non-transgenic mice [165]. Collectively, the studies described demonstrate that human complement transgenic mice display aggravated infections when the infecting *S. pyogenes* strain has the ability to capture complement regulators, and thus, may provide important resources for elucidating the functions of complement-binding virulence factors in human disease progression.

1.9.3 Human plasminogen-transgenic murine models

Interactions between host plasminogen and streptokinase secreted by *S. pyogenes* have been shown to promote tissue invasion and bacterial dissemination. Streptokinase forms a 1:1 complex with plasminogen and anchors to fibrinogen sequestered on the bacterial surface. Together, this trimolecular complex activates the conversion of plasminogen to plasmin, a serine protease that solubilizes fibrin clots, the ECM, and matrix metalloproteinases to promote barrier penetration and tissue damage [166–168]. Unlike human plasminogen, murine plasminogen is highly resistant to activation by streptokinase as highly streptokinase-producing strains and its streptokinase-deletion mutant show no difference in virulence during skin infection of mice [169]. In comparison, streptokinase activity prominently enhances skin lesion development and the progression to lethal infection when human plasminogen is present at the site of skin infection [170], or by preincubation in human plasma, but not plasminogen-depleted plasma, in plasminogen-deficient ($Plg^{-/-}$) mice [171]. Introduction of the human plasminogen *AlPLG1* gene into mice markedly increased *S. pyogenes*-mediated pathogenesis and mortality during skin and subcutaneous infections [172,173]. Notably, increased susceptibility of $AlPLG1^{+}$ mice to *S. pyogenes* was abrogated following streptokinase deletion, and no difference in mortality was observed between $AlPLG1^{+}$ and non-transgenic mice injected intravenously, suggesting that fibrinolysis activity by streptokinase is specifically required to facilitate bacterial access to the vasculature [173]. More recently, treatment of a lead compound CCC-2979 inhibited streptokinase activity and protected $AlPLG1^{+}$ mice from *S. pyogenes* mortality [174]. Together, transgenic expression of human plasminogen is important for modeling fibrinolysis mechanisms used by *S. pyogenes* to accelerate bacterial spread and invasion into surrounding tissue.

1.10   Group A streptococcal vaccines

The global burden of *S. pyogenes* disease is substantial and a vaccine that is successful at preventing the vast range of infections caused by this pathogen could address an impedingly unmet public health demand. Since the upper respiratory tract and skin represent the major reservoirs for all types of *S. pyogenes* infection [175], prevention of these 'natural' colonization states has the potential to prevent all types illness and their severe complications and could possibly save over 500,000 premature deaths every year. Importantly, prevention of even just acute *S. pyogenes* infections would reduce morbidity, have a considerable economic impact through reduced health care expenditure, and improve the quality of life of millions of people worldwide. While efforts to develop a *S. pyogenes* vaccine have been ongoing for almost 100 years [176] no licensed vaccine is currently available, and it is now considered an "impeded vaccine." One major barrier to vaccine development is that approximately 95% of all *S. pyogenes* disease occurs in low- and middle-income regions [10] where vaccine manufacturers have limited commercial interest to pursue development costs due to a lack of return on investments. Furthermore, inadequate epidemiological data in regions where disease is endemic complicates geographical assessments of serotype distribution and potential vaccine coverage. Vaccine development is also obstructed by the lack of suitable and relevant infection models, complex antigenic variability, and safety concerns based on the possibility a vaccine may elicit autoimmune responses. Nevertheless, the biological feasibility for vaccine development is supported by an abundance of pre-clinical and clinical studies that have identified key host-pathogen interactions that contribute to streptococcal diseases and offer promising intervention targets.

1.10.1   M protein-based vaccines

Early work by Rebecca Lancefield supported an important consideration for M protein-based immunity as bactericidal M protein antibodies were discovered to persist for years after streptococcal infection [56]. Years later, human volunteers were immunized with M protein preparations and were found to be protected from subsequent challenge infections [177,178], indicating that type-specific immunity can prevent symptomatic streptococcal

infections. To date, vaccines that focus on enhancing immunity against the cell wall-anchored M protein are well studied candidates with several advancing to clinical trials.

Mechanistically, serum IgG that targets the hypervariable N-terminal region of M protein enhances antibody-mediated complement activation and phagocytosis of *S. pyogenes* [179]*,* and thus, vaccine formulations containing multivalent N-terminal sequences from multiple epidemiologically important serotypes were developed. Vaccines consisting of four [180], six [181,182], eight [183], twenty-six [184–186], and thirty [187] N-terminal serotypes have been shown to elicit high immunogenicity and generate bactericidal antibodies in animals against nearly all vaccine-containing serotypes. Vaccines that have progressed to early stage clinical trials include the hexavalent [182], 26-valent (StreptAvax) [188], and 30-valent [189] formulations, and trials determined that they were safe, immunogenic and evoked bactericidal antibodies. StreptAvax to date is the most advanced *S. pyogenes* vaccine candidate with the successful completion of a Phase II clinical trial [190]. An important concern with generating type-specific immunity is the potential coverage as more than 220 hypervariable streptococcal *emm*-types are differentially distributed globally [191], therefore, a universally protective vaccine based on this surface molecule is challenging. Notably, vaccine-encoded M peptides produce antibodies that recognize a number of non-vaccine containing serotypes [186–189,192], suggesting that immune responses may provide cross-protection and offer extended coverage for regions where the diversity of circulating *emm*-types is high and disease is endemic [191].

An alternative viable approach to overcoming gaps in *emm* type coverage is to target cryptic epitopes found within the highly conserved C-repeat domain of the M protein, which has the potential to induce protection against most, if not all, *S. pyogenes* strains. Conserved M protein vaccine candidates include StreptInCor, containing selected T and B-cell epitopes from the C2 and C3 repeat regions [193–196], SV1 containing five 14-mer amino acids from differing C-repeat regions, and the J8 and J14 vaccines that contain shorter cryptic single minimal B cell epitopes from the C3 repeat region [158,197–205]. StreptInCor induced mucosal IgG and systemic IgG antibodies that led to phagocytosis and death of several strains [196], and protected mice from infection with no cross-reactivity

to cardiac proteins or other tissues [195]. Extensive studies particularly of the J8 vaccine candidate provided further evidence of opsonic antibody induction, long-term B cell memory, and protection against nasal [205,206], skin [199,202], and systemic infections in mice [158,197,198,200,202,207]. Due to the protective responses in animal models, the J8-DT candidate has advanced to clinical trials [208].

1.10.2 Superantigen-based vaccines

Superantigens are secreted mitogenic toxins that have strong and specific reactivity to specific TCRs and Vβ chains and induce profound Vβ-specific T cell activation and proinflammatory cytokine responses. Superantigens are immunologically distinct and while different strains of *S. pyogenes* often encode different combinations of superantigens [209,210], this repertoire appears to be limited to 14 superantigens to date [211]. Superantigens have been implicated in several *S. pyogenes* diseases, including severe and invasive diseases, as well as acute uncomplicated infections and asymptomatic colonization [212], and the lack of protective antibodies against superantigens has been associated with an increased risk for STSS [39,213]. Pooled human IVIG is increasingly used in cases of severe disease as it contains anti-superantigen neutralizing antibodies and reduces mortality in cases of STSS [43,214–216], however, its efficacy can vary [217,218]. Furthermore, specific MHC-II haplotypes are known risk factors for the development of invasive streptococcal disease, an outcome that has been directly linked to superantigens [154,219]. Together, superantigens exhibit features that warrant further study in using toxoid molecules as potential vaccine candidates.

Vaccination with inactive toxoid mutants of SpeA and SpeC show clear protective outcomes in rabbit models streptococcal toxic shock syndrome and sepsis [220–222]. Immunization of HLA-transgenic mice with inactive SpeA toxoid (SpeA$_{TRI}$) generated significant anti-SpeA IgG serum titers that prevented experimental nasopharyngeal infection by *S. pyogenes* MGAS8232 [156,157]. Passive immunization with polyclonal anti-SpeA antibodies also prevented nasopharyngeal infection [157]. Furthermore, the application of using modified TCR-binding defective superantigens to stimulate protective antibody responses could be harnessed for vaccine adjuvant use. By coupling inactive

superantigens with other virulence molecules, superantigens can deliver antigens directly to MHC class II receptors on APCs to mimic antigen presentation and stimulation of T cells in a conventional way. For instance, vaccination of mice with SmeZ toxoid conjugated to ovalbumin significantly improved antigen presentation and resulted in a 1000-10,000-fold increase in anti-ovalbumin IgG titers than immunization with unconjugated ovalbumin alone [223], and further substitution with an MHC class II binding mutant of SmeZ eliminated this enhanced immunity [223]. Immunization with inactive SpeA fused to the cysteine protease SpeB protein produced antibodies that recognized both SpeA and SpeB and protected HLA-transgenic mice from lethal toxic shock syndrome [220]. More recently, a chimeric molecule containing an immunodominant parasitic antigen of *Trypanosoma cruzi* fused to a non-toxic staphylococcal superantigens SEG maintained classical activation of macrophages and provided better control and protection against parasitemia during early stages of *T. cruzi* infection [224]. Overall, these studies encourage testing TCR-binding defective superantigens toxoids conjugated to specific antigens as immune modulators against *S. pyogenes* and other pathogens.

1.10.3 Group A carbohydrate-based vaccines

All serotypes of *S. pyogenes* express the cell wall-anchored Lancefield group A carbohydrate (GAC) containing an immunodominant GlcNAc side chain, which serves as the basis of all rapid diagnostic testing for *S. pyogenes* infection. Due to its conservation across all strains and the correlation between high serum titers of anti-GAC antibodies and negative *S. pyogenes* throat cultures in children [225], the GAC is considered an attractive molecule for a universal *S. pyogenes* vaccine. Passive immunization studies using rabbit anti-GAC antibodies increases the survival of mice significantly following IP challenge with multiple *S. pyogenes* strains [225,226]. Furthermore, active immunization studies using intranasal GAC mixed with cholera toxin B, or subcutaneous conjugated GAC vaccines, showed significantly reduced nasal colonization and mortality against multiple *S. pyogenes* serotypes in murine nasal and systemic infections, respectively [225,227]. A significant concern with a vaccine targeting the GAC is the potential for antibodies that recognize the GlcNAc side chain to have autoreactivity against human tissues, and thus, GAC vaccine formulations have been designed to lack expression of GlcNAc. Antibodies

raised against the polyrhamnose core of GAC lacking GlcNAc have proven identical efficacy in providing broad-spectrum opsonophagocytic activity and passive immunity against IP challenge with *S. pyogenes* [226]. Furthermore, immunization with GAC lacking GlcNAc and conjugated to arginine deiminase prevented bacterial persistence in skin lesions and reduced dissemination into the blood and spleen following cutaneous challenge in BALB/c mice [228]; however, vaccination did not increase survival following subcutaneous injection in *AlPLG1*^{+} transgenic mice [228]. Collectively, these studies highlight an important role for GAC-specific antibodies combatting *S. pyogenes* infection and may provide a promising approach to address the diversity of *S. pyogenes* isolates.

1.10.4 Other vaccine candidates

S. pyogenes expresses many other cell wall-associated and secreted virulence determinants that have undergone pre-clinical vaccine research with encouraging protective results, however, none have progressed to clinical trials. ScpA (C5a peptidase) is found on the surface of all *S. pyogenes* serotypes with a high degree of sequence similarity and is also expressed in human isolates of group B, C, and G streptococci [229]. Antibodies against ScpA have been detected in 90% of adult convalescent-phase sera, and >70% of adults had measurable secretory ScpA-specific IgA in their saliva, demonstrating the high immunogenicity of this virulence factor [230]. Deletion of *scpA* reduces the virulence of *S. pyogenes* in the NALT and on the skin of mice [106,229], which provides strong support to use ScpA as a vaccine target. Protection studies produced recombinant inactive ScpA and demonstrated that subcutaneous or intranasal immunization of ScpA in mice induced ScpA-specific serum IgG and salivary IgA antibodies and serotype-independent protection against several serotypes following intranasal *S. pyogenes* challenge [229,231,232].

Additionally, *S. pyogenes* expresses a diverse number of fibronectin binding proteins that are important in mediating adherence and internalization into host cells, and antibodies directed against these adhesins are thought to prevent bacterial attachment and inhibit colonization. Intranasal immunization with Sfb1 and cholera toxin B subunit as an adjuvant induced protection against a lethal intranasal challenge with *S. pyogenes* [233], but failed to limit bacterial growth in the blood or dissemination to the spleen and liver [234].

Furthermore, immunization with either full-length FbA or its fibronectin binding domain [235], or immunization with Fbp54 orally or subcutaneously [236] were found to significantly reduce mortality following fatal *S. pyogenes* injections. Also expressed within the FCT region is the pilus and the main protein component of the pilus is the T-antigen subunit. Multivalent vaccines that consist of multiple fused T-antigen domains are expected to provide over 95% strain coverage [237] and immunization with multivalent T-antigen vaccines produced opsonophagocytic antibodies in rabbits and protected mice against nasopharyngeal and invasive challenges [62,237,238]. An alternative vaccine antigen that binds fibronectin is the cysteine protease SpeB, which cleaves fibronectin to modulate *S. pyogenes* entry into host cells [239,240] and cleaves the IL-1β precursor to produce active IL-1β [241]. Polyclonal antibodies raised against SpeB provide passive immunity to mice and enhance survival during invasive infection [242]. Additionally, mice actively immunized with SpeB [242], or SpeB fused to SpeA [220], showed significantly reduced mortality from lethal *S. pyogenes* injection. These results, and the fact that nearly all strains have ubiquitous expression of antigenically conserved SpeB, are noteworthy features that suggest SpeB be considered to include within a multicomponent *S. pyogenes* vaccine.

From the studies above, several highly conserved single antigens have demonstrated the ability to induce protective immune responses in animal studies, yet protection is often determined using particular infection models that may require a distinct set of immune responses. A vaccine that targets multiple antigens involved in various mechanisms of disease may offer enhanced protection against the diverse range of infections caused by *S. pyogenes.* Five conserved virulence factors expressed by *S. pyogenes* were formulated as a multicomponent vaccine, designated 5CP, which included sortase A [243], C5a peptidase ScpA, the adhesion and division protein SpyAD, a fragment of the serine protease SpyCEP [244], and SLO [245]. Intranasal immunization of mice with 5CP induced both local and systemic immune responses across multiple serotypes that significantly protected against *S. pyogenes* burden, reduced dermonecrotic lesions, and increased survival against mucosal, skin, and systemic infection models [246]. Parenteral immunization with 5CP, however, failed to reduce *S. pyogenes* burden in nasal tissue, despite induction of high levels of serum IgG [246]. A similar multicomponent vaccine candidate, Combo5,

containing several of the same conserved antigens, including arginine deiminase, ScpA, SpyCEP, SLO, and trigger factor, was tested against cutaneous murine skin infections and pharyngeal infections in nonhuman primates (NHP). In BALB/c mice, Combo5 prevented bacterial dissemination to the blood and spleen, but did not significantly reduce bacterial persistence in skin lesions following superficial skin infection, and did not increase survival following subcutaneous injection in $AlPLG1^+$ transgenic mice [228]. In NHP, Combo5 did not prevent *S. pyogenes* colonization, however, the vaccine did stimulate antibody responses and reduced both pharyngitis and tonsillitis scores [247], highlighting the important use of NHP pharyngeal infection models for assessing vaccine effectiveness. Overall, a successful approach against *S. pyogenes* infections may stem from multicomponent vaccine formulations that contain either multiple epidemiologically relevant M protein subunits or M proteins conserved region peptides in combination with other importantly conserved surface-bound or secreted antigens, which together, could broaden the immune response against *S. pyogenes* and target several mechanisms of disease.

1.11 Rationale and hypotheses

The ability of *S. pyogenes* to colonize and establish infection in humans relies on the collection and collaboration of virulent determinants that overcome host barriers and adapt to the various tissue environments encountered during infection. Despite embodying a minority of the global burden, research on *S. pyogenes* pathogenesis has largely focused on severe and invasive infection models. Moving away from extreme manifestations to models that better represent natural routes of infection, such as the nasopharynx or skin, are critical for understanding pathogenic processes that support initial steps of bacterial colonization. During early infection stages, *S. pyogenes* exploits an assortment of surface molecules that adhere to host tissue and subvert early immune defenses in effort to promote the onset of infection, including the HA capsule and M protein. It remains unclear how HA capsule and M protein expression support acute infections of the nasopharynx or skin, and whether immune responses to the M protein provide significant protection within these limited biological niches. Furthermore, the evaluation of multiple *S. pyogenes* nasopharyngeal infections as a predisposing condition for developing cardiac defects

remains largely unassessed. The work presented here will characterize the virulency of the HA capsule and M protein during superficial infections and provide greater insight into the efficacy of a M protein vaccine in preventing acute *S. pyogenes* infections. It is proposed that HA capsule and M protein expression are necessary for *S. pyogenes* to establish infection of the nasopharynx and skin in HLA-transgenic mice. We also speculate that monovalent M protein vaccinations will protect mice from homologous *S. pyogenes* nasal and skin challenges. Finally, since it is widely considered that the M protein is an autoantigen and driver of destructive immune responses against the heart, we extend our studies to characterize left ventricle heart function following repeated exposure to *S. pyogenes* nasopharyngeal infections. We propose that expression of the M protein will be critical for the development of cardiac dysfunction in our recurring infection model. Together, these studies will provide greater mechanistic understandings into how *S. pyogenes* avoids innate clearance to establish superficial infections and will provide valuable considerations that will help guide future vaccine development strategies against this globally prominent pathogen.

1.12 Specific aims

The specific aims of this research are distributed into the following chapters: In **Chapter 2**, we aim to examine the specific role of the HA capsule during acute infections of the nasopharynx and skin in HLA-transgenic mice. In **Chapter 3**, we aim to assess the efficacy of immunity induced by several different monovalent M proteins by investigating whether M protein vaccination prevents nasopharyngeal and skin challenges by their homologous strains. We also aim to characterize the necessity of M protein expression by *S. pyogenes* MGAS8232 during acute infections. Lastly, in **Chapter 4** we will explore a recurring *S. pyogenes* infection model in HLA-transgenic mice and evaluate whether expression of the M protein influences left ventricle cardiac function using echocardiogram imaging.

Chapter 2: *S. pyogenes* hyaluronic acid capsule promotes experimental nasal and skin infection in HLA-transgenic mice by preventing neutrophil-mediated clearance

2.1   Introduction

Streptococcus pyogenes is a globally prominent and human-adapted bacterial pathogen responsible for an enormous burden of disease [11]. While *S. pyogenes* exists primarily as an asymptomatic commensal in up to 12% of school-aged children [22], more than 600 million cases of pharyngitis and 100 million cases of skin infections are recorded each year, and at least 18.1 million people worldwide currently suffer from serious post-infection sequelae, resulting in approximately 517,000 annual deaths [10,11]. It is widely accepted that most *S. pyogenes* strains that cause severe disease arise from benign pharyngeal or skin infections, and thus, as both a major pathogen and common commensal in humans, *S. pyogenes* has evolved various mechanisms to subvert the human immune system to promote colonization and persistence, and to establish disease [4,123].

S. pyogenes produces a high molecular weight polysaccharide capsule comprised of hyaluronic acid (HA) that presents distinct mucoid colony morphology when grown on solid media. It is composed of repeating disaccharide units of glucuronic acid and GlcNAc and is structurally identical to HA found within the human ECM, thereby making the capsule immunologically inert [248]. The capsule is produced by the *hasABC* genetic locus that encodes a cluster of three genes involved in HA biosynthesis [249–251]. The first gene in the operon, *has*A, encodes hyaluronate synthase [77,252]; the second gene, *hasB*, encodes UDP-glucose 6-dehydrogenase [253]; and the third gene, *hasC,* encodes UDP-glucose pyrophosphorylase [254]. While the enzyme proteins encoded by *hasB* and *hasC* are enzymatically active, they are not essential for HA synthesis by *S. pyogenes* [255,256]. Interestingly, expression of the *hasA* gene is the only fundamental gene required for the production of the HA polymer from UDP-glucuronic and UDP-GlcNAc sugar precursors [77]. The amount of capsule produced can vary widely among individual strains, regulated by growth conditions and in response to changes in the host environment. Maximal HA capsule production occurs during early and mid-exponential phase *in vitro*, followed by capsule shedding during stationary phase [250]. These observations are further supported *in vivo* as introduction of *S. pyogenes* into the pharynx of non-human primates or into the mouse peritoneum induces high levels of HA capsule gene transcription within 1-2 hours

of inoculation [257], suggesting that capsule expression has an important function during early stages of colonization.

Early pioneering studies using encapsulated M18 and M24 serotypes revealed that transposon mutants lacking the HA capsule had ~100-fold increases in the LD_{50} using an invasive intraperitoneal CD1 mouse infection model [258,259]. Additionally, the HA capsule promoted chronic throat colonization, pneumonia, and secondary systemic infections following intratracheal inoculation in mice [260]. These findings suggest that encapsulation of *S. pyogenes* confers a powerful survival advantage during severe and invasive infections in which animals succumb to overwhelming bacteremia. Research using the M24 serotype in a pharyngeal colonization model also demonstrated that capsule expression was strongly selected for *in vivo* [78], and pharyngeal colonization models in non-human primates found that unencapsulated mutants were cleared more quickly from the pharynx of baboons [84]. Taken together, encapsulation likely enhances *S. pyogenes* pathogenesis, yet the mechanism whereby it promotes infection remains unclear. Prior studies have shown that the HA capsule binds to the cell surface ligand CD44 to mediate adherence to epithelium [79,80], which can further induce host cell signaling events that disrupts tight junctions to promote invasion [81]. However, reduced binding efficiencies by encapsulated strains have also been observed [80,85]. Removal of the capsule by genetic inactivation of the *has* operon can also promote robust invasion of cultured epithelial cells, although once internalized, *S. pyogenes* is rapidly killed [261]. Furthermore, by producing a molecule ubiquitously expressed by its host, molecular mimicry enables *S. pyogenes* to avoid detection by host immune surveillance and increases resistance to phagocytosis. In several experiments, unencapsulated mutants display significant susceptibility to complement-dependent phagocytic killing by human blood compared to their encapsulated parental strains [125,259,262].

Although these results demonstrate that HA capsule production promotes invasive disease and encourages survival and persistence in the pharynx, studies in human carriers and primate models have identified mutations that reduced or eliminated capsule production in long-term carriage isolates [263,264]. Furthermore, while most strains of *S. pyogenes*

encode the *has* operon, the capsule is not universally present in all isolates. For example, M4 and M22 serotypes*,* and some M89 serotypes, do not contain the *hasABC* operon and thus cannot express HA capsule [265,266]. Therefore, the HA capsule may promote colonization and dissemination by *S. pyogenes*, but prolonged carriage in humans may be favoured by subsequent down-regulation or loss of capsule production. Regulation of HA capsule expression may consequently offer a useful survival adaptation in environments where defense against complement-mediated phagocytic killing is necessary to circumvent the host innate immune response. Mutations that produce a truncated RocA protein (regulator of Cov) present amplified expression of the *has* operon through transcriptional activation of the repressor *covR* support this and have been identified in *S. pyogenes* types *emm*18 and *emm*3 [83,267].

Overall, it is widely recognized that encapsulation can provide *S. pyogenes* with a survival advantage and promote resistance to complement-mediated phagocytosis *in vitro*, however, the mechanisms whereby the capsule promotes *in vivo* infection merits further investigation [268]. In this work, we aimed to further evaluate the role of the HA capsule in two non-invasive infection models using a precise genetic deletion of the *hasA* gene to provide additional mechanistic insights into how *S. pyogenes* may avoid innate immune clearance mechanisms in order to establish superficial infection. Herein, we demonstrate using the encapsulated *S. pyogenes* MGAS8232 strain that the HA capsule is a key virulence factor for non-invasive skin and nasopharyngeal infection. While removal of the capsule allowed for enhanced invasion of host cells, we demonstrate that the key function for both *in vivo* nasal and skin infections is to protect *S. pyogenes* from neutrophil-mediated killing.

2.2 Materials and Methods

All solutions and media were made using water purified with a MilliQ filtration system (EMD Millipore; Darmstadt, Germany).

2.2.1 Bacterial growth conditions

A complete list of bacterial strains used in this study can be found in **Table 2.**

2.2.1.1 *Escherichia coli*

Molecular cloning experiments utilized the *E. coli* XL1-Blue strain cultured in Luria-Bertani (LB) broth (Thermo Fisher Scientific, Waltham, MA, USA) aerobically at 37°C, or Brain Heart Infusion (BHI; BD Biosciences, Franklin Lakes, NJ, USA) media containing 1.5% (w/v) agar (Thermo Fisher Scientific). Media was supplemented with 150 μg mL^{-1} erythromycin (Sigma-Aldrich Canada, Oakville, ON, Canada) when necessary. A complete list of plasmids used in this study can be found in **Table 2**. Viable frozen stock cultures were maintained and stored in LB broth plus 25% (v/v) glycerol.

2.2.1.2 *Streptococcus pyogenes*

S. pyogenes strains were grown under static conditions at either at either 30°C, 37°C, or 40°C in 10 mL tubes of Todd Hewitt broth (BD Biosciences; Franklin Lakes, NJ, USA) supplemented with 1% (w/v) yeast extract (BD Biosciences) (THY). For solid media preparation, 1.5% agar and/or 1 μg mL^{-1} erythromycin were added to the media when appropriate. Viable frozen stock cultures were created by addition of 25% (v/v) glycerol to THY media.

2.2.2 Deoxyribonucleic acid manipulations

2.2.2.1 Polymerase chain reaction

All polymerase chain reaction (PCR) primers used in this study were designed through New England Biolabs Tm Calculator (https://tmcalculator.neb.com/#!/main) and supplied by Sigma-Aldrich or Integrated DNA Technologies (IDT) and are listed in **Table 3**.

Table 2. Bacterial strains and plasmids used in Chapter 2.

Strain/plasmid	Description[a]	Source
Streptococcus pyogenes		
MGAS8232	M18 serotype isolated from a patient with acute rheumatic fever (GenBank accession: NC_003485.1)	[269]
MGAS8232 Δ*hasA*	*hasA* deletion mutant derived from MGAS8232	This study
MGAS8232 Δ*hasA* +*hasA*	MGAS8232 Δ*hasA* containing complementation plasmid pDCerm expressing the *hasA* gene	This study
Escherichia coli		
XL1-Blue	General cloning strain	Stratagene
Plasmids		
pG+host5	Temperature-sensitive Gram-positive/*E. coli* shuttle vector; Erm[r]	[270]
pG+host5::Δ*hasA*	pG+host5 with *hasA* flanking regions inserted	This study
pDC*erm*	Erm[r] derivative of streptococcus-*E. coli* shuttle vector pDC123 (*erm* of Tn*916ΔE*) replacing *cat*	[96]
pDC*erm*::*hasA*	pDC*erm* expressing *hasA* gene and its native promoter for plasmid-based complementation	This study

[a] Abbreviations: Erm[r] - erythromycin resistance; *cat* - chloramphenicol acetyltransferase

Table 3. Primers used in Chapter 2.

Plasmid	Primer Sequence (5′→ 3′)[1]
Primers for hasA deletion constructs	
hasA up *Bam*HI For	CCC <u>GGATCC</u> TGTTTCCTTAATAAATAGTGTGAT
hasA up *Pst*I Rev	CCC <u>CTGCAG</u> TAAAGTTTTTTTAAAAATAGGCACAATTACACC
hasA down *Pst*I For	CCC <u>CTGCAG</u> AAAAAGGTCACTATTTTTAAATAATATATGCATCGAG
hasA down *Kpn*I Rev	CCC <u>GGTACC</u> TTCACAAGAAACAATAATTCGGCTTGG
Primers for sequencing and screening	
M13 For	GTAAAACGACGGCCAG
M13 Rev	GTCATAGCTGTTTCCTG
hasA Screen For	CTCTAAACTGCCTAACAGTTGGATAACACTC
hasA Screen Rev	GTGCAAATTTTTCTGCGTCTGCC
Primers for generating complements	
hasA Comp XhoI For	CCC <u>CTCGAG</u> GGGTGAAGTTTTTTTAATGGAAGCAC
hasA Comp SpeI Rev	CCC <u>ACTAGTG</u> AGGGAAGAATATCAACAATAGTGACTTCG

[1]Restriction sites (indicated in the primer name) are underlined in the primer sequence

Abbreviations: For, forward; Rev, reverse

Primers were resuspended to a final concentration of 100 μM in MilliQ water. Reactions were comprised of 1 × High-Fidelity buffer (Thermo Fisher Scientific), 2 mM magnesium chloride ($MgCl_2$; Thermo Fisher Scientific), 3 mM deoxyribonucleotide triphosphate (dNTP) mixture (Roche, Basel, Switzerland), and utilized Phusion High-Fidelity DNA polymerase [0.7 μL per 100 $μL^{-1}$ reaction (Thermo Fisher Scientific)]. Forward and reverse primers were added at a final concentration of 1 μM, and 1 μL template DNA was added per 100 μL total reaction volume. All reactions were performed using a MJ Research PTC-200 Thermal Cycler (Bio-Rad Laboratories, Hercules, CA, USA) using the following gene amplification conditions: 98°C for 5 minutes to preheat the thermocycler; 98 °C for 30 seconds for initial denaturation; 0.5°C per second to ramp up to the calculated melting temperature (T_m); 30 seconds at the calculated melting temperature (T_m) to anneal primers; 0.5°C per second to ramp up to 72°C for amplification, 72°C for an extension time calculated as 30 seconds per 1 kb; and repeat for a total of 36 cycles. The final extension step was 72°C for 5 minutes and reactions were held at 4°C to indicate completed PCR reactions. PCR products were visualized (see below) and purified using a QIAquick PCR Purification kit (Qiagen) according to the manufacturer's instructions and eluted in sterile MilliQ water.

2.2.2.2   DNA visualization

DNA was visualized on 1% (w/v) agarose (Thermo Fisher Scientific) in 1 × TAE (40 mM Tris-acetate, 1 mM EDTA) buffer. DNA Samples were mixed 5:1 with DNA loading dye (40% [v/v] glycerol, 0.25% [w/v] bromophenol blue [International Biotechnologies; New Haven, CT, USA]) prior to loading into pre-cast wells in the gel. A standard DNA molecular weight ladder (1 kb; Invitrogen) was included in each gel as a size marker. The PowerPac 200 Electrophoresis Power Supply and Chamber (Bio-Rad Laboratories Inc; Hercules, CA, USA) was used to run the gel at 100 V for 1 hour. Agarose gels were stained with 0.05% (v/v) ethidium bromide in TAE buffer for approximately 20 minutes and visualized under ultraviolet light (Gel DocTM, Bio-Rad Laboratories Inc).

2.2.2.3   Plasmid isolation from *E. coli*

Plasmid DNA was isolated from overnight stationary phase cultures of *E. coli*. Pelleted bacteria were treated using QIAprep spin miniprep kit (Qiagen; Hilden, Germany) as per manufacturer's instructions. Plasmid DNA was eluted in sterile water. A complete list of plasmids used in this study can be found in **Table 2.**

2.2.2.4   Preparation of *E. coli* competent cells

For preparation of rubidium chloride competent cells, an overnight culture of *E. coli* XL1-Blue was grown in LB media aerobically and subcultured 1:100 in PSI broth (0.5% [w/v] Bacto Yeast Extract [BD Biosciences], 2% [w/v] Bacto Tryptone [BD Biosciences], 0.5% [w/v] magnesium sulphate, pH 7.6) and grown aerobically to an optical density at 600 nm (OD_{600}) of 0.5. Bacteria were incubated on ice for 15 minutes followed by centrifugation at 4°C for 5 minutes at $5,000 \times g$. The cell pellet was resuspended in $0.4 \times$ the original volume of TfbI buffer (100 mM rubidium chloride, 50 mM manganese chloride, 30 mM potassium acetate, 10 mM calcium chloride, 15% [v/v] glycerol, pH 5.8) and chilled on ice for 15 minutes. Cells were centrifuged again as mentioned above and resuspended in $0.04 \times$ the original volume of TfbII buffer (75 mM calcium chloride, 10 mM 3-(N-morpholino) propanesulfonic acid [MOPS], 10 mM rubidium chloride, 15% [v/v] glycerol, pH 6.5) and stored in 100 μL aliquots at -80°C until use.

2.2.2.5   *E. coli* transformation

Recombinant plasmids were transformed into rubidium chloride competent *E. coli* XL1 Blue cells using a heat-shock method. Briefly, competent cells were thawed on ice, ligation reactions (~10 μL) were added to cells and cells incubated on ice for 30 minutes. Cells were then placed in a 42°C water bath for 45 seconds and subsequently placed on ice for 2 minutes. Cells were transferred to a new tube with 900 μL LB broth and were incubated aerobically for 1 hour at 37°C. Transformed cultures were then spread (~100 μL) onto LB agar with appropriate antibiotics and grown overnight at 37°C.

2.2.2.6   *S. pyogenes* genomic DNA extraction

For total genomic DNA extractions from *S. pyogenes*, 1 mL of overnight stationary phase cultures centrifuged at $15,000 \times g$ for 1 minute and washed with 0.2 mM sodium acetate. Bacterial cells resuspended in 500 µl TE Glucose and add 50 µl of mutanolysin (Sigma-Aldrich) and 200 µg of lysozyme (Thermo Fisher Scientific) for 1 hour at 37°C. Bacteria were then centrifuged again and resuspended in 500 µL lysis buffer (50 mM EDTA, 0.2% SDS) and left to incubate at 70°C for 1 hour prior to the addition of 50 µL of 5 M potassium acetate for 10 minutes at -80°C. Cells were then pelleted at $15,000 \times g$ for 10 minutes and the supernatant was transferred to a new tube. Phenol-chloroform (800 µl) was added to DNA and tubes were mixed by inverting for 1-2 minutes. The solution was centrifuged at $15,000 \times g$ for 10 minutes and the top layer containing DNA was carefully transferred to a new tube with 0.1x volume of 3M sodium acetate and mixed. Ice-cold 95% ethanol was then added to the DNA solution and placed at-80°C for 10 minutes. Centrifugation was repeated and bacterial DNA pellets were washed once with 1 mL ice-cold 70% ethanol. The resulting DNA was left to air-dry and then resuspended in 100 µL sterile water with and 10 µl of RNAse (Thermo Fisher Scientific) and left overnight at room temperature. Samples were then kept at –20°C until use.

2.2.2.7   Preparation of *S. pyogenes* competent cells

Overnight cultures of *S. pyogenes* were inoculated 1:50 into THY broth supplemented with 0.6% glycine and incubated at 37°C. Hyaluronidase (1 mg mL^{-1}) was added after one hour of incubation and bacteria were left to grow at 37°C until an OD$_{600}$ of ~0.2 was reached. Cells were then pelleted at $6,000 \times g$ for 5 minutes, washed once in $0.4 \times$ the original volume with ice-cold water with 15% [v/v] glycerol, and resuspended again in $0.04 \times$ the original volume in ice-cold water with 15% [v/v] glycerol. Competent cells were stored in 200 µL aliquots at -80°C until use.

2.2.2.8   *S. pyogenes* electroporation

Frozen electrocompetent *S. pyogenes* cells were thawed on ice, and thoroughly mixed with 1-2 µg of desired plasmid DNA. Cells were transferred to a 2 mm electroporation cuvette

and pulsed exponentially at 2500 V and 600 Ω using the Bio-Rad Gene Pulser Xcell. Cells were transferred to 10 mL of THY and incubated at 37°C for 1-2 hours, followed by a sub-inoculation of 1 μg mL^{-1} erythromycin to the media. Cells were allowed to grow for an additional 1-2 hours, followed by centrifugation at 6,000 × g and resuspension in 1 mL THY. Cells were spread onto THY plates containing 1 μg mL^{-1} erythromycin and left at 37°C until colonies were visible.

2.2.2.9 Construction of deletion mutants

References to genomic loci are based on the genome of *S. pyogenes* MGAS8232, a type M18 clinical isolate associated with acute rheumatic fever [269]. In-frame genetic deletion in the gene encoding *hasA* was generated in the Gram-positive *E. coli* shuttle vector, pG$^+$host5 [270] (**Table 2**). Using appropriate PCR amplification primers (refer to **Table 3**), two fragments of base pairs flanking the upstream and downstream regions of *hasA* were amplified from MGAS8232 genome and purified using the QIAquick PCR Purification Kit (Qiagen). Both *hasA* PCR products and plasmid minipreps of pG$^+$host5 were digested using restriction endonucleases (New England Biolabs, Ipswich, MA, USA), mixed with 1 × T4 Ligase Buffer and 40 U T4 DNA Ligase (New England BioLabs Inc.) with an insert:vector molar ratio of 5:1, and left overnight at room temperature. Ligation reactions were directly transformed into rubidium chloride competent *E. coli* XL1-Blue cells and confirmed by DNA sequencing.

The pG$^+$host5 system contains a Gram-positive temperature-sensitive origin of DNA replication and an erythromycin selection marker, which were used to target and replace wildtype genes with its mutant gene via homologous recombination. Details of this process have been previously described [156]. Briefly, deletion constructs (1-2 μg) were electroporated in electrocompetent *S. pyogenes* MGAS8232 cells and grown at 30°C on THY agar supplemented with 1 μg mL^{-1} erythromycin. Visible colonies were cultured in THY broth with erythromycin at 30°C for up to three days. Bacteria were streaked onto THY agar with erythromycin and incubated at 40°C. At this temperature, pG$^+$host5 is unable to replicate, and thus, only cells that have integrated the plasmid remain resistant to erythromycin and grow. Genomic DNA was extracted from individual colonies grown at

40°C and plasmid integration was confirmed by PCR using integration screening primers (**Table 3**). Bacteria with confirmed integrations were subcultured into THY broth without antibiotics and grown at 30°C. Cultures were screened for the loss of the pG+host5 plasmid by replicate plating colonies onto THY with and without erythromycin to identify clones that lost erythromycin resistance, indicating that the plasmid was cured. Sensitive clones were screened by genomic DNA isolation and PCR for the in-frame deletion construct and verified by DNA sequencing.

2.2.2.10   Complementation of *hasA* mutant

For complementation of the *hasA* in-frame genetic deletion, DNA fragments containing the *hasA* open reading frames and its native promoter were amplified from the *S. pyogenes* MGAS8232 genome using complementation primers listed in **Table 3**. Amplified DNA was purified, digested, and inserted into the pDC*erm* complementation plasmid and confirmed by DNA sequencing. The pDC*erm*::*hasA* construct was electroporated into the *S. pyogenes* MGAS8232 Δ*hasA* mutant strain, restoring capsule expression morphologically with *hasA* re-expression.

2.2.3   DNA sequencing and analyses

DNA sequencing was completed by the John P. Robarts Research Institute sequencing facility at Western University in London, Ontario, Canada. Sanger sequencing of PCR and plasmid products were completed with either provided or designated primers (**Table 3**).

For whole genome sequencing, genomic DNA preparations from *S. pyogenes* MGAS8232 wildtype and Δ*hasA* strains were sent for paired end Illumina sequencing at the John P. Robarts Research Institute sequencing facility (University of Western Ontario, London, Ontario). Illumina short-read sequence data were used to generate *de novo* assemblies using SPAdes v3.15 [271], which were annotated using Prokka v1.12 [272]. These assemblies have been deposited at NCBI. Any sequence differences between the strains were determined using Snippy v4.1 (https://github.com/tseemann/snippy). The publicly available *S. pyogenes* MGAS8232 sequence was used as a reference (Bioproject: PRJNA286). SNPs unique to the Δ*hasA* mutant were reported.

2.2.4   Growth curves

S. pyogenes strains were grown from -80 °C freezer stocks and subcultured twice (1:100 dilution) in 10 mL tubes of THY at appropriate conditions stated above. Overnight cultures were added to 100 mL of THY (1:20) and left at 30°C until early exponential phase of growth was reached. OD_{600} readings were measured by a spectrophotometer (DU® 530 Life Sciences UV/Vis Spectrophotometer; Beckman Coulter Canada LP; Mississauga, ON, Canada). Once a logarithmic growth phase was determined, bacterial samples were adjusted to ~0.02 and added to 96-well plates in triplicate, wells containing media only controlled for background absorbances. OD_{600} readings were measured every 15 minutes for 20 hours using the Synergy HTX Multi-Mode Microplate Reader (BioTek, Winooski, VT, USA).

2.2.5   Trichloroacetic acid preparation

To obtain the secreted protein profile, overnight cultures of *S. pyogenes* were subcultured 1:20 into prewarmed THY 100 mL bottles and left at 37°C for 13 hours. Cells were centrifuged at 10,000 × *g* for 15 minutes at 4°C and 90 mL of supernatant was added to 50% trichloroacetic acid (TCA) (Sigma-Aldrich) to a final concentration of 6%. The mixture was chilled on ice for 30 minutes and then precipitated supernatants were spun at 10,000 × *g* for 10 minutes at 4°C. Pellets were washed with ice-cold acetone (Thermo Fisher Scientific) and centrifuged at 10,000 × *g* for 10 minutes. The supernatants were removed, and proteins were resuspended in 1 mL of 8M urea (BioShop Canada Inc; Burlington, ON, Canada) and then stored at -20°C.

2.2.6   Extracellular matrix binding assay

Corning Costar 9018 high-binding 96-well plates (Corning; Kennebuck, ME, USA) were coated with 1 µg of collagen type IV (Sigma-Aldrich) or fibronectin (Calbiochem, EMD Millipore Corporation; Temecula, CA, USA) in carbonate-bicarbonate buffer (0.2M sodium carbonate anhydrous, 0.2M sodium bicarbonate, pH = 9.6) and kept overnight at 4°C. Overnight streptococcal cultures were inoculated 1:20 into pre-warmed THY and grown to mid exponential phase. Cultures were adjusted to OD_{600} of 0.2, centrifuged at

$6,000 \times g$ for 10 minutes, and then resuspended in PBS. While the bacteria were growing, collagen and fibronectin-bound plates were washed three times with PBS and 0.05% (v/v) tween-20 and incubated for 2 hours with 5% (w/v) skim milk at room temperature to block non-specific binding. Plates were washed three times as described and 100 μL containing 10^7 bacterial CFUs were added to the coated wells in triplicate and left at 37°C. After 2.5 hours, plates were washed and fixed with 10% neutral buffered formalin (VWR International; Randor, PA, USA) for 40 minutes. Plates were washed again and 50 μL of 0.5% (w/v) crystal violet (Sigma-Aldrich) in 80% (v/v) sterile MilliQ water and 20% (v/v) methanol was added for 5 minutes at room temperature. Plates were washed five times and the stain was solubilized in 5% (v/v) acetic acid with mild agitation for 10 minutes. Colorimetric absorbances were measured at OD_{590} with the Synergy HTX Multi-Mode Microplate Reader (BioTek).

2.2.7 Human cell culturing

The Detroit 562 (ATCC CCL-138) human pharyngeal cell line (obtained from Dr. Joe Mymryk, Western University) was grown and maintained at 37°C in 5% CO_2 in minimal essential medium (MEM) (Gibco-BRL, Life Technologies, NY, USA.). Cells were grown in sterile 75 cm^2 tissue culture (TC)-treated flasks (Falcon, Corning; Corning, NY, USA) in 14 mL of MEM supplemented with 10% (v/v) heat-inactivated fetal bovine serum (FBS) (Sigma-Aldrich), 100 $\mu g\ mL^{-1}$ streptomycin (Life Technologies), and 100 $U\ mL^{-1}$ penicillin (Life Technologies) at 37°C in 5% CO_2 and washed 3 times every other day with PBS filtered through a 0.2 μm PES filter (Nalgene^{TM}, Thermo Scientific, MA, USA).

The A549 lung epithelial pharyngeal cell line obtained from (obtained from Dr. Joe Mymryk, Western University) was grown and maintained in Dulbecco's modified eagle medium (DMEM) (Gibco-BRL). Cells were grown in 14 mL of DMEM supplemented with 10% (v/v) heat-inactivated FBS (Sigma-Aldrich), 100 μg mL-1 streptomycin (Life Technologies), and 100 $U\ mL^{-1}$ penicillin (Life Technologies) at 37°C in 5% CO_2 and washed 3 times every other day as described.

2.2.7.1 Adhesion assay

Detroit-562 and A549 cells were grown to confluence on 12 or 24 well TC-treated plates (Falcon, Corning). On the day of the experiment, three wells were dissociated with 0.05%

trypsin-EDTA and the average number of cells per well were calculated by trypan blue exclusion (Gibco®, Life Technologies Inc, CA, USA) using a hemocytometer and used to determine the number of bacteria required for a multiplicity of infection (MOI) of 100 per well. During this time, overnight streptococcal cultures were subcultured into pre-warmed THY and grown to OD_{600} of $0.2 - 0.4$. The appropriate volume of *S. pyogenes* was centrifuged at $10,000 \times g$ and pellets were resuspended in the respective serum- and antibiotic-free media. Once cell monolayers were washed three times with filter-sterilized PBS, bacteria (MOI = 100) were inoculated into wells for 2.5 hours at 37°C in 5% CO_2. Background adherence levels were measured by inoculating bacteria into uncoated wells. Following incubation, wells were washed three times with filter-sterilized PBS to clear non-adherent bacteria, and cell monolayers were lysed by adding 500 µl of 0.01% Triton X-100 (VWR International) for 5 minutes followed by disruption of the wells by scraping with a 1 mL pipette tip. Solubilized wells were serially diluted ten-fold and plated onto TSA 5% sheep blood agar plates to enumerate bacteria present.

2.2.7.2   Internalization assay

The internalization assay is a modification of the classical gentamycin protection assay [273]. The assay follows the steps as outlined in Section 2.2.7.1 with *S. pyogenes* inoculated onto a confluent monolayer of Detroit-562 cells for 2.5 hours. Non-adherent bacteria were washed off as described, and MEM supplemented with 100µg mL^{-1} gentamycin (Sigma-Aldrich) was added to the wells for an additional 1.5 hours at 37°C in 5% CO_2 to kill remaining extracellular bacteria. Cells were washed and lysed with 500 µL of 0.01% Triton X-100 (VWR International) for 5 minutes. A 1 mL plastic pipette tip was used to scrape off remaining debris from the bottom of the wells followed by serial dilution and drop plating on TSA 5% sheep blood agar plates, which were left at 37°C overnight to enumerate internalized bacteria.

2.2.8   *Ex vivo* experiments

2.2.8.1   Ethics statement

The use of primary human lymphocytes was reviewed and approved by Western University's Research Ethics Board for Health Sciences Research Involving Human Subjects. (**Appendix 1**). Informed written consent was obtained from all donors. Human venous blood was taken from healthy volunteer donors in accordance with human subject protocol 110859.

2.2.8.2   Whole blood survival assay

Overnight streptococcal cultures were added to pre-warmed THY broth in a 1:20 dilution and grown to early exponential phase. OD_{600} measurements were used to calculate the number of bacteria in 1 mL of culture. The volume of bacteria necessary to prepare the inoculation was calculated, measured, and spun at $6,000 \times g$ for 10 minutes. Bacterial supernatants were poured off and pellets were transferred to new 1.5 mL microfuge tubes and spun at $21,000 \times g$ for 1 minute. The residual supernatant was removed, and the pellet was washed twice in 1 mL Hanks' Balanced Saline Solution (HBSS; Life Technologies, Carlsbad, CA, USA), and spun as above. The supernatant was again removed, and the pellet was reconstituted in HBSS. Heparinized whole blood was collected in heparinized vacuum tubes (BD Biosciences) from healthy adult volunteers and used within 2 hours of collection for experiments. A volume of 10 μL containing 1000 bacterial CFU was added to 990 μL whole human blood in 1.5 mL microfuge tubes and left to incubate at 37°C with rotation. After 30, 60, 90, 120, and 180 minutes, blood tubes containing each streptococcal strain were serially diluted ten-fold and drop plated in triplicate onto 5% TSA blood agar plates at 37°C overnight to enumerate surviving bacteria in the blood at each selected time point.

2.2.8.3   Isolation of human polymorphonuclear neutrophils

Polymorphonuclear neutrophils (PMNs) were isolated using a Ficoll (GE-Healthcare) Histopaque (Sigma-Aldrich) density gradient centrifugation method. Briefly, heparinized blood from human donors was diluted with an equal volume of PBS (Wisent Bioproducts Inc.) and layered carefully onto a dual Ficoll-Histopaque gradient and centrifuged at $396 \times$

g for 20 minutes without braking. The PMN layer was collected and washed with cold RPMI containing 0.05% human serum albumin (RPMI-HSA) and hypnotic lysis with addition of 1 mL ice-cold water to remove residual erythrocytes. PMNs were then collected in RPMI-HSA following centrifugation and adjusted to 4×10^6 cells mL^{-1}.

2.2.8.4   Neutrophil phagocytosis assay

Overnight streptococcal cultures were grown to early exponential phase and diluted to 10^4 CFU mL^{-1} in RPMI containing 10% (v/v) normal human serum for 30 minutes to assist with bacterial opsonization. A bacterial suspension volume of 0.225 mL was co-cultured with 0.025 mL of isolated human PMNs at 4×10^6 cells mL^{-1} (1:10 bacterial CFU to neutrophils) at 37˚C with vigorous shaking. Control samples had no PMNs added to control for growth of the bacteria. Viable bacteria in each reaction mixture were enumerated after 60 mins by lysing cells with 750 µl of 0.025% Triton X-100, followed by serial dilution and plating onto 5% TSA blood agar plates overnight at 37˚C. Percent bacterial survival was calculated as the average bacterial CFUs in the presence of neutrophils divided by bacterial CFUs in no PMN control samples.

2.2.9   *In vivo* experiments

2.2.9.1   Ethics statement

All mouse experiments were conducted in accordance with the Canadian Council on Animal Care Guide to the Care and Use of Experimental Animals. The Animal Use Protocol (AUP) number 2020-041 was approved by the Animal Use Subcommittee at Western University (London, ON, Canada) (**Appendix 2**).

2.2.9.2   Housing and breeding

Mice were bred and housed in the West Valley Barrier Facility (Western University, London, ON, Canada) and moved to either the animal holding facility on the sixth floor of the Dental Sciences Building (Western University, London, ON, Canada) or in Sieben's Drake Research Institute (Western University, London, ON, Canada) for undertaking of

experiments. In both facilities, mice were housed under specific pathogen-free conditions with food and water *ad libitum.*

2.2.9.3 Strains utilized

A list of all mice used in this study can be found in **Appendix 3.** Human MHC class II transgenic mice were bred from McCormick laboratory colonies specifically for this study and were in a C57BL/6 (B6) background. B6 mice expressing the transgenic HLA-DR4 and DQ8 were obtained from the Kotb Laboratory and have been previously described [154,156]. Mice expressing the DQ8 gene alone were outbred from HLA-DR4/DQ8 by selecting for mice containing only the HLA-DQ8 allele. Herein, Human MHC class II transgenic mice will be referred to as B6$_{HLA}$ mice.

2.2.9.4 *S. pyogenes* dose preparation and infection

Preparation of *S. pyogenes* MGAS8232 for nasal inoculation has been previously described [156]. Briefly, *S. pyogenes* was grown in THY broth statically at 37°C and subcultured 1:100 for two days. On the third day, bacteria were subcultured 1:20 into pre-warmed 100 mL bottles of THY and grown to early exponential phase (OD$_{600}$ ~0.2 – 0.4). The appropriate volume of bacteria necessary to prepare the inoculation dose was calculated and centrifuged at 6,000 × g for 10 minutes and the supernatant was then removed. The bacterial pellet was transferred to a 1.5 mL microfuge tube and spun at 21,000 × *g* for one minute. The residual supernatant was removed, and the pellet was washed twice in 1 mL HBSS (Wisent Bioproducts Inc) and resuspended in 150 μL HBSS for murine inoculation. One dose volume was serially diluted and plated to determine the concentration of the bacterial inoculum.

2.2.9.5 Nasopharyngeal infection model

Mice were given 2 mg ml^{-1} neomycin sulphate *ad libitum* in their drinking water two days prior to infection to reduce the nasal microbiota. Mice were anesthetized using FORANE (isoflurane, USP; Baxter Corporation; Mississauga, ON, Canada) and 7.5 μL of bacterial inoculum was administered to each nostril with 15 μL containing 1×10^8 CFUs. The mice were allowed to recover from the anesthetic and monitored for the duration of the

experiment. Mice were euthanized 24- or 48-hours post-infection and and their complete nasal turbinates (cNTs), including the nasal-associated lymphoid tissue (NALT), nasal turbines (NT), and maxillary sinuses (MS), were extracted and homogenized using a glass homogenizer. Murine blood, spleen, liver, kidneys, lungs, and heart were also removed for bacterial enumeration where indicated. Organs were serially diluted in HBSS and plated on TSA supplemented with 5% sheep's blood (BD Biosciences) for bacterial enumeration. Counts less than 25 CFU per 100 µL of cNT were considered below the theoretical limit of detection.

2.2.9.6   Skin infection model

The fur on the lower backs of B6$_{HLA}$ mice between 8-12 weeks old were removed by shaving and hair removal cream the day before infections. *S. pyogenes* was grown and prepared as stated above in Section 2.2.9.4 and resuspended to 5×10^9 CFU per mL in HBSS. Mice were anesthetized and a 50 µL dose containing ~2.5×10^7 CFU was injected subcutaneously into each lower flank. Each day following infection, mice were weighed and lesions at the injection sites were measured using calipers. At 72 hours post-infection, mice were sacrificed and the skin around each injection site was harvested, homogenized, and plated on TSA with 5% sheep's blood (BD Biosciences) overnight at 37°C for bacterial enumeration. Bacterial burden was normalized to the weights of the skin excised and presented as CFU per gram of skin.

2.2.9.7   Neutrophil Depletion

The function of neutrophils during acute infections by *S. pyogenes* was examined in B6$_{HLA}$ mice between 8-12 weeks old. Mice were intraperitonially injected with 250 µg αLy6G monoclonal antibody (clone 1A8) or 250 µg of isotype IgG2a (BioXcell, NH, USA) at 24 hours prior to nasopharyngeal or skin infections. For 48-hour nasopharyngeal infections, mice received a second injection of 250 µg α-Ly6G or isotype at 24 hours following *S. pyogenes* exposure. Neomycin (2 g L^{-1}) was added to water bottles 48 hours before nasal inoculations and bacterial burden was assessed at either 24- or 48-hours following infection. For skin infections, the fur on the lower backs of mice was removed 24-hours

prior to subcutaneous inoculations and mice received a second injection of 250 μg α-Ly6G or isotype 24 hours following skin infections.

2.2.9.8   Macrophage Depletion

The depletion of macrophages in B6$_{HLA}$ mice between 8-12 weeks old has been previously described [274]. Briefly, 200 μL clodronate containing liposomes and control liposomes [Clodrosome® + Encapsome® (Encapsula Nano Sciences)] were intraperitonially injected in mice at both 48 and 4 hours prior to nasopharyngeal infection with *S. pyogenes.* Bacterial burden in cNTs were examined at both 24- and 48-hours following infection.

2.2.10   Multiplex cytokine array

Cytokine and chemokine concentrations were determined from cNTs of B6$_{HLA}$ mice nasally infected with *S. pyogenes*. Uninfected cNT homogenates were collected for background comparisons. Multiplex cytokine array (mouse cytokine/chemokine array 32-Plex) was performed by Eve Technologies (Calgary, AB, Canada) and heat maps were generated using GraphPad Prism (9.3.1). Data on heat maps are normalized median cytokine responses ($X_{normalized} = [(x - x_{min})/(x_{max} - x_{min})]$) from cNT homogenates of all nasally infected mice ($n \geq 3$). Statistical analyses were completed by the appropriate test within groups, quantitative cytokine levels are shown in **Appendix 5**.

2.2.11   Statistical analyses

Data was analyzed using unpaired Student's *t*-test, one-way analysis of variance (ANOVA) with Kruskal-Wallis post-hoc test and Dunn's multiple comparisons test, or two-way ANOVA with Tukey's or Dunnett's multiple comparisons tests and Geisser's Greenhouse correction, as indicated. A *P* value less than 0.05 was determined to be statistically significant, all analyses were completed using Prism software 9.3.1 (GraphPad Software, Inc.; La Jolla, CA, USA).

2.3   Results

2.3.1   Confirmation of HA capsule deletion and complementation in *S. pyogenes* MGAS8232

In order to evaluate the influence of the HA capsule during experimental infection, we used the pG⁺host5 integration plasmid [270] to generate a markerless 1,212-bp in-frame deletion of *hasA* in the M18 serotype rheumatic fever isolate *S. pyogenes* MGAS8232 [269]. M18 serotypes are well known for being highly encapsulated, a phenotype that has been traced to the mutations within the RocA regulatory protein [83]. The *hasA* deletion was confirmed by PCR and DNA sequencing with primers that flanked the deleted *hasA* region (**Table 3**). Compared to the wildtype MGAS8232 genome, the Δ*hasA* mutant strain featured a 1,212 bp deletion (**Figure 1A**). To further confirm the isogenic nature of the *hasA* mutant, whole genome sequencing analysis was performed, which confirmed the correct Δ*hasA* deletion, but also revealed two non-synonymous single nucleotide polymorphisms (SNPs) compared to the wildtype MGAS8232 strain within the *pstI* gene encoding cytosolic protein enzyme I in the phosphoenolpyruvate phosphotransferase system (PTS). These SNPs resulted in two amino acid substitutions ($Leu_{194}Phe$ and $Ser_{306}Phe$) (**Table 4**). Therefore, we generated a complementation strain using the pDC*erm* plasmid [96] (**Table 2**) by expressing the *hasA* gene and its native promoter in the *hasA* mutant background (MGAS8232 Δ*hasA* + *hasA*). As predicted, MGAS8232 Δ*hasA* lost the large mucoid colony phenotype on sheep blood agar compared to wildtype MGAS8232, and capsule production was restored in the *hasA*-complemented strain by pDC*erm*::*hasA* (**Figure 1B**). Genomic deletion and complementation of the HA capsule did not overtly affect the secreted protein profile of *S. pyogenes* MGAS8232, demonstrated by SDS-PAGE (**Figure 1C**). The Δ*hasA* mutant strain grew comparably to wildtype MGAS8232 *in vitro,* ensuring that *hasA* deletion did not have any discernable growth defects (**Figure 1D**). The Δ*hasA* + *hasA* complement strain, however, displayed slower exponential growth, likely due to the pDC*erm* expression system (**Figure 1D**).

Figure 1. Verification of *hasA* gene deletion and complementation in *S. pyogenes* MGAS8232

In-frame genomic deletion of the *hasA* gene in *S. pyogenes* MGAS8232 was generated by standard molecular cloning procedures and complemented back into the mutant by pDC*erm*::*hasA* expression. **A.** Deletion of *hasA* confirmed by PCR using primers flanking the homologous recombination site. PCR products were visualized on a 1% agarose gel stained with ethidium bromide. **B.** Colony morphology differences on TSA + 5% sheep blood agar. **C**. Secreted protein profiles after growth in THY for 18 hours, demonstrated by SDS-PAGE on 12% acrylamide gel stained with Ready Blue. **D**. Growths in THY at 37°C were measured by OD_{600} over 18 hours. Data is presented as mean ± SD of each culture analyzed in triplicate ($n = 3$).

A

bp

MWL · Wildtype · ΔhasA · ΔhasA + hasA

4,000
3,000
2,000
1,650
1,000

B

ΔhasA

ΔhasA + hasA

Wildtype

C

kDa

MWL · Wildtype · ΔhasA · ΔhasA + hasA

75
63
40
35
25

D

OD600

Time (hours)

○ Wildtype
■ ΔhasA
▲ ΔhasA +hasA
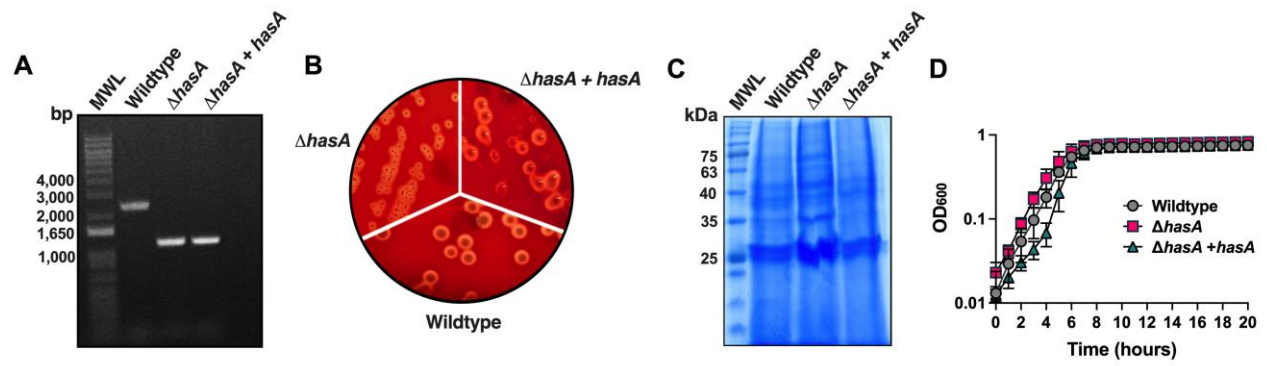
Table 4. SNPs identified through genome wide comparisons of *S. pyogenes* MGAS8232 wildtype and Δ*hasA* strains

Gene	Locus	Protein	Gene size (bp)[b]	Codon number	Reference nucleotide	Competing nucleotide	Nucleotide in codon	Amino acid change
pstI[a]	spyM18_1384	AAL97979.1	1734	194	A	T	1	L > F
pstI[a]	spyM18_1384	AAL97979.1	1734	306	C	T	2	S > F

[a] cytosolic enzyme I in the phosphoenolpyruvate-protein phosphotransferase system

[b] bp, base pairs

2.3.2 HA capsule expression promotes nasopharyngeal infection in B6$_{HLA}$ mice

A major limitation to investigating *S. pyogenes* during acute infections is its human specific tropism. We have recently shown that the use of HLA-transgenic mice enhances streptococcal infections due to the selective specificity of superantigens for human MHC class II molecules [156,275]. In this model *S. pyogenes* MGAS8232 infected cNTs of HLA-transgenic mice ~10,000-fold higher than conventional B6 mice [156]. Since superantigens do not bind mouse MHC-II molecules efficiently, [156,276,277], this model supports the human-specific tropism of *S. pyogenes*. We therefore sought to assess the HA capsule using this established nasopharyngeal infection model. HLA-transgenic mice (herein B6$_{HLA}$ mice) were nasally infected with ~10^8 CFU of live MGAS8232 wildtype or Δ*hasA* strains and murine cNTs were excised 48 hours later for bacterial enumeration. Infection with the Δ*hasA* mutant resulted in a ~1000-fold reduction in bacterial recovery from the nasal mucosa at 48 hours compared to infection by wildtype *S. pyogenes* MGAS8232 (**Figure 2A**). We then confirmed that capsule expression was specifically required for the infection phenotype as B6$_{HLA}$ mice infected with the restored capsule expressing strain Δ*hasA* +*hasA* had in a ~1000-fold increase in recovered bacteria compared to the Δ*hasA* mutant, phenocopying wildtype infection (**Figure 2A**). Consistent with the non-invasive nature of the model [156], mean bacterial dissemination of all strains remained below the limit of detection in the lungs, liver, spleen, heart, and kidneys (**Figure 3**). We conclude that HA capsule expression improves *S. pyogenes* experimental nasopharyngeal infection in B6$_{HLA}$ mice, and removal of the capsule does not increase bacterial dissemination of *S. pyogenes*.

2.3.3 HA capsule expression amplifies cytokines that support monocyte and neutrophil function in the nasopharyngeal environment.

To further assess the nasopharyngeal environment during *S. pyogenes* wildtype and Δ*hasA* infections, we conducted a multiplex cytokine array to evaluate the levels of 32 cytokines and chemokines using cNT homogenates at 48 hours post-infection. Any cytokine that presented an average concentration above 20 pg ml^{-1} within a treatment group was included

in the heat map and presented as normalized median cNT cytokine responses (**Figure 2B**). Quantitative data is shown in **Appendix 5** for all 32 cytokines. As predicted, uninfected mice demonstrated no apparent inflammatory signature from the cNT homogenates whereas robust cytokine responses were evident in wildtype-infected mice and included: Th1-type cytokines (IL-1α and IL-1β); Th17-type cytokines (IL-6 and IL-17); chemokines (KC, IP-10, MCP-1, MIP-1α, MIP-1β, MIG, MIP-2, LIF and LIX); and growth factors (G-CSF) (**Figure 2B, Appendix 5**). In contrast, Δ*hasA*-infected cNTs presented a reduced inflammatory signature and revealed similar cytokine expression profiles as uninfected mice. Particularly, reductions were observed with pro-inflammatory cytokines, such as IL-1β, IL-6, and IL-17, and those involved in monocyte and neutrophil recruitment, including KC, IP-10, MCP-1, MIP-1β, MIG, and G-CSF (**Figure 2B, Appendix 5**). Restoring capsule expression in the Δ*hasA* mutant background induced a moderately inflamed environment, trending for greater concentrations of KC, MIP-1α, MIG, MIP-2, and G-CSF compared to the Δ*hasA* mutant infection. Interestingly, IL-2, IL-12 (p40), IL-15, and IL-9 concentrations were higher in cNTs challenged with Δ*hasA* mutant compared to wildtype or Δ*hasA* + *hasA* strains; however, concentrations for these cytokines did not drastically differ from uninfected murine cNTs (**Figure 2B, Appendix 5**). There were also numerous cytokines that did not show average concentrations above 20 pg ml^{-1} in any treatment groups, were not different between treatment groups, or did not conform to any obvious trends (**Appendix 5**). These results indicate that at 48 hours post-infection, HA capsule expression is associated with higher concentrations of cytokines that support inflammation and monocyte and neutrophil function. In the absence of its HA capsule, *S. pyogenes* cannot remodel the nasopharynx to express favourable inflammatory responses that promote infection.

2.3.4   Nasopharyngeal infection with *S. pyogenes* provokes neutrophil influx in murine nasal turbinates

To gain further insight into the interaction between *S. pyogenes* and host immune cells during nasopharyngeal infection, MGAS8232 wildtype and Δ*hasA*-infected cNTs were harvested and cryopreserved for immunohistochemistry. Due to the possibility that Δ*hasA* mutant would be completely cleared by 48 hours post-infection (**Figure 2A**), infected cNTs

Figure 2. Hyaluronic acid expression by *S. pyogenes* promotes nasal infection in B6$_{HLA}$ mice

B6$_{HLA}$ mice were administered ~10^8 colony forming units (CFUs) of *S. pyogenes* MGAS8232 wildtype, Δ*hasA,* or Δ*hasA* +*hasA* strains intranasally and sacrificed 48 hours later. **A.** Data points represent CFUs from infected complete nasal turbinates (cNTs) of individual B6$_{HLA}$ mice. Bars represent mean ± SEM. Significance was determined by one-way ANOVA with with Kruskal-Wallis post-hoc test (****, $P < 0.0001$; **, $P < 0.01$). The horizontal dotted line indicates limit of detection. **B.** Heat-map of multiplex cytokine array during *S. pyogenes* nasopharyngeal infection. Supernatants from infected cNT homogenates were obtained for cytokine and chemokine analyses. Data shown represent the normalized median cytokine responses ($n \geq 3$ per group). **C.** Immunohistochemistry of murine cNTs at 24 hours post-infection with *S. pyogenes* MGAS8232 wildtype and Δ*hasA*. Sections were stained with α-CD3 (green) for T cells, α-B220 (blue) for B cells, α-*S. pyogenes* (red), and α-Ly6G (white) for neutrophils. Panel is a close-up view from the boxed section. Arrows indicate regions with internalized *S. pyogenes.*

A

B

C
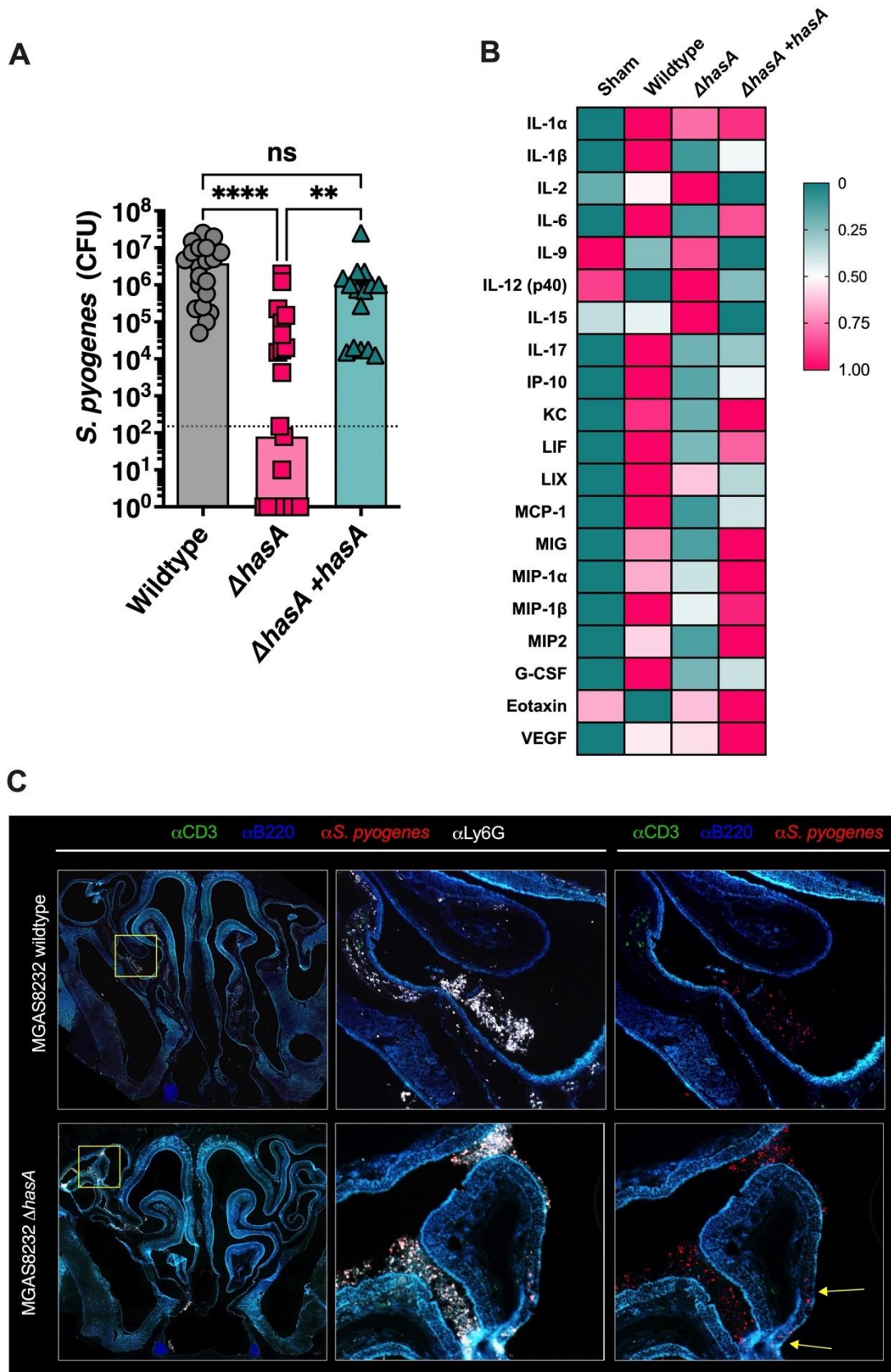
Figure 3. Deletion of the *hasA* gene in *S. pyogenes* MGAS8232 does not enhance bacterial dissemination in B6$_{\text{HLA}}$ mice.

B6$_{\text{HLA}}$ mice were nasally challenged with ~10^8 CFUs of *S. pyogenes* wildtype, Δ*hasA,* or Δ*hasA* +*hasA* strains. Mice were sacrificed 48 hours later and indicated organs were harvested, homogenized, and plated on TSA with 5% sheep blood agar to assess bacterial dissemination. Bacterial CFUs were measured in the **(A)** lungs, **(B)** liver, **(C)** spleen, **(D)** heart, and **(E)** kidneys. Data points represent CFUs of indicated organs from individual mice ($n \geq 4$ per group). Bars represent mean ± SEM. Horizontal dotted line indicates theoretical limit of detection. Significance was determined by one-way ANOVA with Dunnett's multiple comparisons test, data not significant.

A Lungs

CFU/Lung

Wildtype ΔhasA ΔhasA +hasA

B Liver

CFU/Liver

Wildtype ΔhasA ΔhasA +hasA

C Spleen

CFU/Spleen

Wildtype ΔhasA ΔhasA +hasA

D Heart

CFU/Heart

Wildtype ΔhasA ΔhasA +hasA

E Kidneys

CFU/Kidneys

Wildtype ΔhasA ΔhasA +hasA
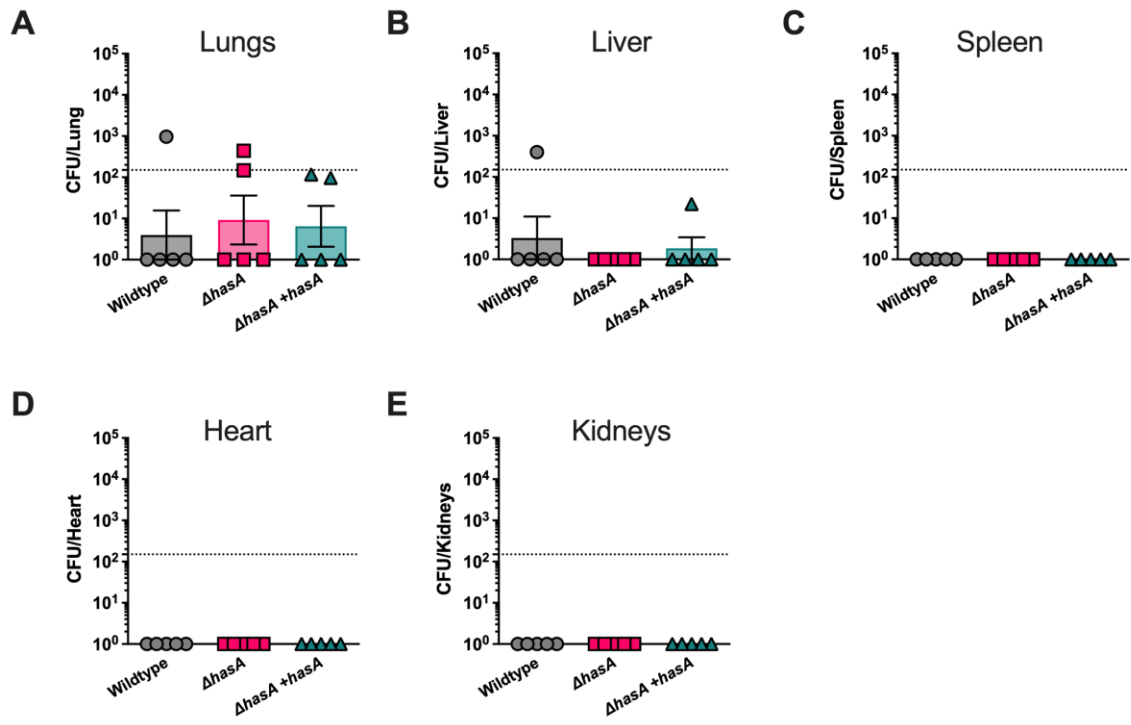
were collected at 24 hours post-infection and sections were stained with α-*S. pyogenes* (red), α-B220 (blue), α-CD3 (green), and α-Ly6G (white) fluorescent antibodies where indicated. Sections revealed that *S. pyogenes* was present with robust α-Ly6G neutrophil signals in both wildtype and Δ*hasA*-infected cNTs (**Figure 2C**). By 24 hours, neutrophils infiltrated to the central areas where *S. pyogenes* resided, whether the HA capsule was expressed or not (**Figure 2C**). Although few differences in immune cell percentages have been detected within the cNTs of wildtype-infected B6$_{HLA}$ mice by 48 hours [156], previous examination of infected nasal passages demonstrated increased trends for neutrophil populations (GR1$^+$) during wildtype *S. pyogenes* MGAS8232 infection [156], entirely consistent with the immunofluorescence (**Figure 2C**). Notably, *S. pyogenes* Δ*hasA,* but not wildtype, was detected within epithelial cells in some areas, denoted by arrows in the right panel. Together, these observations are consistent with a model that neutrophils are recruited to murine cNTs during both MGAS8232 wildtype and Δ*hasA* nasopharyngeal infection.

2.3.5 Bacterial burden and lesion sizes are enhanced by HA capsule expression during *S. pyogenes* skin infection

Pharyngeal colonization by *S. pyogenes* is believed to be the major reservoir for this pathogen in developed countries, yet skin infections (impetigo) tend to be more prevalent in resource-poor settings [278]. Since our findings indicate that experimental nasopharyngeal infection by *S. pyogenes* is notably compromised by deletion of the HA capsule, we next performed a novel skin infection model to further assess whether capsule expression could promote experimental skin infection. To address this, B6$_{HLA}$ mice were intradermally injected in each hind flank with 2.5×10^7 CFUs of wildtype, Δ*hasA,* or Δ*hasA* +*hasA* strains. Animal weights and lesion sizes were measured daily, and at 72 hours post-infection mice were sacrificed and the skin surrounding infection sites were harvested for bacterial enumeration. We observed a ~10% weight decline in mice infected with wildtype *S. pyogenes,* a striking contrast to mice infected with the Δ*hasA* strain that appeared to gain weight over the 72-hour infection period (**Figure 4A**). The Δ*hasA* mutant strain revealed a clear reduction in virulence through considerably smaller lesions and less inflamed tissue over the infection period compared to wildtype-infected mice (**Figures 4B and 4D**).

Figure 4. HA capsule expression enhances *S. pyogenes* burden and lesion sizes during acute skin infection in B6$_{HLA}$ mice.

B6$_{HLA}$ mice were administered ~5 x 10^7 CFUs of wildtype, Δ*hasA,* or Δ*hasA +hasA S. pyogenes* MGAS8232 by intradermal injections in each hind flank. **A.** Weights of B6$_{HLA}$ mice at 24-, 48-, and 72-hours following skin challenge. Data is represented as a percentage of day 0 weight. Data points represent the mean weights ± SEM. **B.** Skin lesion areas of mice following at 24-, 48-, and 72-hours post skin challenge. Data points represent mean lesion areas ± SD. **C.** Data points represent bacterial CFUs from individual skin abscesses normalized to the weight of the excised skin tissue from mice at 72 hours. Bars represent mean ± SEM. The horizontal dotted line indicates limit of detection. Significance was determined by (**A - B**) two-way ANOVA with Dunnett's multiple comparisons test and Geisser's Greenhouse correction (**, $P < 0.01$; ***, $P < 0.001$; ****, $P < 0.0001$), or (**C**) one-way ANOVA with Kruskal Wallis post-hoc test and Dunn's multiple comparisons test (**, $P < 0.01$; ****, $P < 0.0001$). **D.** Representative skin lesion images at 72 hours following skin challenge.

D

Wildtype   Δ*hasA*   Δ*hasA* + *hasA*
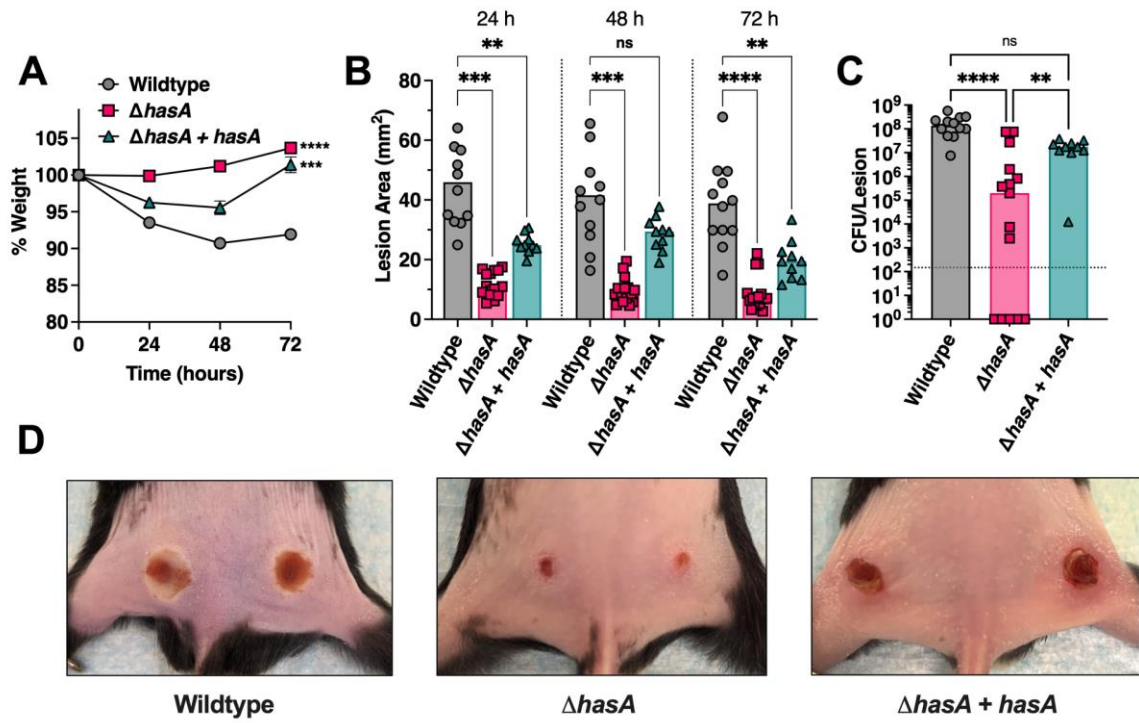
Significantly reduced bacterial CFUs were also recovered from each *ΔhasA*-infected lesion compared to wildtype-infected lesions (**Figure 4C**). Though weight loss and lesion sizes were only partially restored in *ΔhasA* + *hasA*-infected mice, plasmid-based complementation of the HA capsule was effective at restoring bacterial burden, which was comparable to wildtype bacterial recovery (**Figures 4B-D**). Overall, we demonstrate that HA capsule expression in *S. pyogenes* supports virulence during acute skin infections in B6$_{HLA}$ mice.

2.3.6   The HA capsule blocks *S. pyogenes* adherence to pharyngeal tissue

As an organism successfully avoids mucocilliary clearance, it proceeds to target and adhere to the underlying epithelial surface. Multiple studies have described the HA capsule as an important adhesin [79,80], and therefore, we sought to evaluate and compare the adherence of wildtype *S. pyogenes* with its unencapsulated mutant. Collagen type IV and fibronectin make up a significant portion of the nasopharyngeal ECM, and such, bacterial binding to these structures may contribute to streptococcal infection [97,279–281]. Collagen type IV is the primary component of the ECM basement membrane that underlays epithelial cells, and while only a minor component, fibronectin is frequently secreted to facilitate adhesion and migration of host cells [282,283]. Bacterial binding characteristics were assessed by incubating *S. pyogenes* with cell culture wells coated with either collage type IV or fibronectin for 2.5 hours, followed by washing to remove unbound bacteria and staining with crystal violet to visualize adherent bacteria. A decline in both fibronectin binding and collagen type IV binding was observed for the *ΔhasA* mutant (**Figure 5A, B**). These results demonstrate that under *in vitro* growth conditions, *S. pyogenes* can likely adhere to the nasopharyngeal ECM through interactions with both collagen type IV and fibronectin.

Bacterial adherence properties were also evaluated using primary human cell lines, including the lung epithelial cell lines A549 and the pharyngeal cell line Detroit-562 (D562). A549 cells have been shown to promote streptococcal adherence through M protein-fibronectin interactions [284], and D562 cells express similar surface molecules with non-transformed pharyngeal cells and also support induction of streptococcal superantigens and DNAses that are otherwise unexpressed by *S. pyogenes* when cultured

on its own [285,286]. Briefly, exponential phase bacteria were inoculated over confluent cell monolayers for 2 hours and adherent bacteria were enumerated after unbound bacteria were washed off and cells were lysed. There were no significant differences in adherent bacteria between wildtype or Δ*hasA S. pyogenes* using A549 cells, and a slight but significant increase in the amount of Δ*hasA* mutants that adhered to D562 cells (**Figure 5D**). Despite the ability to bind collagen type IV and fibronectin, these results conflict with reports suggesting the HA capsule contributes substantially to bacterial adhesion properties, and suggests that the HA capsule may function in part to mask adhesins on the bacterial cell wall and obstruct adherence, at least with *S. pyogenes* MGAS8232 [78,79].

2.3.7 *S. pyogenes* internalization into pharyngeal tissue is inhibited by HA capsule expression

Histological examination of murine cNTs detected MGAS8232 Δ*hasA,* but not wildtype, within epithelial cells during early stages of nasopharyngeal infection. Thus, we next aimed to characterize the invasive proficiency of *S. pyogenes* MGAS8232 and assess the loss of capsule expression on epithelial cell internalization. D562 cells were infected in a similar fashion to the described adhesion assay and following the washing of non-adherent bacteria the media was replaced and supplemented with gentamycin to target and kill extracellular bacteria. In support of the histological findings, a dramatic ~1000-fold increase in Δ*hasA* mutants were recovered from lysed D562 cells following gentamycin treatment (**Figure 5E**). Given this dramatic phenotype, we also evaluated the complemented strain (Δ*hasA +hasA*) and found that the capsule complementation completely abolished the invasion phenotype of the Δ*hasA* mutant (**Figure 5E**). These data demonstrate that the expression of the HA capsule by *S. pyogenes* MGAS8232 acts to obstruct adhesion and repress internalization into pharyngeal epithelial cells.

2.3.8 HA capsule prevents opsonophagocytosis killing by neutrophils *ex vivo*

A critical step during early colonization events following attachment to pharyngeal or skin epithelial cell surfaces include mechanisms to evade the host immune responses. *S. pyogenes* resistance to bacteriolysis strategies were investigated through the Lancefield

Figure 5. Expression of the hyaluronic acid capsule prevents internalization and adherence to pharyngeal epithelial cells.

Binding of *S. pyogenes* to wells pre-coated with 1 µg of human ECM components **(A)** fibronectin and **(B)** collagen type IV. Adhesion of *S. pyogenes* to **(C)** A549 lung epithelial and **(D)** D562 pharyngeal epithelial cells. Confluent cell monolayers were treated with *S. pyogenes* (MOI of 100) for 2 hours at 37°C + 5% CO_2. Cells were washed with PBS and lysed with Triton X-100 for enumerating remaining adherent bacteria. Bars represent the mean CFUs ± SEM ($n = 3$). Statistical differences evaluated by unpaired *t*-test **(A – D)** (**, $P < 0.01$; ****, $P < 0.0001$). **E.** Internalization of *S. pyogenes* into D562 cells. Confluent D562 cells were cultured with *S. pyogenes* (MOI of 100) for 2 hours at 37°C + 5% CO_2 followed by 1 hour in media supplemented with 100 µg mL^{-1} of gentamycin. Asterisks indicate significant differences (*, $P < 0.05$; ****, $P < 0.0001$) compared to wildtype control by one-way ANOVA with Dunn's multiple comparisons test ($n = 3$).

A Collagen Type IV

B Fibronectin Binding

C A549 Adherence

D D562 Adherence

E D562 Internalization
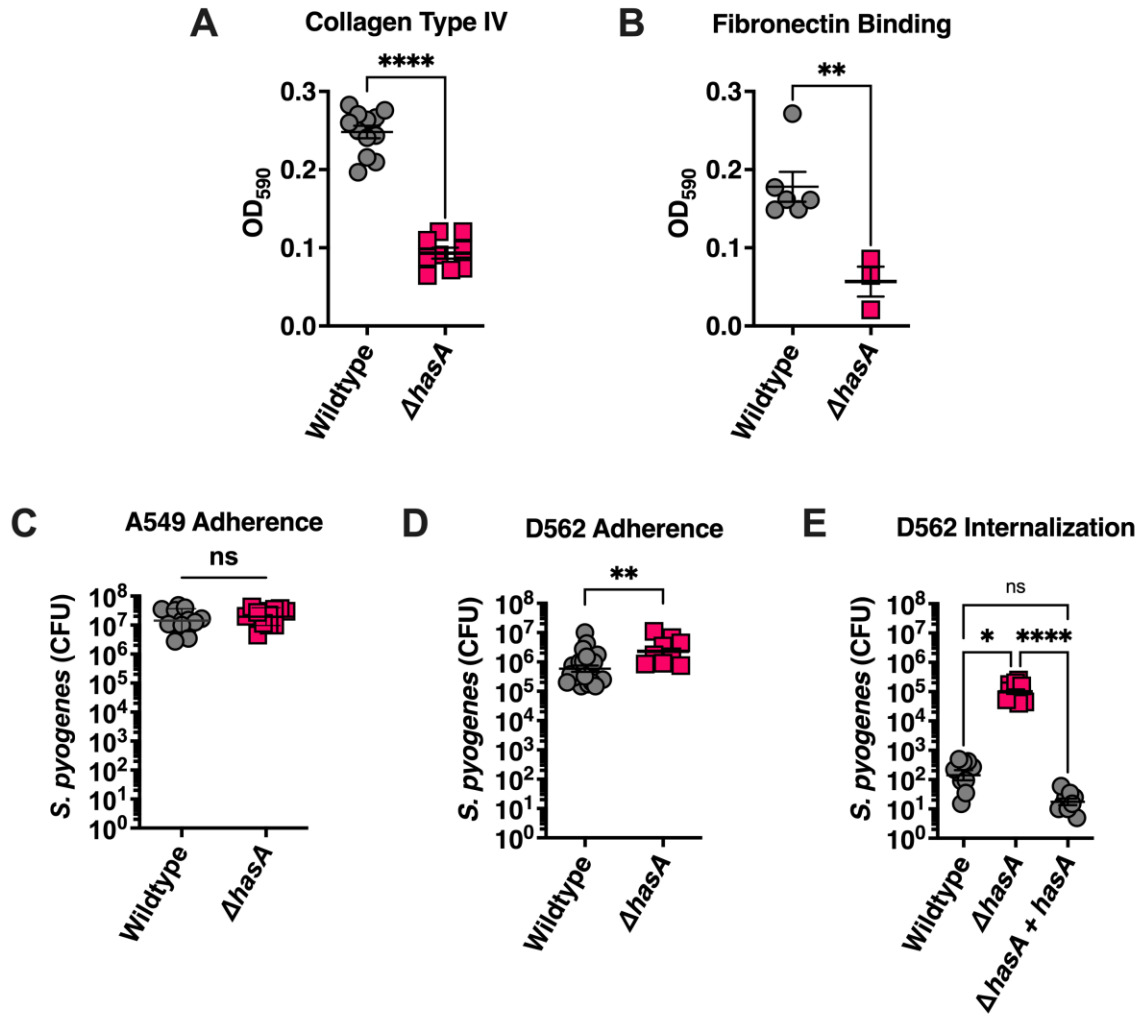
human blood bactericidal assay to explore whether capsule expression improves immune evasion by *S. pyogenes*. An inoculum of ~1000 CFU of each test strain was inoculated into fresh heparinized human blood from multiple non-immune donors for 3 hours with rotation at 37°C, with bacterial CFUs measured at 30, 60, 90, 120, and 180 minutes. Compared with wildtype MGAS8232, growth and survival in whole human blood was markedly attenuated (~3 logs) in the absence of capsule expression (**Figure 6A**). Upon earlier histological assessment of infected murine nasal turbinates, neutrophils accumulated in regions surrounding both *S. pyogenes* wildtype and *ΔhasA*, yet *ΔhasA* strain had significantly less bacterial burden by 48 hours post-infection (**Figure 2A, 2C**). Furthermore, a significant decline in cytokines and chemokines involved in recruiting, modulating, and activating neutrophils were detected at 48 hours post-infection with Δ*hasA* mutant strain (**Figure 2B; Appendix 3**). Therefore, we next sought to examine how the HA capsule resists neutrophil activity specifically. Unencapsulated bacteria were more sensitive to neutrophil-mediated killing demonstrated by a significant decline in Δ*hasA* mutants that survived in the presence of freshly isolated neutrophils (**Figure 6B**). Indeed, increased susceptibility in each condition was rescued through complementation of capsule expression in the mutant strain (**Figure 6A, 6B**). These results have outlined an important role in promoting resistance to killing by neutrophils, and thus, suggests may provide an innate immune role for HA capsule during early stages of acute infection.

2.3.9 Depletion of neutrophils in B6$_{HLA}$ mice restores *S. pyogenes* Δ*hasA* bacterial load during nasopharyngeal infection.

Preventing opsonophagocytic bacterial clearance is one of the main proposed mechanisms for the HA capsule and has been repeatedly investigated using various *in vitro* bacterial survival assays [125,259,262]. Since neutrophil influx is a major feature of our experimental nasopharyngeal model and during natural infections [7], we aimed to explore the importance of neutrophils during nasopharyngeal infection and determine whether preventing phagocyte-mediated killing is a key molecular process by which HA capsule functions in this model. For this purpose, mice were depleted of neutrophils by administering the α-Ly6G monoclonal antibody (**Figure 6C**), which effectively depletes neutrophils from the peripheral blood of mice [287]. Mice were administered rat IgG2a as

an isotype control. We examined the effect of depleting neutrophils at 24- and 48-hours after nasal challenge with MGAS8232 wildtype or Δ*hasA* strains. Following the depletion of neutrophils, no differences in the amount of MGAS8232 wildtype recovered from infected cNTs were observed in neutrophil depleted mice compared to control mice at either 24- or 48-hours post-infection (24 h, $P = 0.5802$; 48 h, $P = 0.2803$), indicating that neutrophil depletion in this model does not impact nasopharyngeal infection by *S. pyogenes* MGAS8232 (**Figure 6D**). As expected, isotype treated mice showed a reduction for the Δ*hasA* mutant at both 24 hours (*, $P < 0.05$) and 48 hours (****, $P < 0.0001$) compared to wildtype-infected control mice (**Figure 6D**). While there was no difference in recovery of the Δ*hasA* mutant between control and neutrophil depleted mice at 24 hours post-infection ($p = 0.9808$), there was a significant increase in the bacterial burden of Δ*hasA* mutants at 48 hours post-infection in neutrophil depleted mice compared to control mice ($p < 0.05$). Furthermore, no statistical differences were observed between Δ*hasA* mutants recovered from neutrophil depleted mice and control mice receiving wildtype *S. pyogenes* ($p = 0.0989$). Overall, these findings suggest neutrophil-mediated clearance mechanisms contribute substantially to the lower burden of unencapsulated *S. pyogenes* in the nasopharynx.

2.3.10 Macrophage depletion in B6$_{HLA}$ mice does not affect *S. pyogenes* Δ*hasA* bacterial load during nasopharyngeal infection.

We next wanted to determine if preventing immune evasion by the HA capsule was specific to neutrophils or if it was shared by other phagocytes. For this purpose, mice were depleted of macrophages by administering clodronate containing liposomes, or empty control liposomes, and infected intranasally with *S. pyogenes* (**Figure 7A**). Following treatment with clodronate liposomes, similar amounts of wildtype *S. pyogenes* were recovered from infected cNTs compared to control liposome-administered mice at both 24- and 48-hours (24h, $p = 0.6826$; 48h, $p = 0.8534$), indicating that macrophage depletion did not impact nasopharyngeal infection by wildtype *S. pyogenes* (**Figure 7B**). As expected, control liposome-administered mice showed a reduction of the Δ*hasA* mutant at both 24 hours ($p < 0.01$) and 48 hours ($p < 0.05$) compared to wildtype-infected control mice (**Figure 7B**). At 24-hours, there was a trend of ~1 log-fold greater recovery of Δ*hasA* CFUs in

Figure 6. The hyaluronic acid capsule is important for resisting *ex vivo* and *in vivo* neutrophil-mediated killing.

A. Whole human blood survival assay. Heparinized blood from human donors were inoculated with ~10^3 CFUs of *S. pyogenes* MGAS832 at 37°C with rotation for 3 hours. Data points represent mean CFUs ± SD at each timepoint. Statistical significance was determine using two-way ANOVA with Dunnett's multiple comparisons tests and Geisser's Greenhouse correction (***, $P < 0.001$). Horizontal line indicates limit of detection **B.** Neutrophil survival assay. Neutrophils were isolated from human blood by density centrifugation and inoculated with opsonized *S. pyogenes* at a multiplicity of infection of 10. Surviving bacteria were enumerated after 60 mins at 37°C with rotation and calculated as the difference between survival in the no neutrophil control and in the presence of neutrophils. Each data point represents *S. pyogenes* CFUs from individual donors. Data shown are the means of percent survival ± SD. Statistical analyses were performed using one-way ANOVA with Kruskal-Wallis post-hoc test and Dunn's multiple comparisons test (*, $P < 0.05$). **C.** Schematic outline for *in vivo* depletion of neutrophils by intraperitoneal injection with 250 µg of αLy6G at 24 hours prior to and 24 hours post-intranasal challenge with 10^8 CFUs of *S. pyogenes* wildtype or Δ*hasA* strains. Control mice received isotype control α-rat IgG2a. **D.** Neutrophil effects on *S. pyogenes* survival in the nasopharynx. Data points represent CFUs from the cNTs of individual mice 48 hours post-nasal infection. Horizontal bars represent the means ± SEM. The horizontal dotted line indicates limit of detection. Significance was determined by two-way ANOVA with Tukey's multiple comparisons (*, $P < 0.05$; **, $P < 0.01$; ****, $P < 0.0001$).
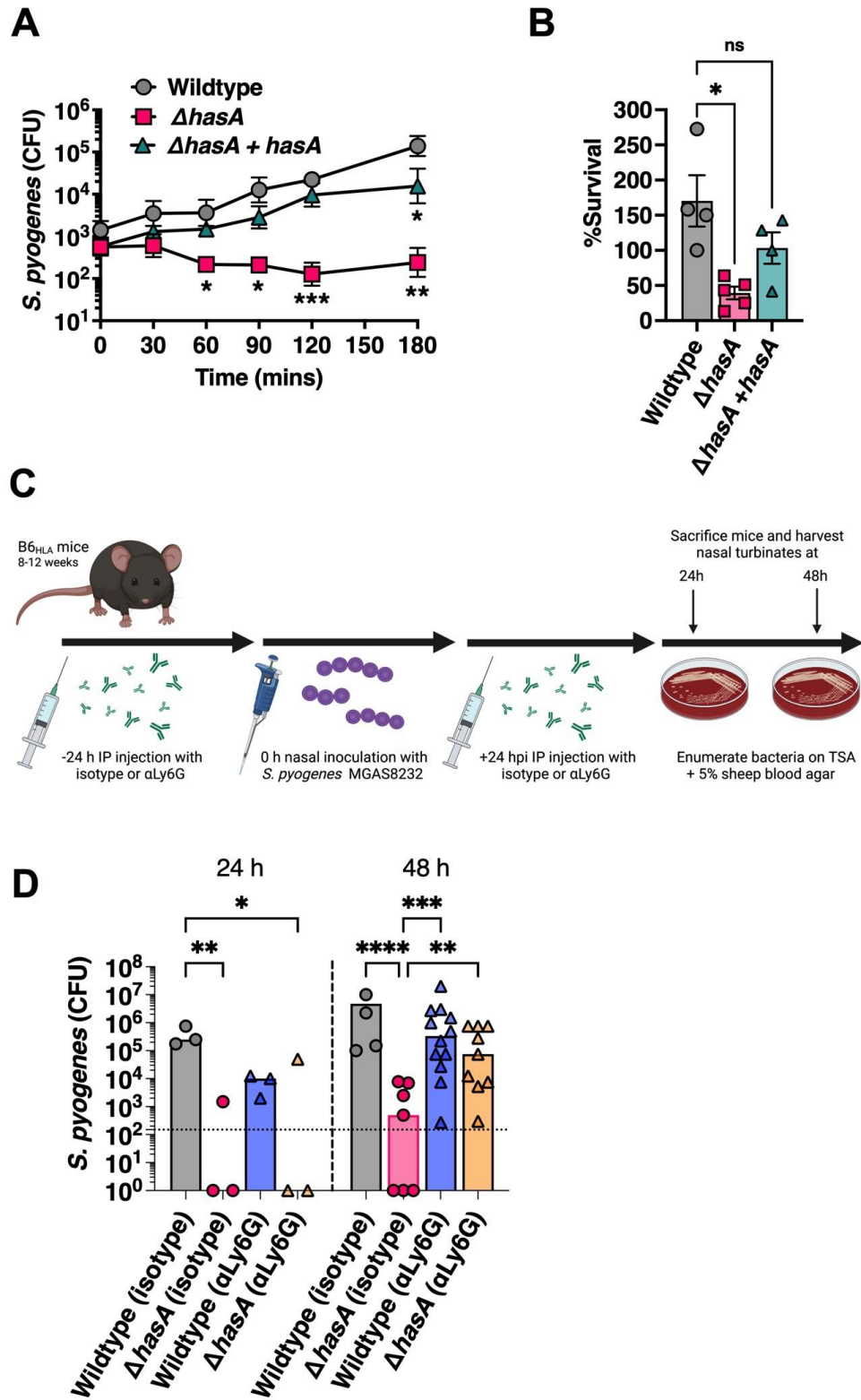
Figure 7. Depletion of macrophages in mice does not affect nasopharyngeal infection by *S. pyogenes*.

A. Schematic outlining clodronate liposome-based depletion of macrophages in B6$_{HLA}$ mice prior to of *S. pyogenes* nasopharyngeal infection with wildtype and Δ*hasA* strains (~10^8 CFUs). **B.** Bacterial burden in murine cNTs at 48 hours post-infection are shown. Each point represents *S. pyogenes* CFUs from individual mice, and the bar represents mean ± SEM. Significant differences were determined by two-way ANOVA with Tukey's multiple comparisons (*, $P < 0.05$; **, $P < 0.01$).

A

B6_HLA mice
8-12 weeks

-48 h IP injection with liposome or clodronate liposome

-4 h IP injection with liposome or clodronate liposome

0 h nasal inoculation with *S. pyogenes* MGAS8232

Sacrifice mice and harvest nasal turbinates at
24h   48h

Enumerate bacteria on TSA + 5% sheep blood agar

B

24 h   48 h

S. pyogenes (CFU)

10^8
10^7
10^6
10^5
10^4
10^3
10^2
10^1
10^0

**   *   *   **

Wildtype (liposomes)
Δ*hasA* (liposomes)
Wildtype (clodronate)
Δ*hasA* (clodronate)
Wildtype (liposomes)
Δ*hasA* (liposomes)
Wildtype (clodronate)
Δ*hasA* (clodronate)

macrophage-depleted mice; however, this was not statistically greater than Δ*hasA* control mice ($p = 0.7883$) and remained significantly lower than control wildtype-infected mice ($p < 0.05$) (**Figure 7B**). At 48-hours, Δ*hasA* mutant CFUs from macrophage-depleted mice remained significantly lower than control wildtype-infected mice ($p < 0.01$). Overall, macrophage depletion by clodronate liposomes did not rescue the low infection phenotype by the Δ*hasA* strain at either 24- or 48-hours and did not significantly influence infection by wildtype *S. pyogenes*. These results suggest that protection against phagocytosis by macrophages is not a key mechanism by which the HA capsule functions during experimental nasopharyngeal infection.

2.3.11 Depletion of neutrophils in B6_{HLA} mice recovers *S. pyogenes* Δ*hasA* bacterial load during acute skin challenge

To examine whether a lack of neutrophils would similarly enhance infection by unencapsulated *S. pyogenes* in the skin, B6$_{HLA}$ mice were depleted of neutrophils as described and challenged with intradermal injections of 2.5×10^7 CFUs wildtype or Δ*hasA* mutant *S. pyogenes* MGAS8232. Following neutrophil depletion, the weights of mice within wildtype or Δ*hasA* mutant infection groups were not significantly different; however, mice exposed to Δ*hasA* showed significantly less weight loss throughout the infection compared to wildtype-infected mice (**Figure 8A**). Irrespective of depletion status, mice infected with the *ΔhasA* mutant revealed considerably smaller lesions and less inflamed injection sites over the infection period compared to wildtype-infected mice (**Figure 8B and 8D**). Neutrophil depletion did not impact lesion sizes, or the amount of wildtype *S. pyogenes* CFUs retrieved from each infected lesion. As expected, control mice the isotype antibody showed a significant reduction of Δ*hasA* mutants within lesions at 72 hours ($p < 0.001$) compared to wildtype-infected control mice (**Figure 8C**). In contrast, neutrophil depleted mice displayed a sharp increase in Δ*hasA* CFUs recovered from each lesion compared to control mice that received infections with the Δ*hasA* mutant, despite presenting with similar lesion sizes (**Figure 8C and 8D**). Overall, these data demonstrate that the *S. pyogenes* HA capsule is important for resisting bacterial killing by neutrophils during experimental skin infection.

Figure 8. The HA capsule is important for resisting neutrophil-mediated killing in the skin

B6$_{HLA}$ mice were administered ~2.5 x 10^7 CFUs of *S. pyogenes* MGAS8232 wildtype, Δ*hasA,* or Δ*hasA* +*hasA* intradermally in each hind flank. Mice received αLy6G or rat IgG2a isotype control antibodies intraperitoneally 24 hours preceding and 24 hours following skin challenge. **A.** Weights of B6$_{HLA}$ mice at 24-, 48-, and 72-hours following *S. pyogenes* skin infection. Data is represented as a percentage of day 0 weight. Data points represent the mean weights ± SD. **B.** Skin lesion areas of mice following at 24-, 48-, and 72-hours after skin challenge. Data points represent the mean lesion areas ± SD. **C.** Data points represent CFUs from individually infected skin abscesses at 72 hours normalized to the weight of the excised skin tissue from each mouse. Bars represent mean ± SEM. The horizontal dotted line indicates limit of detection. Significance was determined by (**A - B**) two-way ANOVA with Dunnett's multiple comparisons test and Geisser's Greenhouse correction and (*, $P < 0.05$, **, $P < 0.01$, ***, $P < 0.001$;), or (**C**) one-way ANOVA with Tukey's multiple comparisons test (***, $P < 0.001$; (****, $P < 0.0001$). **D.** Representative skin lesion images from B6$_{HLA}$ mice 72 hours following skin challenge.

A

B

C

D

| Wildtype (isotype) | ΔhasA (isotype) | Wildtype (αLy6G) | ΔhasA (αLy6G) |
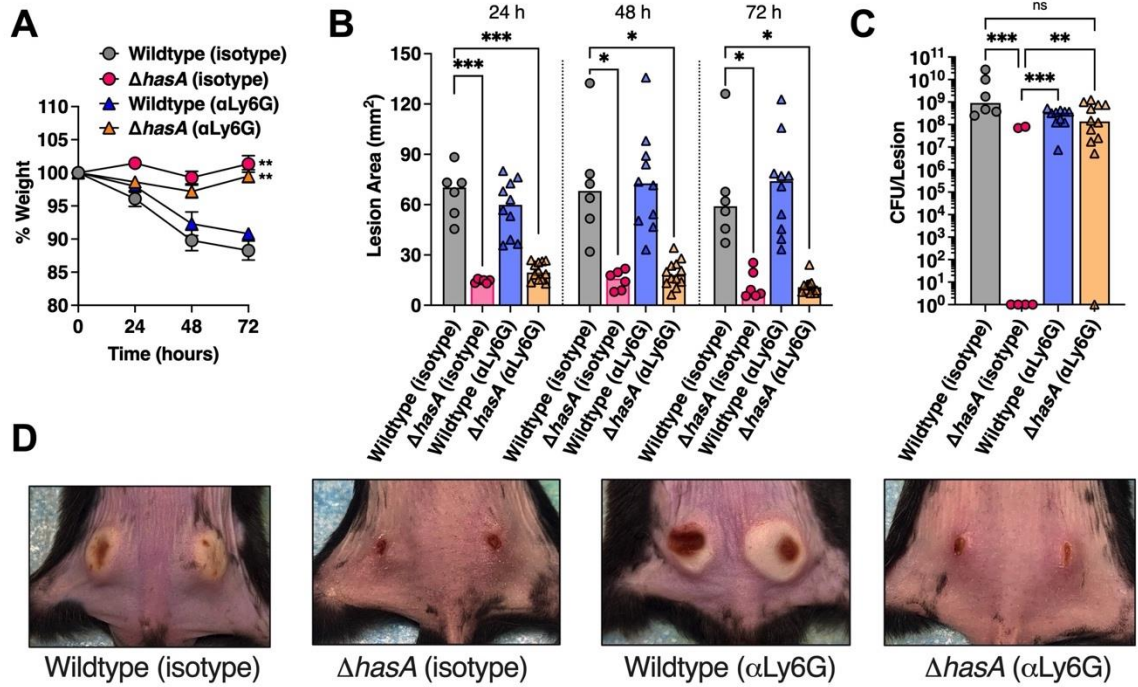
2.4   Discussion

S. pyogenes is a globally prominent bacterial pathogen capable of colonizing the upper respiratory tracts and skin of human hosts where it can cause a wide spectrum of diseases. This human-restricted bacteria maintains an arsenal of virulence factors to both offensively and defensively sense variations in its external environmental and combat diverse selective pressures as it adapts to various tissue sites within a host. Despite representing a minority of cases, previous studies on *S. pyogenes* pathogenesis have largely focused on host-pathogen interactions during invasive infections, where failure to control infection can result in severe morbidity and mortality. As it is widely recognized that superficial infections of the throat and skin, such as pharyngitis and impetigo, often precede these extreme but rare invasive manifestations [264], findings from these studies are not necessarily reflective of mechanisms elicited during natural routes of infection and may inadvertently divert attention onto the coincidental effects of these virulence factors during extreme cases. Therefore, bacterial molecular mechanisms and host immune responses during acute infection stages within these limited biological niches are comparatively less well understood.

Previous work by our team paved extraordinary breakthroughs in developing an experimental nasal infection model in mice that reflects the human-specificity of *S. pyogenes*. This work demonstrated that host sensitivity to superantigen-mediated Vβ-specific T cell activation induces an excessive inflammatory signature of the nasopharyngeal environment that promotes infection [156,157], and thus, a sensitive model that retains human-specific tropism with the use of transgenic mice expressing human MHC-II molecules is critical for accurate understanding the course of pathogenesis and streptococcal-host interactions. Additionally, IL-1β-mediated inflammation mediated by the SpeB protease can promote *S. pyogenes* colonization of the nasopharynx [287]. Nevertheless, additional virulence factors may similarly contribute to infection in this model. Once bacteria out-compete resident microflora and attach to the mucosal epithelium, it must rapidly replicate while successfully avoiding the host's attempt at immune clearance. Consequently, *S. pyogenes* must remodel its external environment and balance superantigen- and SpeB-mediated inflammation while tempering host immune

clearance mechanisms at various stages of infection, each of which may be influenced by strain-specific differences and tissue-specific cues that can affect the outcome of infection.

In the current study, we provide evidence that expression of the HA capsule promoted *S. pyogenes* virulence in murine models of experimental nasal and skin infections. In absence of capsule expression, a ~10,000-fold reduction in mean bacterial CFUs were uncovered within infected nasal turbinates compared to wildtype-infected mice (**Figure 2A**). This reduction was rescued through trans-complementation of the *hasA* gene, which showed similar bacterial burden as wildtype infections (**Figure 2A**). Furthermore, we also demonstrated a loss of virulence using an acute skin infection model. Mice injected intradermally with the Δ*hasA* mutant presented no weight loss, smaller lesions, and significantly less bacterial CFUs within infected skin lesions (**Figure 4**). The Δ*hasA* +*hasA* capsule complement strain rescued the number of Δ*hasA* mutants recovered from the skin, however, weight loss and lesion sizes were not fully re-established with this strain. The moderate restoration of weight loss and lesion sizes may be explained by the incomplete complementation of the *hasA* gene expressed *in trans* using the pDC*erm* plasmid, as erythromycin was not used topically to maintain plasmid expression and replication over the 72-hour infection period. This is supported by the observation of some capsule deficient reversion colonies on plated skin homogenates (data not shown). Therefore, an alternative method to plasmid complementation for the *hasA* gene should be fully explored to validate the necessity of the HA capsule in establishing *S. pyogenes* skin infection. Nevertheless, whole genome sequencing of the wildtype and Δ*hasA* strains revealed >99% identity at the nucleotide level between the strains, with just two SNPs identified in the Δ*hasA* mutant genome within the *pstI* gene of the phosphotransferase system (**Table 4**). In a mouse model of soft tissue infection, a *S. pyogenes* M1T1 Δ*pstI* mutant displayed significantly larger and more severe ulcerative lesions than wildtype-infected mice [288]. While we did not investigate the consequence of these identified SNPs in the Δ*hasA* mutant, a functional PTS has been shown to limit pathogenesis of *S. pyogenes* during skin infections and, thus, would not account for the reduced virulence of the Δ*hasA* mutant in this model.

The findings presented here illustrate an important role of the HA capsule during the pathogenesis of acute infections by *S. pyogenes*; however, this may appear inconsistent with some previous investigations for other encapsulated bacterial pathogens. For example, reduced or eliminated capsule production appears to have advantages for the invasive potential or persistence at mucosal surfaces across multiple bacterial species, including *Streptococcus agalactiae* (Group B *Streptococcus*) [289]*, Streptococcus pneumoniae* [290]*, Neisseria meningitidis* [291,292], and *Haemophilus influenzae* [293]. *S. pneumoniae*, for example, varies capsule expression from its initial abundance to prevent mucus-mediated clearance [294], yet it is subsequently downregulated to expose underlying adherence molecules [295] and to promote biofilm formation [296,297]. Furthermore, our findings also contradict some previous reports where acapsular *S. pyogenes* infected the pharynx as effectively as the parental strain in a baboon model of pharyngeal infection [84], and that frameshift inactivating mutations in the *hasA* or *hasB* genes that deplete capsule production contribute to persistence during asymptomatic carriage [84,263]. However, contradicting evidence for the role of persistence with capsule expression has been previously reported [83]. The use of different strains, and different infections models, have likely have contributed to these disparate findings, and since not all *S. pyogenes* strains encode the *has* operon [298], it is clear that the HA capsule is not an essential virulence factor for all *S. pyogenes* isolates. Nevertheless, our work is entirely consistent with prior work demonstrating an important selective advantage of the HA capsule for survival within the nasopharyngeal environment [259–261].

Inflammation in the nasopharynx has been determined to be broadly beneficial for *S. pyogenes* infection and may support several pathogenic benefits, including disrupting membrane barrier function, promoting dissemination, enhancing nutrient acquisition, and inhibiting competing microbes [299]. Prominent inflammatory T cell activation by SpeA superantigen [157,300] and IL-1β-mediated inflammation by SpeB protease [287] can promote *S. pyogenes* colonization of the nasopharynx. Analogous to previous reports, a consistent inflammatory signature driven by increased concentrations of IL-1β and IL-6 persisted during wildtype and Δ*hasA* +*hasA* infections (**Figure 2B; Appendix 5**). Increased levels of TNF-α and IL-17 were also detected in mice inoculated with wildtype

S. pyogenes but were not statistically significant (**Appendix 5**). Infection with unencapsulated *S. pyogenes*, however, induced a cytokine and chemokine profile that mimicked uninfected mice at 48 hours. Streptococcal nasal infections have previously been shown to induce T_h17 cellular expansion, marked by increased IL-6, TGF-β, TNF-α and IL-1β responses [287,301–303]. Although TGF-β was not assessed in this study, increased IL-6, TNF-α and IL-1β concentrations indirectly suggest that T_h17 responses are induced by wildtype infections and are absent in mice treated with the unencapsulated Δ*hasA* mutant. Interestingly, concentrations of KC, IP-10, MCP-1, MIP-1α, MIG, and G-CSF were reduced in Δ*hasA*-infected cNTs compared to wildtype and Δ*hasA* +*hasA* infections at 48 hours post-infection (**Appendix 5**), yet histological examination revealed prominent neutrophil signals at 24 hours following infection with both wildtype and Δ*hasA* strains (**Figure 2C**). These results indicate that deletion of the HA capsule does not alter neutrophil recruitment to sites of bacterial infection, but rather permits the rapid clearance of unencapsulated bacteria, and thus, neutrophil-modulating cytokines are reduced by 48 hours as Δ*hasA* mutants are less abundant during later stages of infection.

During infection of the nasopharynx, the epithelium and mucus layer form the first defensive barrier against invading pathogens where adherence to epithelial cells or exposed ECM may be exploited to prevent mucosal-mediated removal. In this study, we report that unencapsulated *S. pyogenes* display reduced binding to collagen type IV and fibronectin ECM components, yet pharyngeal epithelial cell adhesion and internalization were significantly greater compared to the encapsulated wildtype strain (**Figure 5A-B, D**). These results present an apparent paradox: unencapsulated *S. pyogenes* mutants exhibit greater adherence properties and become internalized with higher efficiency than encapsulated *S. pyogenes*, however, encapsulation is evidently important during experimental models of systemic and acute infections. While seemingly puzzling, fluctuating levels of HA capsule expression may differentially contribute to adherence and consequently subsequent biofilm formation. During early biofilm formation on keratinocytes, *hasA* transcription levels are downregulated [304] and enzymatic removal of the capsule improves static biofilm formation by many *S. pyogenes* isolates [305], suggesting that capsule expression masks biofilm-associated adhesins. Contrarily, unencapsulated *S. pyogenes* HSC5 are unable to

mature fully into a three-dimensional biofilm structure in a flow cell [306], suggesting that a robust matrix of extracellular polysaccharides may be beneficial for later biofilm formation. Together, a model where the capsule conceals important adhesins that promote binding to epithelial cells is supported, however, mechanisms that disrupt host cellular barriers to expose underlying ECM components may support the binding of encapsulated *S. pyogenes* to the ECM and resist mucosal clearance. *S. pyogenes* may upregulate secretion of the protease SpeB, which can directly degrade components of intercellular junctions [307,308], or streptolysin S, which may activate the host protein calpain and disrupt cell-to-cell linkages allowing *S. pyogenes* to travel across the epithelial barrier and gain access to ECM proteins [309]. Interestingly, scanning electron microscopy has shown that binding interactions between HA and host CD44 on epithelial cells may similarly facilitate extracellular penetration across the epithelium. As HA binds CD44, localized membrane projections (lamellipodia) prompt membrane destabilization of keratinocytes and rupture intercellular bridges with neighbouring cells, which can permit penetration and translocation of extracellular *S. pyogenes* through the epithelium [81]. The authors also observed that unencapsulated mutants may bind cell surfaces, not localized with CD44, but fail to translocate efficiently and remain trapped within membrane-bound vacuoles in the superficial epidermis of keratinocytes. Gaining access to intracellular compartments can protect from complement deposition, specific antibodies, and phagocytic leukocytes; however, unencapsulated *S. pyogenes* are not more virulent in our experimental infection models, are rapidly cleared from the nasal turbinates and skin lesions, and do not spread to other organs (**Figure 3**). Therefore, entry into cells is unlikely a virulent mechanism, but rather a failure of *S. pyogenes* to avoid ingestion by host cells, where encapsulation helps resist internalization and enhances the capacity to invade tissues by an extracellular route to promote *S. pyogenes* infection. While future work is needed to clarify adherence properties of encapsulated and unencapsulated *S. pyogenes,* our work supports that any capsule-mediated adherent properties are less important compared to the capsule's potent protective effect from ingestion and killing by host phagocytes.

Upon infection with *S. pyogenes* the immune system launches a complex innate response that largely depends on the recruitment and activity of neutrophils, macrophages, and

dendritic cells [108,310–313]. In this study we successfully demonstrated that the HA capsule is a key structure that promotes resistance to neutrophil mediated killing *ex vivo* (**Figure 6A, 6B**). These findings, accompanied by the marked infiltration of neutrophils during nasopharyngeal infection (**Figure 2C**), led us to examine interactions between *S. pyogenes* and neutrophils during acute infections. Neutrophils are the most abundant among leukocytes involved in innate responses, acting as both professional detectors that release inflammatory alarms to invading bacteria as well as direct killers via phagocytosis, degranulation, and the formation of NETs. Given the key role of neutrophils in orchestrating host-protective immune responses, it is not surprising that *S. pyogenes* has evolved an impressive number of mechanisms to subvert their recruitment and activity during infection (reviewed in Section 1.8.2), yet they appear to offer no compensation for the loss of activity of the HA capsule during infection. Furthermore, while neutrophil influx during severe infections is protective against *S. pyogenes* [108], we show that depleting neutrophils or macrophages did not affect wildtype MGAS8232 acute infections. These results are in stark contrast to findings where neutrophils are key for pathogenesis and neutrophil ablation by α-Ly6G administration reduces *S. pyogenes* infection of the nasopharynx [287,314], however, conventional C57BL/6 mice were used in these studies with superantigen-mediated inflammation absent. In the presence of a superantigen-driven inflammatory response capable of promoting infection [156], our analysis indicates that neutrophils are not essential for *S. pyogenes* MGAS8232 to establish nasopharyngeal or skin infections. Instead, expression of the HA capsule offered a clear survival advantage that promotes a strong resistance to bacterial clearance by neutrophils. Unencapsulated bacteria are no longer inhibited following the depletion of neutrophils by α-Ly6G administration, which recovered the reduced burden by Δ*hasA* in both nasopharynx and skin (**Figure 6D, 8C**). Despite having a major role in the identification and immune response to pathogens, the function of DCs in response to capsule-mediated protection were not investigated in this study due to the significant decrease of DCs in the cNTs of wildtype *S. pyogenes*-treated mice shown previously [156,315]. Since all major innate immune cells are thought to participate in host protection against *S. pyogenes,* more research is needed to define specific roles, to examine crosstalk, and to address redundancy in responses between individual cell types.

A major question that has yet to be answered is what mechanism of action the HA capsule employs to resist neutrophil-mediated clearing. Since the HA capsule is identical to HA on mammalian tissues, *S. pyogenes* may be avoiding bacterial detection through molecular mimicry, which dampens neutrophil responses to avoid reactivity. Evidence from group B *Streptococcus* revealed that the sialylated capsular polysaccharide binds to Siglec-9 lectin on neutrophils to subvert innate immune detection and evade neutrophil-based killing [316], and thus, future work should determine whether the HA capsule on *S. pyogenes* similarly engages a host inhibitory receptor. Interestingly, both encapsulated and unencapsulated type 18 *S. pyogenes* are equally opsonized by C3 in either plasma or serum [125], suggesting that the HA capsule does not inhibit complement activation or deposition of complement fragments on the bacterial cell wall. Since opsonization does not necessarily lead to phagocytic ingestion, the HA capsule may serve as a physical barrier that interferes with leukocyte access to opsonic complement proteins deposited on the bacterial surface [125]. Similarly, encapsulated *Staphylococcus aureus* resist phagocytosis despite the deposition of C3 on its surface [317]. More recently, the HA capsule has been shown to promote bacterial survival within NETs by resisting a major component and antimicrobial effector, cathelicidin antimicrobial peptide LL-37 [145]. Trapping host antimicrobial peptides before they reach the bacterial cell wall is observed with other bacterial polysaccharide capsules, including *Klebsiella pneumoniae*, *Streptococcus pneumoniae*, and *Pseudomonas aeruginosa,* through the trapping of neutrophil alpha-defensin 1 (HNP-1), beta-defensin 1, and lactoferrin [318,319]. Further work that investigates HA capsule expression and *S. pyogenes* survival within NETs *in vivo* is needed.

Overall, our findings support the hypothesis that the HA capsule is a critical factor at early stages of nasopharyngeal and skin infection. This work provides valuable insight into the host-pathogen interaction of *S. pyogenes,* however, limitations in this study are considered. Different strains of *S. pyogenes* harbour variations in global virulence factor expression, and consequently, express varying amounts of HA capsule. It is likely that distinct strategies to prevent phagocytic ingestion and killing are exploited among individual strains. For example, mutations that produce a truncated RocA (regulator of Cov) protein have amplified expression of the *has* operon through transcriptional activation of the

repressor *covR*, and have been identified in *S. pyogenes* types *emm*18 and *emm*3 [83,267]. Thus, no single strain of *S. pyogenes* should be considered representative of the population as a whole and future studies using additional encapsulated strains are recommended to draw general conclusions on the mechanisms utilized by the HA capsule. The disadvantage that only a limited number of strains are capable of colonizing the mouse nasopharynx due to intrinsic differences in expressed virulence factors exists, and many may become distributed in secondary organs. However, *S. pyogenes* MGAS8232 utilized in this study proficiently infects the nasopharynx and remains localized to the infected tissue site [156]. Furthermore, the skin infection model utilized in this study may be considered distinct from typical superficial *S. pyogenes* skin exposures. Intradermal injections forces *S. pyogenes* to bypass the epidermal skin layers rather than allowing the skin barrier to innately become damaged and broken from exposure to allow bacterial entry. Therefore, the role of the HA capsule in permeating the epithelial skin barrier should be further explored. To conclude, the results presented provide evidence that HA capsule expression by *S. pyogenes* MGAS8232 promotes a strong resistance to killing by neutrophils during acute infection models, and thus, defining strategies by which neutrophils can counteract HA capsule resistance is warranted to combat this leading bacterial pathogen.

Chapter 3: Parenteral vaccination of M proteins do not protect against *S. pyogenes* acute nasopharyngeal or skin infections in HLA-transgenic mice

3.1   Introduction

Streptococcus pyogenes, also recognized as the Lancefield Group A *Streptococcus,* is a human-adapted opportunistic pathogen that causes a substantial burden of acute and chronic diseases worldwide. Although *S. pyogenes* subsists primarily in an asymptomatic carrier state within the upper respiratory tract or on the skin [19,22,29], over 600 million cases of pharyngitis, and 160 million cases of impetigo are reported each year [10]. Importantly, *S. pyogenes* is capable of breaching epithelial barriers and invading host tissue, which can result in severe illnesses such as cellulitis, scarlet fever, puerperal sepsis, bacteremia, pneumonia, streptococcal toxic shock syndrome (STSS), and necrotizing fasciitis [4,123]. Serious postinfectious immune-mediated disorders, including acute poststreptococcal glomerulonephritis (APSGN), acute rheumatic fever (ARF), and rheumatic heart disease (RHD) may also develop as severe consequences to repeated acute infections [8,50,123,320]. Conservative estimates indicate that there are more than 33.4 million prevalent cases of RHD globally, with more than 9.6 million Disability-Adjusted Life Years (DALYs) lost, representing the sum of years of life lost due to premature mortality and years lived with disability from RHD [13]. Together, these diseases account for over half a million deaths per year, serving as a leading cause of infection-related mortality worldwide [10,11].

It is widely accepted that most severe illnesses develop from benign pharyngeal or skin infections, and therefore, preventing the colonization of these biological niches remains a major goal to prevent all types of disease. While this bacterium remains uniformly susceptible to current gold standard treatment strategies, including widespread use of penicillin and other β-lactam antibiotics, treatment failure and resistance to macrolides, clindamycin, and lincosamide are becoming an increasing problem worldwide [321–329]. Efforts to develop a *S. pyogenes* vaccine have been ongoing for almost 100 years [176] yet there is no licensed vaccine available to prevent the vast severity of infections and complications caused by *S. pyogenes*. Vaccine development has faced many challenges including the lack of suitable and relevant infection models, complex antigenic variability, inadequate epidemiological surveillance, and safety concerns based on the possibility a

vaccine may elicit autoimmune responses, and thus, *S. pyogenes* vaccines are considered "impeded vaccines."

Vaccine candidates can be broadly divided into M protein-based and non-M protein-based approaches. Many non-M protein potential candidates, including C5a peptidase [231,232,246], streptococcal carbohydrate [225,226], fibronectin binding proteins [234,236], SpeB cysteine protease [220,242], serine protease [244,246], sortase A [243,246], exotoxins [156,157,221,222,242], and pili [62,330], have demonstrated protective effects in animal infection models, yet none have progressed to clinical trials. To date, the most advanced candidates focus on enhancing immunity against the cell wall-anchored M protein. M proteins are alpha-helical coiled coil immunodominant surface antigens consisting of highly variable N-terminal domains used for epidemiologic molecular typing (*emm*-typing). M proteins are "hallmark" *S. pyogenes* virulent determinants that inhibit amplification of complement-mediated opsonization and uptake by professional phagocytes by preventing the deposition of complement proteins on its surface and facilitating their degradation [111,112,331,113–118,124,161]. M proteins have also been recognized to promote adherence to host epithelial cells [75,89,91,92,94,332,333]. Furthermore, bactericidal M protein antibodies can persist for years after streptococcal infection [56], and are thought to provide serotype-specific immunity against future infections. From these findings, M protein immunity became an attractive target for vaccine researchers. In the 1970s, human volunteers immunized with purified M protein preparations were protected from challenge infections [177,178], indicating that type-specific immunity can prevent symptomatic streptococcal infections. Since then, significant progress has been made in the design and clinical development of multivalent M protein vaccines containing highly purified fused recombinant N-terminal peptide regions from multiple streptococcal *emm*-types, and several have progressed to early-stage human clinical trials [182,189,190]. Clinical trials determined that hexavalent [182], 26-valent (StreptAvax) [188], and 30-valent [189] vaccines were safe and immunogenic, and generated bactericidal antibodies against nearly all vaccine-containing serotypes. StreptAvax to date is the most advanced *S. pyogenes* vaccine candidate with the successful completion of a Phase II clinical trial [190]. Although M proteins exhibit high

genetic diversity, vaccine-encoded M peptides produce antibodies that recognize a number of non-vaccine containing serotypes [187,188,192], suggesting that immune responses can offer extended coverage to *emm*-types found in low-income settings where diversity of circulating *emm*-types is high and disease is endemic [191].

Despite continuing efforts that target the surface M protein as a vaccine candidate, robust data illustrating clear protection with serotype-specific immunity is lacking. Immunoassays that quantitate serological responses, and functional opsonophagocytosis assays that measure bactericidal activity are widely used to assess serotype-specific antibody responses *in vitro,* however, protection against *S. pyogenes* colonization and acute infections have not been established. To our knowledge, serotype-specific immune responses have only shown to protect mice from systemic infection and death using intraperitoneal challenge models [334,335]. Furthermore, recent epidemiological data has suggested that prior exposure with the same M protein serotype does not influence future infection [336]. Together, we consider that M protein immunizations followed by relevant acute experimental infection models are critical to support, or possibly refute, the focus of serotype-specific immunity. Since M protein function has primarily been studied in the context of severe and invasive disease models, the biological role of the streptococcal M protein during acute infections also remains largely unassessed. In the present study, we aim to evaluate the efficacy of immunity induced by various monovalent M protein preparations in mice and determine whether M protein immunizations prevent nasopharyngeal and skin challenges by *S. pyogenes*. The strains used in this study are clinical isolates from patients with diverse streptococcal illnesses, including toxic shock syndrome (MGAS315), scarlet fever (HKU16), acute rheumatic fever (MGAS8232), and invasive disease (NGAS979). We also extended our studies to characterize the necessity of M18 protein expression by *S. pyogenes* MGAS8232 during these non-invasive infection models. Evaluation of host responses to various M proteins in the context of acute infections will provide valuable insight that will guide future vaccine development strategies against *S. pyogenes.*

3.2   Materials and Methods

3.2.1   Bacteria mutant production

A complete list of bacterial strains used in this chapter is found in **Table 5.** Details for bacterial grown conditions and construction of deletion mutants are outlined in Section 2.2. All *S. pyogenes* strains were grown in THY under static conditions at 37°C. In the current work, in-frame deletion of the gene encoding the M18 protein was produced in *S. pyogenes* MGAS8232. Primers were designed to amplify the upstream and downstream regions of *emm18* and replace the *emm18* sequence in *S. pyogenes* MGAS8232 with the deletion construct using the Gram-positive *E. coli* shuttle vector, pG$^+$host5. Primers for *emm18* mutant production are found in **Table 6.**

3.2.2   Protein production

3.2.2.1   Bacterial protein expression

Details on DNA manipulations are described in Section 2.2.2. A complete list of plasmids and primers used in this study are described in **Table 5** and **Table 6** respectively. Briefly, genes encoding M3, M12, M18, and M74 proteins were PCR amplified and inserted into the pET-28a(+) vector with an engineered tobacco etch virus (TEV) protease cleavage site and a His6-tag. Each M protein sequence was modified to lack the predicted signal peptide (using SignalP 5.0 server) and 'LPXTG' cell wall sorting sequence. *E. coli* BL21 (DE3) containing appropriate pET-28a(+) expression constructs (**Table 5**) were grown overnight in LB broth supplemented with 50 µg mL^{-1} kanamycin. Overnight cultures were inoculated 1:100 into 1L LB broth containing 50 µg mL^{-1} kanamycin and grown for 3 hours aerobically at 37°C. Bacteria were then induced with 200 µM isopropyl β-D-1-thiogalactopyranoside (IPTG) and grown aerobically overnight at room temperature. Overnight induced cultures were pelleted at 3,500 × *g* for 10 minutes and resuspended in 10 mL of 20 mM Tris base, 200 mM sodium chloride pH 7.5 buffer containing 10 µL DNaseI (Sigma-Aldrich) and 50 µL of 10 mg mL^{-1} lysozyme (Thermo Fisher Scientific Inc.). Bacteria were left shaking on ice for 30 minutes, followed by 3 rounds of sonication with 50 pulses each, 40% duty cycle and output 4 on a Branson Sonifier (Emerson

Table 5. Bacterial strains and plasmids used in Chapter 3.

Strain/Plasmid	Description	Source
Streptococcus pyogenes		
MGAS315	M3 serotype, isolated from a patient with streptococcal toxic shock syndrome in Texas, United States in late 1980's (NCBI RefSeq: NC_004070)	[337]
HKU16	M12 serotype, isolated from a patient with scarlet fever in the Hong Kong 2011 outbreak (NCBI RefSeq NZ_AFRY01000001.1)	[338]
MGAS8232	M18 serotype isolated from a patient with acute rheumatic fever (GenBank accession: NC_003485.1)	[269]
MGAS8232 Δ*emm18*	*emm18* deletion mutant derived from MGAS8232	This study
NGAS979	M74 serotype, isolated from a patient with invasive disease in Ontario, Canada in 2016 (NCBI RefSeq: NZ_CP028140.1)	[339]
Escherichia coli		
XL1-Blue	General cloning strain	Stratagene
BL21 (DE3)	Protein Expression Strain	Novagene
M protein expression plasmid constructs		
pET-28a(+)::TEV::M3	M3 protein inserted into the *Nco*I and *Bam*HI sites of pET-28a(+)::TEV; Kan^r	This study
pET-28a(+)::TEV::M12	M12 protein inserted into the *Nco*I and *Bam*HI sites of pET-28a(+)::TEV; Kan^r	This study
pET-28a(+)::TEV::M18	M18 protein inserted into the *Nco*I and *Bam*HI sites of pET-28a(+)::TEV; Kan^r	This study
pET-28a(+)::TEV::M74	M74 protein inserted into the *Nco*I and *Bam*HI sites of pET-28a(+)::TEV; Kan^r	This study
Plasmids for cloning		
pET-28a(+)	Protein expression vector; N-terminal His-Tag®/thrombin cut site; Kan^r	Novagene
pET-28a(+)::TEV	pET-28a(+) plasmid with modified TEV protease cleavage site; Kan^r	McCormick lab
pG$^+$host5	Temperature-sensitive Gram-positive/*E. coli* shuttle vector; Erm^r	Appligene [270]
pG$^+$host5::Δ*emm18*	pG$^+$host5 with *emm18* flanking regions inserted	This study

Abbreviations: Erm^r, erythromycin resistance; *Cat* - chloramphenicol acetyltransferase; Kan^r, kanamycin resistance; TEV, tobacco etch virus protease cleavage site

Table 6. Primers used in Chapter 3.

Plasmid	Primer Sequence (5′→ 3′)[a]
Primers for M protein expression constructs	
M3 Forward-*Nco*I	GGG<u>CCATGG</u>GCAGCAGCCATCATCATCATCATCACAGCAGCGGCGA AAACTTGTATTTCCAAGGCGATGCTAGGAGTGTTAATGGAGAG
M3 Reverse-*Bam*HI	GGG<u>GGATCC</u> TTACTGTCTCTTAGTTTCCTTCATTGG
M12 Forward-*Nco*I	GGG<u>CCATGG</u>GCAGCAGCCATCATCATCATCATCACAGCAGCGGCGA AAACTTGTATTTCCAAGGCGATCATAGTGATTTAGTCGCAGAA
M12 Reverse-*Bam*HI	GGG<u>GGATCC</u> TTACTGTCTCTTAGTTTCCTTCATTGG
M18-Forward-*NcoI*	GGG<u>CCATGG</u>GCAGCAGCCATCATCATCATCATCACAGCAGCGGCGA AAACTTGTATTTCCAAGGCGCACCTCTTACTCGAGCTACAGCA
M18-Reverse-*Bam*HI	GGG<u>GGATCC</u> TTACTGTCTCTTAGTTTCCTTCATTGG
M74 Forward-*Nco*I	GGG<u>CCATGG</u>GCAGCAGCCATCATCATCATCATCACAGCAGCGGCGA AAACTTGTATTTCCAAGGCTTCACGGTTACTAGGTCTATGACA
M74 Reverse-*Bam*HI	GGG<u>GGATCC</u> TTACTGTCTCTTAGTTTCCTTCATTGG
Primers for M protein gene chromosomal deletion constructs	
emm18 up *Bam*HI For	CCC<u>GGATCC</u> TTGATGAGTTAGATTGTTTGACAATTGATCTAGTAGAG
emm18 up *Pst*I Rev	CCC<u>CTGCAG</u> TCTATTTGCATCTTTTCTAACCATTATTTGCTCC
emm18 down *Pst*I For	CCC<u>CTGCAG</u> CTAAAACGCAAAGAAGAAAACTAAGCCTTTAGAA
emm18 down *Kpn*I Rev	CCC<u>GGTACC</u> TGTGTCGTCCTTTCCTGATGAGAG
Primers for sequencing and screening	
M13 For	GTAAAACGACGGCCAG
M13 Rev	GTCATAGCTGTTTCCTG
T7 For	TAATACGACTCACTATAGGG
T7 Rev	CGCCAGGGTTTTCCCAGTCACGAC
emm18 Screen For	CAGGAGTTTGTGGGGTTTTGGTTTC
emm18 Screen Rev	CGGTAATTTTTTGAAAAAGTACATCGGTGAG

[a] Underlined sequences in primers indicate restriction endonuclease sites used for cloning purposes.
 Abbreviations: For, forward; Rev, reverse

Industrial Automation; Eden Prairie, MN, USA) with icing between each round. Sonicated cells were centrifuged at $10,000 \times g$ at 4°C for 10 minutes and supernatants were collected for gravity nickel column purification

3.2.2.2   Metal affinity column chromatography protein purification

Supernatants from sonicated bacterial lysates were applied to a charged (100 mM $NiSO_4$) NiNTA affinity column (Novagen, EMD Millipore) and washed with 20 mM Tris base, 200 mM sodium chloride pH 7.5 buffer containing increasing concentrations of imidazole (10 mL each of 15 mM and 30 mM; followed by 5 mL each of 60 mM and 200 mM imidazole). Fractions were analyzed by SDS-PAGE (**Figure 9**) and fractions containing an abundance of the protein of interest were pooled and dialyzed in 1L of 20 mM Tris base, 200 mM sodium chloride pH 7.5 three times for 1 hour per litre. The N-terminal His_6-tags were removed from proteins by the addition of auto-inactivation resistant His_6-TEV [340] for 48 hours at 4°C. The protein solution was reapplied to a charged Ni-NTA affinity column (Novagen, EMD Millipore) to remove His_6-TEV and obtain a purified protein sample. Pure proteins were then dialyzed three times against 1 L of 20mM Tris base, 200 mM sodium chloride pH 7.5 buffer for one hour per litre. Protein homogeneity was assessed by SDS-PAGE.

3.2.2.3   Protein quantification

Concentration of purified proteins were determined using Pierce^{TM} BCA Protein Assay kit (Thermo Fisher Scientific Inc.) according to manufacturer's instructions. Briefly, the protein of interest was mixed with bicinchoninic acid (BCA) for 30 minutes at 37°C. Protein concentrations were determined through comparison to bovine serum albumin (BSA) as a reference protein at standard concentrations. Colourimetric detection was measured at an optical density of 562 nm using a Synergy^{TM} H4 Hybrid Multi-Mode Microplate Reader (BioTek, Fisher Scientific Inc.).

3.2.3   Protein visualization

3.2.3.1   Sodium dodecyl sulphate polyacrylamide gel electrophoresis

Protein samples were mixed 3:1 with 4 × Laemmeli buffer (240 mM Tris-HCl pH 6.8, 8% [w/v] SDS, 40% [v/v] glycerol, 0.01% [w/v] bromophenol blue, 1% [v/v] β-mercaptoethanol) and boiled for 5 minutes. Samples were then loaded into 15% polyacrylamide resolving gels (15% [v/v] acrylamide/bisacrylamide [37.5:1] aqueous solution, 0.25% [v/v] 1.5 M Tris-HCl pH 8.8, 0.1% [w/v] SDS, 0.1 % [w/v] ammonium persulfate [APS], 0.15% [v/v] tetramethylethylenediamine [TEMED]) with 5% polyacrylamide stacking gel (5% [v/v] acrylamide/bisacrylamide [37.5:1] aqueous solution, 25% [v/v] 0.5 M Tris-HCl pH 6.8, 1.3% [w/v] SDS, 0.1 % [w/v] APS, 0.2% [v/v] TEMED). Samples ran for 30 minutes at 80 V and then 1 hour at 150 V (Mini-PROTEAN System, Bio-Rad Laboratories Inc.) using Tris-Glycine electrophoresis buffer (192 mM glycine, 25 mM Tris, 0.1% [w/v] SDS, pH 8.3). Polyacrylamide gels were stained for 1 hour with Ready Blue stain (Thermo Fisher Scientific). Protein sample molecular weights were compared to PM008 protein marker (New England BioLabs Inc.)

3.2.3.2   Western blot

Protein samples from unstained SDS-PAGE gels were transferred onto polyvinylidine difluoride (PVDF) membrane (EMD Millipore) that was presoaked in 100% methanol and Western blot transfer buffer (20% [v/v] methanol, 48 mM Tris base, 39 mM glycine, 0.037% [w/v] SDS) for 5 minutes each. The prepared PVDF membrane and SDS-PAGE gel were assembled in a Mini Trans-Blot® Cell (Bio-Rad Laboratories Inc.) with Western blot transfer buffer for 1 hour at 100 V or overnight at 25 V with a cold block at 37°C. The PVDF membrane was then blocked for 30 minutes with 5% (w/v) skim milk powder in Tris buffered saline (TBS; 100 mM Tris, 1.5 M sodium chloride, pH 7.5). Following blocking, the membrane was incubated for 1 hour with appropriate primary antibody (**Appendix 4**) diluted 1:10,000 in 1% (w/v) skim milk in TBS. To remove residual antibody, PVDF membrane was washed three times in TBS with 0.01% (v/v) tween-20 (TBS-T) for 10 minutes per wash. Appropriate secondary antibody (**Appendix 4**) was

Figure 9. M protein plasmid constructs and purification by nickel column chromatography

A. All recombinant M protein genes were cloned into pET-28a(+) expression plasmids with His$_6$ purification tags and TEV cleavage tags. Recombinant proteins were designed to lack the signal peptide sequence (predicted by SignalP-5.0 server) and the 'LPXTG' cell wall sorting sequence. aa, amino acid. **B – D.** Protein expression was induced from *E. coli* BL21 (DE3) using IPTG and M proteins were purified from cell lysates using nickel-affinity column chromatography. **B.** Cell lysates were applied to a NiSO$_4$-charged column and fractions were eluted with increasing concentrations of imidazole. M protein-containing fractions were pooled, dialysed to remove imidazole, and incubated with TEV for 48 hours at 4ºC. **C.** Samples were passed through a charged nickel column again to remove cleaved His$_6$-tagged TEV. **D.** Fractions of purified, cleaved M proteins were collected and dialyzed into Tris NaCl and diluted to the required concentration. All visualization was done using 12% v/v SDS-PAGE. FT, flowthrough; P, purified M protein. Column labels indicate millimolar concentration of imidazole in the wash buffers.

A

503 aa

His | TEV | rM3 protein — –pET-28a(+)

499 aa

His | TEV | rM12 protein — –pET-28a(+)

326 aa

His | TEV | rM18 protein — –pET-28a(+)

381 aa

His | TEV | rM74 protein — –pET-28a(+)

B

kDa | FT | 15 | 30 | 60 | 200

75
63
48
35
25
20

C

kDa | FT | 15 | 30 | 60 | 200

75
63
48
35
25
20

D

kDa | P

75
63
48
35
25
20
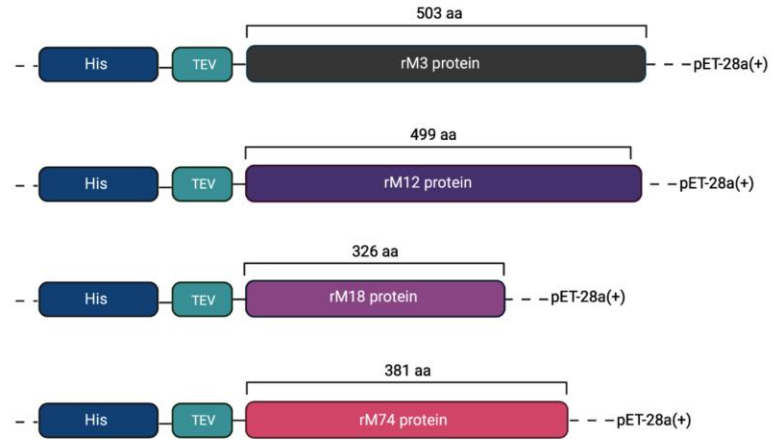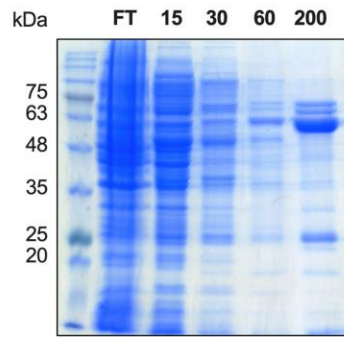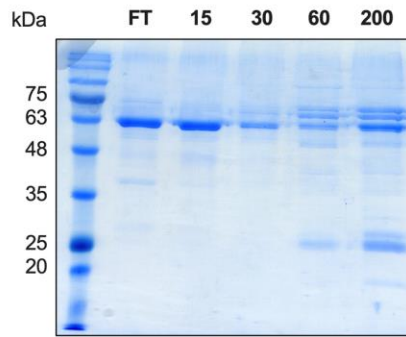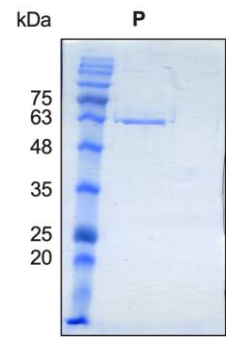
diluted 1:10,000 in 1% (w/v) skim milk powder in TBS and incubated with the PVDF membrane for 1 hour in the dark at room temperature. The membrane was washed three times with TBS-T as above and imaged on a LI-COR® Odyssey Imaging System (LI-COR Biosciences; Lincoln, NE, USA).

3.2.4   Antibody generation

Purified recombinant M18 protein in 20mM Tris, 200mM NaCl (pH 7.5), was sent to ProSci Inc (Poway, CA, USA) for production of polyclonal rabbit anti-M18 antibodies. New Zealand white rabbits were immunized with 200 μg of M18 protein with complete Freund's adjuvant (CFA) at week 0 and boosted with 100 μg M18 protein with incomplete Freund's adjuvant (IFA) at weeks 2, 4 and 6. Preimmunized serum was collected at week 0, followed by immunized serum collected at weeks 5 and 7 with terminal bleed taken at week 8. Serum samples were assessed for anti-M18 antibody titers using enzyme-linked immunosorbent assay (ELISA) and aliquoted and stored at -80°C until use.

3.2.4.1   Adhesion assay

Details for human cell culturing and epithelial cell adhesion assay procedures are outlined in Section 2.2.7. Briefly, Detroit-562 and A549 cells were grown to confluence on 12 or 24 well TC-treated plates and exponential phase *S. pyogenes* were inoculated onto cells at a MOI of 100 for 2.5 hours at 37°C in 5% CO_2. Following incubation, non-adherent bacteria were washed off and epithelial cells were lysed with Triton-X100 (VWR International) and serially diluted ten-fold to enumerate remaining bacteria present.

3.2.5   *Ex vivo* experiments

3.2.5.1   Ethics statement

The use of primary human lymphocytes was reviewed and approved by Western University's Research Ethics Board for Health Sciences Research Involving Human Subjects (**Appendix 1**). Informed written consent was obtained from all donors.

3.2.5.2   Immune evasion assays

Experimental procedure details for whole blood survival assay, isolation of neutrophils, and neutrophil survival assay are found in Section 2.2.8. Whole blood was collected in heparinized vacuum tubes (BD Biosciences) from healthy adult volunteers and used directly for determining whole blood survival or for density gradient separation and isolation of PMNs. For whole blood survival assay, ~1000 CFUs of *S. pyogenes* were inoculated into whole human blood at 37°C and the number of surviving bacteria were enumerated after 30, 60, 90, 120, and 180 minutes with rotation. For neutrophil survival assay, *S. pyogenes* was added to 10% (v/v) normal serum for 30 minutes to assist with bacterial opsonization prior to incubation with isolated human PMNs at 1:10. After 60 mins, PMNs were lysed, and survival was calculated as the average bacterial CFUs in the presence of neutrophils divided by bacterial CFUs in no PMN control samples.

3.2.6   *In vivo* experiments

3.2.6.1   Ethics statement

All mouse experiments were approved by the Animal Use Subcommittee at Western University (London, ON, Canada) under AUP number 2021-041-D (**Appendix 2**). A list of all mice used in this study can be found in **Appendix 3**. All *in vivo* experimental procedures were conducted in accordance with Canadian Council on Animal Care Guide to the Care and Use of Experimental Animals.

3.2.6.2   Mice

Mice utilized in this study were conventional C57BL/6 (B6) mice and transgenic B6 mice expressing HLA-DR4 and DQ8 (B6$_{HLA}$ mice) and are listed in **Appendix 3**. Transgenic mice were bred by the McCormick laboratory as described in Section 2.2.9.2. Conventional C57Bl/6 mice were obtained from the Jackson Laboratory.

3.2.6.3   Vaccination experiments

Vaccination of 6-8 week old B6$_{HLA}$ mice has been previously described [156] Briefly, mice received 1 μg of recombinant protein in 200 μL (100 μL 20mM Tris base, 200 mM sodium chloride, pH 7.5; 100 μL Imject^{TM} Alum adjuvant [Thermo Fisher Scientific]) subcutaneously under isoflurane anesthetic. Control mice received saline solution (PBS) and adjuvant only. Vaccinations followed a four-week schedule with subcutaneous immunizations on days 0, 14, and 28. Where applicable, infection experiments occurred two-weeks post vaccination on day 42 (see below) (**Figure 10**), followed by euthanasia and collection of terminal bleeds for assessment of serum IgG antibody levels.

3.2.7   Antibody titer analysis

ELISA was performed to measure serum IgG antibody titers from terminal bleeds of mice following immunizations. 96-well plates (Corning Costar 9018 [NY, USA]) were coated with 100 μL of recombinant protein (10 μg mL^{-1}) in a 0.01 M sodium carbonate buffer (pH 9.6) and incubated overnight at room temperature wrapped in aluminum foil. The coating solution was removed, and plates were washed three times in PBS (Wisent Bioproducts Inc.; Saint-Bruno, QU, Canada) with 0.05% tween-20 (PBS-T). Plates were blocked with 200 μL of PBS with 0.02% tween-20 and 1% bovine serum albumin (BSA) for 2 hours at room temperature and then washed three times. Serum samples were diluted 1:100 in PBS containing 0.02% tween-20 and 0.01% BSA to a final volume of 100 μL per well followed by 1:4 serial dilutions to a final concentration of 1:204,800. Plates were incubated at room temperature for 2 hours and washed three times with PBS-T. Goat anti-mouse horseradish peroxidase (HRP)-conjugated secondary antibody (Sigma-Aldrich) (**Appendix 4**) was added at a dilution 1:10,000 to a final volume of 100 μL per well in PBS with 0.02% tween-20 and 1% BSA and incubated at room temperature for 2 hours. Following rigorous washing, 100 μL per well of tetramethylbenzidine (TMB) was added and plates were developed for 15 minutes at room temp shieled from light. Colour change was neutralized by adding 50 μL per well of 1 N H_2SO_4 and absorbances were measured at OD$_{450}$ with subtracting OD$_{570}$ readings to adjust for background fluorescence. Antibody titers were calculated as the reciprocal of the lowest serum dilution with readings four-fold above

Figure 10. Schedule for M protein vaccination and acute *S. pyogenes* infections in B6$_{HLA}$ mice.

A. M protein vaccination with nasopharyngeal infection protocol. B6$_{HLA}$ mice were subcutaneously vaccinated with 1 µg recombinant M protein in alum every 2 weeks for a total of three injections. Two weeks following the last vaccination, mice were intranasally challenged with the appropriate *S. pyogenes* strain. Mice were sacrificed 2 days later for enumeration of bacteria within nasal turbinates. **B.** M protein vaccination with skin infection protocol. Using the same vaccination schedule, mice were challenged with an intradermal injection with the appropriate *S. pyogenes* strain. On each day following infection, mice were weighed and lesions at injection sites were measured. At 3 days post-infection, mice were sacrificed and the skin around each injection site was harvested for bacterial enumeration.

A

Subcutaneous injections
M protein (1 ug) in alum

Nasal challenge
with *S. pyogenes*

Sacrifice

Day

0   14   28   42   44

B

Subcutaneous injections
M protein (1 ug) in alum

Skin challenge
with *S. pyogenes*

Sacrifice

Day

0   14   28   42 43 44 45

Measure lesions and
weigh mice daily
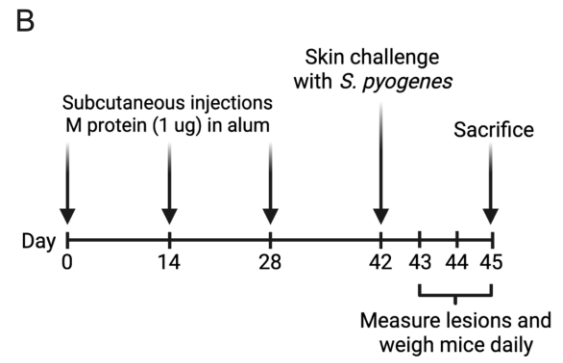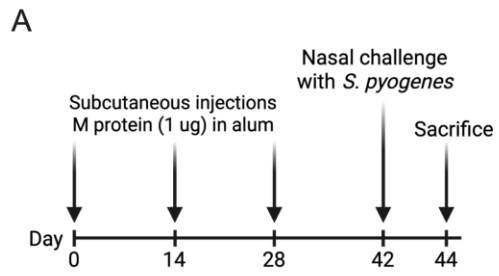
background.

3.2.8   Acute infections

Preparation of *S. pyogenes* for nasal and skin infections were completed according to Section 2.2.9. For nasal inoculations, B6$_{HLA}$ mice were given 2 mg ml^{-1} neomycin sulphate in their drinking water, which was provided *ad libitum,* two days prior to infection. At infection, mice were anesthetized using FORANE (isoflurane, USP; Baxter Corporation; Mississauga, ON, Canada) and 7.5 µL of *S. pyogenes* inoculum was administered to each nostril with 15 µL containing ~10^8 CFUs. Mice were sacrificed 48 hours post-infection and cNTs were harvested for bacterial enumeration. Murine blood, spleen, liver, kidneys, lungs, and heart were also removed for bacterial enumeration where indicated. For skin inoculations, the fur on the lower backs of mice were removed by shaving and hair removal cream the day before infections. At infection, mice were anesthetized and a 50 µL dose containing ~2.5×10^7 CFUs were injected intradermally into each lower flank. Each day following infection, mice were weighed and lesions at the injection sites were measured using calipers. At 72 hours post-infection, mice were sacrificed and the skin around each injection site was harvested for bacterial enumeration. Bacterial burden was normalized to the weights of the skin excised and presented as CFU per gram of skin.

3.2.9   Multiplex cytokine array

Cytokine and chemokine concentrations in cNT homogenates of mice nasally infected with *S. pyogenes* were measured according to Section 2.2.10 using the 32-Plex array from Eve Technologies (Calgary, AB, Canada). Uninfected cNT homogenates were collected for background comparisons. Data on heat maps is presented as normalized median cytokine responses ($X_{normalized} = [(x - x_{min})/(x_{max} - x_{min})]$) from cNT homogenates of all nasally infected mice ($n \geq 3$). Statistical analyses were completed by the appropriate test within groups, quantitative cytokine levels are shown in **Appendix 6**.

3.2.10   Statistical analyses

Data was analyzed using unpaired Mann-Whitney Student's *t*-test, or one-way ANOVA with Dunnett's multiple comparisons, or two-way ANOVA with Šídák's multiple comparisons test and Geisser's Greenhouse correction, as indicated. A *P* value less than 0.05 was determined to be statistically significant, all analyses were completed using Prism software 9.3.1 (GraphPad Software, Inc.; La Jolla, CA, USA).

3.3   Results

3.3.1   HLA dependence for *S. pyogenes* MGAS315, HKU16, MGAS8232, and NGAS979 during nasopharyngeal infection

Previous work reported by our research team revealed that transgenic expression of HLA class II molecules in mice enhanced *S. pyogenes* MGAS8232 nasopharyngeal infection compared to conventional B6 mice, with SpeA superantigen activity driving this response [156]. To confirm that multiple streptococcal strains share this HLA-dependent phenotype, we inoculated both conventional B6 and transgenic B6$_{HLA}$ mice intranasally with ~10^8 bacterial CFUs of *S. pyogenes* MGAS315, HKU16, or NGAS979. Conventional B6 mice presented very low cNT bacterial burden for each streptococcal strain, however, all strains notably infect the nasopharynx of B6$_{HLA}$ mice (**Figure 11**). Nasal infections with *S. pyogenes* MGAS315, HKU16, and MGAS8232 demonstrated at least ~10,000-fold greater bacterial recovery in B6$_{HLA}$ mice at 48 hours post-infection compared to B6 mice (**Figure 11A-C**), and *S. pyogenes* NGAS979 bacterial CFUs were enhanced by ~100-fold (**Figure 11D**). These findings support that transgenic expression of HLA molecules is important for modeling nasopharyngeal infections in mice using *S. pyogenes* MGAS315, HKU16, MGAS8232, and NGAS979 strains.

3.3.2   Skin infection in B6$_{HLA}$ mice by *S. pyogenes* MGAS315, HKU16, MGAS8232, and NGAS979.

Since HLA-dependent phenotypes exist for each streptococcal strain, we next sought to determine whether these strains were suitable to cause acute skin infections in B6$_{HLA}$ mice. B6$_{HLA}$ mice were injected intradermally with ~2.5 x 10^7 CFUs of *S. pyogenes* MGAS315, HKU16, MGAS8232, or NGAS979 in each hind flank on their lower backs and monitored daily for weights and lesion sizes. Infected mice steadily lost weight at 24- and 48-hours post-infection and showed signs of recovered weight by 72-hours (**Figure 12A**). *S. pyogenes* MGAS315 and MGAS8232 provoked larger and more inflamed lesions compared to HKU16 and NGAS979 (**Figure 12D**). MGAS8232 displayed peak lesion sizes at 48-hours post-infection whereas lesions caused by MGAS315, HKU16, and

Figure 11. HLA-dependent phenotype of *S. pyogenes* MGAS315, HKU16, MGAS8232, and NGAS979 strains.

Conventional B6 and transgenic B6$_{HLA}$ mice were intranasally administered ~10^8 CFUs of *S. pyogenes* MGAS315, HKU16, MGAS8232, and NGAS979 strains. Data points represent bacterial CFUs from nasal turbinates of individual mice 48 hours post-nasal challenge. Bars represent mean ± SD. Horizontal dotted line indicates limit of detection. Significance determined by unpaired Mann-Whitney *t*-test (*, $P < 0.05$; ***, $P < 0.001$).

A MGAS315

B HKU16

C MGAS8232
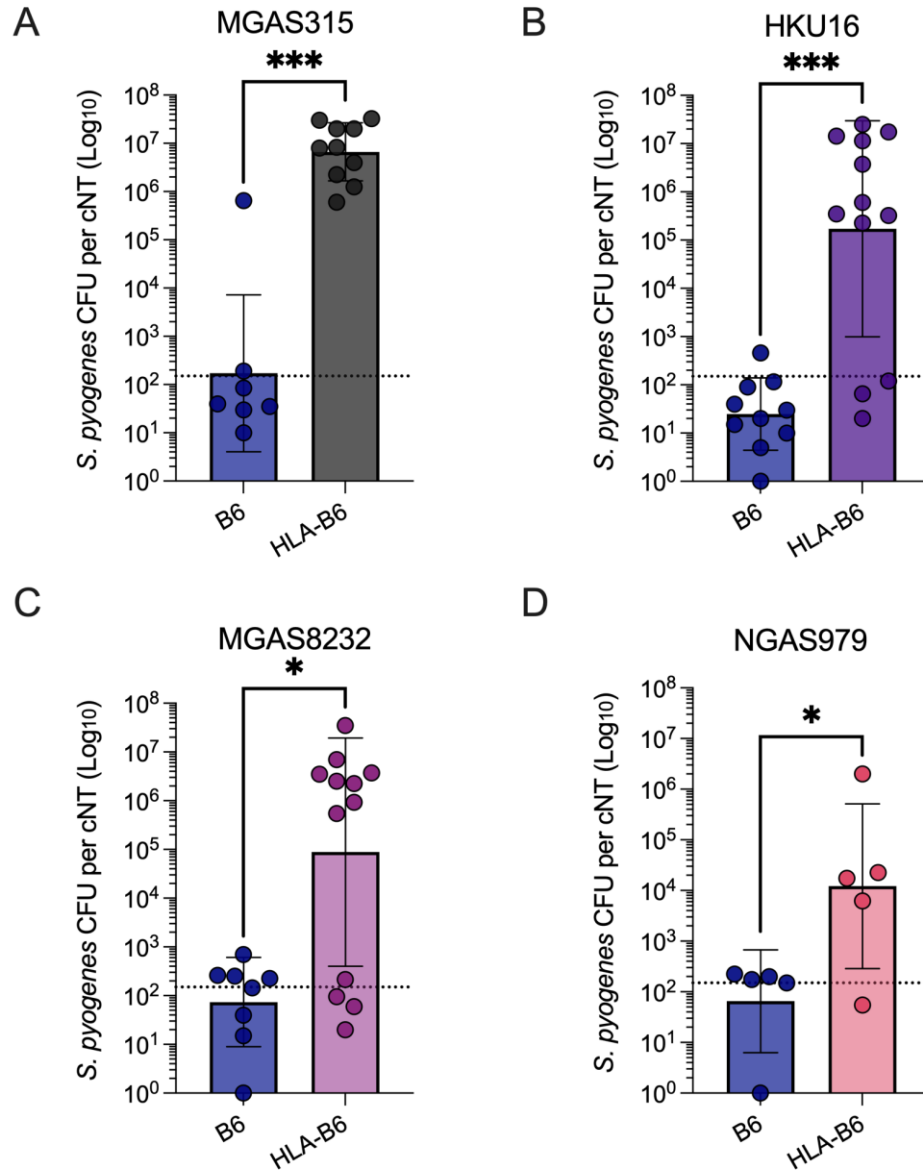
D NGAS979

NGAS979 grew steadily larger over the 72-hour period (**Figure 12B**). All strains presented similar bacterial burdens with ~10^9 CFUs recovered from individual abscesses (**Figure 12C**). Despite variation in the size and appearance of lesions caused by each strain, *S. pyogenes* MGAS315, HKU16, MGAS8232, and NGAS979 can all produce skin infections in B6$_{HLA}$ mice with evidence of bacterial replication.

3.3.3   Generation and purification of recombinant M proteins

Expression constructs for the M3, M12, M18, and M74 proteins encoded by *S. pyogenes* MGAS315, HKU16, MGAS8232, and NGAS979 were designed and produced in this study. Recombinant protein constructs were generated by amplifying *emm* genes from their respective *S. pyogenes* genomes with sequences designed to contain the extracellular domains and lack the ~42 amino acid signal peptides and 'LPXTG' cell wall sorting sequences. Primers were designed to add nucleic acid sequences for a His$_6$-Tag and a TEV protease cleave site between the His$_6$-Tag, and recombinant M protein sequences, including appropriate restriction enzyme sites for cloning into the pET-28a(+) expression vector (**Figure 9A; Table 6**). Recombinant M protein constructs were expressed in *E. coli* BL21 (DE3) by IPTG induction and purified from cell lysates using two-step nickel-affinity column chromatography (**Figures 9B-D**). Purified recombinant proteins were visualized on SDS-PAGE (**Figure 13**).

3.3.4   Serum IgG antibodies generated against recombinant M proteins do not prevent acute *S. pyogenes* nasopharyngeal infections

A major goal for a *S. pyogenes* vaccine is to prevent colonization and infection at all major biological niches, which include the upper respiratory tract and the skin. We first sought to determine whether parenteral vaccinations with recombinant M proteins would protect B6$_{HLA}$ mice from nasopharyngeal infection. Mice were subcutaneously injected with 1 ug of recombinant M protein in alum 3 times at two-week intervals before nasal challenge with the appropriate *S. pyogenes* strain (**Figure 10A**). To our surprise, mice vaccinated with any of M3, M12, M18, or M74 proteins presented no differences in nasopharyngeal bacterial burdens compared to control mice following infection with their respective strain

Figure 12. *S. pyogenes* MGAS315, HKU16, MGAS8232, and NGAS979 cause acute skin infection in mice.

B6$_{HLA}$ mice were administered ~2.5 x 10^7 CFUs of *S. pyogenes* MGAS315, HKU16, MGAS8232, or NGAS979 intradermally in each hind flank. **A**. Weights of mice at 24-, 48-, and 72-hours following *S. pyogenes* skin challenge. Weights represented as a percentage (%) of day 0 weight. **B.** Skin lesion areas at 24-, 48-, and 72-hours post-infection. Bars represent mean ± SD. **C.** Data points represent bacterial CFUs from individual infected skin abscesses normalized to the weight of the excised skin tissue from mice at 72-hours. Bars represent mean ± SD. Horizontal line indicates limit of detection. Significance analysed by one-way ANOVA; data not significant. **D.** Photographic representation of skin lesions at 72-hours post-skin challenge with *S. pyogenes*.

A

B

C

D
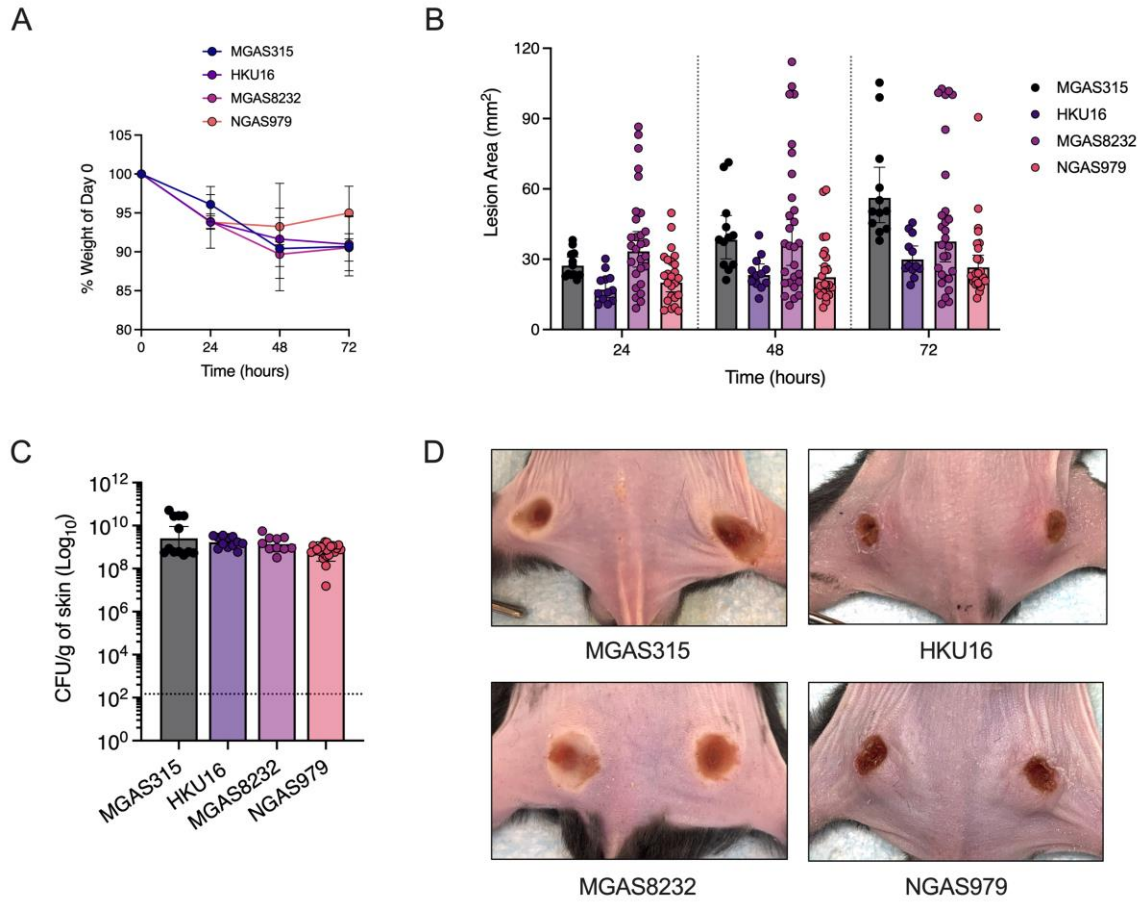
Figure 13. Purified recombinant M proteins.

Recombinant M3, M12, M18, and M74 proteins were induced from *E. coli* BL21 (DE3) by IPTG and purified by nickel column chromatography. Protein visualization was shown using 12% v/v SDS-PAGE stained with Ready Blue.
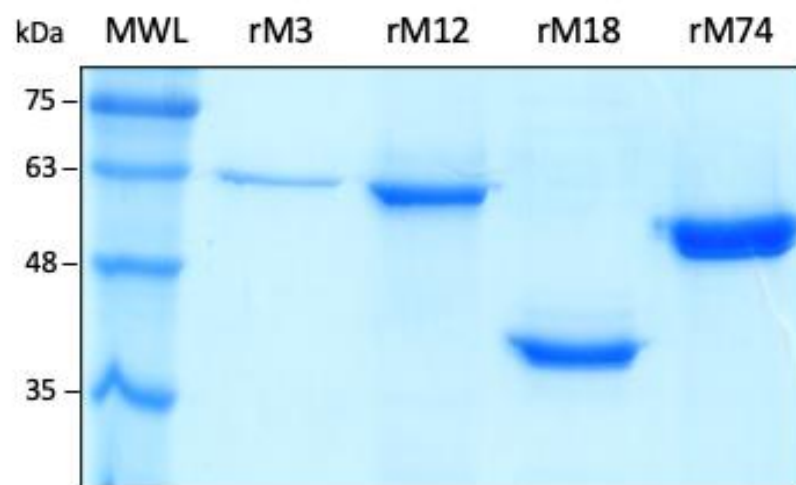
(**Figure 14**). Serum analyses of all experimental mice confirmed that vaccinations with recombinant M proteins generated significantly high serum levels of M protein-specific IgG antibodies compared to control mice (**Figure 14**), and therefore, these results indicate that serum IgG antibodies against streptococcal M proteins are not protective against nasopharyngeal infection in B6$_{HLA}$ mice.

3.3.5 Serum IgG antibodies generated against recombinant M proteins do not prevent acute *S. pyogenes* skin infections

It was next investigated whether M protein-specific IgG antibodies induced by parenteral vaccinations could protect against the other major reservoir of acute *S. pyogenes* infections, the skin. The vaccination regime was repeated in B6$_{HLA}$ mice, followed by intradermal skin challenge with appropriate *S. pyogenes* strains two weeks succeeding the final immunization (**Figure 10B**). Mice vaccinated with recombinant M proteins displayed no discernable protective phenotype against skin infection by their respective *S. pyogenes* strain. Vaccinated mice revealed comparable weight loss and lesion size development over the course of infection compared to control PBS-immunized mice (**Figure 15A, 15B**). Bacterial loads within lesions were also similar between control and M protein-vaccinated mice (**Figure 15C**) despite mice demonstrating significantly higher serum M protein-specific IgG levels post-vaccination (**Figure 15D**). These results further indicate that serum IgG antibodies against streptococcal M proteins are not protective against acute skin infections by *S. pyogenes* in B6$_{HLA}$ mice.

3.3.6 Generation of a M18 protein-knockout mutant strain in *S. pyogenes* MGAS8232

M proteins are thought to promote virulence through adhesion and immune evasion mechanisms, and such, the lack of protection following immunization was unexpected. Therefore, we sought to examine the effect of knocking out expression of the M protein on acute infections. Standard molecular cloning techniques were used to generate an in-frame clean deletion of the M18 protein, encoded by the *emm18* gene, within the *S. pyogenes* MGAS8232 genome. The deletion mutant was confirmed by DNA sequencing and

Figure 14. Subcutaneous vaccination with monovalent M proteins do not protect against *S. pyogenes* nasopharyngeal infection in B6$_{HLA}$ mice.

B6$_{HLA}$ mice were immunized subcutaneously with 1 μg of recombinant (**A**) M3, (**B**) M12, (**C**) M18, or (**D**) M74 protein in alum three times at 2-week intervals, or PBS in alum for control mice. At 2 weeks post-vaccination, mice were intranasally challenged with ~10^8 CFUs of the homologous *S. pyogenes* strain and sacrificed 48 hours later for bacterial enumeration. CFU data points represent bacterial recovery from cNTs of individual immunized mice. Bars represent mean CFUs ± SD. The horizontal line indicates limit of detection. Significance determined by unpaired Mann-Whitney *t*-test**,** data not significant. Serum anti-M protein IgG titers from (**A**) M3, (**B**) M12, (**C**) M18, or (**D**) M74 protein-vaccinated and control mice. Antibody titers were calculated as the reciprocal of the lowest serum dilution with readings four-fold above background. Bars represent mean ± SD serum IgG titers calculated for individual mice by ELISA. Significance determined by unpaired Mann-Whitney *t*-test (******, *P* < 0.01).

A   M3-alum

CFUs   M3-IgG

B   M12-alum

CFUs   M12-IgG

C   M18-alum

CFUs   M18-IgG

D   M74-alum

CFUs   M74-IgG
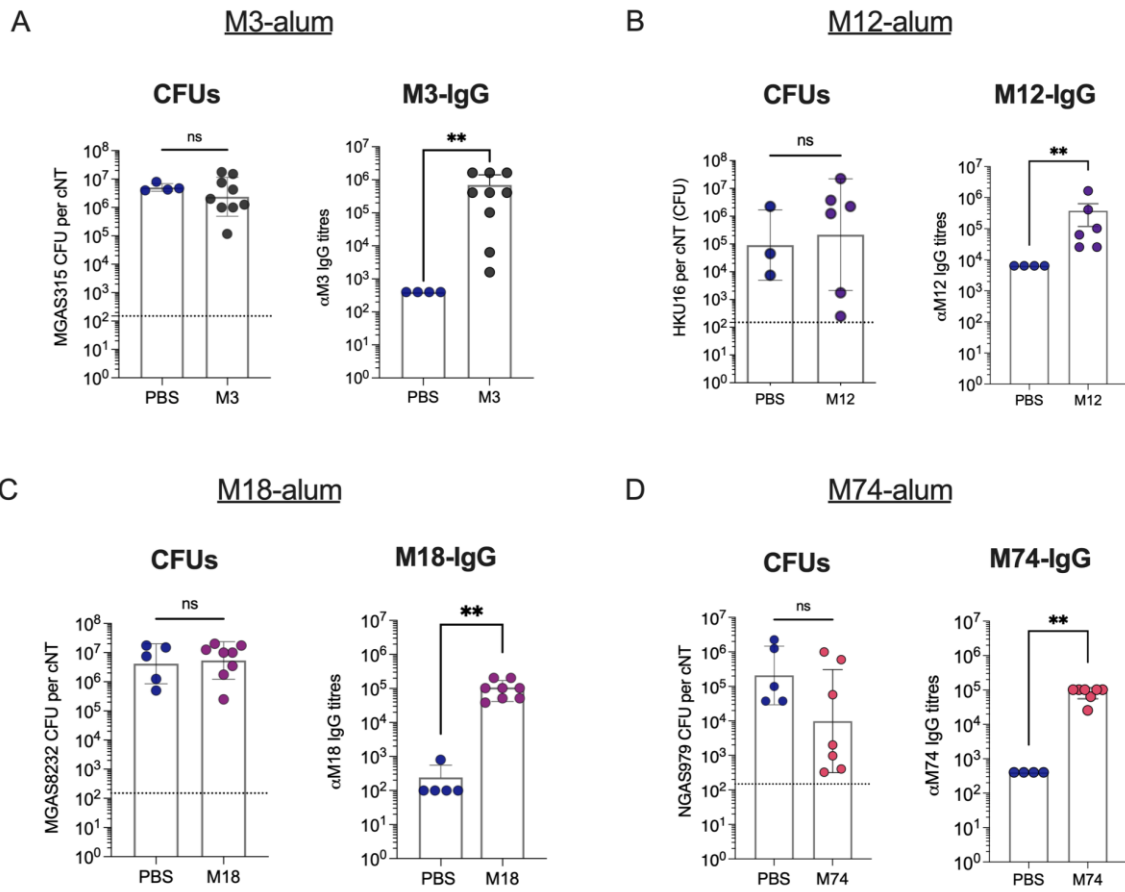
Figure 15. Subcutaneous vaccination with recombinant intact M proteins do not prevent acute skin infection by *S. pyogenes* in B6$_{HLA}$ mice

B6$_{HLA}$ mice were immunized subcutaneously with 1 µg of recombinant M proteins in alum three times at 2-week intervals or PBS in alum for control mice. Mice were administered ~2.5 x 10^7 CFUs of homologous *S. pyogenes* strains intradermally in each hind flank 2-weeks post-vaccination and sacrificed 72 hours later for bacterial enumeration. **A**. Weights of mice at 24-, 48-, and 72-hours following skin challenge. Weights represented as a percentage (%) of day 0 weight. **B**. Skin lesion areas at 24-, 48-, and 72-hours post-infection. Bars represent mean ± SD. For each vaccine experiment significance was determined by (**A - B**) two-way ANOVA with Šídák's multiple comparisons test and Geisser's Greenhouse correction, data not significant. **C.** Bacterial CFUs from individual lesions normalized to the weight of skin excised. Bars represent mean ± SD. Significance was determined by unpaired Mann-Whitney *t*-tests, data not significant. **D.** M protein-specific IgG antibody serum titers. Antibody titers were calculated as the reciprocal of the lowest serum dilution with readings four-fold above background. Data points represent IgG titers calculated for each individual mouse by ELISA. Bars represent mean ± SD. Significance was determined by unpaired Student's *t* test (*, $P <$ 0.05; **, $P < 0.01$). **E.** Representative images of skin lesions at 72 hours post-infection.

A <u>Weights</u>
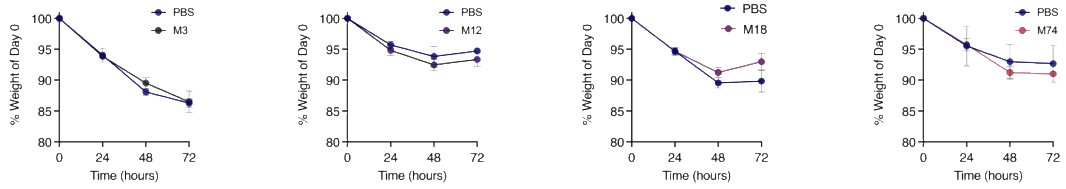
B <u>Lesion sizes</u>
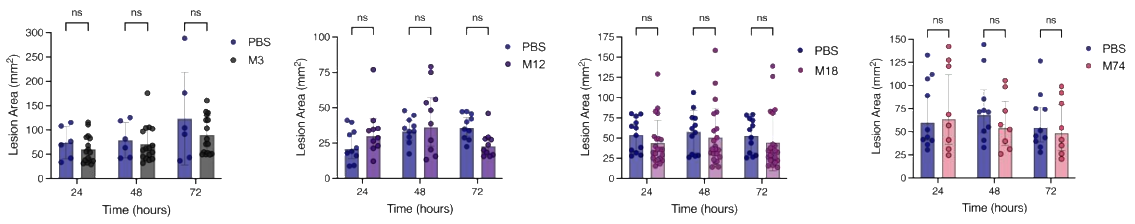
C <u>CFUs in skin lesions</u>
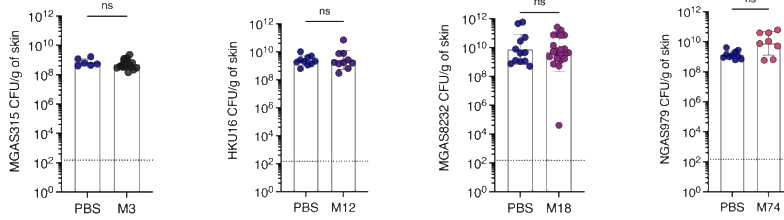
D <u>IgG titres in serum</u>
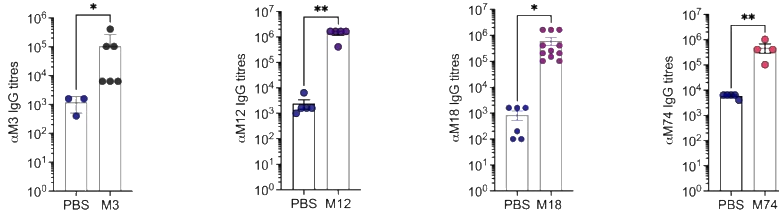
E <u>Skin lesion photographs</u>
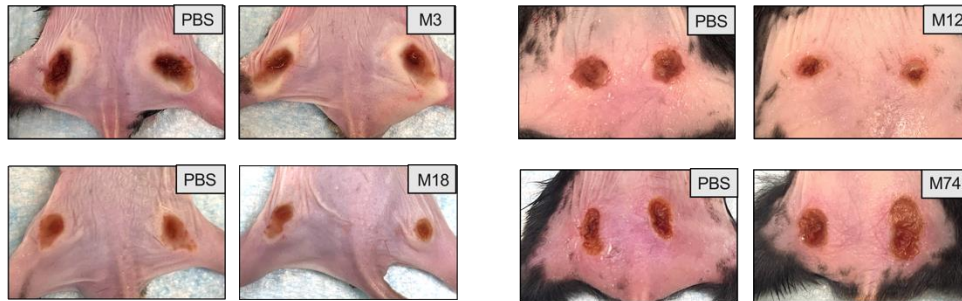
validated using PCR amplification with primers flanking the deleted region. Compared to the wildtype MGAS8232 genome, the Δ*emm18* mutant strain contained a 1,167 bp deletion within the *emm18* encoded region (data not shown). Recombinant M18 protein was used to immunize rabbits (Pro Sci Incorporated) and produce polyclonal rabbit serum containing α-M18 antibodies. Expression of the M18 protein from wildtype MGAS8232 was illustrated by Western blot using rabbit α-M18 serum, which also emphasized the absence of M18 expression in the Δ*emm18* mutant compared to wildtype and Δ*hasA* strains (**Figure 16A**). Furthermore, deletion of the *emm18* gene did not impact the secreted protein profile, which was assessed through trichloroacetic acid preparations of wildtype and Δ*emm18* MGAS8232 and visualized by SDS-PAGE (**Figure 16B**). Bacterial growth was similar between wildtype and Δ*emm18* strains *in vitro* in THY media, which ensured that the deleted *emm18* gene had no detrimental effect on the growth rate of *S. pyogenes* (**Figure 16C**).

3.3.7   Characterization of *S. pyogenes* MGAS8232 Δ*emm18 in vitro*

Bacterial adherence properties of wildtype and Δ*emm18* MGAS8232 were then evaluated using A549 lung epithelial cells and D562 pharyngeal cells. Briefly, we incubated exponential phase bacteria over confluent monolayers for two hours, washed off non-adherent bacteria, and then lysed cells to determine the remaining adherent bacteria. There were no significant differences in the amount of adherent wildtype or Δ*emm18* adherent bacteria recovered from A549 and D562 cells (**Figure 16D, E**), suggesting that M18 protein expression does not mediate adherence to these epithelial cells. Additionally, the Lancefield human blood bactericidal assay was used explore the contribution of the M18 protein to bacterial immune evasion. Following the inoculation of wildtype or Δ*emm18* cultures into fresh heparinized human blood, the Δ*emm18* mutant had reduced growth and survival of compared to wildtype MGAS8232 in whole human blood (**Figure 16F**), supporting that M18 protein resists killing in blood. We next sought to examine how the M18 protein contributes to survival against neutrophils specifically and found that Δ*emm18* mutant was more sensitive to neutrophil-mediated killing than wildtype MGAS8232. This was demonstrated by a significant decline in the survival of *Δemm18* in the presence of

freshly isolated neutrophils (**Figure 16G**). These results outline an important feature by the M18 protein in promoting resistance to neutrophil killing.

3.3.8 M18 protein expression by *S. pyogenes* MGAS8232 does not promote nasopharyngeal infection in B6$_{HLA}$ mice

Although M protein-specific antibodies offered no defense from nasopharyngeal and skin infections, we next pursued to investigate whether *S. pyogenes* requires this surface protein at all during these acute infection models. We first assessed the necessity of the M18 protein during nasopharyngeal infection and infected mice with ~10^8 CFUs of wildtype or Δ*emm18* MGAS8232. Nasal turbinates were collected 48 hours post-infection to assess nasopharyngeal bacterial burdens and cytokine responses during infection. Consistent with previous findings, mice presented high bacterial loads of wildtype *S. pyogenes* MGAS8232 in their nasopharynx, and this was not significantly different than the number of bacteria recovered from Δ*emm18*-infected mice (**Figure 17A**), suggesting that M18 protein expression is not essential to establish nasopharyngeal infection of B6$_{HLA}$ mice. Consistent with the non-invasive nature of the model [156], mean bacterial dissemination of *S. pyogenes* wildtype and Δ*emm18* remained below the limit of detection in the lungs, liver, spleen, heart, and kidneys (**Figure 18**), concluding that removal of the M18 protein does not increase *S. pyogenes* dissemination.

Cytokine responses in cNT homogenates were then assessed by a multiplex cytokine array to evaluate the levels of 32 cytokines during infection. Any cytokine that presented an average concentration above 20 pg ml^{-1} within a treatment group was included in the heat map and presented as normalized median cNT cytokine responses (**Figure 17B**). Quantitative cytokine data is shown in the supplemental data (**Appendix 6**). As shown previously, uninfected mice do not naturally express an inflammatory signature within their cNTs, whereas concentrations of Th1-type cytokines (IL-1α and IL-1β); Th17-type cytokines (IL-6 and IL-17); chemokines (KC, IP-10, MCP-1, MIP-1α, MIP-1β, MIG, MIP-2, LIF and LIX); and growth factors (G-CSF) are vigorously induced during wildtype *S. pyogenes* infections (**Appendix 6**). Interestingly, infection by the Δ*emm18* mutant paralleled a wildtype-induced inflammatory environment

Figure 16. Generation and characterization of the *S. pyogenes* Δ*emm18* mutant strain.

A. Western Blot using rabbit anti-M18 polyclonal serum demonstrated absence of M18 protein from the Δ*emm18* mutant strain. **B.** *S. pyogenes* wildtype and Δ*emm18* strains were grown in THY for 18-hours and the secreted protein profiles were assessed by SDS-PAGE on 12% acrylamide gel stained with Coomassie. **C.** Growths of *S. pyogenes* wildtype and Δ*emm18* in THY at 37°C was measured by OD_{600} over the course of 18 hours. Data is presented as mean ± SD of each culture analyzed in triplicate. **D.** Adhesion of *S. pyogenes* to D562 pharyngeal epithelial cells. **E.** Adhesion of *S. pyogenes* to A549 lung epithelial cells. Confluent cell monolayers were treated with *S. pyogenes* (MOI of 100) for 2 hours at 37°C + 5% CO_2. Non-adherent bacteria were washed with PBS, and cells were lysed with Triton X-100 for enumerating remaining adherent bacteria. Data was evaluated using unpaired *t*-test, data not significant (*n* = 3). **F.** Whole human blood survival assay. Heparinized blood from human donors were incubated with ~10^3 bacterial CFUs of wildtype or Δ*emm18 S. pyogenes* MGAS832 at 37°C with rotation for 3 hours. Data points represent geometric mean CFUs ± SD. Horizontal line indicates limit of detection. **G.** Neutrophil survival assay. Neutrophils were isolated from human blood by density centrifugation and inoculated with opsonized wildtype and Δ*emm18* strains at a MOI of 10. Surviving bacteria were determined after 60 min at 37°C with rotation and was calculated as the difference between surviving bacteria with no neutrophils and in the presence of neutrophils. Data shown are the means of percent survival ± SD (*n* ≥ 3 per group). Statistical analyses were performed using unpaired Mann-Whitney *t*-test (*, *P* < 0.05).

A

MWL Wildtype Δ*emm18* Δ*hasA*

kDa
75
48
35
25
20

B

MWL Wildtype Δ*emm18*

kDa
75
48
35
25
20

C *in vitro* growths

OD$_{600}$ vs Time (hours)

- Wildtype
- Δ*emm18*

D A549 adherence

S. pyogenes (CFU)

Wildtype   Δ*emm18*

E D562 adherence

ns

S. pyogenes (CFU)

Wildtype   Δ*emm18*

F Whole blood survival

- Wildtype
- Δ*emm18*

S. pyogenes (CFU) vs Time (mins)

G Neutrophil survival

*

%Survival
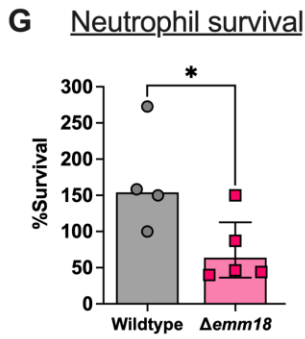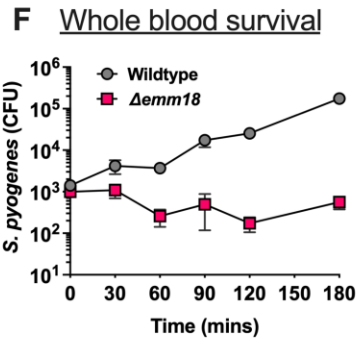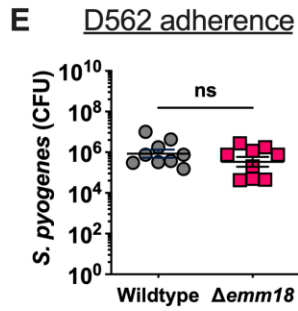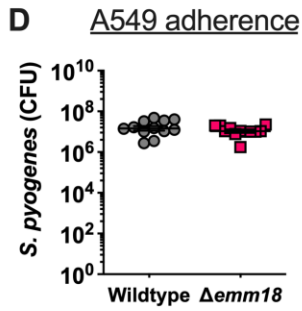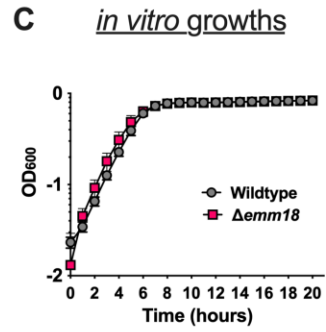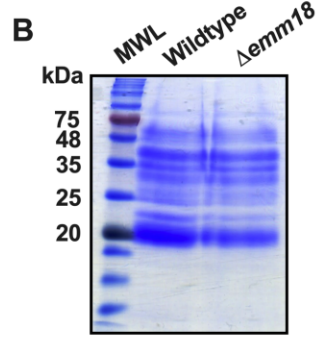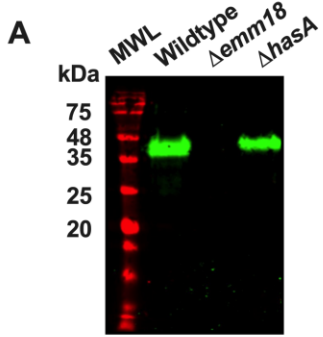
Wildtype   Δ*emm18*

Figure 17. M18 protein expression by *S. pyogenes* MGAS8232 is expendable during acute nasopharyngeal infection in B6$_{HLA}$ mice

A. Nasopharyngeal burden from *S pyogenes* MGAS8232 wildtype and Δ*emm18* infections. B6$_{HLA}$ mice were administered ~10^8 CFUs of *S. pyogenes* intranasally. Data points represent bacterial CFUs from cNTs of individual mice 48 hours post-nasal challenge. Bars represent mean ± SD. Horizontal dotted line indicates limit of detection. Significance determined by unpaired Mann-Whitney *t*-test ($P = 0.2381$, data not significant). **B.** Heat-map of cNT cytokine and chemokine responses during *S. pyogenes* MGAS8232 wildtype and Δ*emm18* nasopharyngeal infections. Data shown represent normalized median cytokine responses from infected cNTs ($n \geq 3$ per group).

A

B

Figure 18. Deletion of the *emm18* gene in *S. pyogenes* MGAS8232 does not enhance bacterial dissemination in B6$_{HLA}$ mice.

B6$_{HLA}$ mice were nasally challenged with *S. pyogenes* MGAS8232 and sacrificed 48 hours later. Organs were harvested, homogenized, and plated on TSA with 5% sheep blood agar to determine bacterial dissemination. Bacterial CFUs were measured in the **(A)** lungs, **(B)** liver, **(C)** spleen, **(D)** heart, and **(E)** kidneys. Bars represent mean ± SD. Horizontal dotted line indicates limit of detection. Significance determined by unpaired Mann-Whitney *t*-test, data not significant ($n \geq 5$).

A Lungs **B** Liver **C** Spleen **D** Kidneys **E** Heart
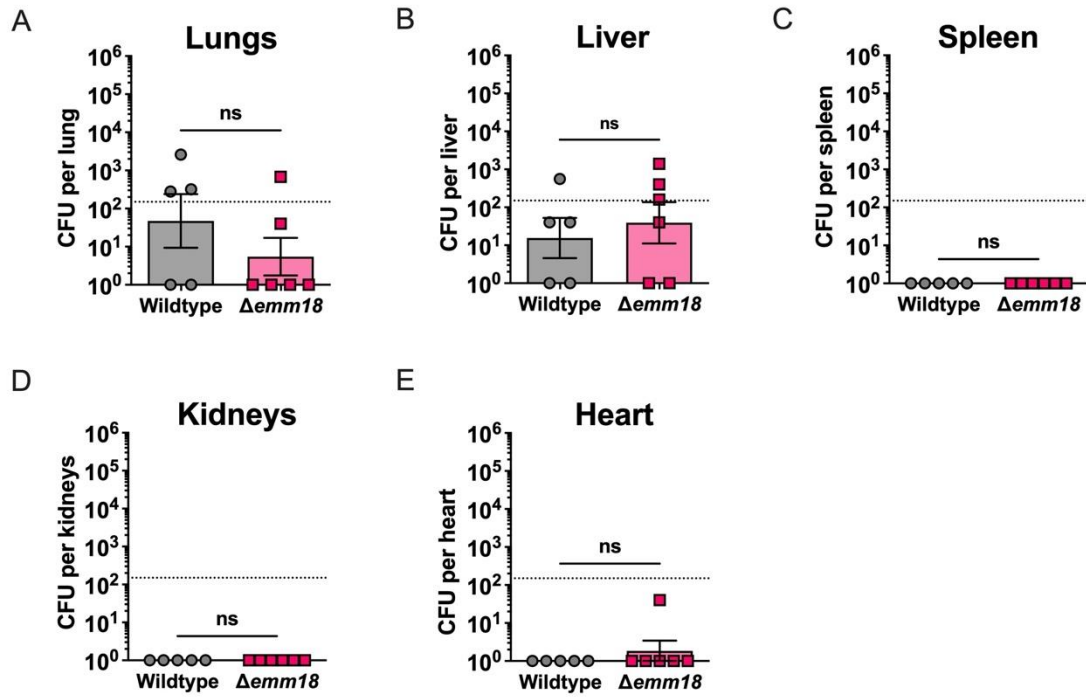
with no significant cytokine differences (**Figure 17B**; **Appendix 6).** These results suggest that removal of the M18 protein continues to support inflammation within the nasopharynx and does not alter bacterial burden during nasopharyngeal infection.

3.3.9 M18 protein expression by *S. pyogenes* MGAS8232 does not promote bacterial density during skin infection

We next aimed to assess whether M protein expression promotes infection by the other major reservoir of *S. pyogenes*, the skin. B6$_{HLA}$ mice were injected intradermally in each hind flank with wildtype or *Δemm18* and showed weight loss at 24- and 48-hours and exhibited signs of recovery by 72-hours (**Figure 19A**). Although lesions from *Δemm18*-infected mice showed dramatically reduced areas over the course of the infection compared to wildtype-infected mice (**Figure 19B, 19D**), they revealed no differences in bacterial load within these lesions at 72-hours (**Figure 19C**). Unexpectantly, *Δemm18*-infected mice trended for greater bacterial recovery within lesions, however, bacterial CFUs were not significantly higher than wildtype-infected mice (**Figure 19D**). Overall, we conclude that expression of M18 protein does not offer a competitive advantage for *S. pyogenes* MGAS8232 to establish acute infections of the nasopharynx or skin in B6$_{HLA}$ mice.

Figure 19. M18 protein expression by *S. pyogenes* MGAS8232 does not promote bacterial density during skin infection in B6_{HLA} mice.

B6_{HLA} mice were intradermally administered ~2.5 x 10^7 CFUs in each hind flank with *S. pyogenes* MGAS8232 wildtype or Δ*emm18*. **A.** Weights of B6_{HLA} mice at 24-, 48-, and 72-hours following skin challenge. Weights represented as a percentage (%) of day 0 weight. **B.** Skin lesion areas following skin challenge at 24-, 48-, and 72-hours post-infection. Bars represent mean ± SD. Significance determined by two-way Šídák ANOVA (****, $P < 0.0001$). **C.** Bacterial CFUs from individual infected skin abscesses normalized to the weight of excised skin tissue at 72 hours. Bars represent mean ± SD. Significance determined by unpaired *t*-test ($P = 0.2720$, data not significant). **D.** Photographic representation of skin lesions at 72-hours post-skin challenge with *S. pyogenes* MGAS8232 wildtype and Δ*emm18* strains.
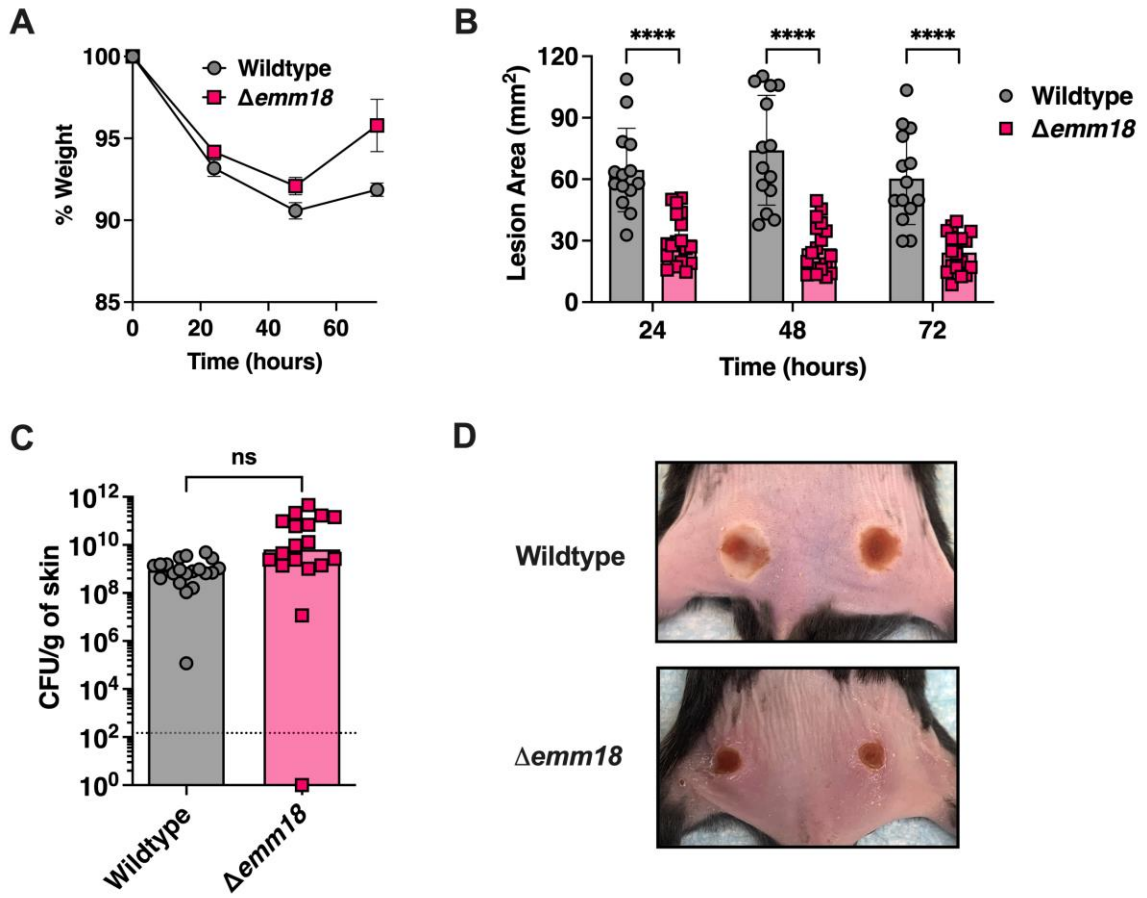
3.4   Discussion

Protective immunity against *S. pyogenes* has historically been ascribed to the accumulation of protective antibodies against type-specific regions of the M protein. Vaccines consisting of four [180], six [181,182], eight [183], twenty-six [184–186], and thirty [187] N-terminal peptides from various serotypes have demonstrated bactericidal responses, yet protection from disease has not been established. In the present study, mice were immunized with distinct monovalent M protein vaccines and subjected to acute experimental infections to either provide support or possibly refute the focus of serotype-specific immunity. Since pharyngitis and impetigo are the most common manifestations, we evaluated the effectiveness of monovalent M protein vaccines in preventing experimental nasopharyngeal and skin infections. While this work supports that M protein vaccination induces high systemic levels of M protein-specific IgG, these responses fail to prevent infection by *S. pyogenes* in the nasopharynx and skin of B6$_{HLA}$ mice. We also show that genetic deletion of the M18 protein in *S. pyogenes* MGAS8232 did not reduce nasopharyngeal or skin bioburdens. Our findings indicate that peripheral antibodies raised against M proteins are not protective against acute experimental infections and suggest that subcutaneous M protein vaccinations may not be optimal strategies for *S. pyogenes* vaccine development.

In the current study, we leveraged our previously described robust B6$_{HLA}$ model [157] to further our understanding of streptococcal-host interactions with a focused goal to evaluate serotype-mediated protection. M3 serotypes, including MGAS315, are common causes of pharyngeal and severe invasive infections globally with unusual high rates of morbidity and mortality [341]. The M12 serotype HKU16 strain is representative of a massive scarlet fever outbreak in the Far East [143,342], and the M18 serotype MGAS8232 strain is a pharyngeal isolate from an acute rheumatic fever outbreak in Utah [269]. Lastly, NGAS979 is an M74 serotype skin isolate from Thunder Bay, representative of an explosive invasive strain that expanded across Canada beginning in 2015 [339]. Notably, each of these strains infect the nasopharynx of mice in an HLA-dependent manner (**Figure 11**), which reinforces that HLA expression is important for modeling infections in mice across a number of contemporary *S. pyogenes* strains. Pharyngeal colonization is considered the

major reservoir for *S. pyogenes* in developed countries and skin infections (impetigo) are much more prevalent in resource poor settings [278], and thus, the ability to cause acute skin infection in $B6_{HLA}$ mice was next examined. MGAS315 and MGAS8232 produced larger lesions and prompted greater weight loss over the 72-hour infection period compared to mice injected with HKU16 or NGAS979 strains, but bacterial recovery by each strain was comparable (**Figure 12**). Since NGAS979 belongs to *emm*-type pattern D typically associated with skin tropism [343], it was anticipated to cause more severe soft tissue infections, however, lesions were smaller than those caused by MGAS315 and MGAS8232 strains and bacterial burden remained confined to the injection site (data not shown). The $B6_{HLA}$ infection model does have limitations whereby many superantigens are not functionally active, likely due to the inability of most streptococcal superantigens to target mouse Vβs [156,157], however, *S. pyogenes* NGAS979 encodes SpeA [339] which has been shown to promote infection in $B6_{HLA}$ mice [156]. Furthermore, the role of plasminogen remains an important issue for all murine models as streptokinase activates human, but not mouse, plasminogen. By binding human plasminogen, streptokinase clears fibrin clots and ECM components in skin tissue, permitting bacteria to enter deeper tissue and blood more readily [167]. Since streptokinase is not active in $B6_{HLA}$ mice, this may represent a limitation for this model in *S. pyogenes* skin pathogenesis. In our skin infection model, *S. pyogenes* does not enter the blood and spread to other organs (data not shown) and it remains possible that these strains have reduced virulence in absence of human plasminogen, yet the plasminogen system is only one of many factors implicated in skin invasion [344]. Additionally, intradermal injections force bacteria to bypass the epidermal skin layer and may not reflect the superficial aspect of *S. pyogenes* skin infections as it is known to enter only broken skin [345]. Models that more closely mimic physiological conditions under natural conditions, such as the skin scarification method [345], should be considered for future studies. Nevertheless, each of the strains used in this study were able to colonize and cause acute nasopharyngeal and skin infections in $B6_{HLA}$ mice, and this led us to explore whether M protein-based immunizations generated antibody-mediated protection using these models.

As expected, M3, M12, M18, and M74 immunizations mounted robust systemic M protein-specific IgG titers, but these M protein antibodies were not protective against acute nasopharyngeal or skin infections in these non-invasive models (**Figure 14, Figure 15**). Previous vaccine studies have shown that humoral responses against M protein can prevent severe disease [334,335], and the results of this study were therefore unexpected. The discrepancy of immunological protection may be explained by the route of vaccine administration. Similar reported studies reveal that parenteral immunization fails to reduce mucosal infection by *S. pyogenes,* despite induction of high levels of serum IgG [246,335], yet the same vaccine administered by the intranasal route was able to induce protection against intranasal *S. pyogenes* challenges [246,335]. Interestingly, early human clinical trials using monovalent M3 and M12 protein immunizations significantly reduced rates of throat colonization and clinical illness in only recipients of intranasal vaccination compared with patients immunized systemically [178], and serum antibody responses were not reliable indicators of resistance against pharyngitis or colonization [178]. Recently, Influenza immunization studies demonstrated enhanced antiviral immunity when a protein-based vaccine was administered only intranasally and not by alternate parenteral routes [346], and this was correlated with local IgA secretion rather than circulating antibodies alone [346]. The lack of protection by parenteral immunization may be due to the absence of mucosal recall responses at the targeted site of infection. Parenterally vaccinated mice fail to mount Th17/IgA responses in lungs compared to intranasally vaccinated mice [335], and since lymphocytes primed in the lungs have strong tropism to airways, parenteral immunization may not induce T cell responses with mucosal homing markers [347–349]. Multiple studies demonstrate important protective roles for Th17 cells against intranasal *S. pyogenes* infections [243,301,303], however, priming must occur in the mucosal compartment in order to promote protective immune responses locally. Mucosal immunizations activate antigen-responsive T cells that differentiate into tissue-resident memory T cells (T_{RM}) and respond rapidly to antigen rechallenge, recruiting neutrophils to limit subsequent pathogen exposure [350]. Alternatively, they can be 'pulled' to the infected compartment shortly after their priming. This has been accomplished by adding an intranasal booster immunization to a vaccination strategy that already involves parenteral immunizations, which 'pulls' systemic antigen primed Th17 cells to the targeted

mucosal site to increase resident Th17 memory T cells and accelerate local IgA recall responses; boosting the effects from parenteral vaccination [351,352].

The results of this study are in striking contrast to our previous vaccination work that demonstrate protective effects using subcutaneous immunizations with SpeA. In this work, immunization of B6$_{HLA}$ mice with inactive SpeA toxoid in alum generated serum anti-SpeA IgG antibody titers that prevented experimental nasopharyngeal infection by *S. pyogenes* MGAS8232 [157]. Furthermore, passive immunization with anti-SpeA antibodies prevented nasopharyngeal infection [157], and thus, a protective role for systemic IgG alone cannot be excluded for prevention against acute *S. pyogenes* infections. Likewise, parenteral immunizations have resulted in remarkable protection against a number of mucosal pathogens, including *Haemophilus influenzae* type b, *Streptococcus pneumoniae,* and *Neisseria meningitidis* [353], capable of inducing mucosal effector cells and highly neutralizing antibodies. It was recently demonstrated that protective pneumococcal-responsive IL-17A$^+$CD4$^+$ T$_{RM}$ cells accumulate in the nasopharynx following either intranasal or subcutaneous vaccination of killed pneumococci [350]. While cellular responses following subcutaneous immunizations were not characterized in this study, it cannot be excluded that they could still be contributing to immune responses against *S. pyogenes* via parenteral immunization. Together, protection against upper respiratory tract and skin infections is a requirement for any *S. pyogenes* vaccine, and a subcutaneous-based immunization strategy that induces significant M protein IgG antibodies in serum may not be sufficient by itself to provide immunity against *S. pyogenes*. It will be important to determine in future experiments if intranasal routes of M protein immunizations are more optimal to induce protective serotype-based immunity, and if local, rather than systemic, responses mediate this protection.

An overarching concern with M protein-based vaccines is that there are over 220 known streptococcal *emm*-types identified with varying distributions worldwide, and this presents a possible complication of low coverage for type-specific vaccines. Particularly, the diversity of *emm*-types circulating in low-income countries, where disease is endemic, differs considerably between regions [191,354]. Recent findings have shown that the 30-valent vaccine would protect against the majority of invasive- and pharyngitis-associated

emm-types in North America and Europe and produce cross-reactive antibodies that recognize other additional *emm*-types [37,184,192,355], however, targeting the hypervariable N-terminal region of M proteins does not protect against all globally circulating *S. pyogenes* serotypes [356]. Therefore, it is considered unlikely that a universally protective vaccine will ever arise from just targeting the hypervariable immunogenic region of the M protein. Furthermore, the absence of dominating serotypes through vaccination may select for and replace vaccine-containing serotypes with expanding *emm*-types not included in the vaccine, known as serotype replacement. This would result in a new skewed serotype distribution that would erode the benefit of vaccination and make it difficult and costly to tackle the remaining burden of disease. In resource-poor settings, it is not uncommon for individuals to be co-colonized with multiple strains of *S. pyogenes* at once [357]. If vaccine and non-vaccine containing serotypes compete in a single host, this could unmask minor serotypes that would now benefit from removal of competitors and increase in prevalence. Another important consideration for M protein-based vaccines is the opportunity for antigenic drift. High-frequency, intragenic recombinational events have been reported to occur within repeat regions of M proteins, which has the possibility of producing size variant derivatives of a particular strain and may even generate new serotypes. In the type 6 M protein from *S. pyogenes* D471, recombination events within the A-repeat block of M6 led to a significant decline in the opsonization ability of monoclonal antibodies directed at this region [358]. Furthermore, sequence variations have been identified in nonrepeating N-terminal regions of several strains identified serologically as the same M1 serotype [359,360], which may ultimately affect the efficacy of opsonic antibodies due to antigenic drift. An alternative approach to is to target cryptic epitopes found within the highly conserved C-repeat domain of the M protein, which has the potential to induce protection against most, if not all, *S. pyogenes* strains. Antibodies against highly conserved epitopes may not be considered a result of natural infection [361], but their immunogenicity is enhanced when fused to highly immunogenic carrier proteins. Extensive studies, particularly of the J8 vaccine candidate, show induction of opsonic antibodies, long-term B cell memory, and protection against nasal [205,206], skin [199,202], and systemic infections in mice [158,197,198,200,202,207]. The efficacy of the J8-DT vaccine, however, is greatly

impaired against CovR/S mutants, including the global epidemic hypervirulent strain M1T1 [202].

Furthermore, a remaining major hurdle for M protein-based vaccines is the theoretical possibility of inducing autoantibodies. Although historical studies that administered crude whole M protein preparations to human volunteers demonstrated reduced pharyngeal colonization [177,178,362], there were reports of increased ARF incidences for some immunized participants [363]. This led to a U.S. federal ban on testing *S. pyogenes* vaccines in humans that lasted for over 30 years [364]. Identifying protective from autoimmune epitopes has since remained a focus of M protein vaccine strategies so that vaccine preparations would not activate autoimmune responses. Multiple studies have shown that vaccine formulations targeting type-specific hypervariable N-terminus epitopes are least likely to cross-react with host tissues [181,188,189], and epitopes located in the middle of the mature M proteins, including B and C repeat regions, are more likely to express cross-reactivity [365–370]. However, passive transfer of hypervariable A-repeat region-specific T cells from M5 immunized rats produced valvulitis in naïve rats [366]. Consequently, M protein-based immunizations are unlikely to be universally safe from inducing cross-reactive immune responses, and thus, a vaccine composed of other conserved antigens or multiple bacterial components known to be crucial for infection and survival of *S. pyogenes* may be more successful candidates.

Our findings demonstrated that serum antibodies against the M protein did not prevent acute infections, and this led us to further analyze the necessity of M protein expression during acute infections in B6$_{HLA}$ mice. Chromosomal deletion of the *emm18* gene was created in *S. pyogenes* MGAS8232 and used to infect the nasopharynx and skin of mice. We discovered that removal of M18 protein had no impact on bacterial burden as Δ*emm18* mutant recovery was similar to wildtype at both sites of infection (**Figure 17, Figure 19**). Interestingly, Δ*emm18* mutant displayed significantly smaller skin lesions throughout the 72-hour skin infection model (**Figure 19**), although this did not correlate to lower bacterial load within infected lesions. Previous studies demonstrate that M proteins induce potent inflammatory responses by stimulating T cell proliferation [371] and monocyte and

neutrophil activation [372–375] to promote the secretion of IL-1β, IL-6, TNF-α, and IFNγ. M proteins have also been shown to form complexes with fibrinogen that bind β2 integrins and induce the release of heparin-binding protein from neutrophils and monocytes to promote vascular leakage [372,373], as well as activate NLRP3 inflammasome activation [374]. Conversely, it has also been shown that the B- and C-repeat regions of the M5 protein may have a role in modulating inflammatory potential through induction of anti-inflammatory IL-10 secretion by macrophages, however, IL-10 secretion had no effect on the output of IL-6, TNFα and IL-1β [375]. We propose that robust tissue inflammation induced by M protein expression likely contributes to larger lesion sizes observed in this study and recent reports showing that keratinocytes recognize soluble M protein as a PAMP to release innate inflammatory response alarms [376] support this. Nevertheless, our studies do not support significant proinflammatory cytokine induction by the M protein as no significant differences in proinflammatory cytokines were observed in the nasopharynx of mice inoculated with MGAS8232 wildtype and Δ*emm18* strains (**Figure 17; Appendix 6**), however, cytokine levels within infected skin lesions were not measured. Our experiments also demonstrate the profound effect of resisting phagocytosis by M18 protein expression, while adherence to pharyngeal epithelial cells was unchanged by Δ*emm18* (**Figure 16**). Although its role as a major streptococcal adhesin has been under great debate (reviewed in [70]), evidence that M proteins inhibit complement deposition and prevent opsonophagocytosis has received overwhelming support (reviewed in [124]). Though it remains possible that functionally redundant bacterial components may compensate for deletion of the M protein during acute infections, important limitations to the presented models are considered. B6$_{HLA}$-transgenic mice may be sensitive to proinflammatory effects triggered by superantigens; however, M proteins promote *S. pyogenes* virulence by binding several human-specific, but not mouse, complement inhibitors. Consequently, B6$_{HLA}$ mice are unlikely the most suitable model to fully recapitulate pathogenic mechanisms of M proteins with the innate immune system. Transgenic mouse models that express human C4BP and/or human Factor H demonstrate reduced *S. pyogenes* uptake by neutrophils and greater bacterial burden and dissemination during invasive disease compared to wildtype BALB/c mice [161], and thus, may be more appropriate to model M protein human-specific interactions with complement inhibitors. Furthermore, binding human plasminogen

promotes the degradation of fibrin clots, connective tissue, and the ECM [166]; and introduction of the human plasminogen transgene into mice has been shown to promote M protein-mediated pathogenesis during invasive disease [172]. Further experimentation using mice that are humanized in ways relevant to M protein function may be required to fully elucidate the mechanism of M proteins during acute nasopharyngeal and skin infections, however, the contribution of superantigen activity cannot be accounted for within these models.

To conclude, several M protein monovalent immunizations were performed in this study to assess their ability to generate M protein-specific antibodies *in vivo* and to determine whether these humoral responses were protective against acute *S. pyogenes* infections in B6$_{HLA}$ mice. While this work supports the induction of significant M protein-specific IgG antibodies following immunizations, these responses fail to prevent experimental nasopharyngeal and skin infections by homologous *S. pyogenes* strains. Our findings also reveal that genetic deletion of M18 protein in *S. pyogenes* MGAS8232 did not reduce bacterial burdens in nasal turbinates or skin lesions of mice. Although the majority of *S. pyogenes* vaccine research focuses on enhancing immunity against streptococcal M proteins, this study indicates that parenteral M protein immunizations are not protective against acute infections and are, therefore, not optimal approaches for vaccine consideration. From this work, future studies should focus on defining M protein immune responses using multiple routes of vaccine administration, and to determine whether the functional activity of M proteins is enhanced and necessary for acute infections in the presence of human complement inhibitors. Recent advances in controlled human infection models [377,378] may overcome barriers to describing the importance of M protein in the establishment of acute infections and for defining the efficacy of M protein-based vaccines. Analyzing M proteins from these perspectives will have wide-reaching implications on therapeutic approaches against this globally prominent pathogen.

Chapter 4: Repeated nasopharyngeal challenges with *S. pyogenes* MGAS8232 impairs left ventricle function in HLA-transgenic mice

4.1   Introduction

S. pyogenes is a major bacterial pathogen that continues to cause a vast amount of human illness worldwide, ranging from mild localized infections to life threatening diseases. Importantly, ineffective treatment or recurring *S. pyogenes* infections can provoke autoimmune post-infection sequelae whereby the host's immune system not only generates a response against the invading organism but also against self-antigens [4]. Acute rheumatic fever (ARF) is a delayed multifactorial inflammatory illness that generally appears around 2-3 weeks following *S. pyogenes* pharyngeal and possibly skin infections [8,45,47,320,379]. Together with a positive throat culture or serological evidence of prior *S. pyogenes* infection, diagnosis of ARF involves various combinations of minor and major manifestations that reflect tissue involvement, and these manifestations are outlined in the updated Jones criteria (**Table 1**). Clinical presentations include fever, joint swelling and pain, chorea, subcutaneous nodules on the skin, and carditis. While most clinical features eventually resolve, inflammation and damage to cardiac valves can persist and result in valvular regurgitation or stenosis, and this chronic valvular autoimmune damage is classified as rheumatic heart disease (RHD). Subsequent or repeated streptococcal infections can exacerbate ARF symptoms and valve injury, therefore, secondary antibiotic prophylaxis may reduce the risk of ARF recurrences and slow the progression and severity of disease in patients with established RHD [46,380]. Determinants of ARF and RHD progression are poorly understood, and initial clinical presentations can range from asymptomatic valvular dysfunction to heart failure.

For most human autoimmune diseases, a defining exogenous trigger required for the development of disease is not known, however, prior pharyngitis by *S. pyogenes* is wildly accepted as playing a causal role for development of ARF and RHD [11]. In susceptible individuals, host responses intended to clear streptococcal infections also inadvertently recognize and express immunological cross-reactivity to host tissue through a process known as molecular mimicry. Molecular mimicry occurs when antibody or T cell epitopes are shared between the host and microorganism, which occurs when distinct molecules present either identical or homologous amino acid sequences, or when epitopes are shared by entirely different chemical structures [381]. If cross-reactivity is sufficiently robust, or

if specific autoreactive targets are not normally "visible" to the immune system, there may be a loss of self-tolerance resulting in autoimmune manifestations. In cases of ARF, cross-reactive host antigens can reside in the skin, joints, brain, and heart; however, chronic autoimmune responses against heart valves are the most severe and can lead to RHD and possibly cardiac failure. In support of the molecular mimicry hypothesis, researchers have defined antibody-mediated cross-reactivity as initiators of cardiac autoimmune responses, followed by cellular infiltration of the endocardium and valve tissue. Autoantibodies that react with the valve endothelium form immune complexes and upregulate vascular cell adhesion protein 1 (VCAM1) on the valve surface, which attracts VLA-4 on activated T cells [382–384] and leads to extravasation of autoreactive T cells into the valve. Granulomatous lesions containing both T cells and macrophages can form as a result of this inflammatory process and are mainly mediated by $CD4^+$ T cells [366,385–388]. Persistent inflammatory responses at the valve tissue can destabilize its structural integrity and consequently result in valve dysfunction [389,390]. Examination of humoral responses from ARF/RHD patients and animal models revealed that antibodies that recognize the *S. pyogenes* surface M protein cross-react with similar α-helical coiled-coil host structures, including myosin, tropomyosin, laminin, vimentin, and keratin [381]. Mutations that specifically destabilize the α-helical structure of the M protein prevent its recognition by streptococcal antibodies that cross-react with cardiac myosin [391], supporting that α-helical protein epitopes are important targets of autoantibodies. Similarly, autoreactive T cells isolated from either the peripheral blood or rheumatic mitral valves of ARF and RHD patients have also been shown to react strongly and proliferate in response to M protein and host myosin peptide stimulation [392–394]. Kirvan and colleagues demonstrated that rat T cell lines specific for streptococcal M5 protein can passively transfer valvulitis into naïve rat recipients, characterized by infiltration of $CD4^+$ cells and upregulation of VCAM-1 at the valve endothelium [366]. Autoantibodies that target α-helical structures have also demonstrated cross-reactivity with the immunodominant epitope of the surface group A carbohydrate antigen, *N*-acetyl-β-D-glucosamine (GlcNAc) [395–398]. Although once thought to be conflicting, cross-reactive monoclonal antibodies that arise from molecular mimicry can be polyreactive and recognize epitopes shared by multiple antigens, and thus, epitope redundancy may be an important factor in autoimmune disease development [381].

Since no other known natural host or environmental reservoir of *S. pyogenes* exists, post-streptococcal autoimmune complications are strictly a human condition and modeling these disease complications in animals is particularly challenging. One major barrier in the field of ARF/RHD research has been the lack of a universally accepted and valid animal model. A suitable model requires initiation and progression of the pathological mechanisms to be identical or similar in the animal compared with the human condition. Early experimental work assumed that direct injury to cardiac tissues was produced by *S. pyogenes* toxins, and these studies introduced whole bacteria or crude streptococcal preparations into a variety of animals, including mice, rats, rabbits, guinea pigs, swine, sheep, etc., (reviewed in [399]). Despite numerous attempts, these animals did not present the representative pathology and a relevant animal model for ARF/RHD remained elusive for many years. Currently, the dominant *in vivo* valvulitis model utilizes the Lewis rat [366,370,386,387,400,401]. This model employs an immunization of 500 μg of recombinant M protein emulsified in CFA followed by 2 injections of heat killed *B. pertussis* cells as a Th1-polarizing co-adjuvant at days 1 and 3, a booster immunization at day 7 with M protein in IFA, and rats sacrificed at week 3 [366,370,386,387,400,401]. Although the Lewis rat model does not use a live infection, it was the first model to induce hallmark pathological features of the mitral valve, including infiltration of CD4$^+$ cells and macrophages, upregulation of VCAM-1, and the induction of granulomatous Aschoff bodies [366,386,387]. Autoantibodies that cross-react with various regions of recombinant M5 protein and cardiac myosin were also produced in these animals [387,401]. Together, these observations demonstrated that M protein immune responses stimulate pathological features that closely reflect the human condition, and this model was termed the rat autoimmune valvulitis (RAV) model [386].

While the RAV model has been instrumental in characterizing key aspects involved in the in ARF/RHD responses, the model design and its portrayal of autoimmune development contains limitations. Immunopathological features are detected in the RAV model, but it has not been validated whether animals develop measurable impairments to cardiac function. Recently, electrocardiogram changes including prolongated P-R intervals and echocardiographic identification of mitral valve thickening has been observed [401],

however, extensive characterization of left ventricle function has not been fully demonstrated. With the advantage of a safe, non-invasive, and reproducible technique, echocardiography has become an essential tool for grading the severity of valvular disease and for assessing left ventricle diastolic and systolic functions. In 2001, a WHO expert consultation on ARF and RHD established a consensus for echocardiographic diagnosis of subclinical RHD to enhance its early detection and prevent its advanced disease state [380]. Echocardiographic screening has shown a significant (up to 50-fold) increase in RHD detection in multiple studies of school-aged children compared to conventional methods [402–405]. Furthermore, since the RAV model does not use a live bacterial infection, the omittance of additional bacterial components expressed during infection may provide a secondary signal for disease induction, such as innate immune activation and significant cytokine production. Together, the availability of an animal model that involves live *S. pyogenes* infections, demonstrates key valvular pathological features, and assesses cardiac function through echocardiographic screening is crucial to further our complete understanding of the ARF and RHD disease process.

Although animal models of RHD exist (reviewed in [406]), key mechanisms of disease development remain incomplete due to the lack of a live and relevant infection model. A robust mouse model would be extraordinarily powerful due to the availability of genetically engineered mice, along with genetically defined bacterial strains to evaluate specific *S. pyogenes* virulence factors in disease development. Furthermore, repetitive infections, particularly of the nasopharynx, as a predisposing condition to development of ARF/RHD also remains largely unassessed. In our study, we aim to investigate a genetically susceptible mouse model that involves repeated nasopharyngeal infections with *S. pyogenes* and echocardiogram imaging to evaluate left ventricle function. We further aim to examine the role of the streptococcal M protein on cardiac function by comparing the use of a mutant strain that lacks M protein expression on its surface. Analysis of M protein responses in the context of cardiac imaging will provide valuable insight into the mechanism of valve damage following live infections and will guide future research that assess autoimmune responses triggered by *S. pyogenes* infections.

4.2   Materials and Methods

4.2.1   Bacterial growth conditions

A complete list of bacterial strains used in this chapter are found in **Table 7.** Molecular cloning experiments utilized *E. coli* XL1-Blue with growth conditions outlined in Section 2.2.1. *S. pyogenes* was grown under the same conditions outlined in Section 2.2.1.

4.2.2   Construction of deletion mutants

Details on DNA manipulations are described in Section 2.2.2. A complete list of plasmids and primers used in this chapter are described in **Table 7** and **Table 8** respectively. Briefly, standard molecular cloning techniques were used to generate an in-frame clean deletion of the M18 protein and GlcNAc, encoded by the *emm18* and *gacI* genes respectively, within the *S. pyogenes* MGAS8232 genome. Primers were designed to amplify the upstream and downstream regions of *emm18* and *gacI* and replace the wildtype genomic sequences with the deletion constructs through homologous recombination using the Gram-positive *E. coli* shuttle vector pG$^+$host5. All mutants were confirmed by PCR and DNA sequencing.

4.2.3   *In vivo* experiments

4.2.3.1   Ethics statement

All mouse experiments were conducted in accordance with the Canadian Council on Animal Care Guide to the Care and Use of Experimental Animals. The Animal Use Protocol (AUP) numbers 2017-024-D, and 2020-041-D were approved by the Animal Use Subcommittee at Western University (London, ON, Canada) (**Appendix 2**).

4.2.3.2   Mice

Mice utilized in this study were transgenic C57BL/6 (B6) mice expressing HLA-DR4 and DQ8 (herein referred to as B6$_{HLA}$ mice) as listed in **Appendix 3** and were bred as described in Section 2.2.9.

Table 7. Bacterial strains and plasmids used in Chapter 4.

Strain/Plasmid	Description	Source
Streptococcus pyogenes		
MGAS8232	M18 serotype isolated from a patient with acute rheumatic fever (GenBank accession: NC_003485.1)	[269]
MGAS8232 Δ*emm18*	*emm18* deletion mutant derived from MGAS8232	This study
MGAS8232 Δ*gacI*	*gacI* deletion mutant derived from MGAS8232	This study
Escherichia coli		
XL1-Blue	General cloning strain	Stratagene
Plasmids for cloning		
pG⁺host5	Temperature-sensitive Gram-positive/*E. coli* shuttle vector; Erm^r	Appligene [270]
pG⁺host5::Δ*emm18*	pG⁺host5 with *emm18* flanking regions inserted	This study
pG⁺host5::Δ*gacI*	pG⁺host5 with *gacI* flanking regions inserted	This study

Abbreviations: Erm^r - erythromycin resistance

Table 8. Primers used in Chapter 4.

Primer	Primer Sequence (5′→ 3′)[a]
Primers for *emm18* chromosomal deletion construct	
Emm18 up *Bam*HI For	CCC<u>GGATCC</u> TTGATGAGTTAGATTGTTTGACAATTGATCTAGTAGAG
Emm18 up *Pst*I Rev	CCC<u>CTGCAG</u> TCTATTTGCATCTTTTCTAACCATTATTTGCTCC
Emm18 down *Pst*I For	CCC<u>CTGCAG</u> CTAAAACGCAAAGAAGAAAACTAAGCCTTTAGAA
Emm18 down *Kpn*I Rev	CCC<u>GGTACC</u> TGTGTCGTCCTTTCCTGATGAGAG
Primers for *gacI* chromosomal deletion construct	
gacI up *BamHI* For	CCC<u>GGATCC</u> GGCCAAACCTCATACGATTAGTG
gacI up *PstI* Rev	CCC<u>CTGCAG</u> AGGAATAATGATTAACTTTTTCACGAAAACTTCTCC
gacI down *Pst*I For	CCC<u>CTGCAG</u> GTTAGATTGAAAGGAAATCGTTAAAATGACGGTAA
gacI down *Kpn*I Rev	CCC<u>GGTACC</u> CGAATGACCAATGTCATAATACATTAT
Primers for sequencing and screening	
M13 For	GTAAAACGACGGCCAG
M13 Rev	GTCATAGCTGTTTCCTG
T7 For	TAATACGACTCACTATAGGG
T7 Rev	CGCCAGGGTTTTCCCAGTCACGAC
emm18 Screen For	CAGGAGTTTGTGGGGTTTTGGTTTC
emm18 Screen Rev	CGGTAATTTTTTGAAAAAGTACATCGGTGAG
gacI Screen For	ATTTTTCTTCTTCAGTATCTGTTCTT
gacI Screen Rev	ACTGTTTTGAAATGAAATATTACTTAATAA

[a] Underlined sequences in primers indicate restriction endonuclease sites used for cloning purposes.

Abbreviations: For, forward; Rev, reverse

4.2.3.3   Repetitive infection model

Details on *S. pyogenes* dose preparation and nasopharyngeal inoculation are described in detail in Sections 2.2.9. In this study, baseline echocardiograms were performed on B6$_{HLA}$ mice prior to receiving five nasopharyngeal challenges two weeks apart. Mice were imaged again at week 9 and sacrificed at week 10 or subjected to two additional nasopharyngeal challenges (two weeks apart), followed by echocardiogram acquisition at week 13 and sacrifice at week 14. At euthanasia, terminal bleeds were collected for antibody assessment. A schematic of the repetitive infection model is illustrated in **Figure 20.**

4.2.4   Antibody titer analyses

Serums from terminal bleeds were used to assess IgG antibody levels by ELISA following repetitive infection by *S. pyogenes* as described in detail in Section 3.2.7.

4.2.5   Multiplex cytokine array

For cardiac cytokine array, serums of mice following repeated infections were diluted 2-fold and sent to Eve Technologies (Calgary, AB, Canada) for the evaluation of 9 cytokine concentrations involved in cardiac injury. Cytokine concentrations are found in **Figure 26** and **Appendix 7**. Cytokine and chemokine concentrations in cNT homogenates of mice nasally infected with *S. pyogenes* were measured according to Section 2.2.10 using the 32-Plex array from Eve Technologies (Calgary, AB, Canada). Uninfected cNT homogenates were collected for background comparisons. Data on heat maps is presented as normalized median cytokine responses ($X_{normalized} = [(x - x_{min})/(x_{max} - x_{min})]$) from cNT homogenates of all nasally infected mice ($n \geq 3$). Statistical analyses were completed by completed by one-way ANOVA with Kruskal-Wallis post-hoc test and Dunn's multiple comparisons test. Quantitative cytokine levels are shown in **Appendix 8**.

Figure 20. Model of repeated *S. pyogenes* nasopharyngeal infections in B6$_{HLA}$ mice.
B6$_{HLA}$ mice were exposed to recurrent nasopharyngeal infections of ~10^8 CFUs of *S. pyogenes* MGAS8232 wildtype or $\Delta emm18$ every other week for 13 weeks. Echocardiogram images were taken by the VisualSonics Vevo3100 ultrasound imaging system at week 0, week 9, and week 13. Image analyses were kept blind until the end of the study. At week 14, mice were sacrificed, and their serum and hearts were harvested.
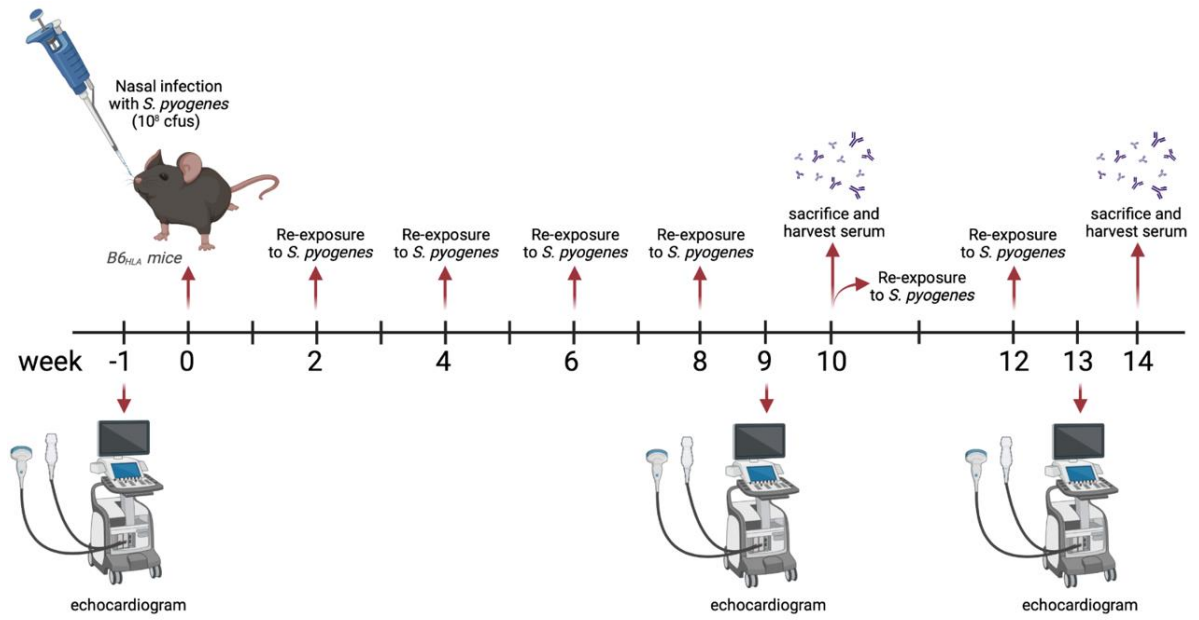
4.2.7   Echocardiogram imaging

4.2.7.1   Animal set-up

Echocardiography was performed to measure basic cardiac function in mice as previously described [407,408]. Briefly, we used an ultra-high frequency linear array transducer (MX550S, 25-55 MHz, center transmit 40Hz, axial resolution 40 μm) coupled to a Vevo® 3100 high resolution imaging system (FUJIFILM VisualSonics; Toronto, Ontario, Canada). Animals were sedated with 3% isoflurane (Baxter International, Deerfield, Illinois, USA) and secured in a supine position on the Vevo mouse handling platform (FUJIFILM VisualSonics; Toronto, Ontario, Canada). The platform was set to 42°C and a heat lamp was closely secured to help maintain core temperature at 37°C. Continuous monitoring of body temperature by a rectal probe was used to aid in heat regulation. Following the removal of fur on the chest by over-the-counter hair removal cream (Nair™), ultrasound gel (Parker Laboratories Fairfield, New Jersey, USA) was applied on the chest. For examination, isoflurane concentrations were reduced to 1-2% to achieve comparable heart rates (HR) during image acquisition. HR were kept consistent between experimental groups (400–500 bpm) and were continuously monitored by electrocardiogram (ECG) recordings obtained from the limb electrodes on mouse handling platform to minimize cardio-depressive effects from the anesthetic. HR values were obtained and reported in real-time together with images. Photographic representation for echocardiogram imaging set-up of an anesthetized mouse is shown in **Figure 21.**

4.2.7.2   Cardiac image acquisition

All animals were scanned and recorded in the parasternal long-axis (PSLAX) view for visualization of the left ventricle (LV) in its maximum dimension from apex to base. B-mode cine loops were recorded and stored for LV image analyses. Particular attention to avoid truncated views or foreshortening of the LV was taken. All animals were scanned in short-axis (SAX) view, taken at the midpapillary level of the LV by rotating transducer position in PSLAX view 90° clockwise. The papillary muscles served as anatomical landmarks for standardized views. M-mode images were assessed in SAX view to determine wall thicknesses. Additionally, all animals were scanned in the apical four-

Figure 21. Echocardiogram image acquisition of an anesthetized mouse.

Preparation of a mouse for an echocardiogram exam using the Vevo® 3100 high resolution imaging system. An anesthetized mouse is placed in a supine position on the pre-warmed mouse handling platform in a nose cone to maintain 1-2% isoflurane sedation level. A rectal probe is inserted into the mouse for continuous monitoring of physiological body temperature with a heat lamp secured close by to aid in heat regulation. The mouse's paws are taped down on or near the electrode pads on the handling platform and electrode cream is used to for ECG monitoring. Heart rates were continuously reported in real-time by ECG recordings. Following the removal of fur on the chest by hair removal cream (Nair™), ultrasound gel is applied, and a MX550S transducer is used for cardiac examinations.

Heat lamp

MX550S transducer

Isoflurane (1-2%)

Electrode pads

Rectal thermometer

Mouse handling platform
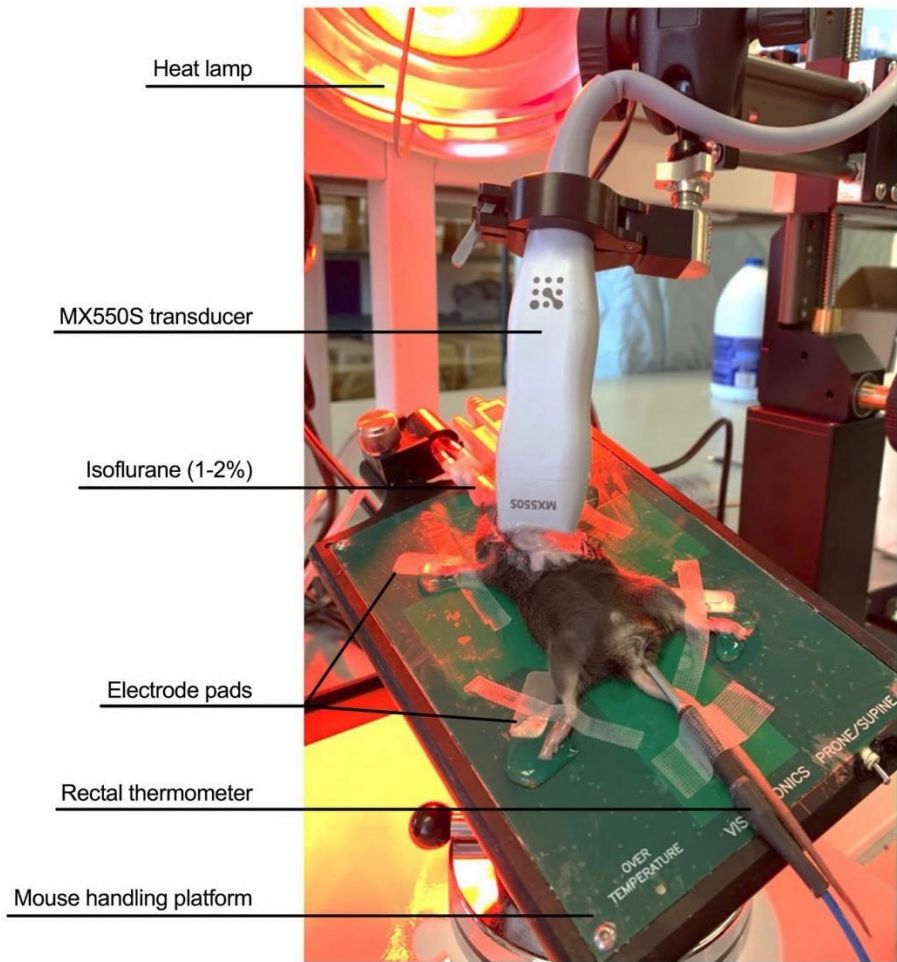
chamber view to allow for recording of colour and pulsed-wave (PW) Doppler flow velocities across the mitral valve. The view was obtained by placing the transducer over the apex and pointing it towards the animal's right shoulder, allowing the beam to cross both ventricles, both atria, and their respective walls and septa. The left atrium (LA) was routinely used as an anatomical marker to locate the mitral valve annulus, which separates the LA and LV. The sample volume was placed parallel to the blood flow and close to the tip of the mitral leaflets where velocity appeared the highest to record maximal transmitral flow velocities. For all image acquisitions, image depth, width and gain settings were used to optimize image quality. All images were acquired are stored digitally in a raw format (DICOM) for further offline analyses.

4.2.8 Echocardiogram analyses

Image analyses were performed by a single blind observer using the dedicated software package VevoLAB Version 5.5.6 (FUJIFILM VisualSonics, Toronto, Ontario, Canada). Despite the high heart rates of rodents, VevoLAB software displays acquired high-resolution images in adjustable slow-motion loops, permitting suitable analyses. Parameters assessed in each image mode are demonstrated in **Figure 22**.

4.2.8.1 Apical four-chamber image analyses

As in humans, LV diastolic function was assessed in mice with B-mode to visualize the apical four-chamber view. Colour and PW Doppler mode were used to extract the direction and velocity of flow. Colour Doppler allowed visualization of the general direction of blood flow, with movement toward the transducer indicated in red, and movement away from the transducer indicated in blue. LV filling velocity was assessed by the ratio between early and late diastolic transmitral Doppler flow velocities. The *E* wave represents the transmitral blood flow velocity during early LV filling phase (passive filling velocity), while the *A* wave represents the transmitral blood flow velocity during the atrial contraction phase (active filling velocity). The *E/A* ratio provides important information regarding the filling dynamics of the LV. The apical four-chamber plane allows extraction of values for *E* and *A* velocities, their ratios, mitral valve E wave deceleration time (DT), isovolumetric

Figure 22. Echocardiographic views of the left side of a mouse heart.

Echocardiogram images of B6$_{HLA}$ mice were acquired using the Vevo3100 imaging system under 1-2% isoflurane anaesthetic. Representative echocardiographic images of **(A)** parasternal long-axis **(B)**, parasternal short-axis in M-mode **(C),** apical four chamber view and **(D),** pulsed-wave Doppler of mitral valve inflow. LV, left ventricle; LA, left atrium; RV, right ventricle; Ao, aorta; LVAW;s, left ventricle anterior wall in systole; LVAW;d, left ventricle anterior wall in diastole; LVPW;s, left ventricle posterior wall in systole; LVPW;d, left ventricle posterior wall in diastole; LVID;s, left ventricle internal diameter in systole; LVID;d, left ventricle internal diameter in diastole; RA, right atrium; MV, mitral valve; E wave, MV early velocity; A wave, MV atrial velocity; NFT, non-flow time; IVRT, isovolumetric relaxation time; IVCT, isovolumetric contraction time; AET, aortic ejection time; MV decel, MV deceleration).

A

Long axis view
(diastole)

Long axis view
(systole)

B   Parameters assessed in Mmode

C   Colour Doppler in apical 4-chamber view

D   Parameters assessed in pulsed wave Doppler
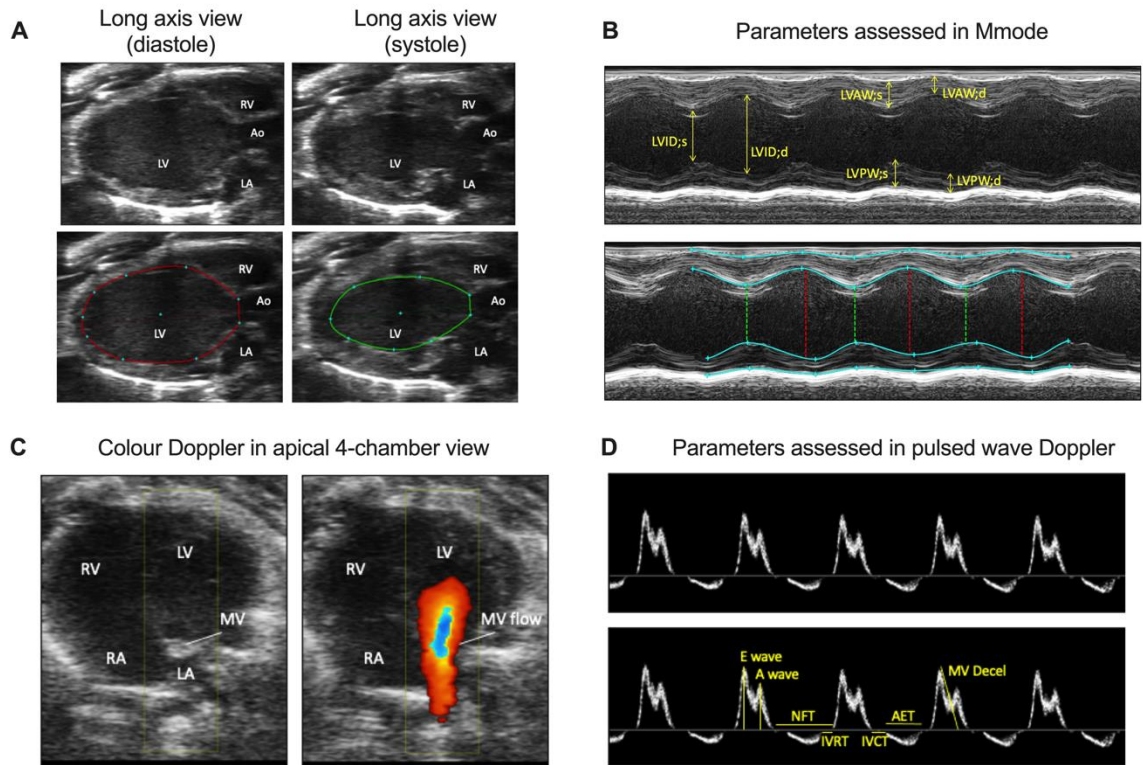
relaxation time (IVRT), isovolumetric contraction time (IVCT), mitral valve orifice, ejection time (ET) and myocardial performance index (MPI; TEI index).

4.2.8.2   Parasternal long-axis and short axis image analyses

Parameters of diastolic function (ejection fraction, EF; cardiac output, CO) were assessed manually in B-mode images derived from PSLAX views by using the LV trace tool in VevoLAB to trace the LV area in both end-diastole and end-systole positions from LV outflow tract to apex. The end of diastole corresponds to the frame in which the LV reaches its maximal extension, while the end of systole corresponds to the minimal size of the LV area. Calculations of 2DE-assessed cardiac volumes and EF were generated by VevoLab from LV traces. All B-mode cine loops were traced three times and averaged to account for inter-beat variability. M-mode images from the midpapillary region of the LV in SAX were analyzed for fractional shortening (FS), LV wall thickness and diameter through manual tracing of the endocardial and epicardial borders. Special care was taken to select cardiac cycles in which no deep breathing occurred to avoid plane movement of the myocardium.

4.2.8.3   Adhesion assay

Details for human cell culturing and epithelial cell adhesion assay procedures are outlined in Section 2.2.7. Briefly, Detroit-562 and A549 cells were grown to confluence on 12 or 24 well TC-treated plates and exponential phase *S. pyogenes* were inoculated onto cells at a MOI of 100 for 2.5 hours at 37°C in 5% CO_2. Following incubation, non-adherent bacteria were washed off and epithelial cells were lysed and serially diluted to enumerate remaining bacteria present.

4.2.9   *Ex vivo* experiments

4.2.9.1   Splenocyte preparation

Spleens were obtained from euthanized mice and immediately stored on ice in 5 mL of complete RPMI (cRPMI) media (RPMI-1640 [Life Technologies Inc.] supplemented with 0.1 mM minimal essential medium non-essential amino acids [Life Technologies Inc.],

10% [v/v] heat-inactivated FBS [Sigma-Aldrich], 100 units mL^{-1} penicillin [Life Technologies Inc.], 100 μg mL^{-1} streptomycin [Life Technologies Inc.], 1 mM sodium pyruvate [Life Technologies Inc.], and 2 mM L-glutamine [Life Technologies Inc.]).Spleens were gently pressed through a sterile 0.2 μm nylon mesh filter and the single-cell suspension was centrifuged at $450 \times g$ for 5 minutes. The cell supernatant was removed, and the pellet was loosened via racking. Red blood cells were lysed by addition of 1 mL ammonium chloride potassium (ACK) lysing buffer (Thermo Fisher Scientific Inc.) for 30 seconds. To stop lysis, 10 mL of PBS, pH 7.5 was added and the cells were spun as above. Cells were resuspended in 7 mL PBS and poured through a sterile 0.2 μm nylon mesh filter to remove cell debris, and the filter was additionally washed with 7 mL of PBS to ensure collection of all living cells. Cells were centrifuged as above, and the supernatant was discarded. Pelleted cells were loosened by racking and resuspended in 4 mL of cRPMI, and live cells were counted using Trypan Blue (Life Technologies Inc.) exclusion and resuspended to a concentration of 1.1×10^6 cells mL^{-1} as required for the indicated assay.

4.2.9.2   Mouse splenocyte activation assay

Mouse splenocytes were seeded at 2×10^5 splenocytes per well in a 96-well plate and were stimulated with 10-fold dilutions of recombinant proteins at the indicated concentrations and left to incubate at 37°C with 5% CO_2 for 18 hours. Cells were spun, and supernatants were removed and stored at -20°C until further experimentation. To assess T cell activation, IL-2 was measured using ELISA (mouse IL-2 ELISA Ready-Set-Go! Kit [Thermo Fisher Scientific Inc.]) according to manufacturer's instructions. Appropriate capture antibody was coated onto 96-well high-bind plates (Corning Costar 9018) overnight at 4°C in supplied carbonate capture buffer. Plates were washed twice with PBS-T wash buffer (PBS with 0.05% [v/v] tween-20) and blocked for 2 hours at room temperature with ELISA assay diluent. Plates were washed as above and supernatant from stimulated cells was added for two hours at room temperature. Plates were washed as above three times and the supplied detection antibody was added for hour. Plates were washed five times as above and supplied TMB was then added for 15 minutes to allow for colour change. Colour reaction was stopped with addition of 1 M H_2SO_4. All plates were read on a Synergy H4 plate reader

(BioTek Instruments Inc.) by assessing absorbance at OD_{450} and subtracting OD_{570}. Concentrations were determined by comparing supernatant concentrations to supplied standards with a limit of detection at 3.125 ng mL^{-1}.

4.2.9.3   Ethics statement

The use of primary human lymphocytes was reviewed and approved by Western University's Research Ethics Board for Health Sciences Research Involving Human Subjects (**Appendix 1**). Informed written consent was obtained from all donors.

4.2.9.4   Immune evasion assays

Experimental procedure details for whole blood survival assay, isolation of neutrophils, and neutrophil survival assay are found in Section 2.2.8. Whole blood was collected in heparinized vacuum tubes (BD Biosciences) from healthy adult volunteers and used directly for determining survival in blood or for density gradient separation and isolation of PMNs. For whole blood survival, ~1000 CFUs of *S. pyogenes* were inoculated into human blood at 37°C with rotation and the number of surviving bacteria were determined after 30, 60, 90, 120, and 180 minutes. For neutrophil survival assay, *S. pyogenes* was opsonized with 10% (v/v) human serum for 30 minutes prior to inoculation into isolated human PMNs at 1:10. After 60 mins PMNs were lysed, and survival was calculated as the average bacterial CFUs in the presence of neutrophils divided by bacterial CFUs in no PMN control samples.

4.2.10   Statistical analyses

Data was analyzed using unpaired Student's *t*-test, one-way ANOVA with Dunnett's multiple comparisons post-hoc test, or two-way ANOVA with Geisser's Greenhouse or Dunnett's multiple comparison test, as indicated. A *P* value less than 0.05 was determined to be statistically significant, all analyses were completed using Prism software 9.3.1 (GraphPad Software, Inc.; La Jolla, CA, USA).

4.3   Results

4.3.1.1   Murine left ventricle structural dimensions remain unchanged following recurring *S. pyogenes* MGAS8232 infections

A novel murine infection model was designed to simulate repetitive strep throat episodes through sequential nasal infections in B6$_{HLA}$ mice (**Figure 20**). Using this model, we sought to identify whether repeated exposure to nasopharyngeal infections by *S. pyogenes* MGAS8232, a bacterial isolate from a patient with ARF [269], incites modifications to cardiac function in mice. B6$_{HLA}$ mice were repetitively inoculated intranasally with either PBS (sham), *S. pyogenes* MGAS8232 wildtype, or MGAS8232 Δ*emm18* that lacks expression of M18 protein on its surface. M-mode echocardiography performed on the LV was acquired by rapid succession of B-mode scans along a single plane displayed over time, which showed motion of the myocardial walls as they contract during systole and relax during diastole (**Figure 22B**). M-mode images provided high temporal resolutions of the motions of the LV wall for assessment of chamber architecture and insight into LV contractile patterns and physiology. Dimensions obtained included LV internal diameters (LVID) and LV anterior wall and posterior wall thicknesses (LVAW and LVPW respectively) at systole and diastole, which was then be used to derive other structural parameters, such as LV mass. After 9 and 13 weeks of biweekly challenges with MGAS8232 wildtype or Δ*emm18,* we observed no changes to LV volumes, LVIDs, or thickness of LVAW or LVPW during systole or diastole compared to control mice (**Figure 23A-H**). Similarly, LV masses were not significantly changed among all treatment groups at weeks 9 and 13 (**Figure 23I**). From these data, we conclude that repetitive infections with *S. pyogenes* MGAS8232 does not initiate LV structural modifications in B6$_{HLA}$ mice.

4.3.1.2   Reduced left ventricle systolic function in B6$_{HLA}$ mice following repeated *S. pyogenes* MGAS8232 exposure

In cine loops obtained from PSLAX images (**Figure 22A**), the LV endocardium was manually traced in systole and diastole to evaluate multiple systolic parameters of LV function. These parameters include ejection fractions, which measures the percentage of

Figure 23. Longitudinal changes of left ventricle structural dimensions in B6_{HLA} mice following repeated *S. pyogenes* MGAS8232 nasopharyngeal infections.
Acquisition of PSLAX and PSAX at baseline, week 9, and week 13 following biweekly nasopharyngeal infections with ~10^8 CFUs of *S. pyogenes* MGAS8232 wildtype and Δ*emm18*. Sham mice were inoculated with PBS. Image analyses provided left ventricle structural dimensions including **(A)** left ventricle internal diameter at end-systole (LVID;s), **(B)** left ventricle internal diameter at end-diastole (LVID;d), **(C)** left ventricle end-systolic volume (LV Vol;s), **(D)** left ventricle end-diastolic volume (LV Vol;d), **(E)** left ventricle anterior wall thickness at end systole (LVAW;s), **(F)** left ventricle anterior wall thickness at end diastole (LVAW;d), **(G)** left ventricle posterior wall thickness at end systole (LVAW;s), **(H)** left ventricle posterior wall thickness at end diastole (LVAW;d), and **(I)** left ventricle mass (LV Mass). Data shown are mean ± SD for $n \geq 4$ per treatment group. Significance determined by Tukey's two-way ANOVA.

Legend:
- Sham
- MGAS8232 Wildtype
- MGAS8232 Δemm18
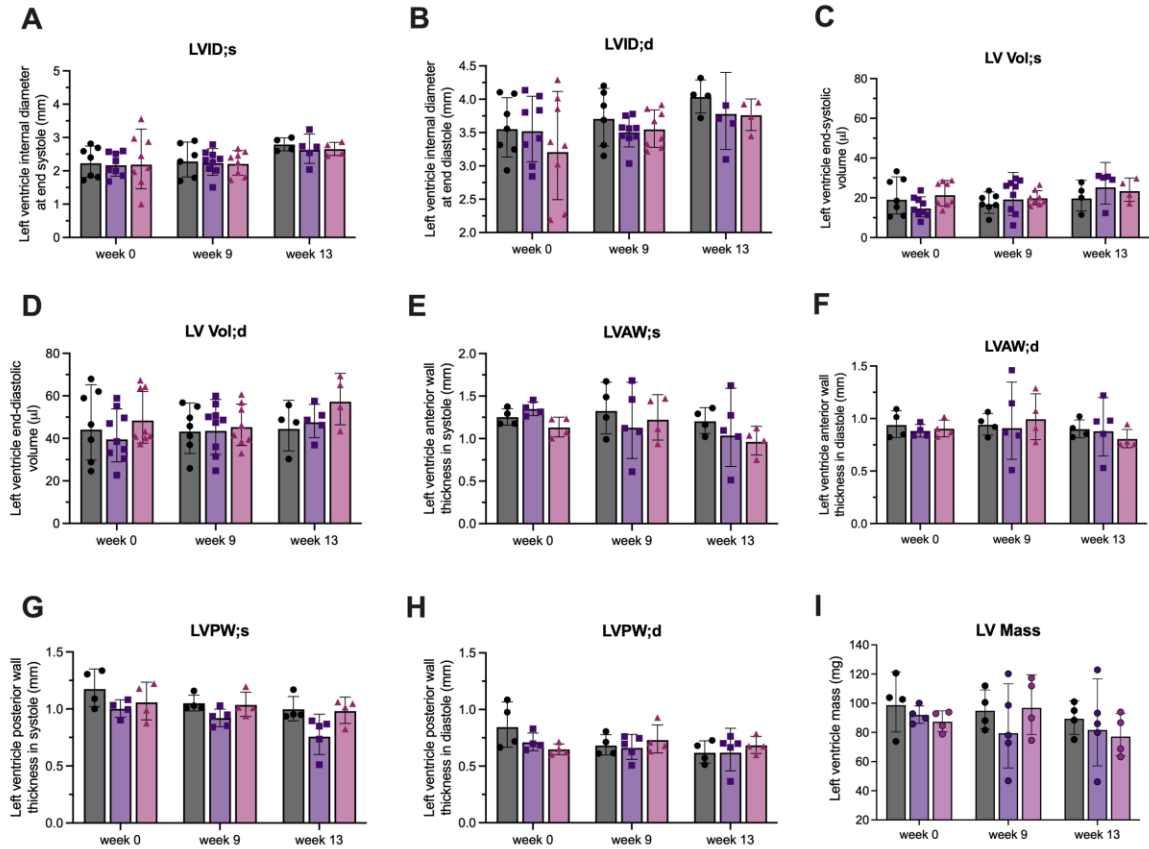
blood that leaves the heart each time it contracts, stroke volume, which measures the amount of blood your heart pumps each time it beats, cardiac output, which measures the volume of blood pumped by the heart per minute, and fractional shortening, which measures the percent change in LV diameter during systole. The LV of mice repetitively exposed to wildtype *S. pyogenes* revealed significantly weakened ejection fractions at both weeks 9 and 13 compared to control mice at each timepoint and when compared to baseline measurements (**Figure 24A**). The ejection fractions of mice repeatedly exposed to Δ*emm18*, however, did not decrease over time and were similar to control mice at both weeks 9 and 13 (**Figure 24A**). Although not statistically different than control mice, mice receiving multiple wildtype infections trended for reduced stroke volumes and cardiac outputs at week 13 compared to those receiving Δ*emm18* infections (**Figure 24B, 24C**). Percent fractional shortening remained unchanged across all treatment groups over time (**Figure 23D**). HR were obtained by ECG and were maintained within an appropriate physiologic range during image acquisition for all ages of mice (**Figure 24E**). Together, these results suggest repeated exposure to *S. pyogenes* MGAS8232 wildtype may reduce myocardium contractibility in mice.

4.3.2 Reduced left ventricle diastolic function in B6$_{HLA}$ mice following repeated *S. pyogenes* MGAS8232 exposure

Transmitral inflow Doppler obtained in apical 4-chamber view (**Figure 22C**) is useful for measuring blood flow across the mitral valve and evaluation of LV diastolic function in mice. Doppler indexes were measured in VevoLAB after all images were acquired and included peak early and late mitral inflow velocities (*E*-wave, *A*-wave), the ratio of peak early to late filling velocities of mitral inflow (*E/A*), deceleration time (DT) of the *E*-wave, deceleration of the *E*-wave (MV Decel), and isovolumetric relaxation time (IVRT) (**Figure 22D**). Additional systolic parameters, such as isovolumetric contraction time (IVCT), ejection time (ET), and no flow times (NFT) were also measured (**Figure 22D**). These measurements enable calculations of myocardial performance index (MPI), MV orifice, and MV pressure half time (PHT).

Figure 24. Reduced ejection fractions in B6$_{HLA}$ mice following multiple *S. pyogenes* MGAS8232 nasopharyngeal infections.

Echocardiogram analyses of mice taken at baseline, week 9, and week 13 following biweekly nasopharyngeal infections with ~10^8 CFUs of *S. pyogenes* MGAS8232 wildtype and Δ*emm18* mutant. Sham mice were inoculated with PBS. Left ventricle systolic function assessed by **(A)** percent ejection fraction, **(B)** fractional shortening, **(C)** stroke volume, and **(D)** cardiac output. **(E)** Heart rates of anesthetized mice during image acquisition. Data shown are mean ± SD for $n \geq 4$ per treatment group. Significance determined by Tukey's two-way ANOVA (*, $P < 0.05$; **, $P < 0.01$).

A Ejection Fractions

B Stroke Volume

C Cardiac Output

D Fractional Shortening

E Heart Rate

Legend:
- Sham
- MGAS8232 Wildtype
- MGAS8232 Δemm18
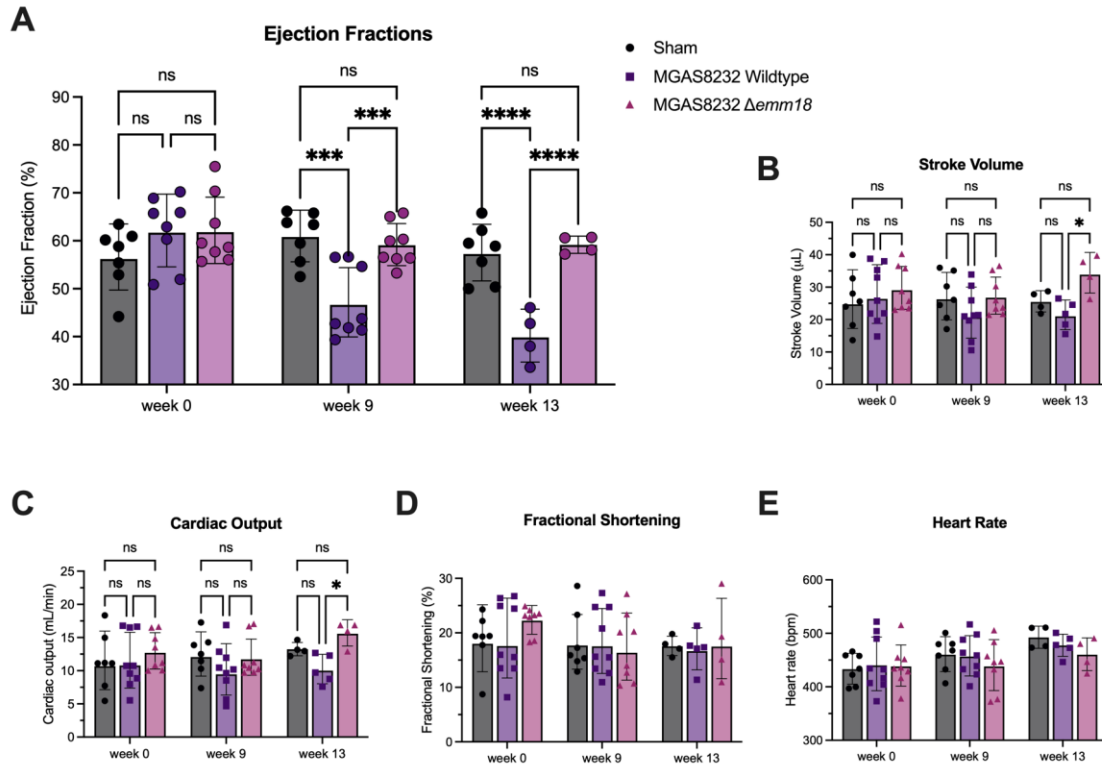
Peak blood flow velocities across the mitral valve revealed elevated left atrial pressure in mice repetitively infected with wildtype MGAS8232 compared to control mice at both weeks 9 and 13. This was illustrated by significantly higher *E/A* ratios, which represents disrupted pressure differences between the left atria and ventricle during early and late diastole (**Figure 25A**). Notably, mice repeatedly challenged with the Δ*emm18* mutant did not demonstrate any differences in *E/A* ratios compared to control mice at week 9 or 13 (**Figure 25A**). Restrictive filling of the LV in wildtype-infected mice likely arose from the reduction of peak late-diastolic transmitral velocities *A*-waves, which were statistically lower than control and Δ*emm18*-infected mice at 13 weeks (**Figure 25C**). Peak early diastolic transmitral velocities, *E*-waves, remained constant among the treatment groups following repeated infections (**Figure 25B**). Other PW Doppler parameters, including IVRT, MV decel, DT, AET, NFT, and MPI, were similarly unaffected from multiple infections (**Figure 25D, F-J**). IVCT was elongated in mice receiving wildtype *S. pyogenes* infections at weeks 9 and 13 but was only significantly longer than control and Δ*emm18*-infected mice at week 9 (**Figure 25E**). MV orifice areas and MV PHT did not statistically differ between control mice and mice receiving *S. pyogenes* infections (**Figure 25K, L**). Together, these results suggest that repetitive exposure to M18 protein may induce defects to cardiac function as LV filling dynamics were altered in B6$_{HLA}$ mice receiving *S. pyogenes* MGAS8232 wildtype, but not Δ*emm18* mutant infections.

4.3.3   Multiple nasopharyngeal challenges with *S. pyogenes* do not trigger cardiomyocyte damage

While severe abnormalities in RHD are due to valvular problems rather than myocardial damage, the involvement of myocarditis is often observed during acute stages of disease development. Myocarditis is characterized by myocyte necrosis and indicators for identifying myocardial injury include elevated serum levels of cardiac troponin T (cTnT) and cardiac troponin I (cTnI) as they are released by damaged myocytes. We next aimed to elucidate whether myocardial damage was evident together with reduced EF and elevated *E/A* ratios in wildtype *S. pyogenes*-infected mice. Cytokines that indicate

Figure 25. Elevated mitral valve *E/A* ratios in B6$_{HLA}$ mice receiving multiple *S. pyogenes* MGAS8232 nasopharyngeal infections.

Pulsed-wave Doppler echocardiography revealed diastolic parameters in mice at weeks 0, 9, and 13, following biweekly nasopharyngeal infections with *S. pyogenes* MGAS8232 wildtype and Δ*emm18* (10^8 CFUs). Sham mice were inoculated with PBS. **(A)** *E/A* ratios of peak early- and late-diastolic transmitral velocities; **(B)** mitral valve early velocity (*E*-wave); **(C)** mitral valve atrial velocity (*A*-wave); **(D)** isovolumetric contraction time (IVCT); **(E)** isovolumetric relaxation time (IVRT); **(F)** non-flow time (NFT); **(G)** aortic ejection time (AET); **(H)** MV deceleration time; **(I)** MV deceleration acceleration; **(J)** mitral valve orifice area; **(K)** myocardial performance index (MPI); and **(L)** mitral valve pressure half time (PHT). Data points represent values from individual B6$_{HLA}$ mice. Bars represent mean ± SD for $n \geq 4$ per treatment group. Significance determined by Tukey's two-way ANOVA, (*, $P < 0.05$; **, $P < 0.01$).

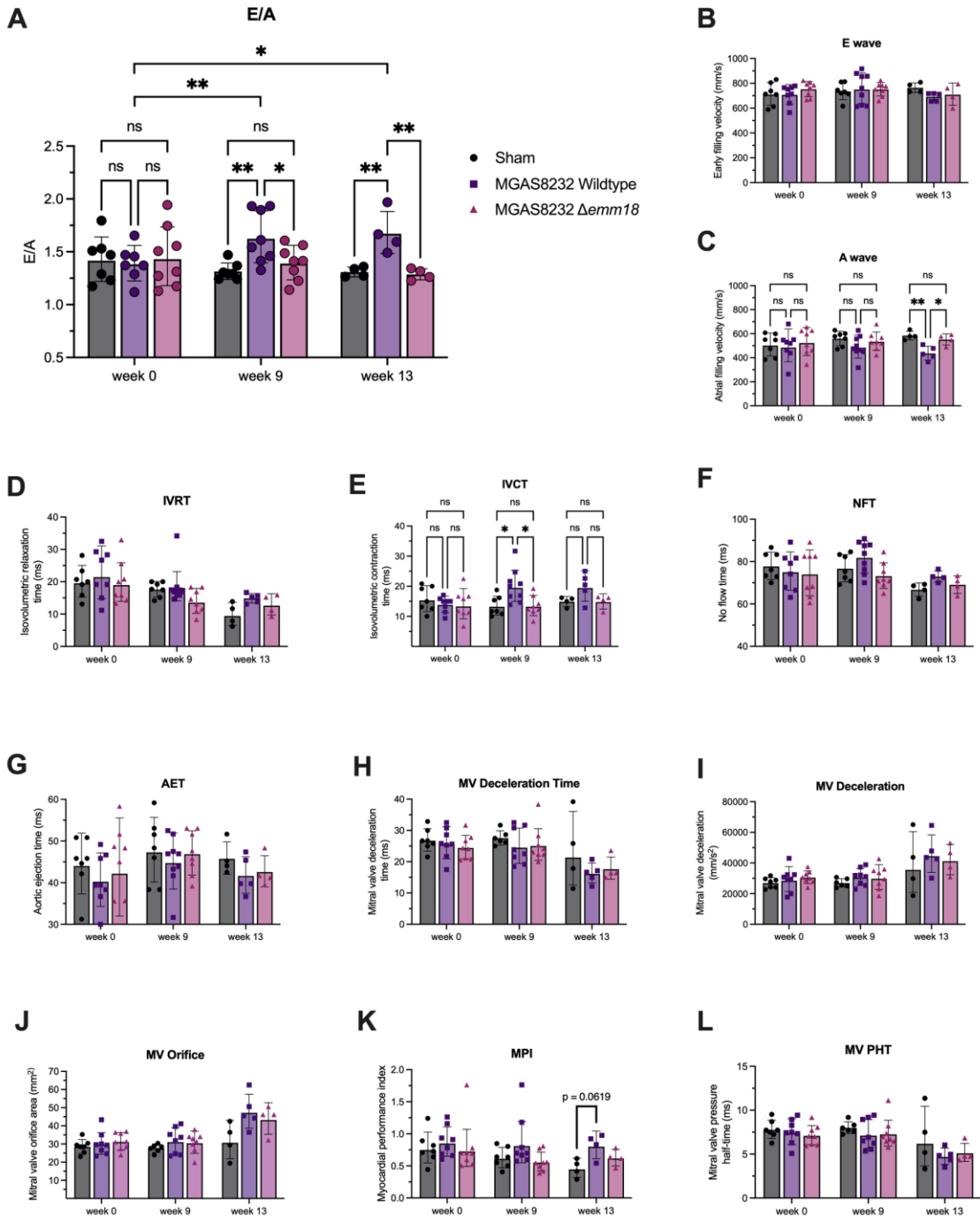myocardial tissue injury, including cTnT and cTnI, were measured in endpoint serums collected at weeks 9 and 13 by a highly sensitive multiplex cardiac cytokine array (Eve Technologies) and compared to control PBS-inoculated mice at both time points. There were no differences in levels of serum cTnT or cTnI at either week 9 or 13 in control mice or mice that received multiple infections with *S. pyogenes* wildtype or Δ*emm18* (**Figure 26A, 26B**). Serum concentrations of other cytokines associated with myocardial injury, including sCD40L, CXCL16, Endocan-I, Light, Oncostatin-M, PLGF-2, and Follistatin, were similarly measured by and presented no differences at both weeks 9 and 13 in *S. pyogenes*-infected or control mice (**Appendix 7**). Normal serum levels of cTnT and cTnI demonstrate that inflammation rather than myocardial necrosis is likely responsible for subverted left atrial pressures in mice repeatedly challenged with wildtype *S. pyogenes* nasopharyngeal infections.

4.3.4 Suppression of *S. pyogenes*-specific antibodies following repeated nasopharyngeal infections

The central role of immunity to a pathogen is to prevent reinfection with the same organism through production of neutralizing antibodies, yet little is known about the induction of strain-specific responses and immunological outcomes from multiple streptococcal infections. The presence of M type-specific antibodies in patients many years after infection provides evidence that life-long strain-specific immunity can develop following *S. pyogenes* infection, however, not all individuals demonstrate type-specific antibodies after a known symptomatic exposure [409]. While it is assumed that *S. pyogenes*-specific antibodies arise with subsequent exposure, it is not entirely understood or demonstrated whether immunity is acquired or persists following sequential challenges with the same streptococcal strain. To determine whether repeated nasopharyngeal infections could boost *S. pyogenes*-specific antibody responses, IgG responses to M18 protein and SpeA superantigen were measured by ELISA using endpoint serums collected from all mice at weeks 10 and 14. Interestingly, multiple nasopharyngeal challenges with MGAS8232 wildtype did not significantly increase serum IgG responses to M18 protein or SpeA at week 10 or week 14 (**Figure 27**). M18 and SpeA IgG titers demonstrated an increased trend from week 10 to week 14 in wildtype and Δ*emm18*-infected mice, however, titers

Figure 26. B6_{HLA} mice repeatedly infected with *S. pyogenes* MGAS8232 do not express increased serum levels of cardiac troponin-I or troponin-T.

Multiplex cytokine array from serums of mice repeatedly exposed to biweekly MGAS8232 wildtype and Δ*emm18* mutant nasopharyngeal infections at weeks 10 and 14. Control mice received PBS inoculations. Data points represent the mean ± SEM of serum cardiac **(A)** troponin-I and **(B)** troponin-T concentrations (pg mL^{-1}) from individual mice ($n \geq 3$ mice per group). Significance was determined by Tukey's two-way ANOVA, data not significant.

A

Troponin-I

B

Troponin-T
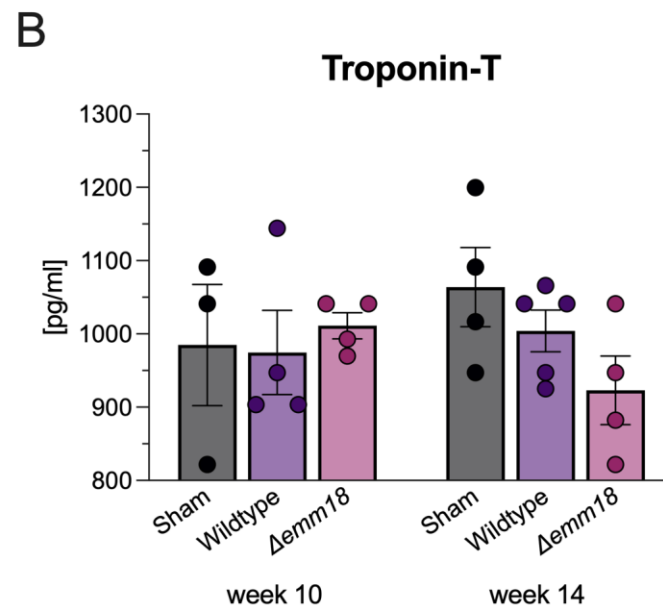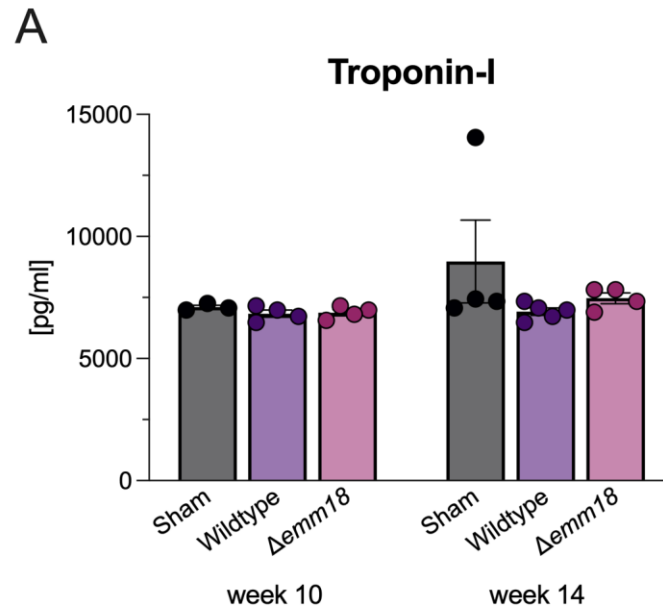
were not statistically higher than control PBS-inoculated mice (**Figure 27**). Therefore, multiple infections with *S. pyogenes* MGAS8232 did not enhance serum M18 protein or SpeA-specific IgG responses, indicating that serotype-specific immunity does not develop following reinfection with the same strain in our model.

4.3.5   B6$_{HLA}$ mice are protected against subsequent *S. pyogenes* nasal challenge following two sequential infections

To explore whether sequential infections would prevent reinfection with the same strain, mice received two nasal challenges with *S. pyogenes* MGAS8232 two weeks apart, which allowed mice to fully clear the bacteria within their nasal turbinates before subsequent challenge [156]. Two weeks following their second infection, mice were rechallenged with a third infection by the same strain, and nasal turbinates were collected 48 hours later to measure colonizing bacteria. Surprisingly, mice demonstrated a 10,000-fold reduction in bacterial burden compared to naïve mice receiving their first and only challenge (**Figure 28**). Although multiple infections with *S. pyogenes* did not amplify M18 or SpeA-specific serum IgG levels (**Figure 27**), two sequential infections provide resistance to rechallenge by the same strain. These observations suggest that either M18 protein and SpeA-specific immunity is not essential to prevent reinfection and are not generated with repeated infections, or protection against *S. pyogenes* infection is not antibody-mediated.

4.3.6   T cell unresponsiveness following repeated *S. pyogenes* MGAS8232 nasopharyngeal infections.

M18 protein and SpeA IgG titers were not significantly elevated after multiple nasopharyngeal infections, and thus, we next considered an alternative explanation for the protective effects observed with subsequent challenge. Following repeated infections, T cell responsiveness to streptococcal superantigens were evaluated by a splenocyte activation assay. While conventional B6 mice are not typically sensitive to streptococcal superantigen stimulation, our research group has previously shown that B6$_{HLA}$ mice demonstrate enhanced splenocyte proliferation with SpeA stimulation targeting mouse TCR Vβ8$^+$ T cells and streptococcal mitogenic exotoxin Z (SmeZ) superantigen targeting

Figure 27. Sequential *S. pyogenes* MGAS8232 nasopharyngeal challenges do not amplify M18 protein- and SpeA-specific IgG serum levels.

B6$_{HLA}$ were exposed to multiple biweekly nasal infections with *S. pyogenes* MGAS8232 wildtype or Δ*emm18*. Serums were collected at 10 and 14 weeks following initial challenge and used to assess IgG titers to **(A)** M18 protein and **(B)** SpeA using ELISA ($n \geq 3$). Data points represent the geometrics means ± SEM from individual mice. Antibody titers were calculated as the reciprocal of the lowest serum dilution with readings four-fold above background. Significance determined by one-way ANOVA with Dunnett's post-hoc test, data not significant.

A

M18 IgG Titres

B

SpeA IgG Titres
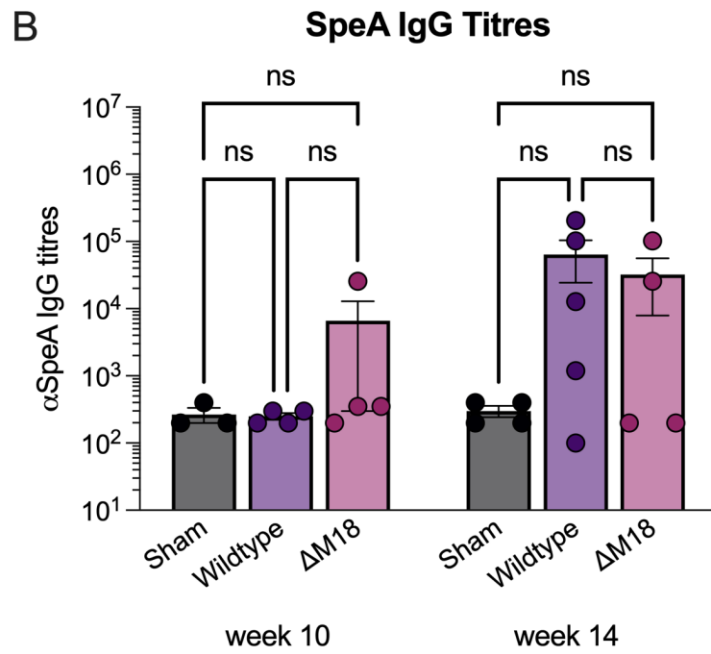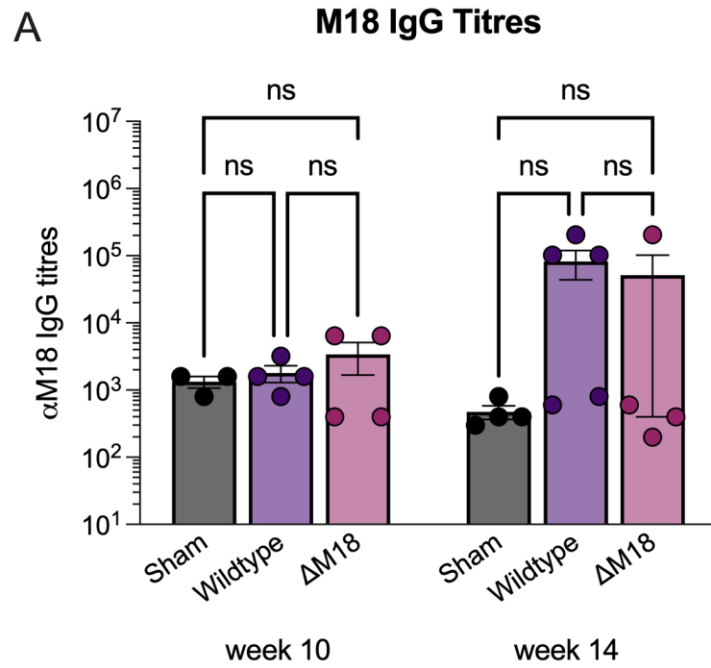
Figure 28. Protection against *S. pyogenes* nasopharyngeal challenge following two sequential infections.

B6$_{HLA}$ mice were infected intranasally twice with ~10^8 CFUs *S. pyogenes* MGAS8232 wildtype at two weeks apart, and then rechallenged to the same strain two weeks later. Protection against subsequent *S. pyogenes* infection was examined by measuring bacterial burden in cNTs 48 hours after the third nasopharyngeal challenge (*S. pyogenes* x3) compared to naïve mice with no prior exposure (*S. pyogenes* x1). Data is shown as mean bacterial CFUs ± SEM recovered from individual mice ($n \geq 4$). Horizontal line indicates limit of detection. Significance was determined by unpaired Mann-Whitney *t*-test (**, $P <$ 0.01).
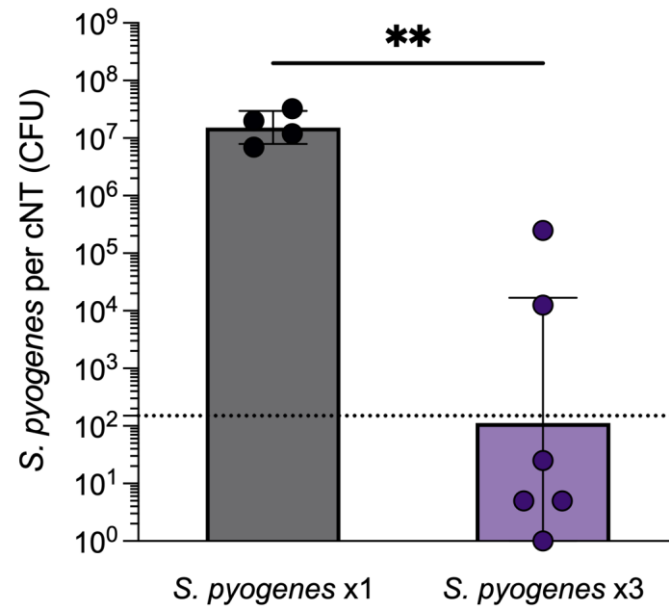
mouse TCR Vβ11$^+$ T cells [156,157]. T cell activation by the M18 protein, however, has not been previously defined. Splenocytes from control mice and mice repeatedly infected with MGAS8232 wildtype or Δ*emm18* were processed and incubated with increasing concentrations of SpeA, SmeZ, or M18 protein for 18 hours. Culture supernatants were then analyzed for IL-2 as a marker for T cell activation using ELISA. As expected, uninfected mice exhibited high IL-2 concentrations following SpeA stimulation and were activated by SmeZ to a lesser extent (**Figure 29A**), however, mice that received repeated MGAS8232 wildtype or Δ*emm18* infections responded poorly to SpeA stimulation (**Figure 29B, 29C**). Responses to SmeZ stimulation were unchanged following multiple *S. pyogenes* infections. This data suggests that sequential *S. pyogenes* infections may impair Vβ8$^+$ T cell activation, but other subsets (i.e., Vβ11) remain responsive. Splenocytes from control mice showed very little activation from increasing M18 protein stimulation, with levels of IL-2 gradually amplifying with increasing M18 protein stimulant concentrations to levels similar to SmeZ stimulated cells (**Figure 29A**). Mice that received multiple infections with MGAS8232 wildtype or Δ*emm18* showed no significant difference in T cell activation from M18 protein stimulation compared to uninfected mice (**Figure 29**), demonstrating that repeated exposure to the M18 protein specifically did not subvert T cell responses.

4.3.7 Generation and characterization of a *S. pyogenes* Δ*gacI* mutant strain lacking expression of the GlcNAc side chain

A long-term goal of our research is to identify *S. pyogenes* antigens that play a role in immunological cross-reactivity and lead to valvular damage. Since echocardiogram imaging denoted that expression of M18 protein by *S. pyogenes* MGAS8232 reduced LV function in mice with repeated infections, this repetitive infection model is now equipped to study the importance of additional virulence factors in disease development. Patients with ARF and valvular heart disease have demonstrated elevated levels of antibodies that recognize and bind GlcNAc, immunodominant side chain of the Lancefield GAC, which similarly shares cross-reactive epitopes with several host proteins [395–398]. Therefore, molecular mimicry by the GlcNAc side chain may contribute to autoimmune responses

Figure 29. Activation of murine splenocytes by streptococcal superantigens and M18 protein following multiple *S. pyogenes* MGAS8232 nasopharyngeal infections.

B6$_{HLA}$ mice were exposed to biweekly **(A)** PBS inoculations or nasopharyngeal infections with *S. pyogenes* MGAS8232 **(B)** wildtype or **(C)** Δ*emm18* strains and sacrificed at week 14. Murine splenocytes were then stimulated with indicated concentrations of SpeA and SmeZ superantigens, or M18 protein for 18 hours. IL-2 concentrations were measured in culture supernatants by ELISA as a marker for T cell activation. Data represents mean ± SEM of triplicate values from mice exposed to each treatment ($n \geq 3$). Protein stimulants are indicated in the colour-coded legends.

A

Sham

B

Wildtype

C

Δemm18
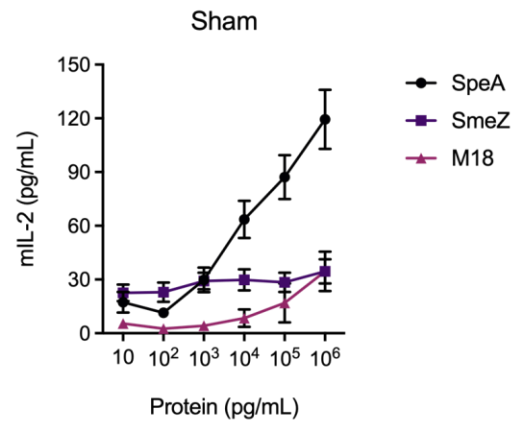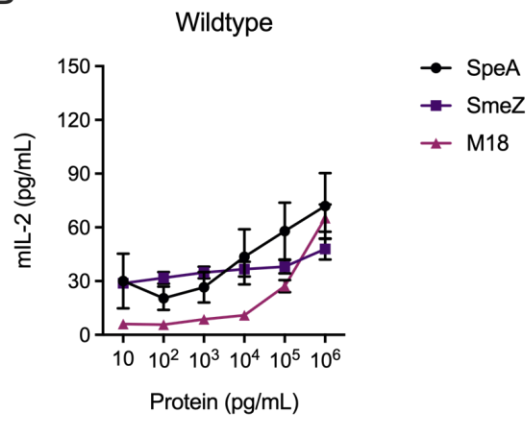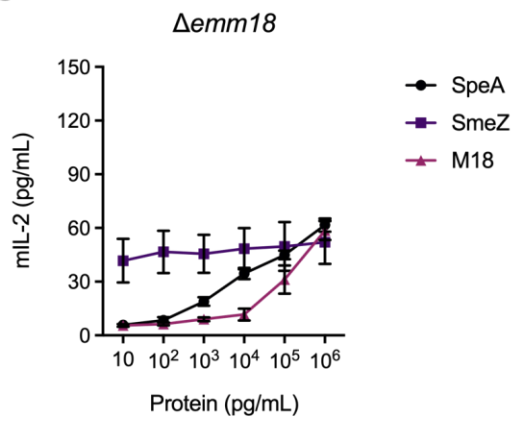
that promote cardiac dysfunction. In order to determine whether the GlcNAc side chain stimulates valve damage, the specific role of the GlcNAc side chain must first be assessed in B6$_{HLA}$ mice. An isogenic mutant of the GlcNAc side chain in *S. pyogenes* MGAS8232 was generated by an in-frame genetic deletion of the glycosyltransferase encoded by the *gacI* gene [226]. The deletion mutant was confirmed by DNA sequencing and validated using PCR amplification using screening primers within the deleted region (**Table 8**). Compared to the wildtype MGAS8232, and Δ*emm18,* genomes, the Δ*gacI* mutant strain contained a 567 bp deletion within the *gacI* encoded region (**Figure 30A**). Bacterial growths *in vitro* and TCA preparations were similar between wildtype and Δ*gacI* strains, which ensured that deletion of the *gacI* gene had no detrimental effect on the growth patterns or secreted protein profile of *S. pyogenes* MGAS8232 (**Figure 30B**, **30C**). Bacterial adherence was then evaluated using A549 lung and D562 pharyngeal epithelial cells, and no differences in the number of adherent bacteria were recovered from either wildtype or Δ*gacI* inoculated cells (**Figure 30D, 30E**). Additionally, wildtype and Δ*gacI* strains were inoculated into fresh heparinized human blood and isolated neutrophils to further characterize immune evasion properties of GlcNAc. Growth and survival of Δ*gacI* was comparable with wildtype MGAS8232 in whole human blood (**Figure 30F**) and while Δ*gacI* survival was reduced compared to wildtype in the presence of neutrophils, it was not statistically significant (**Figure 30G**). These results indicate that the GlcNAc side chain does not substantially contribute to adherence or immune evasion properties by *S. pyogenes* MGAS8232 under these conditions.

4.3.8   The GlcNAc side chain contributes to *S. pyogenes* MGAS8232 nasopharyngeal infection in B6$_{HLA}$ mice but is not essential.

Before determining if the Δ*gacI* mutant impairs cardiac function in mice, the role of the GlcNAc side chain during acute nasopharyngeal infection must first be assessed. B6$_{HLA}$ mice were infected with ~10^8 CFUs of *S. pyogenes* MGAS8232 wildtype or Δ*gacI* and cNTs were collected 48 hours later to assess bacterial burden and cytokine responses during infection. Consistent with previous findings, mice expressed high loads of *S pyogenes* in the nasal turbinates of wildtype-infected mice, yet Δ*gacI* bacterial recovery was variable

Figure 30. Generation and characterization of the *S. pyogenes* MGAS8232 Δ*gacI* mutant strain.

(A) Primers flanking the *gacI* gene demonstrated a 567 bp deletion by PCR from the Δ*gacI* mutant genome compared to *S. pyogenes* MGAS8232 wildtype, and Δ*emm18* strains **(B)** Secreted protein profiles of *S. pyogenes* from TCA preparations after 18 hours of growth in THY. SDS-PAGE on 12% acrylamide gel stained with Ready Blue. **(C)** *S. pyogenes* growths *in vitro* in THY at 37°C measured by OD_{600} absorbances over 18 hours. Data is presented as mean ± SD of each culture analyzed in triplicate ($n = 3$). Adhesion of *S. pyogenes* to **(D)** A549 lung and **(E)** D562 pharyngeal epithelial cells. Confluent cell monolayers were treated with *S. pyogenes* (MOI of 100) for 2 hours at 37°C + 5% CO_2. Cells were washed with PBS and lysed with Triton X-100 to examine adherent bacteria. **(F)** Whole human blood survival assay. Heparinized blood from human donors were inoculated with ~10^3 CFUs of *S. pyogenes* wildtype or Δ*gacI* at 37°C with rotation for 3-hours. Data points represent geometric mean CFUs ± SD. **(G)** Neutrophil survival assay. Neutrophils were isolated from human blood by density centrifugation and inoculated with *S. pyogenes* (MOI of 10) for 60 min at 37°C with rotation. Results were calculated as the difference between surviving bacteria in the no neutrophil control and in the presence of neutrophils. Data shown are the means %survival ± SD ($n \geq 3$ per group). All statistical analyses were performed using unpaired Mann-Whitney *t*-test.

A

bp — MWL — Neg — WT — Δ*emm*18 — Δ*gacI*

1000
850
600
500
400

B

kDa — MWL — WT — Δ*gacI*

75
63
48
35
25
20

C *in vitro* growth

OD$_{600}$ vs Time (hours)
- Wildtype
- Δ*gacI*

D A549 adherence

S. pyogenes (CFU) — Wildtype — Δ*gacI*

E D562 adherence

S. pyogenes (CFU) — Wildtype — Δ*gacI*

F Whole blood survival

S. pyogenes (CFU) vs Time (mins)
- Wildtype
- Δ*gacI*

G Neutrophil survival

%Survival — Wildtype — Δ*gacI*

$P = 0.100$
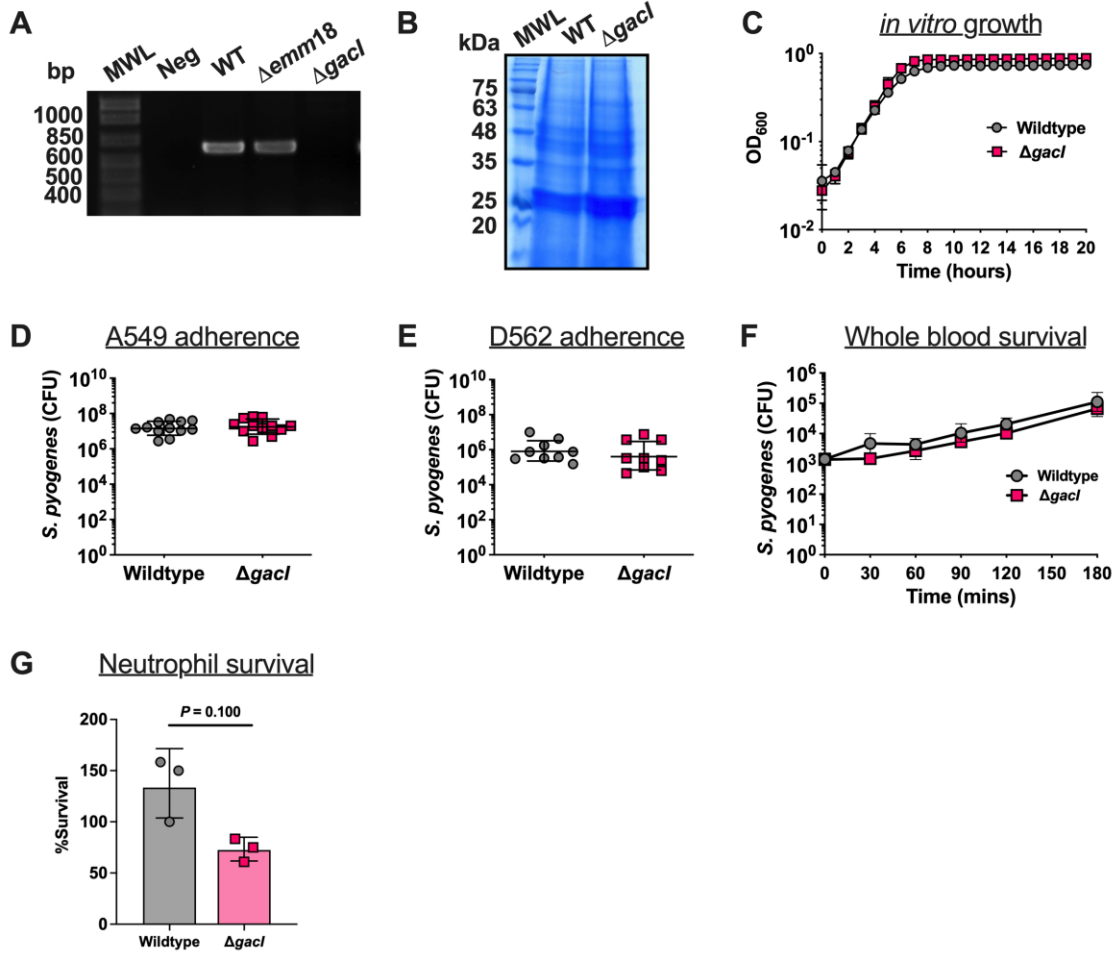
and revealed a statistically detectable attenuation of bacterial CFUs (*, $P = 0.0481$) (**Figure 31A**). These results suggest that GlcNAc side chain contributes to nasopharyngeal infection by *S. pyogenes* MGAS8232 but is likely not essential. Cytokine responses within cNTs of Δ*gacI*-infected mice were then assessed by a multiplex cytokine array for the presence of 32 cytokines and chemokines. Any cytokine that presented an average concentration above 20 pg ml^{-1} within a treatment group was included in the heat map and presented as normalized median cNT cytokine responses (**Figure 31B**). Quantitative data is shown in the Appendices (**Appendix 8**). Concentrations of Th1-type cytokines (IL-1α and IL-1β); Th17-type cytokines (IL-6 and IL-17); chemokines (KC, IP-10, MCP-1, MIP-1α, MIP-1β, MIG, MIP-2, LIF and LIX); and growth factors (G-CSF) were vigorously induced during wildtype *S. pyogenes* infections (**Figure 31B, Appendix 8**). Interestingly, infection by the Δ*gacI* mutant mostly paralleled an inflammatory environment with no significant differences in any cytokine concentration compared to infection with wildtype *S. pyogenes* (**Figure 31B, Appendix 8**). Reductions in IL-6 and IL-17 concentrations, and increased levels of KC, MIP-1α, and VEGF are noted, but were not statistically different than concentrations found during wildtype infection. These results suggest that removal of the GlcNAc side chain in *S. pyogenes* MGAS8232 continues to support inflammation within the nasopharynx, despite detectable reductions in bacterial burden. Consistent with the non-invasive nature of the model [156], mean bacterial dissemination of MGAS8232 wildtype remained below the limit of detection in the lungs, liver, spleen, heart, and kidneys (**Figure 32**). Infection with the Δ*gacI* mutant detected six cases of *S. pyogenes* above the limit of detection in the lungs and four cases of in liver (**Figure 32**), however, these counts did not significantly increase the mean bacterial recovery within the lungs or liver compared to MGAS8232 wildtype. There was no recovery of the Δ*gacI* in the spleen, heart, or kidneys (**Figure 32**) and thus, removal of the GlcNAc side chain did not overtly increase bacterial dissemination of *S. pyogenes* following acute nasopharyngeal infection.

Figure 31. Deletion of the *gacI* gene in *S. pyogenes* MGAS8232 results in a detectable reduction to nasopharyngeal burden.

B6$_{HLA}$ mice were administered ~10^8 CFUs of *S. pyogenes* MGAS8232 wildtype or Δ*gacI* intranasally. **(A)** Data points represent bacterial CFUs recovered from cNTs of individual mice 48 hours post-nasal challenge. Bars represent median CFUs. Horizontal dotted line indicates limit of detection. Significance determined by unpaired Mann-Whitney *t*-test (*, $P < 0.05$). **(B)** Heat-map of multiplex cytokine array from cNT homogenates during infection. Data shown are presented as normalized median cytokine responses from each treatment group ($n \geq 3$ per group).

A
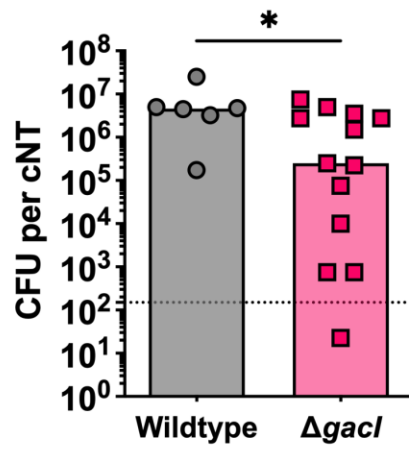
B
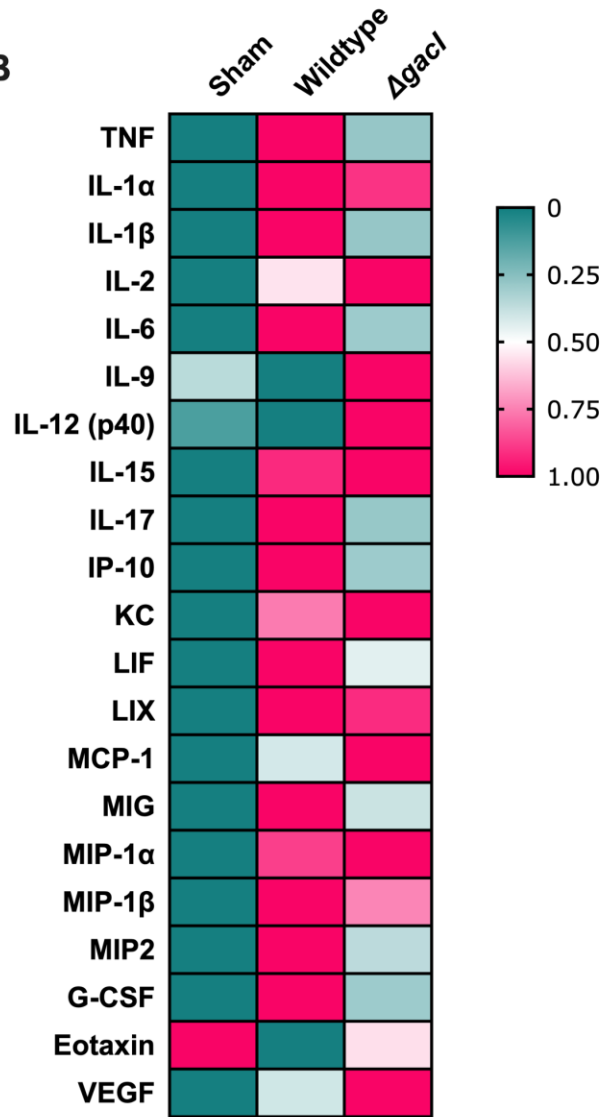
Figure 32. Nasopharyngeal infection with *S. pyogenes* MGAS8232 Δ*gacI* does not enhance bacterial dissemination in B6$_{HLA}$ mice.

B6$_{HLA}$ mice were nasally challenged with $\sim 10^8$ CFUs of *S. pyogenes* wildtype or Δ*gacI* strains. Mice were sacrificed 48 hours later, and organs were harvested, homogenized, and plated on TSA with 5% sheep blood agar to assess bacterial dissemination. Bacterial CFUs were measured in the **(A)** lungs, **(B)** liver, **(C)** spleen, **(D)** heart, and **(E)** kidneys. Data points represent bacterial CFUs in indicated organs from individual mice ($n \geq 4$ per group). Bars represent mean ± SEM. Horizontal dotted line indicates theoretical limit of detection. Significance was determined by unpaired Student's *t*-test, data not significant.

4.4   Discussion

Despite a documented decline in industrialized countries over the past 6 decades [44], ARF and RHD remain as important causes of cardiovascular morbidity and mortality worldwide today [46]. While current rodent models have helped describe inflammatory responses involved in valve pathogenesis, there is an urgent need for models to not only support productive infection by *S. pyogenes,* but also assess the outcomes on heart function to accurately evaluate clinical features of disease progression. In the current study, echocardiography was used to assess LV features and determine whether the M18 protein expression drives cardiac disease development following repeated *S. pyogenes* MGAS8232 nasopharyngeal infections. Our principal findings revealed that repeated *S. pyogenes* MGAS8232 infections resulted in elevated *E/A* ratios and reduced ejection fractions compared to control mice, while mice exposed to MGAS8232 Δ*emm18* presented no changes to LV parameters. To date, this would be the first report that cardiac function is influenced by multiple homologous infections with *S. pyogenes,* and the first study associating M protein expression with defects to LV function through live infections.

Monitoring LV function is a key element in understanding the pathophysiology of cardiac disease models during experimental studies. RHD is a chronic and progressive form of damage to mitral valves that provokes defective diastolic filling mechanisms and lead to deficient pumping mechanisms and systolic dysfunction. Diastole is the relaxation phase of the heart that facilitates normal LV filling, provides sufficient blood volumes, and maintains normal cardiac output. As in humans, diastolic function in mice is evaluated by blood flow across the mitral valve, measured by the ratio between early (*E*) and late (*A*) transmitral blood flow velocities (*E/A*), IVRT, and *E*-wave deceleration time [407,408,410,411]. Since increased LV filling pressures can lead to myocardial stiffness and result in diastolic dysfunction, *E/A* ratios provide important information about LV filling dynamics and diastolic impairments. Following biweekly nasopharyngeal infections with *S. pyogenes* MGAS8232, echocardiography demonstrated significantly higher *E/A* ratios (from ~1.38 at t = 0 weeks, to ~1.62 at t = 9 weeks, and ~1.67 at at t = 13 weeks) compared to control mice receiving PBS inoculations (**Figure 25A**), suggesting that LV

filling dynamics have modified. Important implications are considered when assessing these velocities as they are highly dependent on HR and anesthesia [407,408,410]. In this study, mean HR of wildtype-infected mice were comparable with Δ*emm18*-infected and control mice (**Figure 24E**), highlighting that *E*- and *A*-wave differences were not due to manipulation of HR between treatment groups. Particularly, *A*-waves had slightly reduced at 9 weeks and had significantly reduced by week 13 following repeated MGAS8232 wildtype infections (**Figure 25C**). *A*-waves and *E*-waves were otherwise unchanged across treatment groups over time (**Figure 25B, C**). Since the *A*-wave is produced by atrial contraction and smaller *A*-waves can arise from a 'stiffer' LV, these observations suggest that MGAS8232 wildtype*,* but not Δ*emm18,* may induce myocardial stiffness and modify LV filling dynamics across the mitral valve. Diastolic dysfunction can also develop from abnormal LV relaxation due to distorted IVRT or *E*-wave deceleration times, however, we detected no statistical differences in these parameters between treatment groups (**Figure 25D, H**).

New diastolic guidelines by the American Society of Echocardiography and European Society of Cardiology recommend that if *E/A* ratios are >0.8 but <2 additional signals with greater reliability should be acquired alongside *E/A* for accurate assessment, including annular tissue velocities and left atrium size [407,410]. The emergence of tissue Doppler imaging (TDI) allowed for myocardial tissue to be evaluated as moving targets where myocardial motion can be determined by measuring peak early (e') and late (a') mitral annular velocities in diastole. Movement of the mitral annulus is recommended to more appropriately estimate diastolic dysfunction as it directly reflects left atrium pressure and indirectly reflects LV end-diastolic pressure, which is indicative of myocardial stiffness [407,408,410]. Mitral *E*/e' measurements were not obtained in this work due to the acquisition of TDI software after initiation of the study. Furthermore, it is recommended that precaution be taken when interpreting *E* and e' values as their myocardial velocities are less reliable under certain pathological conditions, such as significant mitral regurgitation, mitral annular calcification, and mitral stenosis [407]. Mitral regurgitation is typically diagnosed by the presence of turbulent flows in colour Doppler, which displays a mosaic of blood flow colours across the mitral valve [46,48,407,408,410,412]. While

advanced RHD is known to involve regurgitation, no mouse in this study exhibited the classic mosaic blood flow across the mitral valve with colour Doppler, suggesting that mitral regurgitation was not apparent at the times of image acquisition at weeks 9 and 13. Advanced RHD also involves mitral valve inflammation and fibrosis that can result in valve thickening on echocardiography [48,412], and is present in 56-100% of rheumatic carditis patients [44]. As a result, the mitral valve can become stiff and disrupt left atrial pressure in response to chronic pressure overload. Neither wildtype nor Δ*emm18*-infected mice showed evidence of mitral valve thickening following *S. pyogenes* exposure as mitral valve orifice areas did not statistically differ from control mice (**Figure 25J**). Thus, in the absence of regurgitation or significant valve thickening, E/e' should be used in future studies to support our findings.

Another major finding of this study was that mice sequentially challenged with *S. pyogenes* MGAS8232 demonstrated significantly reduced ejection fractions, indicating defective systolic pumping mechanisms. Systole is the contraction phase of the heart that ensures the arteries are supplied with an adequate amount of oxygenated blood. Ejection fractions are valuable indications of LV function as it measures changes in LV volumes between systole and diastole. Ejection fractions significantly declined ~15% at 9 weeks and ~22% at 13 weeks (from 61.7% at t = 0 weeks, to 46.6 at t = 9 weeks, to ~39.8% at t = 13 weeks) (**Figure 24A**). Whether longer exposure to *S. pyogenes* results in further reductions will require deeper investigation. In contrast, mice infected with Δ*emm18* demonstrated only a ~2% decline in ejection fractions at both weeks 9 and 13 (from 61.8% at t = 0 weeks, to 59.0 at t = 9 weeks, to ~59.1% at t = 13 weeks). Other systolic variables, including fractional shortening, stroke volume, and cardiac output were also obtained from these images and calculated from measurements of LV wall thickness and chamber dimensions. Fractional shortening remained unchanged among treatment groups over time (**Figure 24D**), and stroke volumes and cardiac outputs were only significantly reduced at week 13 compared to Δ*emm18*-infected mice and did not statistically differ from control mice (**Figure 24B, C**). These results suggest that wildtype-infected mice may be starting to present reduced myocardium contractibility over time, however, the data is not significantly different than control mice. The IVCT period, when the mitral valve closes

and before LV ejection, was significantly prolonged in wildtype-infected mice compared to control mice and Δ*emm18*-infected mice (**Figure 24E**). When defects in LV filling become apparent and LV function deteriorates, the IVCT period will become elongated due to a reduced rate of myocardial contractability and systolic dysfunction [407,408,413]. While wildtype-infected mice showed significantly longer IVCTs at week 9, ICVTs at week 13 were not significantly larger than control mice. Taken together, reduced ejection fractions suggest that multiple *S. pyogenes* infections impairs systolic function, which may progress over time shown by reductions in stroke volumes and cardiac outputs. Furthermore, LV images in M-mode were used to measure thickness of the anterior and posterior walls and LV internal diameters during systole and diastole, however, these dimensions were unchanged in mice across all treatment groups (**Figure 23E-H**) and were within normal ranges for echocardiographic architectural dimensions of healthy mice [407].

Importantly, implications for echocardiographic assessments are considered. When compared to reference values for control/healthy C57BL/6 mice obtained by over 300 echocardiogram exams performed across 10 different laboratories, *E/A* ratios of 1.52 ± 0.40 for heart rates >450 bpm and 1.42 ± 0.26 for heart rates <450 bpm are considered "normal" [407]. While wildtype-infected mice exhibited significantly greater *E/A* ratios compared to Δ*emm18*-infected and control mice, most values reported are still within the referenced normal range for C57BL/6 mice. Therefore, while we did see a difference across treatment groups, associating these values to specific disease state and cardiac dysfunction is premature. Inferences for ejection fractions were similarly considered and referenced to "normal" values. Nearly all heart rates at week 13 were above 450 bpm and contained ejection fraction values well below the normal range (71% ± 11) following wildtype *S. pyogenes* exposure [407]. There was a wide range of values reported for most echocardiographic parameters assessed, including control healthy mice, and this is likely, in part, due to the low level of experience with echocardiographic image acquisition and analyses by the primary investigator. Nevertheless, the primary investigator remained blinded to the treatment groups during acquisition and analyses to prevent potential biases with manual measurements.

Since reductions to LV diastolic and systolic functions following recurring *S. pyogenes* infections were observed, we next determined whether myocardial damage was also present. Continued alterations to LV filling dynamics can result in left atrial enlargement and increased wall stress, which may predispose patients to varying degrees of endocardium, myocardium, and/or pericardium injury. The existence of primary myocardial involvement in the occurrence of ARF episodes or RHD (rheumatic myocarditis) remains controversial. Granulomatous lesions have been observed in the ventricular myocardium of ARF and RHD patients [385,386,414] and in rodents with valvulitis in the RAV model [386,401], however, significant myocyte necrosis is usually not shown. Serum levels of cardiac troponins have emerged as very specific and sensitive markers of myocardial damage in both humans and animal myocarditis models as they are released by damaged myocytes during cardiac injury. Using endpoint serums collected at week 14, levels of cTnI and cTnT were non-invasively measured, and mice exposed to MGAS8232 wildtype expressed no differences in cTnI and cTnT serum levels compared to Δ*emm18*-infected or control mice (**Figure 26**). These results show that myocyte necrosis was not detected using this methodology following multiple *S. pyogenes* infections, and that myocardial injury, and such myocardial damage, does not sufficiently account for the occurrence of altered LV function in this model. These data are in accordance with a study of 95 ARF patients that detected no changes of cTnI levels or echocardiographic myocardial deformities in patients presenting varying stages of carditis, suggesting that there is not significant myocardial involvement during ARF [415]. Furthermore, echocardiographic analysis of LV function has been shown to normalize following valve replacement surgery in ARF patients with active carditis and congestive heart failure [416], which supports the absence of a significant role for myocarditis during valvular disease. Cardiac troponin levels are typically a time-dependant phenomenon with a half-life of 2 hours in serum [417] however, persistent cTnT elevations can remain present for up to 14 days due to the slow dissociation of cTnT from sarcomeres and release from the cells during necrosis [417,418]. In our study, the delay between echocardiogram assessment at week 13 and endpoint blood collection was 1 week only, and thus, we believe that the negative predictive levels of cardiac troponins over time did not limit the validity of these results at this timepoint. This final blood draw, however, occurred 2 weeks following the

last streptococcal infection, therefore, cTnI and cTnT levels should also be measured at an earlier timepoint to further corroborate these findings. Although this study reported the systematic use of echocardiography and cTnI assessment to detect the presence myocardial damage, immunohistologic evidence is required to support the absence of myocardial damage and confirm that altered LV function is related only to the extent of valvular damage.

During ARF and RHD, cross-reacting antibodies are believed to initiate host tissue injury by binding to the valve endothelium to promote inflammation, neovascularization, lymphocyte infiltration, and valve scarring [397,398]. In support of the molecular mimicry hypothesis, antibody responses against both the streptococcal M protein and host myosin have been previously identified in ARF and RHD patients and in rodent models [419–421]. Furthermore, using superantigen-neutralization activity as a readout, serum samples from a cohort of ARF/RHD patients revealed neutralizing antibodies for 10 distinct superantigens and 2 variants of the SmeZ superantigen compared with non-ARF/RHD individuals and healthy controls [422]. In the current study, mice repeatedly exposed to *S. pyogenes* MGAS8232 infections did not demonstrate significantly increased serum IgG responses to either the M18 protein or SpeA compared to control mice at weeks 10 and 14 (**Figure 27**)*,* despite evidence that multiple nasopharyngeal challenges offer protection against subsequent infection (**Figure 28**). Early studies demonstrated the presence and persistence of M type-specific antibodies in patients convalescing from pharyngitis that last for as long as 32 years after an infection [56], and have even been identified in a recovered ARF patient 45 years later [409]. These reports led to the belief that M protein-specific antibodies persist for extended periods of time, possibly even conferring lifelong type-specific immunity. Recently, Pandey et al., demonstrated that two homologous pyoderma infections within a 3-week period does indeed establish specific memory B cell responses that are enduring and protective [361]. Repeated infections with either the same or different strains also led to a broadening of the antibody repertoire, shown by the induction of antibodies to the IL-8 protease, SpyCEP [361]. Since it is widely believed that additional *S. pyogenes* exposures can enhance antibody responses, it was hypothesized that mice sequentially exposed to the same streptococcal strain would indeed present higher

strain-specific antibody levels. While our results were unexpected, there are reports of children that do not develop type-specific antibodies following known streptococcal infections [423], and reports of just 12% of children with pyoderma developing antibodies against the infecting strain [424]. One explanation for the detection of low M18 and SpeA antibody levels may be due to binding of their antigens during an active infection, which may temporarily deplete antibodies from the serum, rendering interpretation of antibody titers difficult during an active infection. Following repeated pyoderma challenges with the M91 serotype *S. pyogenes* NS27 in BALB/c mice, M91-specific IgG levels had risen, and then quickly declined in mice in the days following each infection [361]. In this study, however, endpoint serum samples from mice were collected two weeks after their last *S. pyogenes* challenge and are unlikely to explain low peripheral titers. Besides, B6$_{HLA}$ mice clear *S. pyogenes* MGAS8232 from their cNTs within 6 days following inoculation, and thus, mice in this study were not actively infected with *S. pyogenes* during serum collection. Furthermore, IgG titers to the M91 N-terminal peptide were generally low both during and following sequential pyoderma infections compared to levels measured following immunization [361]. Our observations may also be explained by hyperimmune stimulation. Given that superantigens function to activate T cells in a TCR Vβ-specific manner, studies have analyzed T lymphocyte populations with specific TCR Vβ regions from ARF/RHD patients as an indirect readout of possible superantigen activity and to determine whether superantigen-mediated T cell activation influences RHD progression. A cohort of ARF/RHD patients showed an increased percentage of peripheral blood CD3$^+$ T cells with a reduced percentage of Vβ2$^+$CD8$^+$ T cells compared with healthy controls, and the authors hypothesized that anergic or apoptotic responses to exogenous superantigen were responsible [425]. Bhatnagar et al., similarly demonstrated diminished IL-2 levels from CD8$^+$ T cells, but not CD4$^+$ T cells, isolated from ARF/RHD patients with SpeA treatment [426]. Focusing on T cells that infiltrated heart valves in RHD patients, increased Vβ-specific responses were detected in 8 of 15 RHD valves, with no alterations in control valves [427]. Contrarily, other studies detected no alterations in 19 Vβ gene families from 9 patients with ARF at admission, or at 6-weeks or 6-months post-admission [428]. By targeting T cells, superantigens stimulate uncontrolled cytokine responses that simultaneously recruit and then subvert the activity of effector cells, impeding the host's

ability to combat infections. Human tonsils exposed to superantigens develop B cell apoptosis with marked reductions in Ig synthesis [429]. Impaired antibody responses against *S. pyogenes* have similarly been identified in patients with recurrent streptococcal tonsillitis [430]. Patients displayed significantly reduced SpeA titers, SpeA perturbation of germinal center T follicular helper cell populations, and SpeA-induced killing of germinal center B cells through aberrant granzyme B and perforin expression [430]. Furthermore, it was recently shown that immunization with wildtype SpeA rendered Vβ8$^+$ T cells poorly responsive, ultimately protecting mice from nasopharyngeal infection [157]. Since SpeA exposure is known to induce Vβ-specific T-cell unresponsiveness [157], these studies suggest that repeated superantigen exposure during sequential nasopharyngeal infections may have profound perturbations on the host adaptive immune system. In our study, splenocytes from both wildtype and Δ*emm18*-infected mice exhibited reduced IL-2 levels with SpeA stimulation compared to uninfected mice (**Figure 29**), which supports this indication. Further research using flow cytometry to study the impact of sequential infections on Vβ8$^+$ T cell populations is necessary to confirm these findings. As noted by other investigators, Vβ analysis of T cell populations may not provide definitive answers as ARF symptoms often develop weeks after pharyngitis and pathogenic T cells may not skew in the periphery [428], however, elevated amounts of both peripheral B and T lymphocytes have been identified in ARF patients compared to those with uncomplicated pharyngitis [431]. After an ARF episode, T cell expansion peaked at ~6 weeks and declined by ~12 weeks, and no expansion of T cells were identified the periphery of RHD patients [431]. Based on this data, analysis of numerically different Vβ-specific T cell populations may have to be analyzed at specific times following infection and studied both in the periphery and heart. Splenocyte proliferation assays in this study also revealed that wildtype and Δ*emm18*-infected mice did not show increased T cell activation in response to M18 protein stimulation (**Figure 29B, C**). These results conflict with previous investigations where both peripheral blood and valve-infiltrating human T cells from ARF/RHD patients react strongly and proliferate from M protein stimulation, and also cross-reacted with both myocardium and valve-derived proteins [392–394,432–435]. While T cells in our study were unresponsive to SpeA, splenocytes from wildtype-infected mice secreted twice the amount of IL-2 compared to control mice from stimulation with

10^5 and 10^6 pg mL^{-1} of M18 protein (**Figure 29**), suggesting that T cell responses are not completely inert against the M protein. Why Δ*emm18*-infected mice similarly demonstrated increasing T cell activation with M18 stimulation, despite not being exposed to the protein during infections requires further in-depth analyses of the antigen-specificities of activated T cell clones from these mice and their cross-reactive properties. Further characterization of T cell responses to M protein, other bacterial antigens, and other possible host autoantigens are needed to elucidate potential autoimmune T cell responses following *S. pyogenes* infections. In light of the described findings, it seems likely that repeated exposure to superantigens induced abnormal T cell-dependent responses that may be provoking unresponsiveness. This superantigen-induced unresponsiveness could be a host defensive strategy to balance immunity and tolerance that minimizes superantigen activation and escapes harmful attacks by autoreactive lymphocytes. This may provide a reason for why splenocytes are not easily activated into clonal expression after sequential *S. pyogenes* infections. Although anergy is under complex regulation, and it remains unknown how long this anergic state may last *in vivo*, superantigen-induced anergy could be of help in understanding, or possibly combatting, the pathophysiological mechanisms in ARF and RHD.

Since many ARF patients have no indication of a preceding *S. pyogenes* infection, correct diagnosis of ARF relies heavily on serologic evidence, such as elevated antibody responses to SLO or DNase B [44]. Serological evidence may also be useful when streptococcal cultures are not recovered from patients presenting ARF symptoms, likely due to cardiac symptoms occurring at least two weeks following a streptococcal infection [44]. Antibodies against the streptococcal GAC have been shown to remain elevated for at least 1 year and even up to 20 years in patients with valvulitis, and correlate with poor prognosis of valvular heart disease [396]. Removal of inflamed valves from rheumatic patients has also been associated with a significant decline in anti-GAC antibodies from patient serum [436]. Due to similar alpha-helical structures and glycosylated proteins, antibodies from patients with ARF have also been shown to cross-react with GlcNAc [395–398], which may support a role for anti-GAC antibodies in immunological cross-reactivity against the heart. Together, measuring antibody responses against SLO, DNase B, or GlcNAc would

indicate whether antibodies developed against *S. pyogenes* following multiple infections, and for potential insights into cross-reactive immune responses.

The results of this study have important implications for *S. pyogenes* infections and LV heart function; however, it is difficult to arrive at any conclusions regarding the induction of autoimmunity. This assumption warrants further investigations that explore immunological responses to host antigens. The fact that immune responses to cardiac myosin can induce myocarditis in animal models in the absence of infection [400,437–442] strengthens the role of cardiac myosin as an immunodominant host autoantigen, and thus, antibody and T cell responses to cardiac myosin need to be further explored. However, antibodies against myosin are not sufficient to induce experimental autoimmune myocarditis (EAM) via passive transfer, and immune responses to myosin do not develop initially in EAM but later in the disease process [437,443,444]. Furthermore, myosin is an intracellular protein present in the myocardium and not in valvular tissue, and anti-myosin antibodies do not recognize intact myocytes [443], therefore, initial damage through another cardiac antigen likely comes first. Autoantibodies that recognize cardiac myosin have been shown to cross-react with laminin, an ECM glycoprotein located in the valve endothelial underlying basement membrane [398]. Following endothelial cell disruption and exposure of the underlying ECM, laminin becomes exposed and may contribute to binding of cross-reactive antibodies and subsequent inflammation of valvular tissue. Autoantibodies against collagen types I and IV have similarly been demonstrated in ARF patients [420], yet streptococcal proteins that are cross-reactive with collagen have not been identified [420,445]. One theory describes the generation of anti-collagen antibodies as a mechanism independent from molecular mimicry. Streptococcal M proteins may bind and aggregate collagen directly, via the peptide-associated with rheumatic fever (PARF) amino acid sequence, promoting conformational changes in collagen structure that influence collagen presentation and cause it to be recognized as an autoantigen [445–448]. Furthermore, valve endothelial damage that exposes the underlying ECM may trigger production of autoantibodies against basement-membrane collagen, initiating the pathological process. Collagen, the principal protein component of the valve ECM, is mainly found as densely packed interweaving bundles of fibers that provide the valve with

structural and mechanical strength, and thus, disruption of collagen organization compromises the structural integrity of heart valves leading to valve pathology [389]. Rheumatic patients have higher deposition of collagen on their mitral valves with evidence of fibrosis and valve thickening when compared to non-rheumatic mitral valves [449]. Collectively, studies have demonstrated that immune responses to host myosin, laminin, and collagen are evident in ARF and RHD patients and their role in disease pathology warrants deeper investigation. Since myosin, laminin, and collagen are typically immunologically inaccessible in healthy hearts, they are unlikely to be initial targets of autoimmune disease development. It may be possible that cellular infiltration of inflammatory T cells and macrophages releases a cytokine storm (via superantigen stimulation) and stimulates valvular interstitial cells to overexpress fibrillar collagen, leading to valve structural disarray [390]. Repeated immunological disruption of the valvular endothelium and ECM would expose hidden antigens, triggering epitope spreading to myosin, laminin, and collagen, which then dominate succeeding autoimmunity.

The pathogenesis of ARF and RHD results from three principal risk factors: exposure to a specific *S. pyogenes* strain and usually a throat infection, a genetically susceptible host, and an aberrant immune response that triggers autoimmunity [47,50,381,450]. Our model included inoculating B6$_{HLA}$ mice with sequential biweekly nasal infections of *S. pyogenes* MGAS8232 (**Figure 20**), which was designed to mimic the recurrent acute infections that precede ARF, exacerbate ARF symptoms, and lead to RHD. Firstly, *S. pyogenes* MGAS8232 is a serotype M18 strain and pharyngeal isolate from a patient with ARF [269,451], and is therefore assumed to express distinct "rheumatogenic" properties that stimulate autoimmune consequences. Although several M protein serotypes have been historically associated with ARF, M18 serotypes have been connected to ARF outbreaks in the U.S. for decades [269,452–454], with rates of ARF disappearing as the proportion of circulating *emm18*-types declined [454]. Secondly, several studies have implicated HLA class II molecules to confer increased susceptibility of developing ARF and RHD, and in our model, we utilized transgenic C57Bl/6 mice expressing HLA-DR4/DQ8 alleles. Associations between HLA class II alleles and ARF/RHD have encountered HLA-DR4

alleles in significantly higher frequencies in Caucasian American [455,456] and Saudi Arabian populations [457] with ARF/RHD, however, discrepancies exist as to which alleles confer susceptibility across various population groups around the world [50,458–460]. The role of specific MHC class II molecules in ARF/RHD development may be driven entirely by their ability to present particular autoreactive peptides, however, the ability of MHC class II molecules to function as receptors for streptococcal superantigens may also contribute to the activation and dysregulation of autoreactive T cells. Thymic negative selection of self-reactive T cells is a key element of central immune tolerance but autoreactive T cells can escape this process and populate the peripheral immune system [461,462]. Since superantigens "force" the activation of a large percentage of exposed T cells, it is reasonable to hypothesize that some of the T cells targeted by superantigens will be self-reactive. Therefore, we envision a potential scenario where susceptible HLA alleles present antigenic peptides to peripheral T cells that have escaped immune tolerance and superantigens activate and exacerbate these autoreactive T cell responses, which then cross-react with antigens they are unable to identify as self and initiate the autoimmune process. It has long been proposed that superantigens may be important triggers for a variety of autoimmune diseases [463–465] and risk factors for invasive streptococcal disease have been linked to differential superantigen inflammatory responses driven by different HLA alleles [152–154]. Therefore, it is of great interest to evaluate animal models that express these human factors to account for the potential susceptibility of disease development. Taken together, transgenic rodent models that express HLA molecules may represent more appropriate and susceptible *in vivo* models for both *S. pyogenes* infection and autoimmune disease development.

The dominant model currently used to investigate ARF/RHD pathology is the RAV model, which contributed substantially to our current understanding of the central autoimmune theories supporting ARF/RHD features. This model provided evidence that immune responses against cardiac myosin can develop following immunization with streptococcal M5 and M6 proteins, however, important limitations and unanswered questions still remain. The molecular mimicry theory of RHD disease development assumes that epitope mimicry of a single antigen between pathogens, such as M protein, and human proteins,

such as myosin, is both necessary and sufficient to induce autoimmune disease. This mono-causal theory implies that incidences of RHD would then be directly related to the number of genetically susceptible individuals and their probability of acquiring an infection capable of triggering autoimmune disease, yet only a fraction of those infected with *S. pyogenes* infection develop autoimmune sequalae [460]. Genetic predisposition may account for part of the susceptibility to RHD, but it does not explain the large proportion of individuals who develop immunity to a molecular mimic (M protein) following infection and yet do not develop disease. Therefore, molecular mimicry may be *necessary* to provoke autoimmunity, but incidences of RHD following exposure to *S. pyogenes* suggests that it is not *sufficient.* This might explain why purified M protein or myosin by themselves without an adjuvant are inadequate to produce valvulitis experimentally [466,467]. If autoimmune diseases are multi-causal and induced by a combination of molecular mimicry and bystander activation, then two or more immunological events are required to induce autoimmune disease, which supports the lower prevalence of RHD worldwide. Presence of an appropriate cofactor at the time a molecular mimic is encountered, such as those provided by cytokines or infectious triggers of innate immune responses, can determine how autoreactive T cells are co-stimulated with cross-reactive antigens to influence whether any particular immunological trigger abrogates ongoing autoimmune processes [466]. Bystanders can lower the threshold of antigen stimulation required to induce autoimmune responses and increase the rate at which autoimmune disease develops. In our study of recurrent infections, streptococcal superantigens are active in B6$_{HLA}$ mice, and nasopharyngeal infection by *S. pyogenes* MGAS8232 stimulates significant release of Th1-type cytokines and activation of polyclonal T cells [156,157]. It is possible that some T cells targeted by superantigens will include subsets of autoreactive cells that drive autoimmune development with re-exposure and T cell reactivation. However, this theory implies that any immunological stimulus (infection, or adjuvant) would provide a bystander effect for any given antigen, but adjuvants in the RAV model are not interchangeable. Replacing CFA with IFA, Emulsigen®, or Montanide ISA50V adjuvants, failed to induce valvulitis using *S. pyogenes* M5 protein [468] and were unsuitable alternatives to CFA. The use of CFA is mandatory in some experimental models of autoimmune diseases and it is thought that the mycobacterial components produce a

specific rather than non-specific form of immune responses, such as promoting DC maturation, signaling Th1 skewing, and strong delayed-type hypersensitivity against autoantigens [469]. As adjuvants were not used in this study, repeated mitogenic exposure to superantigens during biweekly infections could support bystander activation to the M protein. Superantigens have been shown to exaggerate animal models of autoimmunity, including rheumatoid arthritis [470,471] and multiple sclerosis [472,473]. Chronic cutaneous lupus erythematous patients, compared with acute cutaneous lupus erythematous patients, exhibited oligo-clonal expansion of $V\beta8^+$ and $V\beta13^+$ T cells from skin lesions [474]. Type I diabetes patients have also demonstrated an expanded $V\beta7^+$ population in the pancreas with diverse CDR3β sequences and without Vα skewing [475]. Thus, in multiple autoimmune settings, T cells from affected autoimmune patients may often exhibit altered Vβ profiles with polyclonal Vβ-restricted responses, which is consistent with superantigen-induced responses. Although Vβ profiles were not investigated in this study, murine splenocytes showed reduced activation by SpeA at week 14 and no difference in SmeZ responsiveness, which supports that specific T cell populations may be exhausted following multiple infections by *S. pyogenes*. Overall, there is a complex network of factors in the pathogenesis of autoimmune diseases, in which the role of superantigens has not yet been elucidated but may play an important role. More work is needed to define how general or specific bystander requirements must be in order to determine whether superantigens have a role in ARF/RHD.

This work provides valuable insight into the physiological consequences from repeated exposure to acute *S. pyogenes* nasopharyngeal infections. Although our model is suitable to represent nasopharyngeal infections in mice, it is still not completely analogous to strep throat in humans. Future studies should assess antibody and T cell-mediated responses following multiple *S. pyogenes* infections with the same or multiple strains, as well as in a more human-like model, such as non-human primates [476]. Moreover, while this study focused on just one strain of *S. pyogenes*, future work should assess other isolates, including M5 and M6 serotypes, that have previously demonstrated cross-reactivity to cardiac proteins [366,370,386,387,400]. It will be important to assess cardiac function following infections with various strains and their respective M protein mutants to confirm

that M protein expression directly provokes cardiac complications. Furthermore, due to limitations in murine colony breeding, a minimal number of animals were used in these experiments and future work should utilize a greater number of animals to reach profound biological significance. Lastly, ARF is multifactorial in origin and can affect multiple organs including the heart, brain, joints, connective tissues and skin [46,320,381], and patients may develop various combinations of clinical symptoms. Approximately 30% of ARF patients present both cardiac and neurobehavioral complications [10], and arthritis is observed in up to 70% of patients with ARF [399]. Therefore, an animal model that exhibits several of the Jones diagnostic characteristics observed in ARF (**Table 1**) would be advantageous to accurately identify early immune responses involved in the multiple complications associated with ARF, and to evaluate therapeutic interventions, and the safety and efficacy of vaccine candidates.

To conclude, this work demonstrated that repeated nasal infections with *S. pyogenes* MGAS8232 resulted in elevated *E/A* ratios and reduced ejection fractions compared to control mice and Δ*emm18* mutant infections. This was illustrated by echocardiographic detection of significantly higher *E/A* ratios and reduced ejection fractions in following MGAS8232 wildtype infections. The lack of elevated cardiac troponin serum levels suggested that myocardial damage was not present and unable to explain the defects in LV function. While we showed that antibody levels to M18 protein and SpeA were not significantly elevated from multiple infections, T cell responsiveness was perturbed, which likely prevented subsequent infections. To our knowledge, this thesis presents the first use of echocardiogram imaging to detect changes to LV function in mice following repeated *S. pyogenes* infections. From this work, there is now a template to assess other strains and various antigens through mutagenesis, which offers a different approach to current animal models of valvulitis that use M protein immunizations. We concluded this work with the construction of a *S. pyogenes* Δ*gacI* mutant that will be used in future studies to investigate the role of GlcNAc in LV dysfunction following repeated infections. Findings from our work may help guide future research that investigates the safety and efficacy of vaccine candidates that may have remarkable advancements in preventing the ~300,000 deaths and ~10.5 million DALYs associated with ARF and RHD each year [477].

Chapter 5: Conclusions

5.1   Conclusions

On a global scale, *S. pyogenes* is responsible for an enormous burden of morbidity and mortality and a vaccine that is safe and effective at preventing the vast range of infections caused by this organism would have a substantial impact on the health of millions of people worldwide. Since no licensed vaccine is currently available it is crucial to develop a better understanding of the factors that influence infection, and therefore, this thesis aimed to explore the biological role of the HA capsule and M protein by *S. pyogenes* MGAS8232 during early stages of nasopharyngeal and skin infections. This work also aimed to characterize the efficacy of a M protein vaccine in preventing acute *S. pyogenes* infections and determine whether M protein expression influences left ventricle cardiac function using echocardiogram imaging. Together, this work provided key understandings on how *S. pyogenes* exploits host-pathogen interactions to successfully colonize and establish infection within these limited biological niches and insights on the physiological complications following acute infections.

In Chapter 2, our findings support the hypothesis that HA capsule expression is crucial for *S. pyogenes* MGAS8232 pathogenesis by promoting a strong resistance to immune clearance by neutrophils in murine models of experimental nasal and skin infections. In absence of capsule expression, infection with Δ*hasA* revealed a 10,000-fold reduction in bacterial CFUs recovered from nasal turbinates compared to wildtype-infected mice, which was rescued through trans-complementation of the *hasA* gene (**Figure 2A**). Furthermore, mice injected intradermally with Δ*hasA* presented no weight loss, smaller lesions, and significantly less bacterial CFUs in skin lesions than wildtype-infected mice (**Figure 4**). Similarly, infection with the HA capsule complement strain rescued the number of Δ*hasA* CFUs recovered from the skin. While future work is needed to clarify adherence properties of encapsulated and unencapsulated *S. pyogenes in vivo,* we showed that any capsule-mediated adherent properties are less important than providing protection from neutrophil killing during acute infections. We demonstrated that MGAS8232 Δ*hasA* had attenuated survival in human blood and with neutrophils *in vitro* compared to wildtype and capsule complement strains (**Figure 6A, 6B**), and depleting neutrophils *in vivo* through α-Ly6G administration recovered the reduced burden by Δ*hasA* in both nasopharynx and skin

(**Figure 6D, 8C**). Future studies using additional strains are recommended to draw general conclusions, define specific molecular mechanisms utilized by the HA capsule to resist neutrophil-mediated clearance, and to explore possible redundant mechanisms across individual immune cell types.

In Chapter 3, our findings unexpectantly refute the hypothesis that serotype-specific immunity against the M protein prevents superficial *S. pyogenes* infections by homologous strains. While this work provided support that parenteral immunizations with M3, M12, M18, and M74 proteins induced robust systemic M protein-specific IgG, these responses failed to prevent infection by *S. pyogenes* in the nasopharynx and skin of $B6_{HLA}$ mice (**Figure 14, Figure 15**). Since protection against upper respiratory tract and skin infections is a requirement for any *S. pyogenes* vaccine, induction of systemic M protein IgG is not sufficient by itself to provide immunity against *S. pyogenes*. Thus, the results of this study indicate that subcutaneous M protein immunizations are not optimal for vaccine consideration and future studies should focus on defining protective M protein immune responses using multiple routes of vaccine administration. The findings of this chapter also reveal that genetic deletion of M18 protein in *S. pyogenes* MGAS8232 had no impact on bacterial burden in nasal turbinates or skin lesions of mice as Δ*emm18* mutant recovery was similar to wildtype at both sites of infection (**Figure 17, Figure 19**). While it remains possible that functionally redundant bacterial components may compensate for deletion of M18 protein during acute infections, M proteins bind several human-specific complement inhibitors to promote bacterial immune evasion. Therefore, future experimentation should utilize mice that are humanized in ways more relevant to M protein function to fully elucidate the necessity of M protein during acute nasopharyngeal and skin infections, and to further explore whether M protein immunizations are protective against acute *S. pyogenes* infections.

Lastly, in Chapter 4 we implemented a recurring *S. pyogenes* infection model to evaluate whether M protein expression is a possible driver of cardiac disease development by using echocardiography to assess LV features in mice. The principal findings of this chapter revealed that repeated biweekly nasopharyngeal exposure to *S. pyogenes* MGAS8232 elevated left atrial pressures, illustrated by significantly elevated *E/A* ratios, and weakened

ejection fractions in mice compared to control inoculations of PBS or infections with MGAS8232 Δ*emm18* (**Figure 24, Figure 25**). These findings are the first to report that left ventricle function is directly influenced by multiple homologous infections with *S. pyogenes* and that M18 protein expression is associated with modifications to these parameters. It will be important to assess cardiac function following infections with various strains and their respective M protein mutants to confirm that M protein expression specifically provokes cardiac defects. Interestingly, the lack of elevated cardiac troponin serum levels suggested that myocardial damage was not present and could not explain the LV defects (**Figure 26**). Our findings also demonstrate that M18 protein and SpeA IgG responses were not significantly elevated following multiple infections (**Figure 27**), which may be due to superantigen-induced T cell unresponsiveness (**Figure 29**). Analysis of numerically different Vβ-specific T cell populations at specific times in both the periphery and heart following sequential infections is needed to corroborate these findings. While the results of this study have important implications for *S. pyogenes* infections and initiation of severe heart complications, it is difficult to arrive at any conclusions regarding the induction of autoimmunity. Future studies should focus on assessing host responses to both bacterial and host antigens following multiple infections to determine whether host immunity becomes perturbed with multiple *S. pyogenes* exposures, and for insights into possible cross-reactive immune responses. From the work presented in this chapter, there is now a differentiated live infection model to assess various bacterial components in disease development, and we conclude this work with construction of a *S. pyogenes* MGAS8232 Δ*gacI* mutant strain for future studies to examine GlcNAc expression as another possible contributor to cardiac complications following repeated infections.

Together, the work presented in this thesis has provided greater mechanistic understandings into how *S. pyogenes* exploits its surface virulent determinants to avoid innate clearance and reveals physiological insights on the development of severe complications following multiple superficial infections. This work has also provided valuable immune considerations that will help guide future vaccine development strategies against this globally prominent pathogen.

References

1.   Beres SB, Musser JM. Contribution of exogenous genetic elements to the group A Streptococcus metagenome. PLoS One. 2007;2: e800. doi:10.1371/journal.pone.0000800

2.   Bessen DE, McShan WM, Nguyen S V., Shetty A, Agrawal S, Tettelin H. Molecular epidemiology and genomics of group A Streptococcus. Infect Genet Evol. 2015;33: 393–418. doi:10.1016/j.meegid.2014.10.011

3.   Maruyama F, Watanabe T, Nakagawa I. Streptococcus pyogenes Genomics. In: Ferretti JJ, Stevens DL, Fischetti VA, editors. Streptococcus pyogenes: Basic Biology to Clinical Manifestations. University of Oklahoma Health Sciences Center; 2016. pp. 171–249. Available: https://www.ncbi.nlm.nih.gov/books/NBK333426/

4.   Cunningham MW. Pathogenesis of group A streptococcal infections. Clin Microbiol Rev. 2000;13: 470–511. doi:10.1128/CMR.13.3.470-511.2000

5.   Lancefield RC. THE ANTIGENIC COMPLEX OF STREPTOCOCCUS HAEMOLYTICUS : I. DEMONSTRATION OF A TYPE-SPECIFIC SUBSTANCE IN EXTRACTS OF STREPTOCOCCUS HAEMOLYTICUS. J Exp Med. 1928;47: 91–103. doi:10.1084/JEM.47.1.91

6.   Tanz RR, Shulman ST. Chronic pharyngeal carriage of group A streptococci. Pediatr Infect Dis J. 2007/01/30. 2007;26: 175–176. doi:10.1097/01.inf.0000255328.19808.be00006454-200702000-00015 [pii]

7.   Walker MJ, Barnett TC, McArthur JD, Cole JN, Gillen CM, Henningham A, et al. Disease Manifestations and Pathogenic Mechanisms of Group A Streptococcus. Clin Microbiol Rev. 2014;27: 264–301. doi:10.1128/CMR.00101-13

8.   Cunningham MW. Post-Streptococcal Autoimmune Sequelae: Rheumatic Fever and Beyond. *Streptococcus pyogenes* : Basic Biology to Clinical Manifestations. 2016. Available: http://www.ncbi.nlm.nih.gov/pubmed/26866235

9.   Marijon E, Mirabel M, Celermajer DS, Jouven X. Rheumatic heart disease. Lancet (London, England). 2012;379: 953–64. doi:10.1016/S0140-6736(11)61171-9

10.   Carapetis JR, Steer AC, Mulholland EK, Weber M. The global burden of group A streptococcal diseases. Lancet Infect Dis. 2005;5: 685–694. doi:S1473-3099(05)70267-X [pii] 10.1016/S1473-3099(05)70267-X

11.   Carapetis JR, Steer AC, Mulholland EK, Weber M. The global burden of group A streptococcal diseases. Ferretti JJ, Stevens DL, Fischetti VA, editors. Lancet Infect Dis. 2005;5: 685–94. doi:10.1016/S1473-3099(05)70267-X

12. O'Brien KL, Beall B, Barrett NL, Cieslak PR, Reingold A, Farley MM, et al. Epidemiology of invasive group A *Streptococcus* disease in the United States, 1995-1999. Clin Infect Dis. 2002/07/13. 2002;35: 268–276. doi:10.1086/341409

13. Watkins DA, Johnson CO, Colquhoun SM, Karthikeyan G, Beaton A, Bukhman G, et al. Global, Regional, and National Burden of Rheumatic Heart Disease, 1990–2015. N Engl J Med. 2017;377: 713–722. doi:10.1056/NEJMoa1603693

14. 2008 WORLD POPULATION Data Sheet. Popul English Ed. 2008; 133. Available: http://www.prb.org/pdf06/06WorldDataSheet.pdf

15. World Health Organization. Epidemiology and management of common skin diseases in children in developing countries. Geneva: World Health Organization. 2005. p. 54. doi:/entity/maternal_child_adolescent/documents/fch_cah_05_12/en/index.html

16. Carapetis JR. Rheumatic Heart Disease in Developing Countries. N Engl J Med. 2007;357: 439–441. doi:10.1056/NEJMp078039

17. Bessen DE. Tissue tropisms in group A Streptococcus: what virulence factors distinguish pharyngitis from impetigo strains? Curr Opin Infect Dis. 2016;29: 295–303. doi:10.1097/QCO.0000000000000262

18. Martin J. The Streptococcus pyogenes Carrier State. In: Ferretti JJ, Stevens DL, Fischetti VA, editors. Streptococcus pyogenes: Basic Biology to Clinical Manifestations. University of Oklahoma Health Sciences Center; 2016. pp. 587–600. Available: http://www.ncbi.nlm.nih.gov/pubmed/27466665

19. Martin JM, Green M, Barbadora KA, Wald ER. Group A streptococci among school-aged children: clinical characteristics and the carrier state. Pediatrics. 2004;114: 1212–9. doi:10.1542/peds.2004-0133

20. Anja A, Beyene G, S/Mariam Z, Daka D. Asymptomatic pharyngeal carriage rate of Streptococcus pyogenes, its associated factors and antibiotic susceptibility pattern among school children in Hawassa town, southern Ethiopia. BMC Res Notes. 2019;12: 564. doi:10.1186/s13104-019-4601-9

21. Oliver J, Malliya Wadu E, Pierse N, Moreland NJ, Williamson DA, Baker MG. Group A Streptococcus pharyngitis and pharyngeal carriage: A meta-analysis. PLoS Negl Trop Dis. 2018;12: 1–17. doi:10.1371/journal.pntd.0006335

22. Shaikh N, Leonard E, Martin JM. Prevalence of streptococcal pharyngitis and streptococcal carriage in children: a meta-analysis. Pediatrics. 2010;126: e557-64. doi:10.1542/peds.2009-2648

23. Schwartz RH, Wientzen RL, Pedreira F, Feroli EJ, Mella GW, Guandolo VL. Penicillin V for Group A Streptococcal Pharyngotonsillitis: A Randomized Trial of Seven vs Ten Days' Therapy. JAMA J Am Med Assoc. 1981;246: 1790–1795.

doi:10.1001/jama.1981.03320160022023

24. Danchin MH, Rogers S, Selvaraj G, Kelpie L, Rankin P, Vorich R, et al. The burden of group A streptococcal pharyngitis in Melbourne families. Indian J Med Res Suppl. 2004;119: 144–147.

25. Wald ER, Dashefsky B, Feidt C, Chiponis D, Byers C. Acute rheumatic fever in western Pennsylvania and the Tristate area. Pediatrics. 1987;80: 371–374.

26. Veasy GL, Wieldmeier Susan E, Orsmond GS, Ruttenberg, Herbert D. Resurgence of Acute Rheumatic Fever in the Intermountain Area of the United States. N Engl J Med. 1987;316: 421–427.

27. Weiss K, Laverdière M, Lovgren M, Delorme J, Poirier L, Béliveau C. Group A Streptococcus carriage among close contacts of patients with invasive infections. Am J Epidemiol. 1999;149: 863–868. doi:10.1093/oxfordjournals.aje.a009902

28. DeMuri GP, Wald ER. The group a streptococcal carrier state reviewed: Still an enigma. J Pediatric Infect Dis Soc. 2014;3: 336–342. doi:10.1093/jpids/piu030

29. Johnson DR, Kurlan R, Leckman J, Kaplan EL. The human immune response to streptococcal extracellular antigens: clinical, diagnostic, and potential pathogenetic implications. Clin Infect Dis. 2010;50: 481–490. doi:10.1086/650167

30. Mustafa Z, Ghaffari M. Diagnostic Methods, Clinical Guidelines, and Antibiotic Treatment for Group A Streptococcal Pharyngitis: A Narrative Review. Front Cell Infect Microbiol. 2020;10: 1–10. doi:10.3389/fcimb.2020.563627

31. Pfoh E, Wessels MR, Goldmann D, Lee GM. Burden and economic cost of group A streptococcal pharyngitis. Pediatrics. 2008;121: 229–234. doi:10.1542/peds.2007-0484

32. Cole C, Gazewood J. Diagnosis and treatment of impetigo. Am Fam Physician. 2007;75: 859–864.

33. Ferrieri P, Dajani AS, Wannamaker LW, Chapman SS. Natural history of impetigo. J Clin Invest. 1972;51: 2863–2871. doi:10.1172/jci107109

34. Bowen AC, Mahé A, Hay RJ, Andrews RM, Steer AC, Tong SYC, et al. The global epidemiology of impetigo: A systematic review of the population prevalence of impetigo and pyoderma. PLoS One. 2015;10. doi:10.1371/journal.pone.0136789

35. Lamagni TL, Darenberg J, Luca-Harari B, Siljander T, Efstratiou A, Henriques-Normark B, et al. Epidemiology of Severe Streptococcus pyogenes Disease in Europe. J Clin Microbiol. 2008;46: 2359–2367. doi:10.1128/JCM.00422-08

36. Davies HD, McGeer A, Schwartz B, Green K, Cann D, Simor AE, et al. Invasive

group A streptococcal infections in Ontario, Canada. Ontario Group A Streptococcal Study Group. N Engl J Med. 1996;335: 547–554. Available: http://www.ncbi.nlm.nih.gov/entrez/query.fcgi?cmd=Retrieve&db=PubMed&dopt=Citation&list_uids=8684408

37. O'Loughlin RE, Roberson A, Cieslak PR, Lynfield R, Gershman K, Craig A, et al. The epidemiology of invasive group A streptococcal infection and potential vaccine implications: United States, 2000-2004. Clin Infect Dis. 2007;45: 853–862. doi:10.1086/521264

38. McCormick JK, Yarwood JM, Schlievert PM. Toxic shock syndrome and bacterial superantigens: An update. Annu Rev Microbiol. 2001;55: 77–104. doi:10.1146/annurev.micro.55.1.77

39. Proft T, Sriskandan S, Yang L, Fraser JD. Superantigens and streptococcal toxic shock syndrome. Emerg Infect Dis. 2003;9: 1211–1218. doi:10.3201/eid0910.030042

40. Dahl PR, Perniciaro C, Holmkvist KA, O'Connor MI, Gibson LE. Fulminant group A streptococcal necrotizing fasciitis: clinical and pathologic findings in 7 patients. J Am Acad Dermatol. 2002;47: 489–92. Available: http://www.ncbi.nlm.nih.gov/pubmed/12271288

41. Misiakos EP, Bagias G, Patapis P, Sotiropoulos D, Kanavidis P, Machairas A. Current concepts in the management of necrotizing fasciitis. Front Surg. 2014;1: 36. doi:10.3389/fsurg.2014.00036

42. Angoules AG, Kontakis G, Drakoulakis E, Vrentzos G, Granick MS, Giannoudis P V. Necrotising fasciitis of upper and lower limb: A systematic review. Inj Int J Care Inj. 2007;38. doi:10.1016/j.injury.2007.10.030

43. Kaul R, McGeer A, Norrby-Teglund A, Kotb M, Schwartz B, O'Rourke K, et al. Intravenous immunoglobulin therapy for streptococcal toxic shock syndrome--a comparative observational study. The Canadian Streptococcal Study Group. Clin Infect Dis. 2000/05/29. 1999;28: 800–807. doi:10.1086/515199

44. Gewitz MH, Baltimore RS, Tani LY, Sable CA, Shulman ST, Carapetis J, et al. Revision of the Jones Criteria for the diagnosis of acute rheumatic fever in the era of Doppler echocardiography: a scientific statement from the American Heart Association. Circulation. 2015;131: 1806–18. doi:10.1161/CIR.0000000000000205

45. Martin WJ, Steer AC, Smeesters PR, Keeble J, Inouye M, Carapetis J, et al. Post-infectious group A streptococcal autoimmune syndromes and the heart. Autoimmun Rev. 2015;14: 710–725. doi:10.1016/j.autrev.2015.04.005

46. Carapetis JR, Beaton A, Cunningham MW, Guilherme L, Karthikeyan G, Mayosi BM, et al. Acute rheumatic fever and rheumatic heart disease. Nat Rev Dis Prim.

2016;2: 1–24. doi:10.1038/nrdp.2015.84

47.   Guilherme L, Kalil J. Rheumatic fever and rheumatic heart disease: Cellular mechanisms leading autoimmune reactivity and disease. J Clin Immunol. 2010;30: 17–23. doi:10.1007/s10875-009-9332-6

48.   Vijayalakshmi IB, Vishnuprabhu RO, Chitra N, Rajasri R, Anuradha T V. The efficacy of echocardiographic criterions for the diagnosis of carditis in acute rheumatic fever. Cardiol Young. 2008;18: 586–592. doi:10.1017/S1047951108003107

49.   Singh PIPK, Carapetis JR, Buadromo EM, Samberkar PN, Steer AC. The high burden of rheumatic heart disease found on autopsy in Fiji. Cardiol Young. 2008;18: 62–69. doi:10.1017/S1047951107001734

50.   Hurst JR, Kasper KJ, Sule AN, McCormick JK. Streptococcal pharyngitis and rheumatic heart disease: the superantigen hypothesis revisited. Infect Genet Evol. 2018;61: 160–175. doi:10.1016/j.meegid.2018.03.006

51.   Nordstrand A, Norgren M, Holm SE. Pathogenic mechanism of acute post-streptococcal glomerulonephritis. Scand J Infect Dis. 1999;31: 523–537. doi:10.1080/00365549950164382

52.   Eison TM, Ault BH, Jones DP, Chesney RW, Wyatt RJ. Post-streptococcal acute glomerulonephritis in children: clinical features and pathogenesis. Pediatr Nephrol. 2011;26: 165–180. doi:10.1007/s00467-010-1554-6

53.   Kirvan CA, Swedo SE, Snider LA, Cunningham MW. Antibody-mediated neuronal cell signaling in behavior and movement disorders. J Neuroimmunol. 2006;179: 173–179. doi:10.1016/j.jneuroim.2006.06.017

54.   Kirvan CA, Swedo SE, Kurahara D, Madeleine W. Streptococcal mimicry and antibody-mediated cell signaling in the pathogenesis of Sydenham ' s chorea. Autoimmunity. 2006;39: 20–29. doi:10.1080/08916930500484757

55.   Williams KA, Swedo SE. Post-infectious autoimmune disorders: Sydenham's chorea, PANDAS and beyond. Brain Res. 2015;1617: 144–154. doi:10.1016/j.brainres.2014.09.071

56.   Lancefield RC. Persistence of type-specific antibodies in man following infection with group A streptococci. J Exp Med. 1959;110: 271–92. doi:10.1084/jem.110.2.271

57.   Bessen DE. Molecular Basis of Serotyping and the Underlying Genetic Organization of Streptococcus pyogenes. Streptococcus pyogenes: Basic Biology to Clinical Manifestations. University of Oklahoma Health Sciences Center; 2016. Available: http://www.ncbi.nlm.nih.gov/pubmed/26866230

58. Frost HR, Laho D, Sanderson-Smith ML, Licciardi P, Donath S, Curtis N, et al. Immune Cross-Opsonization Within *emm* Clusters Following Group A *Streptococcus* Skin Infection: Broadening the Scope of Type-Specific Immunity. Clin Infect Dis. 2017;65: 1523–1531. doi:10.1093/cid/cix599

59. Sanderson-Smith M, De Oliveira DMP, Guglielmini J, McMillan DJ, Vu T, Holien JK, et al. A systematic and functional classification of *Streptococcus pyogenes* that serves as a new tool for molecular typing and vaccine development. J Infect Dis. 2014;210: 1325–38. doi:10.1093/infdis/jiu260

60. McGregor KF, Spratt BG, Kalia A, Bennett A, Bilek N, Beall B, et al. Multilocus Sequence Typing of Streptococcus pyogenes Representing Most Known emm Types and Distinctions among Subpopulation Genetic Structures. J Bacteriol. 2004;186: 4285–4294. doi:10.1128/JB.186.13.4285-4294.2004

61. Loh JMS, Tsai J-YC, Proft T. The ability of Group A streptococcus to adhere to immortalized human skin versus throat cell lines does not reflect their predicted tissue tropism. Clin Microbiol Infect. 2017 [cited 27 Jul 2017]. doi:10.1016/j.cmi.2017.03.011

62. Mora M, Bensi G, Capo S, Falugi F, Zingaretti C, Manetti AGO, et al. Group A *Streptococcus* produce pilus-like structures containing protective antigens and Lancefield T antigens. Proc Natl Acad Sci. 2005;102: 15641–15646. doi:10.1073/pnas.0507808102

63. Falugi F, Zingaretti C, Pinto V, Mariani M, Amodeo L, Manetti AGO, et al. Sequence Variation in Group A Streptococcus Pili and Association of Pilus Backbone Types with Lancefield T Serotypes. J Infect Dis. 2008;198: 1834–1841. doi:10.1086/593176

64. Steemson JD, Moreland NJ, Williamson D, Morgan J, Carter PE, Proft T. Survey of the bp/tee genes from clinical group A streptococcus isolates in New Zealand-implications for vaccine development. [cited 2 Jul 2019]. doi:10.1099/jmm.0.080804-0

65. Kratovac Z, Manoharan A, Luo F, Lizano S, Bessen DE. Population genetics and linkage analysis of loci within the FCT region of *Streptococcus pyogenes*. J Bacteriol. 2007;189: 1299–1310. doi:10.1128/JB.01301-06

66. Bessen DE, Kumar N, Hall GS, Riley DR, Luo F, Lizano S, et al. Whole-genome association study on tissue tropism phenotypes in group A Streptococcus. J Bacteriol. 2011;193: 6651–63. doi:10.1128/JB.05263-11

67. Kreikemeyer B, Podbielski A, Beckert S, Braun-Kiewnick A. Group A streptococcal RofA-type global regulators exhibit a strain-specific genomic presence and regulation pattern. Microbiology. 2002;148: 1501–1511. doi:10.1099/00221287-148-5-1501

68. Luo F, Lizano S, Bessen DE. Heterogeneity in the polarity of Nra regulatory effects on streptococcal pilus gene transcription and virulence. Infect Immun. 2008;76: 2490–2497. doi:10.1128/IAI.01567-07

69. Kreikemeyer B, Mciver KS, Podbielski A. Virulence factor regulation and regulatory networks in Streptococcus pyogenes and their impact on pathogen-host interactions. [cited 23 Jun 2019]. doi:10.1016/S0966-842X(03)00098-2

70. Ryan PA, Juncosa B. Group A Streptococcal Adherence. In: Ferretti JJ, Stevens DL, Fischetti VA, editors. Streptococcus pyogenes: Basic Biology to Clinical Manifestations. University of Oklahoma Health Sciences Center; 2016. pp. 521–545. Available: http://www.ncbi.nlm.nih.gov/pubmed/26866229

71. Brouwer S, Barnett TC, Rivera-Hernandez T, Rohde M, Walker MJ. *Streptococcus pyogenes* adhesion and colonization. FEBS Lett. 2016;590: 3739–3757. doi:10.1002/1873-3468.12254

72. Hasty DL, Ofek I, Courtney HS, Doyle RJ. Multiple adhesins of streptococci. Infect Immun. 1992;60: 2147–52. Available: http://www.ncbi.nlm.nih.gov/pubmed/1587582

73. Theocharis AD, Manou D, Karamanos NK. The extracellular matrix as a multitasking player in disease. FEBS J. 2019;286: 2830–2869. doi:10.1111/FEBS.14818

74. Beachey EH, Courtney HS. Bacterial adherence: the attachment of group A streptococci to mucosal surfaces. Rev Infect Dis. 1987;9 Suppl 5: S475-81. Available: http://www.ncbi.nlm.nih.gov/pubmed/3317744

75. Courtney HS, Ofek I, Hasty DL. M protein mediated adhesion of M type 24 Streptococcus pyogenes stimulates release of interleukin-6 by HEp-2 tissue culture cells. FEMS Microbiol Lett. 1997;151: 65–70. doi:10.1016/S0378-1097(97)00139-0

76. Courtney HS, Von Hunolstein C, Dale JB, Bronze MS, Beachey EH, Hasty DL. Lipoteichoic acid and M protein: dual adhesins of group A streptococci. Microb Pathog. 1992;12: 199–208. doi:10.1016/0882-4010(92)90054-R

77. Dougherty BA, Van De Rijn I. Molecular characterization of *hasA* from an operon required for hyaluronic acid synthesis in group A streptococci. J Biol Chem. 1994;269: 169–175.

78. Wessels MR, Bronze MS. Critical role of the group A streptococcal capsule in pharyngeal colonization and infection in mice. Proc Natl Acad Sci U S A. 1994/12/06. 1994;91: 12238–12242. Available: http://www.ncbi.nlm.nih.gov/pubmed/7991612

79. Cywes C, Stamenkovic I, Wessels MR. CD44 as a receptor for colonization of the

pharynx by group A *Streptococcus*. J Clin Invest. 2000;106: 995–1002. doi:10.1172/JCI10195

80. Schrager HM, Albertí S, Cywes C, Dougherty GJ, Wessels MR. Hyaluronic acid capsule modulates M protein-mediated adherence and acts as a ligand for attachment of group A *Streptococcus* to CD44 on human keratinocytes. J Clin Invest. 1998;101: 1708–1716. doi:10.1172/JCI2121

81. Cywes C, Wessels MR. Group A *Streptococcus* tissue invasion by CD44-mediated cell signalling. Nature. 2001;414: 648–652. doi:10.1038/414648a

82. Cywes C, Wessels MR. Group A Streptococcus tissue invasion by CD44-mediated cell signalling. Nature. 2001;414: 648–652. doi:10.1038/414648a

83. Lynskey NN, Goulding D, Gierula M, Turner CE, Dougan G, Edwards RJ, et al. RocA truncation underpins hyper-encapsulation, carriage longevity and transmissibility of serotype M18 group A streptococci. PLoS Pathog. 2013;9: e1003842. doi:10.1371/journal.ppat.1003842

84. Ashbaugh CD, Moser TJ, Shearer MH, White GL, Kennedy RC, Wessels MR. Bacterial determinants of persistent throat colonization and the associated immune response in a primate model of human group A streptococcal pharyngeal infection. Cell Microbiol. 2000;2: 283–292. doi:10.1046/j.1462-5822.2000.00050.x

85. Hollands A, Pence MA, Timmer AM, Osvath SR, Turnbull L, Whitchurch CB, et al. Genetic Switch to Hypervirulence Reduces Colonization Phenotypes of the Globally Disseminated Group A *Streptococcus* M1T1 Clone. J Infect Dis. 2010;202: 11–19. doi:10.1086/653124

86. Ellen RP, Gibbons RJ. M protein-associated adherence of Streptococcus pyogenes to epithelial surfaces: prerequisite for virulence. Infect Immun. 1972;5: 826–830.

87. Abbot EL, Smith WD, Siou GPS, Chiriboga C, Smith RJ, Wilson JA, et al. Pili mediate specific adhesion of *Streptococcus pyogenes* to human tonsil and skin. Cell Microbiol. 2007;9: 1822–1833. doi:10.1111/j.1462-5822.2007.00918.x

88. Ryan PA, Pancholi V, Fischetti VA. Group A streptococci bind to mucin and human pharyngeal cells through sialic acid-containing receptors. Infect Immun. 2001;69: 7402–7412. doi:10.1128/IAI.69.12.7402-7412.2001

89. Frick IM, Schmidtchen A, Sjöbring U. Interactions between M proteins of Streptococcus pyogenes and glycosaminoglycans promote bacterial adhesion to host cells. Eur J Biochem. 2003;270: 2303–2311. doi:10.1046/j.1432-1033.2003.03600.x

90. Simpson WA, Beachey EH. Adherence of group A streptococci to fibronectin on oral epithelial cells. Infect Immun. 1983;39: 275–279.

91. Wang JR, Stinson MW. Streptococcal M6 protein binds to fucose-containing glycoproteins on cultured human epithelial cells. Infect Immun. 1994;62: 1268–1274.

92. Okada N, Liszewski MK, Atkinson JP, Caparon M. Membrane cofactor protein (CD46) is a keratinocyte receptor for the M protein of the group A Streptococcus. Proc Natl Acad Sci. 1995;92: 2489–93. doi:10.1073/pnas.92.7.2489

93. Feito MJ, Sánchez A, Oliver MA, Pérez-Caballero D, Rodríguez de Córdoba S, Albertí S, et al. Membrane cofactor protein (MCP, CD46) binding to clinical isolates of Streptococcus pyogenes: Binding to M type 18 strains is independent of Emm or Enn proteins. Mol Immunol. 2007;44: 3571–3579. doi:10.1016/j.molimm.2007.03.012

94. Berkower C, Ravins M, Moses AE, Hanski E. Expression of different group A streptococcal M proteins in an isogenic background demonstrates diversity in adherence to and invasion of eukaryotic cells. Mol Microbiol. 1999;31: 1463–75. doi:10.1046/j.1365-2958.1999.01289.x

95. Ozeri V, Rosenshine I, Mosher DF, Fässler R, Hanski E. Roles of integrins and fibronectin in the entry of Streptococcus pyogenes into cells via protein F1. Mol Microbiol. 1998;30: 625–37. Available: http://www.ncbi.nlm.nih.gov/pubmed/9822827

96. Jeng A, Sakota V, Li Z, Datta V, Beall B, Nizet V. Molecular Genetic Analysis of a Group A Streptococcus Operon Encoding Serum Opacity Factor and a Novel Fibronectin-Binding Protein, SfbX. J Bacteriol. 2003;185: 1208–1217. doi:10.1128/JB.185.4.1208-1217.2003

97. Kreikemeyer B, Oehmcke S, Nakata M, Hoffrogge R, Podbielski A. Streptococcus pyogenes fibronectin-binding protein F2: expression profile, binding characteristics, and impact on eukaryotic cell interactions. J Biol Chem. 2004;279: 15850–15859. doi:10.1074/jbc.M313613200

98. Krishnan V. Pilins in gram-positive bacteria: A structural perspective. IUBMB Life. 2015;67: 533–543. doi:10.1002/iub.1400

99. Margarit y Ros I. Streptococcus pyogenes Pili. Streptococcus pyogenes : Basic Biology to Clinical Manifestations. University of Oklahoma Health Sciences Center; 2016. Available: http://www.ncbi.nlm.nih.gov/pubmed/26866226

100. Becherelli M, Manetti AGO, Buccato S, Viciani E, Ciucchi L, Mollica G, et al. The ancillary protein 1 of *Streptococcus pyogenes* FCT-1 pili mediates cell adhesion and biofilm formation through heterophilic as well as homophilic interactions. Mol Microbiol. 2012;83: 1035–1047. doi:10.1111/j.1365-2958.2012.07987.x

101. Crotty Alexander LE, Maisey HC, Timmer AM, Rooijakkers SHM, Gallo RL, von

Köckritz-Blickwede M, et al. M1T1 group A streptococcal pili promote epithelial colonization but diminish systemic virulence through neutrophil extracellular entrapment. J Mol Med. 2010;88: 371–381. doi:10.1007/s00109-009-0566-9

102. Manetti AGO, Zingaretti C, Falugi F, Capo S, Bombaci M, Bagnoli F, et al. Streptococcus pyogenes pili promote pharyngeal cell adhesion and biofilm formation. Mol Microbiol. 2007;64: 968–983. doi:10.1111/j.1365-2958.2007.05704.x

103. Kang HJ, Baker EN. Intramolecular isopeptide bonds give thermodynamic and proteolytic stability to the major pilin protein of *Streptococcus pyogenes*. J Biol Chem. 2009;284: 20729–20737. doi:10.1074/jbc.M109.014514

104. Echelman DJ, Alegre-Cebollada J, Badilla CL, Chang C, Ton-That H, Fernández JM. CnaA domains in bacterial pili are efficient dissipaters of large mechanical shocks. Proc Natl Acad Sci U S A. 2016;113: 2490–2495. doi:10.1073/pnas.1522946113

105. Lynskey NN, Reglinski M, Calay D, Siggins MK, Mason JC, Botto M, et al. Multi-functional mechanisms of immune evasion by the streptococcal complement inhibitor C5a peptidase. PLoS Pathog. 2017;13: 1–29. doi:10.1371/journal.ppat.1006493

106. Ji Y, McLandsborough L, Kondagunta A, Cleary PP. C5a peptidase alters clearance and trafficking of group A streptococci by infected mice. Infect Immun. 1996/02/01. 1996;64: 503–510. Available: http://www.ncbi.nlm.nih.gov/pubmed/8550199

107. Terao Y, Mori Y, Yamaguchi M, Shimizu Y, Ooe K, Hamada S, et al. Group A streptococcal cysteine protease degrades C3 (C3b) and contributes to evasion of innate immunity. J Biol Chem. 2008;283: 6253–6260. doi:10.1074/jbc.M704821200

108. Zinkernagel AS, Timmer AM, Pence MA, Locke JB, Buchanan JT, Turner CE, et al. The IL-8 Protease SpyCEP/ScpC of Group A Streptococcus Promotes Resistance to Neutrophil Killing. Cell Host Microbe. 2008;4: 170–178. doi:10.1016/j.chom.2008.07.002

109. McKenna S, Huse KK, Giblin S, Pearson M, Majid Al Shibar MS, Sriskandan S, et al. The Role of Streptococcal Cell-Envelope Proteases in Bacterial Evasion of the Innate Immune System. J Innate Immun. 2021; 1–20. doi:10.1159/000516956

110. Hyland KA, Wang B, Cleary PP. Protein F1 and Streptococcus pyogenes resistance to phagocytosis. Infect Immun. 2007;75: 3188–3191. doi:10.1128/IAI.01745-06

111. Morfeldt E, Berggård K, Persson J, Drakenberg T, Johnsson E, Lindahl E, et al. Isolated Hypervariable Regions Derived from Streptococcal M Proteins

Specifically Bind Human C4b-Binding Protein: Implications for Antigenic Variation. J Immunol. 2001;167: 3870–3877. doi:10.4049/jimmunol.167.7.3870

112. Berggård K, Johnsson E, Morfeldt E, Persson J, Stålhammar-Carlemalm M, Lindahl G. Binding of human C4BP to the hypervariable region of M protein: a molecular mechanism of phagocytosis resistance in Streptococcus pyogenes. Mol Microbiol. 2001;42: 539–551. doi:10.1046/J.1365-2958.2001.02664.X

113. Carlsson F, Berggård K, Stålhammar-Carlemalm M, Lindahl G. Evasion of phagocytosis through cooperation between two ligand-binding regions in Streptococcus pyogenes M protein. J Exp Med. 2003;198: 1057–1068. doi:10.1084/JEM.20030543

114. Pérez-Caballero D, Albertí S, Vivanco F, Sánchez-Corral P, Rodríguez De Córdoba S. Assessment of the interaction of human complement regulatory proteins with group A *Streptococcus*. Identification of a high-affinity group A *Streptococcus* binding site in FHL-1. Eur J Immunol. 2000;30: 1243–1253. doi:10.1002/(SICI)1521-4141(200004)30:4<1243::AID-IMMU1243>3.0.CO;2-D

115. Horstmann RD, Sievertsen HJ, Knobloch J, Fischetti VA. Antiphagocytic activity of streptococcal M protein: selective binding of complement control protein factor H. Proc Natl Acad Sci U S A. 1988;85: 1657–61. doi:10.1073/pnas.85.5.1657

116. Agrahari G, Liang Z, Glinton K, Lee SW, Ploplis VA, Castellino FJ. *Streptococcus pyogenes* Employs Strain-dependent Mechanisms of C3b Inactivation to Inhibit Phagocytosis and Killing of Bacteria. J Biol Chem. 2016;291: 9181–9189. doi:10.1074/jbc.M115.704221

117. Kotarsky H, Hellwage J, Johnsson E, Skerka C, Svensson HG, Lindahl G, et al. Identification of a domain in human factor H and factor H-like protein-1 required for the interaction with streptococcal M proteins. J Immunol. 1998;160: 3349–3354.

118. Pérez-Caballero D, García-Laorden I, Cortés G, Wessels MR, de Córdoba SR, Albertí S. Interaction between complement regulators and *Streptococcus pyogenes*: binding of C4b-binding protein and factor H/factor H-like protein 1 to M18 strains involves two different cell surface molecules. J Immunol. 2004;173: 6899–904. doi:10.4049/jimmunol.173.11.6899

119. Whitnack E, Beachey EH. Inhibition of complement-mediated opsonization and phagocytosis of *Streptococcus pyogenes* by D fragments of fibrinogen and fibrin bound to cell surface M protein. J Exp Med. 1985;162: 1983–1997. doi:10.1084/jem.162.6.1983

120. Carlsson F, Sandin C, Lindahl G. Human fibrinogen bound to Streptococcus pyogenes M protein inhibits complement deposition via the classical pathway. Mol Microbiol. 2005;56: 28–39. doi:10.1111/J.1365-2958.2005.04527.X

121. Ly D, Taylor JM, Tsatsaronis JA, Monteleone MM, Skora AS, Donald CA, et al. Plasmin(ogen) acquisition by group A Streptococcus protects against C3b-mediated neutrophil killing. J Innate Immun. 2014;6: 240–250. doi:10.1159/000353754

122. Pandiripally V, Gregory E, Cue D. Acquisition of Regulators of Complement Activation by Streptococcus pyogenes Serotype M1. Infect Immun. 2002;70: 6206. doi:10.1128/IAI.70.11.6206-6214.2002

123. Walker MJ, Barnett TC, McArthur JD, Cole JN, Gillen CM, Henningham A, et al. Disease Manifestations and Pathogenic Mechanisms of Group A Streptococcus. Clin Microbiol Rev. 2014;27: 264–301. doi:10.1128/CMR.00101-13

124. Laabei M, Ermert D. Catch Me if You Can: Streptococcus pyogenes Complement Evasion Strategies. J Innate Immun. 2019;11: 3–12. doi:10.1159/000492944

125. Dale JB, Washburn RG, Marques MB, Wessels MR. Hyaluronate capsule and surface M protein in resistance to opsonization of group A streptococci. Infect Immun. 1996;64: 1495–501. doi:10.1128/iai.64.5.1495-1501.1996

126. Dinkla K, Sastalla I, Godehardt AW, Janze N, Chhatwal GS, Rohde M, et al. Upregulation of capsule enables Streptococcus pyogenes to evade immune recognition by antigen-specific antibodies directed to the G-related alpha2-macroglobulin-binding protein GRAB located on the bacterial surface. Microbes Infect. 2007;9: 922–931. doi:10.1016/J.MICINF.2007.03.011

127. Medina E, Schulze K, Chhatwal GS, Guzmán CA. Nonimmune Interaction of the SfbI Protein of Streptococcus pyogenes with the Immunoglobulin G F(ab′)2 Fragment. Infect Immun. 2000;68: 4786. doi:10.1128/IAI.68.8.4786-4788.2000

128. Åkesson P, Moritz L, Truedsson M, Christensson B, Von Pawel-Rammingen U. IdeS, a highly specific immunoglobulin G (IgG)-cleaving enzyme from Streptococcus pyogenes, is inhibited by specific IgG antibodies generated during infection. Infect Immun. 2006;74: 497–503. doi:10.1128/IAI.74.1.497-503.2006

129. Collin M, Svensson MD, Sjöholm AG, Jensenius JC, Sjöbring U, Olsén A. EndoS and SpeB from *Streptococcus pyogenes* inhibit immunoglobulin-mediated opsonophagocytosis. Infect Immun. 2002;70: 6646–51. Available: http://www.ncbi.nlm.nih.gov/pubmed/12438337

130. Collin M, Olsen A. EndoS, a novel secreted protein from Streptococcus pyogenes with endoglycosidase activity on human IgG. EMBO J. 2001;20: 3046–3055. doi:10.1093/emboj/20.12.3046

131. Sjögren J, Okumura CY, Collin M, Nizet V, Hollands A. Study of the IgG endoglycosidase EndoS in group A streptococcal phagocyte resistance and virulence. BMC Microbiol. 2011;11: 120. doi:10.1186/1471-2180-11-120

132. Collin M, Olsén A. Effect of SpeB and EndoS from *Streptococcus pyogenes* on human immunoglobulins. Infect Immun. 2001;69: 7187–7189. doi:10.1128/IAI.69.11.7187-7189.2001

133. Timmer AM, Timmer JC, Pence MA, Hsu LC, Ghochani M, Frey TG, et al. Streptolysin O promotes group A *Streptococcus* immune evasion by accelerated macrophage apoptosis. J Biol Chem. 2009;284: 862–871. doi:10.1074/jbc.M804632200

134. Miyoshi-Akiyama T, Takamatsu D, Koyanagi M, Zhao J, Imanishi K, Uchiyama T. Cytocidal effect of *Streptococcus pyogenes* on mouse neutrophils *in vivo* and the critical role of streptolysin S. J Infect Dis. 2005;192: 107–116. doi:10.1086/430617

135. Tsatsaronis JA, Walker MJ, Sanderson-Smith ML, Walker M, Barnett T, McArthur J, et al. Host responses to group A *Streptococcus*: Cell death and inflammation. Chitnis CE, editor. PLoS Pathog. 2014;10: e1004266. doi:10.1371/journal.ppat.1004266

136. Bastiat-Sempe B, Love JF, Lomayesva N, Wessels MR. Streptolysin O and NAD-glycohydrolase prevent phagolysosome acidification and promote group A Streptococcus survival in macrophages. MBio. 2014;5: e01690-14. doi:10.1128/mBio.01690-14

137. Bricker AL, Cywes C, Ashbaugh CD, Wessels MR. NAD+-glycohydrolase acts as an intracellular toxin to enhance the extracellular survival of group A streptococci. Mol Microbiol. 2002;44: 257–69. doi:10.1046/j.1365-2958.2002.02876.x

138. Sharma O, O'Seaghdha M, Velarde JJ, Wessels MR. NAD+-glycohydrolase promotes intracellular survival of group A *Streptococcus*. PLoS Pathog. 2016;12: 1–21. doi:10.1371/journal.ppat.1005468

139. Carr A, Sledjeski DD, Podbielski A, Boyle MDP, Kreikemeyer B. Similarities between complement-mediated and streptolysin S-mediated hemolysis. J Biol Chem. 2001;276: 41790–41796. doi:10.1074/jbc.M107401200

140. Thapa R, Ray S, Keyel PA. Interaction of Macrophages and Cholesterol-Dependent Cytolysins: The Impact on Immune Response and Cellular Survival. Toxins (Basel). 2020;12. doi:10.3390/TOXINS12090531

141. Buchanan JT, Simpson AJ, Aziz RK, Liu GY, Kristian SA, Kotb M, et al. DNase expression allows the pathogen group A *Streptococcus* to escape killing in neutrophil extracellular traps. Curr Biol. 2006;16: 396–400. doi:10.1016/j.cub.2005.12.039

142. Sumby P, Barbian KD, Gardner DJ, Whitney AR, Welty DM, Long RD, et al. Extracellular deoxyribonuclease made by group A *Streptococcus* assists pathogenesis by enhancing evasion of the innate immune response. Proc Natl Acad

Sci U S A. 2005;102: 1679–1684. doi:10.1073/pnas.0406641102

143. Brouwer S, Barnett TC, Ly D, Kasper KJ, De Oliveira DMP, Rivera-Hernandez T, et al. Prophage exotoxins enhance colonization fitness in epidemic scarlet fever-causing *Streptococcus pyogenes*. Nat Commun. 2020;11: 5018. doi:10.1038/s41467-020-18700-5

144. Chang A, Khemlani A, Kang H, Proft T. Functional analysis of *Streptococcus pyogenes* nuclease A (SpnA), a novel group A streptococcal virulence factor. Mol Microbiol. 2011;79: 1629–42. doi:10.1111/j.1365-2958.2011.07550.x

145. Cole JN, Pence MA, Von Köckritz-Blickwede M, Hollands A, Gallo RL, Walker MJ, et al. M Protein and Hyaluronic Acid Capsule Are Essential for In Vivo Selection of covRS Mutations Characteristic of Invasive Serotype M1T1 Group A Streptococcus. 2010. doi:10.1128/mBio.00191-10

146. Frick I-M, Akesson P, Rasmussen M, Schmidtchen A, Björck L. SIC, a secreted protein of *Streptococcus pyogenes* that inactivates antibacterial peptides. J Biol Chem. 2003;278: 16561–6. doi:10.1074/jbc.M301995200

147. Lauth X, Von Köckritz-Blickwede M, McNamara CW, Myskowski S, Zinkernagel AS, Beall B, et al. M1 Protein Allows Group A Streptococcal Survival in Phagocyte Extracellular Traps through Cathelicidin Inhibition. J Innate Immun. 2009;1: 202. doi:10.1159/000203645

148. Nyberg P, Rasmussen M, Björck L. α2-Macroglobulin-Proteinase Complexes Protect Streptococcus pyogenes from Killing by the Antimicrobial Peptide LL-37 *. J Biol Chem. 2004;279: 52820–52823. doi:10.1074/JBC.C400485200

149. Johansson L, Thulin P, Sendi P, Hertzén E, Linder A, Åkesson P, et al. Cathelicidin LL-37 in Severe Streptococcus pyogenes Soft Tissue Infections in Humans. Infect Immun. 2008;76: 3399. doi:10.1128/IAI.01392-07

150. Cheng S, Baisch J, Krco C, Savarirayan S, Hanson J, Hodgson K, et al. Expression and function of HLA-DQ8 (DQA1*0301/DQB1*0302) genes in transgenic mice. Eur J Immunogenet. 1996;23: 15–20.

151. Sun H, Ringdahl U, Homeister JW, Fay WP, Engleberg NC, Yang AY, et al. Plasminogen is a critical host pathogenicity factor for group A streptococcal infection. Science. 2004;305: 1283–6. doi:10.1126/science.1101245

152. Kotb M, Norrby-Teglund A, McGeer A, El-Sherbini H, Dorak MT, Khurshid A, et al. An immunogenetic and molecular basis for differences in outcomes of invasive group A streptococcal infections. Nat Med. 2002;8: 1398–1404. doi:10.1038/nm800

153. Llewelyn M, Sriskandan S, Peakman M, Ambrozak DR, Douek DC, Kwok WW, et al. HLA class II polymorphisms determine responses to bacterial superantigens.

J Immunol. 2004;172: 1719–1726. Available:
http://www.ncbi.nlm.nih.gov/entrez/query.fcgi?cmd=Retrieve&db=PubMed&dopt
=Citation&list_uids=14734754

154. Nooh MM, El-Gengehi N, Kansal R, David CS, Kotb M. HLA transgenic mice
provide evidence for a direct and dominant role of HLA class II variation in
modulating the severity of streptococcal sepsis. J Immunol. 2007;178: 3076–3083.
doi:178/5/3076 [pii]

155. Park HS, Francis KP, Yu J, Cleary PP. Membranous cells in nasal-associated
lymphoid tissue: a portal of entry for the respiratory mucosal pathogen group A
Streptococcus. J Immunol. 2003;171: 2532–2537. Available:
http://www.ncbi.nlm.nih.gov/entrez/query.fcgi?cmd=Retrieve&db=PubMed&dopt
=Citation&list_uids=12928403

156. Kasper KJ, Zeppa JJ, Wakabayashi AT, Xu SX, Mazzuca DM, Welch I, et al.
Bacterial superantigens promote acute nasopharyngeal infection by *Streptococcus
pyogenes* in a human MHC Class II-dependent manner. PLoS Pathog. 2014;10:
e1004155. doi:10.1371/journal.ppat.1004155

157. Zeppa JJ, Kasper KJ, Mohorovic I, Mazzuca DM, Haeryfar SMM, McCormick JK.
Nasopharyngeal infection by *Streptococcus pyogenes* requires superantigen-
responsive Vβ-specific T cells. Proc Natl Acad Sci. 2017;114: 10226–10231.
doi:10.1073/pnas.1700858114

158. Pandey M, Calcutt A, Ozberk V, Chen Z, Croxen M, Powell J, et al. Antibodies to
the conserved region of the M protein and a streptococcal superantigen
cooperatively resolve toxic shock-like syndrome in HLA-humanized mice. Sci
Adv. 2019;5: eaax3013. doi:10.1126/sciadv.aax3013

159. Caswell CC, Han R, Hovis KM, Ciborowski P, Keene DR, Marconi RT, et al. The
Scl1 protein of M6-type group A Streptococcus binds the human complement
regulatory protein, factor H, and inhibits the alternative pathway of complement.
Mol Microbiol. 2008;67: 584–596. doi:10.1111/J.1365-2958.2007.06067.X

160. Blom AM, Magda M, Kohl L, Shaughnessy J, Lambris JD, Ram S, et al. Factor H-
IgG Chimeric Proteins as a Therapeutic Approach against the Gram-Positive
Bacterial Pathogen Streptococcus pyogenes. J Immunol. 2017;199: 3828–3839.
doi:10.4049/JIMMUNOL.1700426

161. Ermert D, Shaughnessy J, Joeris T, Kaplan J, Pang CJ, Kurt-Jones EA, et al.
Virulence of group A streptococci is enhanced by human complement inhibitors.
Wessels MR, editor. PLOS Pathog. 2015;11: e1005043.
doi:10.1371/journal.ppat.1005043

162. Gustafsson MCU, Lannergård J, Nilsson OR, Kristensen BM, Olsen JE, Harris
CL, et al. Factor H binds to the hypervariable region of many *Streptococcus
pyogenes* M proteins but does not promote phagocytosis resistance or acute

virulence. PLoS Pathog. 2013;9: e1003323. doi:10.1371/journal.ppat.1003323

163. Giannakis E, Jokiranta TS, Ormsby RJ, Duthy TG, Male DA, Christiansen D, et al. Identification of the Streptococcal M Protein Binding Site on Membrane Cofactor Protein (CD46). J Immunol. 2002;168: 4585–4592. doi:10.4049/JIMMUNOL.168.9.4585

164. Lovkvist L, Sjolinder H, Wehelie R, Aro H, Norrby-Teglund A, Plant L, et al. CD46 Contributes to the severity of group A streptococcal infection. Infect Immun. 2008/06/25. 2008;76: 3951–3958. doi:10.1128/IAI.00109-08

165. Matsui H, Sekiya Y, Nakamura M, Murayama SY, Yoshida H, Takahashi T, et al. CD46 transgenic mouse model of necrotizing fasciitis caused by Streptococcus pyogenes infection. Infect Immun. 2009/09/10. 2009;77: 4806–4814. doi:10.1128/IAI.00577-09

166. Baker SK, Strickland S. A critical role for plasminogen in inflammation. J Exp Med. 2020;217. doi:10.1084/JEM.20191865

167. Walker MJ, McArthur JD, McKay F, Ranson M. Is plasminogen deployed as a *Streptococcus pyogenes* virulence factor? Trends Microbiol. 2005;13: 308–13. doi:10.1016/j.tim.2005.05.006

168. Monea S, Lehti K, Keski-Oja J, Mignatti P. Plasmin Activates Pro-Matrix Metalloproteinase-2 With a Membrane-Type 1 Matrix Metalloproteinase-Dependent Mechanism. J Cell Physiol. 2002;192: 160–170. doi:10.1002/jcp.10126

169. Yakovlev SA, Rublenko M V, Izdepsky VI, Makogonenko EM. Brief Communication: Activating effect of the plasminogen activaotrs in plasminogens of different mammalia species. Thromb Res. 1995;79: 423–428.

170. Khil J, Im M, Heath A, Ringdahl U, Mundada L, Cary Engleberg N, et al. Plasminogen Enhances Virulence of Group A Streptococci by Streptokinase-Dependent and Streptokinase-Independent Mechanisms. J Infect Dis. 2003;188: 497–505. doi:10.1086/377100

171. Li Z, Ploplis Victoria A, Fench EL, Boyle MDP. Interaction between Group A Streptococci and the Plasmin(ogen) System Promotes Virulence in a Mouse Skin Infection Model on JSTOR. J Infect Dis. 1999;179: 907–914. Available: https://www-jstor-org.proxy1.lib.uwo.ca/stable/30111809?sid=primo&seq=1#metadata_info_tab_contents

172. Sanderson-Smith ML, Dinkla K, Cole JN, Cork AJ, Maamary PG, McArthur JD, et al. M protein mediated plasminogen binding is essential for the virulence of an invasive Streptococcus pyogenes isolate. FASEB J. 2008;22: 2715–2722. Available: https://ro.uow.edu.au/scipapers

173. Sun H, Ringdahl U, Homeister JW, Fay WP, Engleberg NC, Yang AY, et al. Plasminogen is a critical host pathogenicity factor for group A streptococcal infection. Science. 2004/08/31. 2004;305: 1283–6. doi:10.1126/science.1101245

174. Sun H, Xu Y, Sitkiewicz I, Ma Y, Wang X, Yestrepsky BD, et al. Inhibitor of streptokinase gene expression improves survival after group A Streptococcus infection in mice. Proc Natl Acad Sci U S A. 2012/02/15. 2012;109: 3469–3474. doi:10.1073/pnas.1201031109

175. Fiorentino TR, Beall B, Mshar P, Bessen DE. A genetic-based evaluation of the principal tissue reservoir for group A streptococci isolated from normally sterile sites. J Infect Dis. 1997;176: 177–182. Available: http://www.ncbi.nlm.nih.gov/pubmed/9207364

176. Dale JB, Batzloff MR, Cleary PP, Courtney HS, Good MF, Grandi G, et al. Current approaches to Group A Streptococcal vaccine development. Ferretti JJ, Stevens DL, Fischetti VA, editors. Streptococcus pyogenes : Basic Biology to Clinical Manifestations. University of Oklahoma Health Sciences Center; 2016. Available: http://www.ncbi.nlm.nih.gov/pubmed/26866216

177. Fox EN, Waldman RH, Wittner MK, Mauceri AA, Dorfman A. Protective Study with a Group A Streptococcal M Protein Vaccine Infectivity challenge of human volunteers. J Clin Invest. 1973;52: 1995–1892.

178. D'alessandri R, Plotkin G, Kluge RM, Wittner MK, Fox EN, Dorfman A, et al. Protective Studies with Group A Streptococcal M Protein Vaccine. III. Challenge of Volunteers after Systemic or Intranasal Immunization with Type 3 or Type 12 Group A Streptococcus. Source J Infect Dis. 1978;138: 712–718. Available: https://about.jstor.org/terms

179. Jones KF, Fischetti VA. The importance of the location of antibody binding on the M6 protein for opsonization and phagocytosis of group A M6 streptococci. J Exp Med. 1988;167: 1114–1123. doi:10.1084/JEM.167.3.1114

180. Dale JB, Chiang EY, Lederer J. Recombinant Tetravalent Group A Streptococcal M Protein Vaccine. J Immunol. 1993;151: 2188–2194. doi:10.1016/0264-410X(96)00050-3

181. Dale JB. Multivalent group a streptococcal vaccine designed to optimize the immunogenicity of six tandem M protein fragments. Vaccine. 1999;17: 193–200. doi:10.1016/S0264-410X(98)00150-9

182. Kotloff KL, Corretti M, Palmer K, Campbell JD, Reddish M a, Hu MC, et al. Safety and immunogenicity of a recombinant multivalent group a streptococcal vaccine in healthy adults: phase 1 trial. JAMA. 2004;292: 709–15. doi:10.1001/jama.292.6.709

183. Dale JB, Simmons M, Chiang EC, Chiang EY. Recombinant, octavalent group A

streptococcal M protein vaccine. Vaccine. 1996;14: 944–948. doi:10.1016/0264-410X(96)00050-3

184. Shulman ST, Tanz RR, Dale JB, Beall B, Kabat W, Kabat K, et al. Seven-year surveillance of north American pediatric group A streptococcal pharyngitis isolates. Clin Infect Dis. 2009;49: 78–84. doi:10.1086/599344

185. Shulman ST, Tanz RB, Kabat W, Kabat K, Cederlund E, Patel D, et al. Group A streptococcal pharyngitis serotype surveillance in North America, 2000-2002. Clin Infect Dis. 2004;39: 325–332. doi:10.1086/421949

186. Hu MC, Walls MA, Stroop SD, Reddish MA, Beall B, Dale JB. Immunogenicity of a 26-Valent Group A Streptococcal Vaccine. Infect Immun. 2002;70: 2171–2177. doi:10.1128/IAI.70.4.2171-2177.2002

187. Dale JB, Penfound T a., Chiang EY, Walton WJ. New 30-valent M protein-based vaccine evokes cross-opsonic antibodies against non-vaccine serotypes of group A streptococci. Vaccine. 2011;29: 8175–8178. doi:10.1016/j.vaccine.2011.09.005

188. McNeil S a, Halperin S a, Langley JM, Smith B, Warren A, Sharratt GP, et al. Safety and immunogenicity of 26-valent group a streptococcus vaccine in healthy adult volunteers. Clin Infect Dis. 2005;41: 1114–1122.

189. Pastural É, McNeil SA, MacKinnon-Cameron D, Ye L, Langley JM, Stewart R, et al. Safety and immunogenicity of a 30-valent M protein-based group a streptococcal vaccine in healthy adult volunteers: A randomized, controlled phase I study. Vaccine. 2020;38: 1384–1392. doi:10.1016/j.vaccine.2019.12.005

190. McNeil SA, Halperin SA, Langley JM, Smith B, Baxendale DM, Warren A, et al. A double-blind, randomized phase II trial of the safety and immunogenicity of 26-valent group A streptococcus vaccine in healthy adults. Int Congr Ser. 2006;1289: 303–306. doi:10.1016/j.ics.2005.12.002

191. Steer AC, Law I, Matatolu L, Beall BW, Carapetis JR. Global *emm* type distribution of group A streptococci: systematic review and implications for vaccine development. Lancet Infect Dis. 2009;9: 611–6. doi:10.1016/S1473-3099(09)70178-1

192. Dale JB, Penfound TA, Tamboura B, Sow SO, Nataro JP, Tapia M, et al. Potential coverage of a multivalent M protein-based group A streptococcal vaccine. Vaccine. 2013;31: 1576–1581. doi:10.1016/j.vaccine.2013.01.019

193. Guilherme L, Postol E, Ferreira FM, DeMarchi LMF, Kalil J. StreptInCor: a model of anti-Streptococcus pyogenes vaccine reviewed. Auto-Immunity Highlights. 2013;4: 81. doi:10.1007/S13317-013-0053-8

194. de Sá-Rocha LC, Demarchi LMMF, Postol E, Sampaio RO, de Alencar RE, Kalil J, et al. StreptInCor, a Group A Streptococcal Adsorbed Vaccine: Evaluation of

Repeated Intramuscular Dose Toxicity Testing in Rats. Front Cardiovasc Med. 2021;0: 294. doi:10.3389/FCVM.2021.643317

195.   Postol E, Alencar R, Higa FT, Freschi de Barros S, Demarchi LMF, Kalil J, et al. StreptInCor: a candidate vaccine epitope against S. pyogenes infections induces protection in outbred mice. PLoS One. 2013;8. doi:10.1371/JOURNAL.PONE.0060969

196.   Guilherme L, Postol E, Freschi de Barros S, Higa F, Alencar R, Lastre M, et al. A vaccine against S. pyogenes: Design and experimental immune response. Methods. 2009;49: 316–321. doi:10.1016/J.YMETH.2009.03.024

197.   Pandey M, Batzloff MR, Good MF. Mechanism of protection induced by group A Streptococcus vaccine candidate J8-DT: Contribution of B and T-cells towards protection. PLoS One. 2009;4. doi:10.1371/journal.pone.0005147

198.   Pandey M, Wykes MN, Hartas J, Good MF, Batzloff MR. Long-Term Antibody Memory Induced by Synthetic Peptide Vaccination Is Protective against Streptococcus pyogenes Infection and Is Independent of Memory T Cell Help . J Immunol. 2013;190: 2692–2701. doi:10.4049/jimmunol.1202333

199.   Mills J-LS, Jayashi Flores CM, Reynolds S, Wun C, Calcutt A, Baker S Ben, et al. M-protein based vaccine induces immunogenicity and protection from Streptococcus pyogenes when delivered on a high-density microarray patch (HD-MAP). npj Vaccines. 2020;5: 74. doi:10.1038/s41541-020-00222-2

200.   Batzloff MR, Hayman WA, Davies MR, Zeng M, Pruksakorn S, Brandt ER, et al. Protection against Group A Streptococcus by Immunization with J8–Diphtheria Toxoid: Contribution of J8- and Diphtheria Toxoid–Specific Antibodies to Protection. J Infect Dis. 2003;187: 1598–1608. doi:10.1086/374800

201.   Sekuloski S, Batzloff MR, Griffin P, Parsonage W, Elliott S, Hartas J, et al. Evaluation of safety and immunogenicity of a group A streptococcus vaccine candidate (MJ8VAX) in a randomized clinical trial. Moreland NJ, editor. PLoS One. 2018;13: e0198658. doi:10.1371/journal.pone.0198658

202.   Pandey M, Langshaw E, Hartas J, Lam A, Batzloff MR, Good MF. A synthetic M protein peptide synergizes with a CXC chemokine protease to induce vaccine-mediated protection against virulent streptococcal pyoderma and bacteremia. J Immunol. 2015;194: 5915–25. doi:10.4049/jimmunol.1500157

203.   McNeilly C, Cosh S, Vu T, Nichols J, Henningham A, Hofmann A, et al. Predicted Coverage and Immuno-Safety of a Recombinant C-Repeat Region Based Streptococcus pyogenes Vaccine Candidate. PLoS One. 2016;11: e0156639. doi:10.1371/JOURNAL.PONE.0156639

204.   Reynolds S, Pandey M, Dooley J, Calcutt A, Batzloff M, Ozberk V, et al. Preclinical safety and immunogenicity of Streptococcus pyogenes (Strep A)

peptide vaccines. Sci Reports 2021. 2021;11: 1–13. doi:10.1038/s41598-020-80508-6

205. Batzloff MR, Hartas J, Zeng W, Jackson DC, Good MF. Intranasal Vaccination with a Lipopeptide Containing a Conformationally Constrained Conserved Minimal Peptide, a Universal T Cell Epitope, and a Self-Adjuvanting Lipid Protects Mice from Group A Streptococcus Challenge and Reduces Throat Colonization. J Infect Dis. 2006;194: 325–330. doi:10.1086/505146

206. Bessen D, Fischetti VA. Synthetic peptide vaccine against mucosal colonization by Group A Streptcococci Protection against a Heterologous M Serotype with Shared C Repeat Region Epitopes. J Immunol. 1990;145: 1251–1256. Available: http://www.jimmunol.org/

207. Caro-Aguilar I, Ottinger E, Hepler RW, Nahas DD, Wu C, Good MF, et al. Immunogenicity in mice and non-human primates of the Group A Streptococcal J8 peptide vaccine candidate conjugated to CRM197. Human Vaccines and Immunotherapeutics. 2013. pp. 488–496. doi:10.4161/hv.23224

208. Steer AC, Carapetis JR, Dale JB, Fraser JD, Good MF, Guilherme L, et al. Status of research and development of vaccines for *Streptococcus pyogenes*. Vaccine. 2016; 6–11. doi:10.1016/j.vaccine.2016.03.073

209. Banks DJ, Beres SB, Musser JM. The fundamental contribution of phages to GAS evolution, genome diversification and strain emergence. Trends Microbiol. 2002/11/07. 2002;10: 515–521. doi:S0966842X02024617 [pii]

210. Reglinski M, Sriskandan S, Turner CE. Identification of two new core chromosome-encoded superantigens in *Streptococcus pyogenes*; *speQ* and *speR*. J Infect. 2019. doi:10.1016/j.jinf.2019.02.005

211. Commons RJ, Smeesters PR, Proft T, Fraser JD, Robins-Browne R, Curtis N. Streptococcal superantigens: Categorization and clinical associations. Trends Mol Med. 2014;20: 48–62. doi:10.1016/j.molmed.2013.10.004

212. Proft T, Fraser JD. Streptococcal Superantigens: Biological properties and potential role in disease. In: Ferretti JJ, Stevens DL, Fischetti VA, editors. Streptococcus pyogenes: Basic Biology to Clinical Manifestations. University of Oklahoma Health Sciences Center; 2016. pp. 445–486.

213. Eriksson BK, Andersson J, Holm SE, Norgren M. Invasive group A streptococcal infections: T1M1 isolates expressing pyrogenic exotoxins A and B in combination with selective lack of toxin-neutralizing antibodies are associated with increased risk of streptococcal toxic shock syndrome. J Infect Dis. 1999;180: 410–418. Available: http://www.ncbi.nlm.nih.gov/entrez/query.fcgi?cmd=Retrieve&db=PubMed&dopt=Citation&list_uids=10395857

214. Sriskandan S, Ferguson M, Elliot V, Faulkner L, Cohen J. Human intravenous immunoglobulin for experimental streptococcal toxic shock: bacterial clearance and modulation of inflammation. J Antimicrob Chemother. 2006;58: 117–124. doi:10.1093/jac/dkl173

215. Norrby-Teglund A, Kaul R, Low DE, McGeer A, Andersson J, Andersson U, et al. Evidence for the presence of streptococcal-superantigen-neutralizing antibodies in normal polyspecific immunoglobulin G. Infect Immun. 1996;64: 5395–5398.

216. Stegmayr B, Björck S, Holm S, Nisell J, Rydvall A, Settergren B. Septic shock induced by group A streptococcal infection: clinical and therapeutic aspects. Scand J Infect Dis. 1992;24: 589–97. doi:10.3109/00365549209054644

217. Rajagopalan G, Patel R, Kaveri S V, David CS. Comment on: Human intravenous immunoglobulin for experimental streptococcal toxic shock: bacterial clearance and modulation of inflammation. J Antimicrob Chemother. 2006; 157–159. doi:10.1093/jac/dkl437

218. Schrage B, Duan G, Yang LP, Fraser JD, Proft T. Different Preparations of Intravenous Immunoglobulin Vary in Their Efficacy to Neutralize Streptococcal Superantigens: Implications for Treatment of Streptococcal Toxic Shock Syndrome. Clin Infect Dis. 2006;43: 743–749. Available: https://academic.oup.com/cid/article/43/6/743/327410

219. Kotb M, Norrby-Teglund A, McGeer A, El-Sherbini H, Dorak MT, Khurshid A, et al. An immunogenetic and molecular basis for differences in outcomes of invasive group A streptococcal infections. Nat Med. 2002;8: 1398–1404. doi:10.1038/nm1202-800

220. Ulrich RG. Vaccine based on a ubiquitous cysteinyl protease and streptococcal pyrogenic exotoxin A protects against Streptococcus pyogenes sepsis and toxic shock. J Immune Based Ther Vaccines. 2008;6: 8. doi:10.1186/1476-8518-6-8

221. Roggiani M, Stoehr JA, Olmsted SB, Matsuka Y V, Pillai S, Ohlendorf DH, et al. Toxoids of streptococcal pyrogenic exotoxin A are protective in rabbit models of streptococcal toxic shock syndrome. Clements JD, editor. Infect Immun. 2000;68: 5011–5017. doi:10.1128/IAI.68.9.5011-5017.2000

222. McCormick JK, Tripp TJ, Olmsted SB, Matsuka Y V, Gahr PJ, Ohlendorf DH, et al. Development of streptococcal pyrogenic exotoxin C vaccine toxoids that are protective in the rabbit model of toxic shock syndrome. J Immunol. 2000;165: 2306–12. doi:10.4049/jimmunol.165.4.2306

223. Radcliff FJ, Loh JMS, Ha B, Schuhbauer D, McCluskey J, Fraser JD. Antigen targeting to major histocompatibility complex class II with streptococcal mitogenic exotoxin Z-2 M1, a superantigen-based vaccine carrier. Clin Vaccine Immunol. 2012;19: 574–586. doi:10.1128/CVI.05446-11

224. Antonoglou MB, Sánchez Alberti A, Redolfi DM, Bivona AE, Fernández Lynch MJ, Noli Truant S, et al. Heterologous Chimeric Construct Comprising a Modified Bacterial Superantigen and a Cruzipain Domain Confers Protection Against Trypanosoma cruzi Infection. Front Immunol. 2020;11: 1–14. doi:10.3389/fimmu.2020.01279

225. Sabharwal H, Michon F, Nelson D, Dong W, Fuchs K, Manjarrez RC, et al. Group A *Streptococcus* (GAS) carbohydrate as an immunogen for protection against GAS infection. J Infect Dis. 2006;193: 129–35. doi:10.1086/498618

226. van Sorge NM, Cole JN, Kuipers K, Henningham A, Aziz RK, Kasirer-Friede A, et al. The Classical Lancefield Antigen of Group A Streptococcus Is a Virulence Determinant with Implications for Vaccine Design. Cell Host Microbe. 2014;15: 729–740. doi:10.1016/j.chom.2014.05.009

227. Kabanova A, Margarit I, Berti F, Romano MR, Grandi G, Bensi G, et al. Evaluation of a Group A Streptococcus synthetic oligosaccharide as vaccine candidate. Vaccine. 2010;29: 104–114. doi:10.1016/j.vaccine.2010.09.018

228. Rivera-Hernandez T, Pandey M, Henningham A, Cole J, Choudhury B, Cork AJ, et al. Differing efficacies of lead group A streptococcal vaccine candidates and full-length M protein in cutaneous and invasive disease models. MBio. 2016;7. doi:10.1128/MBIO.00618-16/FORMAT/EPUB

229. Park HS, Cleary PP. Active and passive intranasal immunizations with streptococcal surface protein C5a peptidase prevent infection of murine nasal mucosa-associated lymphoid tissue, a functional homologue of human tonsils. Infect Immun. 2005/11/22. 2005;73: 7878–7886. doi:73/12/7878 [pii]10.1128/IAI.73.12.7878-7886.2005

230. O'connor SP, Darip D, Fraley K, Nelson CM, Kaplan EL, Cleary PP. The Human Antibody Response to Streptococcal C5a Peptidase. Source J Infect Dis. 1991;163: 109–116.

231. Ji Y, Carlson B, Kondagunta A, Cleary PP. Intranasal immunization with C5a peptidase prevents nasopharyngeal colonization of mice by the group A Streptococcus. Infect Immun. 1997;65: 2080–7.

232. Cleary PP, Matsuka Y V., Huynh T, Lam H, Olmsted SB. Immunization with C5a peptidase from either group A or B streptococci enhances clearance of group A streptococci from intranasally infected mice. Vaccine. 2004;22: 4332–4341. doi:10.1016/J.VACCINE.2004.04.030

233. Schulze K, Medina E, Chhatwal GS, Guzmán CA. Stimulation of long-lasting protection against *Streptococcus pyogenes* after intranasal vaccination with non adjuvanted fibronectin-binding domain of the SfbI protein. Vaccine. 2003;21: 1958–1964. doi:10.1016/S0264-410X(02)00803-4

234. Mcarthur J, Medina E, Mueller A, Chin J, Currie BJ, Sriprakash KS, et al. Intranasal Vaccination with Streptococcal Fibronectin Binding Protein Sfb1 Fails To Prevent Growth and Dissemination of Streptococcus pyogenes in a Murine Skin Infection Model. Infect Immun. 2004;72: 7342–7345. doi:10.1128/IAI.72.12.7342-7345.2004

235. Terao Y, Okamoto S, Kataoka K, Hamada S, Kawabata S. Protective immunity against *Streptococcus pyogenes* challenge in mice after immunization with fibronectin-binding protein. J Infect Dis. 2005;192: 2081–2091. doi:10.1086/498162/2/192-12-2081-FIG006.GIF

236. Kawabata S, Kunitomo E, Terao Y, Nakagawa I, Kikuchi K, Totsuka K-I, et al. Systemic and Mucosal Immunizations with Fibronectin-Binding Protein FBP54 Induce Protective Immune Responses against Streptococcus pyogenes Challenge in Mice. Infect Immun. 2001;69: 924–930. doi:10.1128/IAI.69.2.924-930.2001

237. Loh JMS, Rivera-Hernandez T, McGregor R, Khemlani AHJ, Tay ML, Cork AJ, et al. A multivalent T-antigen-based vaccine for Group A Streptococcus. Sci Reports 2021 111. 2021;11: 1–10. doi:10.1038/s41598-021-83673-4

238. Loh JMS, Lorenz N, Tsai CJ-Y, Khemlani AHJ, Proft T. Mucosal vaccination with pili from Group A *Streptococcus* expressed on *Lactococcus lactis* generates protective immune responses. Sci Rep. 2017;7: 7174. doi:10.1038/s41598-017-07602-0

239. Kapur V, Topouzis S, Majesky MW, Li L-L, Hamrick MR, Hamill RJ, et al. A conserved *Streptococcus pyogenes* extracellular cysteine protease cleaves human fibronectin and degrades vitronectin. Microb Pathog. 1993;15: 327–346. doi:10.1006/mpat.1993.1083

240. Nyberg P, Rasmussen M, Von Pawel-Rammingen U, Björck L. SpeB modulates fibronectin-dependent internalization of *Streptococcus pyogenes* by efficient proteolysis of cell-wall-anchored protein F1. Microbiology. 2004;150: 1559–1569. doi:10.1099/mic.0.27076-0

241. Kapur V, Majesky MW, Li LL, Black RA, Musser JM. Cleavage of interleukin 1 beta (IL-1 beta) precursor to produce active IL-1 beta by a conserved extracellular cysteine protease from *Streptococcus pyogenes*. Proc Natl Acad Sci U S A. 1993;90: 7676–80. Available: http://www.ncbi.nlm.nih.gov/pubmed/7689226

242. Kapur V, Maffei JT, Greer RS, Li L-L, Adams GJ, Musser JM. Vaccination with streptococcal extracellular cysteine protease (interleukin-1β convertase) protects mice against challenge with heterologous group A streptococci. Microb Pathog. 1994;16: 443–450. doi:10.1006/mpat.1994.1044

243. Fan X, Wang X, Li N, Cui H, Hou B, Gao B, et al. Sortase A induces Th17-mediated and antibody-independent immunity to heterologous serotypes of group a streptococci. PLoS One. 2014;9. doi:10.1371/journal.pone.0107638

244. Turner CE, Kurupati P, Wiles S, Edwards RJ, Sriskandan S. Impact of immunization against SpyCEP during invasive disease with two streptococcal species: Streptococcus pyogenes and Streptococcus equi. Vaccine. 2009;27: 4923–4929. doi:10.1016/j.vaccine.2009.06.042

245. Chiarot E, Faralla C, Chiappini N, Tuscano G, Falugi F, Gambellini G, et al. Targeted amino acid substitutions impair streptolysin O toxicity and group a Streptococcus virulence. MBio. 2013;4: e00387-12. doi:10.1128/mBio.00387-12

246. Bi S, Xu M, Zhou Y, Xing X, Shen A, Wang B. A Multicomponent Vaccine Provides Immunity against Local and Systemic Infections by Group A Streptococcus across Serotypes. MBio. 2019;10. doi:10.1128/mBio.02600-19

247. Rivera-Hernandez T, Carnathan DG, Jones S, Cork AJ, Davies MR, Moyle PM, et al. An experimental group A Streptococcus vaccine that reduces pharyngitis and tonsillitis in a nonhuman primate model. Kaufmann SHE, editor. MBio. 2019;10: e00693-19. doi:10.1128/mBio.00693-19

248. Kendall FE, Heidelberger M, Dawson MH. A serologically inactive polysaccharide elaborated by mucoid strains of group a hemolytic *Streptococcus*. J Biol Chem. 1937;118: 61–69. doi:10.1016/S0021-9258(18)74517-1

249. Dougherty BA, van de Rijn I. Molecular characterization of a locus required for hyaluronic acid capsule production in group A streptococci. J Exp Med. 1992/05/01. 1992;175: 1291–1299. Available: http://www.ncbi.nlm.nih.gov/pubmed/1569398

250. Crater DL, Van de Rijn I. Hyaluronic acid synthesis operon (*has*) expression in group A streptococci. J Biol Chem. 1995;270: 18452–18458. doi:10.1074/jbc.270.31.18452

251. DeAngelis PL, Papaconstantinou J, Weigel PH. Isolation of a *Streptococcus pyogenes* gene locus that directs hyaluronan biosynthesis in acapsular mutants and in heterologous bacteria. J Biol Chem. 1993;268: 14568–71. doi:10.1016/s0021-9258(18)82366-3

252. DeAngelis PL, Papaconstantinou J, Weigel PH. Molecular cloning, identification, and sequence of the hyaluronan synthase gene from group A *Streptococcus pyogenes*. J Biol Chem. 1993;268: 19181–19184. doi:10.1016/s0021-9258(19)36494-4

253. Dougherty BA, Van de Rijn I. Molecular characterization of hasB from an operon required for hyaluronic acid synthesis in group A streptococci. Demonstration of UDP-glucose dehydrogenase activity. J Biol Chem. 1993;268: 7118–7124. doi:10.1016/s0021-9258(18)53153-7

254. Crater DL, Dougherty BA, Van de Rijn I. Molecular characterization of *hasC* from an operon required for hyaluronic acid synthesis in group A streptococci.

Demonstration of UDP-glucose pyrophosphorylase activity. J Biol Chem. 1995;270: 28676–28680. doi:10.1074/jbc.270.48.28676

255. Ashbaugh CD, Albertí S, Wessels MR. Molecular analysis of the capsule gene region of group A *Streptococcus*: the *hasAB* genes are sufficient for capsule expression. J Bacteriol. 1998;180: 4955–9. doi:10.1128/JB.180.18.4955-4959.1998

256. Cole JN, Aziz RK, Kuipers K, Timmer AM, Nizet V, van Sorge NM. A conserved UDP-glucose dehydrogenase encoded outside the hasABC operon contributes to capsule biogenesis in group A *Streptococcus*. J Bacteriol. 2012;194: 6154–61. doi:10.1128/JB.01317-12

257. Gryllos I, Cywes C, Shearer MH, Cary M, Kennedy RC, Wessels MR. Regulation of capsule gene expression by group A Streptococcus during pharyngeal colonization and invasive infection. Mol Microbiol. 2001/10/27. 2001;42: 61–74. doi:2635 [pii]

258. Wessels MR, Moses AE, Goldberg JB, DiCesare TJ. Hyaluronic acid capsule is a virulence factor for mucoid group A streptococci. Proc Natl Acad Sci. 1991;88: 8317–8321. doi:10.1073/pnas.88.19.8317

259. Wessels MR, Goldberg JB, Moses AE, DiCesare TJ. Effects on virulence of mutations in a locus essential for hyaluronic acid capsule expression in group A streptococci. Infect Immun. 1994;62: 433–441.

260. Husmann LK, Yung DL, Hollingshead SK, Scott JR. Role of putative virulence factors of *Streptococcus pyogenes* in mouse models of long-term throat colonization and pneumonia. Infect Immun. 1997;65: 1422–1430. doi:10.1128/iai.65.4.1422-1430.1997

261. Schrager HM, Rheinwald JG, Wessels MR. Hyaluronic acid capsule and the role of streptococcal entry into keratinocytes in invasive skin infection. J Clin Invest. 1996/11/01. 1996;98: 1954–1958. doi:10.1172/JCI118998

262. Moses AE, Wessels MR, Zalcman K, Albertí S, Natanson-Yaron S, Menes T, et al. Relative contributions of hyaluronic acid capsule and M protein to virulence in a mucoid strain of the group A *Streptococcus*. Infect Immun. 1997;65: 64–71.

263. Flores AR, Jewell BE, Olsen RJ, Shelburne SA, Fittipaldi N, Beres SB, et al. Asymptomatic carriage of group A *Streptococcus* is associated with elimination of capsule production. Infect Immun. 2014;82: 3958–67. doi:10.1128/IAI.01788-14

264. Shea PR, Beres SB, Flores AR, Ewbank AL, Gonzalez-Lugo JH, Martagon-Rosado AJ, et al. Distinct signatures of diversifying selection revealed by genome analysis of respiratory tract and invasive bacterial populations. Proc Natl Acad Sci U S A. 2011;108: 5039–5044. doi:10.1073/pnas.1016282108

265. Flores AR, Jewell BE, Fittipaldi N, Beres SB, Musser JM. Human disease isolates of serotype M4 and M22 group A *Streptococcus* lack genes required for hyaluronic acid capsule biosynthesis. MBio. 2012;3: e00413-12. doi:10.1128/mBio.00413-12

266. Turner CE, Abbott J, Lamagni T, Holden MTG, David S, Jones MD, et al. Emergence of a new highly successful acapsular group A *Streptococcus* clade of genotype *emm89* in the United Kingdom. MBio. 2015;6: 1–11. doi:10.1128/mBio.00622-15

267. Lynskey NN, Turner CE, Heng LS, Sriskandan S. A truncation in the regulator RocA underlies heightened capsule expression in serotype M3 group A streptococci. Infect Immun. 2015;83: 1732–1733. doi:10.1128/IAI.02892-14

268. Wessels MR. Capsular Polysaccharide of Group A Streptococcus. Gram-Positive Pathogens. Washington, DC, USA: ASM Press; 2019. pp. 45–54. doi:10.1128/9781683670131.ch4

269. Smoot JC, Barbian KD, Van Gompel JJ, Smoot LM, Chaussee MS, Sylva GL, et al. Genome sequence and comparative microarray analysis of serotype M18 group A *Streptococcus* strains associated with acute rheumatic fever outbreaks. Proc Natl Acad Sci U S A. 2002;99: 4668–4673. Available: http://www.ncbi.nlm.nih.gov/entrez/query.fcgi?cmd=Retrieve&db=PubMed&dopt=Citation&list_uids=11917108

270. Biswas I, Gruss A, Ehrlich SD, Maguin E. High-efficiency gene inactivation and replacement system for gram-positive bacteria. J Bacteriol. 1993;175: 3628–3635. Available: http://www.ncbi.nlm.nih.gov/entrez/query.fcgi?cmd=Retrieve&db=PubMed&dopt=Citation&list_uids=8501066

271. Bankevich A, Nurk S, Antipov D, Gurevich AA, Dvorkin M, Kulikov AS, et al. SPAdes: A new genome assembly algorithm and its applications to single-cell sequencing. J Comput Biol. 2012;19: 455–477. doi:10.1089/cmb.2012.0021

272. Seemann T. Genome analysis Prokka: rapid prokaryotic genome annotation. 2014;30: 2068–2069. doi:10.1093/bioinformatics/btu153

273. Medina E, Goldmann O, Toppel AWW, Chhatwal GSS. Survival of Streptococcus pyogenes within host phagocytic cells: a pathogenic mechanism for persistence and systemic invasion. J Infect Dis. 2003/02/25. 2003;187: 597–603. doi:JID020956 [pii]10.1086/373998

274. Stritzker J, Weibel S, Seubert C, Götz A, Tresch A, van Rooijen N, et al. Enterobacterial tumor colonization in mice depends on bacterial metabolism and macrophages but is independent of chemotaxis and motility. Int J Med Microbiol. 2010;300: 449–456. doi:10.1016/j.ijmm.2010.02.004

275. Rajagopalan G, Polich G, Sen MM, Singh M, Epstein BE, Lytle AK, et al.

Evaluating the role of HLA-DQ polymorphisms on immune response to bacterial superantigens using transgenic mice. Tissue Antigens. 2008;71: 135–45. doi:10.1111/j.1399-0039.2007.00986.x

276. Yeung RSM, Penninger JM, Kündig T, Khoo W, Ohashi PS, Kroemer G, et al. Human CD4 and human major histocompatibility complex class II (DQ6) transgenic mice: supersensitivity to superantigen-induced septic shock. Eur J Immunol. 1996;26: 1074–1082. doi:10.1002/eji.1830260518

277. Sriskandan S, Unnikrishnan M, Krausz T, Dewchand H, Van Noorden S, Cohen J, et al. Enhanced susceptibility to superantigen-associated streptococcal sepsis in human leukocyte antigen-DQ transgenic mice. J Infect Dis. 2001;184: 166–73. doi:10.1086/322018

278. Bessen DE. Tissue tropisms in group A Streptococcus. Curr Opin Infect Dis. 2016;29: 295–303. doi:10.1097/QCO.0000000000000262

279. LeBleu VS, MacDonald B, Kalluri R. Structure and Function of Basement Membranes. Exp Biol Med. 2007;232: 1121–1129. doi:10.3181/0703-MR-72

280. Hanski E, Caparont M. A streptococcus Streptococcus pyogenes (fibronectin receptor/microbial adherence/virulence). 1992. Available: https://www.pnas.org/content/pnas/89/13/6172.full.pdf

281. Nyberg P, Sakai T, Cho KH, Caparon MG, Fä Ssler R, Bjö Rck L. Interactions with fibronectin attenuate the virulence of Streptococcus pyogenes. EMBO J. 2004;23: 2166–2174. doi:10.1038/sj.emboj.7600214

282. Hymes JP, Klaenhammer TR. Stuck in the Middle: Fibronectin-Binding Proteins in Gram-Positive Bacteria. Front Microbiol. 2016;7: 1504. doi:10.3389/fmicb.2016.01504

283. Kosmehl H, Berndt A, Strassburger S, Borsi L, Rousselle P, Mandel U, et al. Distribution of laminin and fibronectin isoforms in oral mucosa and oral squamous cell carcinoma. Br J Cancer. 1999;81: 1071–1079. doi:10.1038/sj.bjc.6690809

284. Cue D, Lam H, Cleary PP. Genetic dissection of the Streptococcus pyogenes M1 protein: Regions involved in fibronectin binding and intracellular invasion. Microb Pathog. 2001. doi:10.1006/mpat.2001.0467

285. Broudy TB, Pancholi V, Fischetti VA. Induction of lysogenic bacteriophage and phage-associated toxin from group a streptococci during coculture with human pharyngeal cells. Infect Immun. 2001;69: 1440–3. doi:10.1128/IAI.69.3.1440-1443.2001

286. Broudy TB, Pancholi V, Fischetti VA. The in vitro interaction of Streptococcus pyogenes with human pharyngeal cells induces a phage-encoded extracellular DNase. Infect Immun. 2002;70: 2805–11. doi:10.1128/IAI.70.6.2805-2811.2002

287. LaRock DL, Russell R, Johnson AF, Wilde S, LaRock CN. Group a streptococcus infection of the nasopharynx requires proinflammatory signaling through the interleukin-1 receptor. Infect Immun. 2020;88. doi:10.1128/IAI.00356-20

288. Gera K, Le T, Jamin R, Eichenbaum Z, McIver KS. The phosphoenolpyruvate phosphotransferase system in group A Streptococcus acts to reduce streptolysin s activity and lesion severity during soft tissue infection. Infect Immun. 2014;82: 1192–1204. doi:10.1128/IAI.01271-13

289. Davies HD, Adair C, McGeer A, Ma D, Robertson S, Mucenski M, et al. Antibodies to capsular polysaccharides of group B Streptococcus in pregnant Canadian women: Relationship to colonization status and infection in the neonate. J Infect Dis. 2001;184: 285–291. doi:10.1086/322029

290. Hanage WP, Kaijalainen T, Saukkoriipi A, Rickcord JL, Spratt BG. A successful, diverse disease-associated lineage of nontypeable pneumococci that has lost the capsular biosynthesis locus. J Clin Microbiol. 2006;44: 743–749. doi:10.1128/JCM.44.3.743-749.2006

291. Hoang LMN, Thomas E, Tyler S, Pollard AJ, Stephens G, Gustafson L, et al. Rapid and fatal meningococcal disease due to a strain of Neisseria meningitidis containing the capsule null locus. Clin Infect Dis. 2005;40. doi:10.1086/427875

292. Johswich KO, Zhou J, Law DKS, St. Michael FF, McCaw SE, Jamieson FB, et al. Invasive potential of nonencapsulated disease isolates of neisseria: Meningitidis. Infect Immun. 2012;80: 2346–2353. doi:10.1128/IAI.00293-12

293. Nizet V, Colina KF, Almquist JR, Rubens CE, Smith AL. A virulent nonencapsulated Haemophilus influenzae. J Infect Dis. 1996;173: 180–186. doi:10.1093/infdis/173.1.180

294. Nelson AL, Roche AM, Gould JM, Chim K, Ratner AJ, Weiser JN. Capsule enhances pneumococcal colonization by limiting mucus-mediated clearance. Infect Immun. 2007;75: 83–90. doi:10.1128/IAI.01475-06

295. Novick S, Shagan M, Blau K, Lifshitz S, Givon-Lavi N, Grossman N, et al. Adhesion and invasion of Streptococcus pneumoniae to primary and secondary respiratory epithelial cells. Mol Med Rep. 2017;15: 65–74. doi:10.3892/mmr.2016.5996

296. Muñoz-Elías EJ, Marcano J, Camilli A. Isolation of Streptococcus pneumoniae biofilm mutants and their characterization during nasopharyngeal colonization. Infect Immun. 2008;76: 5049–5061. doi:10.1128/IAI.00425-08

297. Sanchez CJ, Kumar N, Lizcano A, Shivshankar P, Hotopp JCD, Jorgensen JH, et al. Streptococcus pneumoniae in biofilms are unable to cause invasive disease due to altered virulence determinant production. PLoS One. 2011;6. doi:10.1371/journal.pone.0028738

298. Flores AR, Jewell BE, Fittipaldi N, Beres SB, Musser JM. Human disease isolates of serotype M4 and M22 group A *Streptococcus* lack genes required for hyaluronic acid capsule biosynthesis. MBio. 2012. doi:10.1128/mBio.00413-12

299. Lupp C, Robertson ML, Wickham ME, Sekirov I, Champion OL, Gaynor EC, et al. Host-mediated inflammation disrupts the intestinal microbiota and promotes the overgrowth of Enterobacteriaceae. Cell Host Microbe. 2007;2: 119–29. doi:10.1016/j.chom.2007.06.010

300. Dan JM, Havenar-Daughton C, Kendric K, Al-Kolla R, Kaushik K, Rosales SL, et al. Recurrent group A Streptococcus tonsillitis is an immunosusceptibility disease involving antibody deficiency and aberrant TFH cells. Sci Transl Med. 2019;11: eaau3776. doi:10.1126/scitranslmed.aau3776

301. Dileepan T, Linehan JL, Moon JJ, Pepper M, Jenkins MK, Cleary PP. Robust antigen specific Th17 T cell response to group A *Streptococcus* is dependent on IL-6 and intranasal route of infection. PLoS Pathog. 2011/10/04. 2011;7: e1002252. doi:10.1371/journal.ppat.1002252

302. Linehan JL, Dileepan T, Kashem SW, Kaplan DH, Cleary PP, Jenkins MK. Generation of Th17 cells in response to intranasal infection requires TGF-β1 from dendritic cells and IL-6 from CD301b+ dendritic cells. Proc Natl Acad Sci U S A. 2015;112: 12782–7. doi:10.1073/pnas.1513532112

303. Wang B, Dileepan T, Briscoe S, Hyland KA, Kang J, Khoruts A, et al. Induction of TGF-beta1 and TGF-beta1-dependent predominant Th17 differentiation by group A streptococcal infection. Proc Natl Acad Sci U S A. 2010/03/17. 2010;107: 5937–5942. doi:10.1073/pnas.0904831107

304. Marks LR, Mashburn-Warren L, Federle MJ, Hakansson AP. Streptococcus pyogenes biofilm growth in vitro and in vivo and its role in colonization, virulence, and genetic exchange. J Infect Dis. 2014;210: 25–34. doi:10.1093/infdis/jiu058

305. Šmitran A, Opavski NV, Erić-Marinković J, Gajić I, Ranin L. Adherence and biofilm production of invasive and non-invasive isolates of Streptococcus pyogenes after hyaluronidase treatment. Arch Biol Sci. 2013;65: 1353–1361. doi:10.2298/ABS1304353S

306. Cho KH, Caparon MG. Patterns of virulence gene expression differ between biofilm and tissue communities of Streptococcus pyogenes. Mol Microbiol. 2005;57: 1545–1556. doi:10.1111/J.1365-2958.2005.04786.X

307. Sumitomo T, Nakata M, Higashino M, Terao Y, Kawabata S. Group A streptococcal cysteine protease cleaves epithelial junctions and contributes to bacterial translocation. J Biol Chem. 2013;288: 13317–13324. doi:10.1074/jbc.M113.459875

308. Sumitomo T, Mori Y, Nakamura Y, Honda-Ogawa M, Nakagawa S, Yamaguchi M, et al. Streptococcal cysteine protease-mediated cleavage of desmogleins is involved in the pathogenesis of cutaneous infection. Front Cell Infect Microbiol. 2018;8: 10. doi:10.3389/fcimb.2018.00010

309. Sumitomo T, Nakata M, Higashino M, Jin Y, Terao Y, Fujinaga Y, et al. Streptolysin S contributes to group A streptococcal translocation across an epithelial barrier. J Biol Chem. 2011;286: 2750–2761. doi:10.1074/jbc.M110.171504

310. Goldmann O, Rohde M, Chhatwal GS, Medina E. Role of macrophages in host resistance to group A streptococci. Infect Immun. 2004/04/23. 2004;72: 2956–2963. Available: http://www.ncbi.nlm.nih.gov/entrez/query.fcgi?cmd=Retrieve&db=PubMed&dopt=Citation&list_uids=15102808

311. Mishalian I, Ordan M, Peled A, Maly A, Eichenbaum MB, Ravins M, et al. Recruited Macrophages Control Dissemination of Group A Streptococcus from Infected Soft Tissues. J Immunol. 2011;187: 6022–6031. doi:10.4049/JIMMUNOL.1101385

312. Loof TG, Rohde M, Chhatwal GS, Jung S, Medina E. The Contribution of Dendritic Cells to Host Defenses against Streptococcus pyogenes. J Infect Dis. 2007;196: 1794–1803. doi:10.1086/523647

313. Döhrmann S, Cole JN, Nizet V. Conquering Neutrophils. PLoS Pathog. 2016;12. doi:10.1371/JOURNAL.PPAT.1005682

314. Tanaka M, Kinoshita-Daitoku R, Kiga K, Sanada T, Zhu B, Okano T, et al. Group A Streptococcus establishes pharynx infection by degrading the deoxyribonucleic acid of neutrophil extracellular traps. Sci Reports 2020 101. 2020;10: 1–11. doi:10.1038/s41598-020-60306-w

315. Costalonga M, Cleary P, Fischer L, Zhao Z. Intranasal bacteria induce Th1 but not Treg or Th2. Mucosal Immunol. 2009;2: 85. doi:10.1038/MI.2008.67

316. Carlin AF, Uchiyama S, Chang Y-C, Lewis AL, Nizet V, Varki A. Molecular mimicry of host sialylated glycans allows a bacterial pathogen to engage neutrophil Siglec-9 and dampen the innate immune response. Blood. 2009;113: 3333. doi:10.1182/BLOOD-2008-11-187302

317. Peterson,' PK, Kim Y, Wilkinson BJ, Schmeling D, Michael AF, Quie2 PG. Dichotomy Between Opsonization and Serum Complement Activation by Encapsulated Staphylococci. Infect Immun. 1978;20: 770–775.

318. Llobet E, Tomás JM, Bengoechea JA. Capsule polysaccharide is a bacterial decoy for antimicrobial peptides. Microbiol. 2008;154: 3877–3886. doi:10.1099/MIC.0.2008/022301-0

319. Campos MA, Vargas MA, Regueiro V, Llompart CM, Albertí S, Bengoechea JA. Capsule Polysaccharide Mediates Bacterial Resistance to Antimicrobial Peptides. Infect Immun. 2004;72: 7107. doi:10.1128/IAI.72.12.7107-7114.2004

320. Cunningham MW. Rheumatic Fever, Autoimmunity, and Molecular Mimicry: The Streptococcal Connection. Int Rev Immunol. 2014;33: 314–329. doi:10.3109/08830185.2014.917411

321. Hasenbein ME, Warner JE, Lambert KG, Cole SE, Onderdonk AB, McAdam AJ. Detection of Multiple Macrolide- and Lincosamide-Resistant Strains of Streptococcus pyogenes from Patients in the Boston Area. J Clin Microbiol. 2004;42: 1559–1563. doi:10.1128/JCM.42.4.1559-1563.2004

322. Kaplan EL, Johnson DR, Del Rosario MC, Horn DL. Susceptibility of group A beta-hemolytic streptococci to thirteen antibiotics: examination of 301 strains isolated in the United States between 1994 and 1997. Pediatr Infect Dis J. 1999;18: 1069–1072. Available: http://www.ncbi.nlm.nih.gov/entrez/query.fcgi?cmd=Retrieve&db=PubMed&dopt=Citation&list_uids=10608626

323. Facinelli B, Spinaci C, Magi G, Giovanetti E, Varaldo PE. Association between erythromycin resistance and ability to enter human respiratory cells in group A streptococci. Lancet. 2001;358: 30–33. doi:10.1016/S0140-6736(00)05253-3

324. Varaldo PE, Debbia EA, Nicoletti G, Pavesio D, Ripa S, Schito GC, et al. Nationwide Survey in Italy of Treatment of Streptococcus pyogenes Pharyngitis in Children: Influence of Macrolide Resistance on Clinical and Microbiological Outcomes. Clin Infect Dis. 1999;29: 869–873. doi:10.1086/520451

325. Cattoir V. Mechanisms of antibiotic resistance, Streptococcus pyogenes: Basic Biology to Clinical Manifestations. 2016. doi:10.1128/9781555819286.ch17

326. York MK, Gibbs L, Perdreau-Remington F, Brooks GF. Characterization of Antimicrobial Resistance in Streptococcus pyogenes Isolates from the San Francisco Bay Area of Northern California. J Clin Microbiol. 1999;37: 1727. doi:10.1128/jcm.37.6.1727-1731.1999

327. Martin JM, Green M, Barbadora KA, Wald ER. Erythromycin-resistant group A streptococci in schoolchildren in Pittsburgh. N Engl J Med. 2002;346: 1200–1206. doi:10.1056/NEJMOA013169

328. Johnson AF, LaRock CN. Antibiotic Treatment, Mechanisms for Failure, and Adjunctive Therapies for Infections by Group A Streptococcus. Front Microbiol. 2021;0: 3163. doi:10.3389/FMICB.2021.760255

329. Brook I. Penicillin failure in the treatment of streptococcal pharyngo-tonsillitis. Curr Infect Dis Rep. 2013;15: 232–235. doi:10.1007/s11908-013-0338-0

330. Young PG, Moreland NJ, Loh JM, Bell A, Atatoa Carr P, Proft T, et al. Structural conservation, variability, and immunogenicity of the T6 backbone pilin of serotype M6 *Streptococcus pyogenes*. Infect Immun. 2014;82: 2949–2957. doi:10.1128/IAI.01706-14

331. Ly D, Taylor JM, Tsatsaronis JA, Monteleone MM, Skora AS, Donald CA, et al. Plasmin(ogen) acquisition by group A *Streptococcus* protects against C3b-mediated neutrophil killing. J Innate Immun. 2014;6: 240–50. doi:10.1159/000353754

332. Courtney HS, Bronze MS, Dale JB, Hasty DL. Analysis of the role of M24 protein in group A streptococcal adhesion and colonization by use of omega-interposon mutagenesis. Infect Immun. 1994;62: 4868–73. Available: http://www.ncbi.nlm.nih.gov/pubmed/7927767

333. Rohde M, nat habil rer, Patrick Cleary P, Cleary PP. Adhesion and invasion of Streptococcus pyogenes into host cells and clinical relevance of intracellular streptococci. Streptococcus pyogenes : Basic Biology to Clinical Manifestations. University of Oklahoma Health Sciences Center; 2016. Available: http://www.ncbi.nlm.nih.gov/pubmed/26866223

334. Dale JB, Chiang EC. Intranasal Immunization with Recombinant Group A Streptococcal M Protein Fragment Fused to the B Subunit of Escherichia coli Labile Toxin Protects Mice against Systemic. Source J Infect Dis. 1995;171: 1038–1041. Available: https://about.jstor.org/terms

335. Mortensen R, Christensen D, Hansen LB, Christensen JP, Andersen P, Dietrich J. Local Th17/IgA immunity correlate with protection against intranasal infection with Streptococcus pyogenes. PLoS One. 2017;12: e0175707. doi:10.1371/JOURNAL.PONE.0175707

336. Campbell PT, Tong SYC, Geard N, Davies MR, Worthing KA, Lacey JA, et al. Longitudinal analysis of group A Streptococcus emm types and emm clusters in a high prevalence setting reveals past infection does not prevent future infection. J Infect Dis. 2019;3000: 1–9. doi:10.1093/infdis/jiz615

337. Musser JM, Hauser AR, Kim MH, Schlievert PM, Nelson K, Selander RK. *Streptococcus pyogenes* causing toxic-shock-like syndrome and other invasive diseases: clonal diversity and pyrogenic exotoxin expression. Proc Natl Acad Sci U S A. 1991;88: 2668–2672.

338. Tse H, Bao JYJ, Davies MR, Maamary P, Tsoi H-W, Tong AHY, et al. Molecular characterization of the 2011 Hong Kong scarlet fever outbreak. J Infect Dis. 2012;206: 341–51. doi:10.1093/infdis/jis362

339. Teatero S, McGeer A, Tyrrell GJ, Hoang L, Smadi H, Domingo M-C, et al. Canada-Wide Epidemic of emm74 Group A Streptococcus Invasive Disease. Open Forum Infect Dis. 2018;5: ofy085. doi:10.1093/ofid/ofy085

340. Kapust RB, Tozser J, Fox JD, Anderson DE, Cherry S, Copeland TD, et al. Tobacco etch virus protease: mechanism of autolysis and rational design of stable mutants with wild-type catalytic proficiency. Protein Eng. 2001;14: 993–1000.

341. Beres SB, Sylva GL, Barbian KD, Lei B, Hoff JS, Mammarella ND, et al. Genome sequence of a serotype M3 strain of group A *Streptococcus*: phage-encoded toxins, the high-virulence phenotype, and clone emergence. Proc Natl Acad Sci U S A. 2002;99: 10078–10083.

342. Hurst JR, Brouwer S, Walker MJ, McCormick JK. Streptococcal superantigens and the return of scarlet fever. PLoS Pathog. 2021;17: 1–6. doi:10.1371/journal.ppat.1010097

343. McMillan DJ, Drèze P-A, Vu T, Bessen DE, Guglielmini J, Steer AC, et al. Updated model of group A *Streptococcus* M proteins based on a comprehensive worldwide study. Clin Microbiol Infect. 2013;19: E222-9. doi:10.1111/1469-0691.12134

344. McKay FC, McArthur JD, Sanderson-Smith ML, Gardam S, Currie BJ, Sriprakash KS, et al. Plasminogen Binding by Group A Streptococcal Isolates from a Region of Hyperendemicity for Streptococcal Skin Infection and a High Incidence of Invasive Infection. Infect Immun. 2004;72: 364–370. doi:10.1128/IAI.72.1.364-370.2004

345. Pandey M, Good MF. A Superficial Skin Scarification Method in Mice to Mimic Streptococcus pyogenes Skin Infection in Humans. Methods Mol Biol. 2020;2136: 287–301. doi:10.1007/978-1-0716-0467-0_22

346. Oh JE, Song E, Moriyama M, Wong P, Zhang S, Jiang R, et al. Intranasal priming induces local lung-resident B cell populations that secrete protective mucosal antiviral IgA. Sci Immunol. 2021;6. doi:10.1126/SCIIMMUNOL.ABJ5129

347. Agace WW. Tissue-tropic effector T cells: generation and targeting opportunities. Nat Rev Immunol 2006 69. 2006;6: 682–692. doi:10.1038/nri1869

348. Turner DL, Farber DL. Mucosal resident memory CD4 T cells in protection and immunopathology. Front Immunol. 2014;5: 331. doi:10.3389/FIMMU.2014.00331/BIBTEX

349. Thome JJC, Farber DL. Emerging concepts in tissue-resident T cells: lessons from humans. Trends Immunol. 2015;36: 428–435. doi:10.1016/J.IT.2015.05.003

350. O'Hara JM, Redhu NS, Cheung E, Robertson NG, Patik I, Sayed S El, et al. Generation of protective pneumococcal-specific nasal resident memory CD4+ T cells via parenteral immunization. Mucosal Immunol. 2020;13: 172–182. doi:10.1038/s41385-019-0218-5

351. Christensen D, Mortensen R, Rosenkrands I, Dietrich J, Andersen P. Vaccine-

induced Th17 cells are established as resident memory cells in the lung and promote local IgA responses. Mucosal Immunol. 2017;10: 260–270. doi:10.1038/mi.2016.28

352. Ozberk V, Reynolds S, Huo Y, Calcutt A, Eskandari S, Dooley J, et al. Prime-pull immunization with a bivalent m-protein and spy-cep peptide vaccine adjuvanted with caf®01 liposomes induces both mucosal and peripheral protection from covr/s mutant streptococcus pyogenes. MBio. 2021;12: 1–15. doi:10.1128/MBIO.03537-20/FORMAT/EPUB

353. Zhang Q, Finn A. Mucosal immunology of vaccines against pathogenic nasopharyngeal bacteria. J Clin Pathol. 2004;57: 1015. doi:10.1136/JCP.2004.016253

354. Smeesters PR, McMillan DJ, Sriprakash KS, Georgousakis MM. Differences among group A streptococcus epidemiological landscapes: consequences for M protein-based vaccines? Expert Rev Vaccines. 2009;8: 1705–1721. doi:10.1586/ERV.09.133

355. Engel ME, Stander R, Vogel J, Adeyemo AA, Mayosi BM. Genetic susceptibility to acute rheumatic fever: a systematic review and meta-analysis of twin studies. PLoS One. 2011;6: e25326. doi:10.1371/journal.pone.0025326

356. Giffard PM, Tong SYC, Holt DC, Ralph AP, Currie BJ. Concerns for efficacy of a 30-valent M-protein-based *Streptococcus pyogenes* vaccine in regions with high rates of rheumatic heart disease. PLoS Negl Trop Dis. 2019;13: e0007511. doi:10.1371/JOURNAL.PNTD.0007511

357. Carapetis J, Gardiner D, Currie B, Mathews JD. Multiple strains of Streptococcus pyogenes in skin sores of aboriginal Australians. J Clin Microbiol. 1995;33: 1471. doi:10.1128/jcm.33.6.1471-1472.1995

358. Jones KF, Hollingsheado SK, Scottf JR, Fischetti VA. Spontaneous M6 protein size mutants of group A streptococci display variation in antigenic and opsonogenic epitopes (antigenic variation/intragenic repeats/surface proteins/phagocytosis/monoclonal antibodies). Proc Nati Acad Sci USA. 1988;85: 8271–8275.

359. Harbaugh MP, Podbielski A, Hügl S, Cleary PP. Nucleotide substitutions and small-scale insertion produce size and antigenic variation in group A streptococcal M1 protein. Mol Microbiol. 1993;8: 981–991. doi:10.1111/J.1365-2958.1993.TB01642.X

360. Penney TJ, Martin DR, Williams LC, De Malmanche SA, Bergquist PL. A single emm gene-specific oligonucleotide probe does not recognise all members of the Streptococcus pyogenes M type 1. FEMS Microbiol Lett. 1995;130: 145–150. doi:10.1111/j.1574-6968.1995.tb07711.x

361. Pandey M, Ozberk V, Calcutt A, Langshaw E, Powell J, Rivera-Hernandez T, et al. Streptococcal Immunity Is Constrained by Lack of Immunological Memory following a Single Episode of Pyoderma. Wessels MR, editor. PLOS Pathog. 2016;12: e1006122. doi:10.1371/journal.ppat.1006122

362. Polly SM, Waldman RH, High P, Wittner MK, Dorfman A. Protective Studies with a Group A Streptococcal M Protein Vaccine. II. Challenge of Volunteers after Local Immunization in the Upper Respiratory Tract. 1975;131: 217–224. Available: https://www.jstor.org/stable/30081569

363. Massell BF. Rheumatic Fever Following Streptococcal Vaccination. JAMA. 1969;207: 1115. doi:10.1001/jama.1969.03150190037007

364. Food and Drug Administration. Revocation of Status of Specific Products; Group A Streptococcus. Federal Register. 2005. Available: www.fda.gov/dockets/ecomments.

365. Cunningham MW, Antone SM, Smart M, Liu R, Kosanke S. Molecular analysis of human cardiac myosin-cross-reactive B- and T-cell epitopes of the group A streptococcal M5 protein. Infect Immun. 1997;65: 3913–3923.

366. Kirvan CA, Galvin JE, Hilt S, Kosanke S, Cunningham MW. Identification of streptococcal M-protein cardiopathogenic epitopes in experimental autoimmune valvulitis. J Cardiovasc Transl Res. 2014;7: 172–181. doi:10.1007/s12265-013-9526-4

367. Quinn A, Ward † Kent, Fischetti VA, Hemric M, Cunningham MW. Immunological Relationship between the Class I Epitope of Streptococcal M Protein and Myosin. Infect Immun. 1998;66: 4418–4424.

368. Pruksakorn S, Currie B, Brandt E, Phornphutkul C, Hunsakunachal S, Manmontri A, et al. Identification of T cell autoepitopes that cross-react with the C-terminal segment of the M protein of group A streptococci. Int Immunol. 1994;6: 1235–1244. doi:10.1093/INTIMM/6.8.1235

369. Vashishtha A, Fischetti VA. Surface-exposed conserved region of the streptococcal M protein induces antibodies cross-reactive with denatured forms of myosin. J Immunol. 1993;150: 4693–4701. Available: http://www.jimmunol.org/content/150/10/4693

370. Lymbury RS, Olive C, Powell KA, Good MF, Hirst RG, LaBrooy JT, et al. Induction of autoimmune valvulitis in Lewis rats following immunization with peptides from the conserved region of group A streptococcal M protein. J Autoimmun. 2003;20: 211–217. doi:10.1016/S0896-8411(03)00026-X

371. Påhlman LI, Olin AI, Darenberg J, Mörgelin M, Kotb M, Herwald H, et al. Soluble M1 protein of Streptococcus pyogenes triggers potent T cell activation. Cell Microbiol. 2008;10: 404–414. doi:10.1111/J.1462-5822.2007.01053.X

372. Påhlman LI, Mörgelin M, Eckert J, Johansson L, Russell W, Riesbeck K, et al. Streptococcal M protein: a multipotent and powerful inducer of inflammation. J Immunol. 2006;177: 1221–8. doi:177/2/1221 [pii]

373. Herwald H, Cramer H, Mörgelin M, Russell W, Sollenberg U, Norrby-Teglund A, et al. M Protein, a Classical Bacterial Virulence Determinant, Forms Complexes with Fibrinogen that Induce Vascular Leakage. Cell. 2004;116: 367–379. doi:10.1016/S0092-8674(04)00057-1

374. Valderrama JA, Riestra AM, Gao NJ, Larock CN, Gupta N, Ali SR, et al. Group A streptococcal M protein activates the NLRP3 inflammasome. Nat Microbiol 2017 210. 2017;2: 1425–1434. doi:10.1038/s41564-017-0005-6

375. Movert E, Lienard J, Valfridsson C, Nordströ T, Johansson-Lindbom B, Carlsson F. Streptococcal M protein promotes IL-10 production by cGAS-independent activation of the STING signaling pathway. PLoS Pathog. 2018;14. doi:10.1371/journal.ppat.1006969

376. Persson ST, Wilk L, Mörgelin M, Herwald H. Vigilant Keratinocytes Trigger Pathogen-Associated Molecular Pattern Signaling in Response to Streptococcal M1 Protein. Infect Immun. 2015;83: 4673. doi:10.1128/IAI.00887-15

377. Osowicki J, Azzopardi KI, McIntyre L, Rivera-Hernandez T, Ong C-LY, Baker C, et al. A Controlled Human Infection Model of Group A Streptococcus Pharyngitis: Which Strain and Why? Papasian CJ, editor. mSphere. 2019;4: e00647-18. doi:10.1128/mSphere.00647-18

378. Osowicki J, Azzopardi KI, Baker C, Waddington CS, Pandey M, Schuster T, et al. Controlled human infection for vaccination against Streptococcus pyogenes (CHIVAS): Establishing a group A Streptococcus pharyngitis human infection study. Vaccine. 2019;37: 3485–3494. doi:10.1016/j.vaccine.2019.03.059

379. Cunningham MW. Streptococcus and rheumatic fever. Curr Opin Rheumatol. 2012;24: 408–416. doi:10.1097/BOR.0b013e32835461d3

380. World Health Organization. WHO Expert Consultation on Rheumatic Fever and Rheumatic Heart Disease. WHO Tech Rep Ser. 2001;923.

381. Cunningham MW. Molecular Mimicry, Autoimmunity, and Infection: The Cross-Reactive Antigens of Group A Streptococci and their Sequelae. Fischetti VA, Novick RP, Ferretti JJ, Portnoy DA, Braunstein M, Rood JI, editors. Microbiol Spectr. 2019;7. doi:10.1128/microbiolspec.GPP3-0045-2018

382. Laffon A, Garcia-Vicuna R, Humbria A, Postigo AA, Corbi AL, De Landazuri MO, et al. Upregulated expression and function of VLA-4 fibronectin receptors on human activated T cells in rheumatoid arthritis. J Clin Invest. 1991;88: 546–552. doi:10.1172/JCI115338

383. Yednock TA, Cannon C, Fritz LC, Sanchez-Madrid F, Steinman L, Karin N. Prevention of experimental autoimmune encephalomyelitis by antibodies against a4B1 integrin. Nature. 1992;356: 63–66. Available: https://www.nature.com/articles/356063a0.pdf?origin=ppub

384. Waugh RE, Kim M, Hyun Y-M, Chung H-L, Mcgrath JL. Activated Integrin VLA-4 Localizes to the Lamellipodia and Mediates T Cell Migration on VCAM-1. J Immunol. 2009;183: 359–369. doi:10.4049/jimmunol.0803388

385. Fraser WJ, Haffejee Z, Cooper K. Rheumatic Aschoff nodules revisited: an immunohistological reappraisal of the cellular component. Histopathology. 1995;27: 457–461. doi:10.1111/j.1365-2559.1995.tb00310.x

386. Quinn A, Kosanke S, Fischetti VA, Factor SM, Cunningham MW. Induction of autoimmune valvular heart disease by recombinant streptococcal M protein. Infect Immun. 2001/05/12. 2001;69: 4072–4078. doi:10.1128/IAI.69.6.4072-4078.2001

387. Gorton D, Govan B, Olive C, Ketheesan N. B- and T-Cell Responses in Group A *Streptococcus* M-Protein- or Peptide-Induced Experimental Carditis. Infect Immun. 2009;77: 2177–2183. doi:10.1128/IAI.01514-08

388. Kemeny E, Grieve T, Marcus R, Sareli P, Zabriskie JB. Identification of mononuclear cells and T cell subsets in rheumatic valvulitis. Clin Immunol Immunopathol. 1989;52: 225–37. Available: http://www.ncbi.nlm.nih.gov/pubmed/2786783

389. Goodwin RL, Kheradvar A, Norris RA, Price RL, Potts JD. Collagen Fibrillogenesis in the Mitral Valve: It's a Matter of Compliance. J Cardiovasc Dev Dis. 2021;8. doi:10.3390/JCDD8080098

390. Liu AC, Joag VR, Gotlieb AI. The Emerging Role of Valve Interstitial Cell Phenotypes in Regulating Heart Valve Pathobiology. Am J Pathol. 2007;171: 1407. doi:10.2353/AJPATH.2007.070251

391. McNamara C, Zinkernagel AS, Macheboeuf P, Cunningham MW, Nizet V, Ghosh P. Coiled-coil irregularities and instabilities in group A *Streptococcus* M1 are required for virulence. Science. 2008/03/08. 2008;319: 1405–8. doi:10.1126/science.1154470

392. Guilherme L, Oshiro SE, Faé KC, Cunha-Neto E, Renesto G, Goldberg AC, et al. T-cell reactivity against streptococcal antigens in the periphery mirrors reactivity of heart-infiltrating T lymphocytes in rheumatic heart disease patients. Infect Immun. 2001;69: 5345–5351. doi:10.1128/IAI.69.9.5345-5351.2001

393. Faé KC, Silva DD da, Oshiro SE, Tanaka AC, Pomerantzeff PMA, Douay C, et al. Mimicry in Recognition of Cardiac Myosin Peptides by Heart-Intralesional T Cell Clones from Rheumatic Heart Disease. J Immunol. 2006;176: 5662–5670. doi:10.4049/JIMMUNOL.176.9.5662

394. Ellis NMJ, Li Y, Hildebrand W, Fischetti VA, Cunningham MW. T Cell Mimicry and Epitope Specificity of Cross-Reactive T Cell Clones from Rheumatic Heart Disease. J Immunol. 2005;175: 5448–5456. doi:10.4049/JIMMUNOL.175.8.5448

395. Shikhman AR, Cunningham MW. Immunological mimicry between N-acetyl-beta-D-glucosamine and cytokeratin peptides. Evidence for a microbially driven anti-keratin antibody response. J Immunol. 1994;152: 4375–4387.

396. Dudding BA, Ayoub EM. Persistence of streptococcal group A antibody in patients with rheumatic valvular disease. J Exp Med. 1968;128: 1081–1098. doi:10.1084/JEM.128.5.1081

397. Adderson EE, Cunningham MW. Region Genes-Acetylglucosamine/Anti-Myosin Antibody V N Carditis: Human Anti-Monoclonal Antibodies from Rheumatic Molecular Analysis of Polyreactive. J Immunol. 1998;161: 2020–2031. Available: http://www.jimmunol.org/content/161/4/http://www.jimmunol.org/content/161/4/2 020.full#ref-list-1

398. Galvin JE, Hemric ME, Ward K, Cunningham MW. Cytotoxic mAb from rheumatic carditis recognizes heart valves and laminin. J Clin Invest. 2000;106: 217–224. doi:10.1172/JCI7132

399. Rafeek RAM, Sikder S, Hamlin AS, Andronicos NM, McMillan DJ, Sriprakash KS, et al. Requirements for a Robust Animal Model to Investigate the Disease Mechanism of Autoimmune Complications Associated With ARF/RHD. Front Cardiovasc Med. 2021;0: 389. doi:10.3389/FCVM.2021.675339

400. Galvin JE, Hemric ME, Kosanke SD, Factor SM, Quinn A, Cunningham MW. Induction of myocarditis and valvulitis in lewis rats by different epitopes of cardiac myosin and its implications in rheumatic carditis. Am J Pathol. 2002/01/12. 2002;160: 297–306. doi:10.1016/S0002-9440(10)64373-8

401. Sikder S, Price G, Alim MA, Gautam A, Scott Simpson R, Margaret Rush C, et al. Group A streptococcal M-protein specific antibodies and T-cells drive the pathology observed in the rat autoimmune valvulitis model. https://doi.org/101080/0891693420191605356. 2019;52: 78–87. doi:10.1080/08916934.2019.1605356

402. Marijon E, Ou P, Celermajer DS, Ferreira B, Mocumbi AO, Jani D, et al. Prevalence of rheumatic heart disease detected by echocardiographic screening. N Engl J Med. 2007/08/03. 2007;357: 470–476. doi:10.1056/NEJMoa065085

403. Beaton A, Okello E, Lwabi P, Mondo C, McCarter R, Sable C. Echocardiography screening for rheumatic heart disease in ugandan schoolchildren. Circulation. 2012;125: 3127–3132. doi:10.1161/CIRCULATIONAHA.112.092312

404. Carapetis JR, Hardy M, Fakakovikaetau T, Taib R, Wilkinson L, Penny DJ, et al. Evaluation of a screening protocol using auscultation and portable

echocardiography to detect asymptomatic rheumatic heart disease in Tongan schoolchildren. Nat Clin Pract Cardiovasc Med 2008 57. 2008;5: 411–417. doi:10.1038/ncpcardio1185

405. Bhaya M, Panwar S, Beniwal R, Panwar RB. High Prevalence of Rheumatic Heart Disease Detected by Echocardiography in School Children. Echocardiography. 2010;27: 448–453. doi:10.1111/j.1540-8175.2009.01055.x

406. Rush CM, Govan BL, Sikder S, Williams NL, Ketheesan N. Animal models to investigate the pathogenesis of rheumatic heart disease. Front Pediatr. 2014;2: 116. doi:10.3389/fped.2014.00116

407. Zacchigna S, Paldino A, Falcão-Pires I, Daskalopoulos EP, Dal Ferro M, Vodret S, et al. Towards standardization of echocardiography for the evaluation of left ventricular function in adult rodents: a position paper of the ESC Working Group on Myocardial Function. Cardiovasc Res. 2021;117: 43–59. doi:10.1093/CVR/CVAA110

408. Lindsey ML, Kassiri Z, I Virag JA, de Castro Brás LE, Scherrer-Crosbie M, Jai V, et al. REVIEW Guidelines in Cardiovascular Research. Am J Physiol Hear Circ Physiol. 2018;314: 733–752. doi:10.1152/ajpheart.00339.2017.-Cardiovascular

409. Bencivenga JF, Johnson DR, Kaplan EL. Determination of group a streptococcal anti-M type-specific antibody in sera of rheumatic fever patients after 45 years. Clin Infect Dis. 2009;49: 1237–1239. doi:10.1086/605673/2/49-8-1237-TBL001.GIF

410. Nagueh SF, Smiseth OA, Appleton CP, Byrd BF, Dokainish H, Edvardsen T, et al. Recommendations for the Evaluation of Left Ventricular Diastolic Function by Echocardiography: An Update from the American Society of Echocardiography and the European Association of Cardiovascular Imaging. J Am Soc Echocardiogr. 2016;29: 277–314. doi:10.1016/J.ECHO.2016.01.011

411. Lang RM, Badano LP, Mor-Avi V, Afilalo J, Armstrong A, Ernande L, et al. Recommendations for cardiac chamber quantification by echocardiography in adults: An update from the American society of echocardiography and the European association of cardiovascular imaging. Eur Heart J Cardiovasc Imaging. 2015;28: 1–39. doi:10.1093/ehjci/jev014

412. Atalay S, Uçar T, Özçelik N, Ekici F, Tutar E. Echocardiographic evaluation of mitral valve in patients with pure rheumatic mitral regurgitation. Turk J Pediatr. 2007;49: 148–153.

413. Yumoto Y, Satoh S, Fujita Y, Koga T, Kinukawa N, Nakano H. Noninvasive measurement of isovolumetric contraction time during hypoxemia and acidemia: Fetal lamb validation as an index of cardiac contractility. Early Hum Dev. 2005;81: 635–642. doi:10.1016/J.EARLHUMDEV.2005.04.004

414. Chopra P, Narula J, Kumar AS, Sachdeva S, Bhatia ML. Immunohistochemical characterisation of Aschoff nodules and endomyocardial inflammatory infiltrates in left atrial appendages from patients with chronic rheumatic heart disease. Int J Cardiol. 1988;20: 99–105. doi:10.1016/0167-5273(88)90319-1

415. Kamblock J, Payot L, Iung B, Costes P, Gillet T, Le Goanvic C, et al. Does rheumatic myocarditis really exists? Systematic study with echocardiography and cardiac troponin I blood levels. Eur Heart J. 2003;24: 855–862. doi:10.1016/S0195-668X(02)00825-4

416. Essop MR, Wisenbaugh T, Sareli P, Johannesburg F, Africa S. Evidence Against a Myocardial Factor as the Cause of Left Ventricular Dilation in Active Rheumatic Cardifis. JACC. 1993;22: 826–829.

417. Katus HA, Remppis A, Neumann FJ, Scheffold T, Diederich KW, Vinar G, et al. Diagnostic Efficiency of Troponin T Measurements in Acute Myocardial Infarction. Circulation. 1991;83: 902–912. Available: http://ahajournals.org

418. Cardinaels EPM, Mingels AMA, Van Rooij T, Collinson PO, Prinzen FW, Van Dieijen-Visser MP. Time-Dependent Degradation Pattern of Cardiac Troponin T Following Myocardial Infarction. Clin Chem. 2013;59: 1083–1090. doi:10.1373/CLINCHEM.2012.200543

419. Fenderson PG, Fischetti VA, Cunningham MW. Tropomyosin shares immunologic epitopes with group A streptococcal M proteins. J Immunol. 1989;142: 2475–81. Available: http://www.ncbi.nlm.nih.gov/pubmed/2466896

420. Martins TB, Hoffman JL, Augustine NH, Phansalkar AR, Fischetti VA, Zabriskie JB, et al. Comprehensive analysis of antibody responses to streptococcal and tissue antigens in patients with acute rheumatic fever. Int Immunol. 2008;20: 445–52. doi:10.1093/intimm/dxn004

421. Garcia AF, Yamaga KM, Anne Shafer L, Bollt O, Tam EK, Cunningham MW, et al. Cardiac Myosin Epitopes Recognized by Autoantibody in Acute and Convalescent Rheumatic Fever. Pediatr Infect Dis J. 2016;35: 1021–1026. doi:10.1097/INF.0000000000001235

422. Yang LPH, Eriksson BKG, Harrington Z, Curtis N, Lang S, Currie BJ, et al. Variations in the protective immune response against streptococcal superantigens in populations of different ethnicity. Med Microbiol Immunol. 2006;195: 37–43. doi:10.1007/s00430-005-0245-6

423. Flores AE, Johnson DR, Kaplan EL, Wannamaker LW. Factors Influencing Antibody Responses to Streptococcal M Proteins in Humans. J Infect Dis. 1983;147: 1–15. doi:10.1093/INFDIS/147.1.1

424. Bisno AL, Nelson KE. Type-Specific Opsonic Antibodies in Streptococcal Pyoderma. Infect Immun. 1974;10: 1356–1361.

425. Carrión F, Fernandez M, Iruretagoyena M, Coelho Andrade L., Odete-Hilário M, Figueroa F. Selective depletion of Vβ2+CD8+ T cells in peripheral blood from rheumatic heart disease patients. J Autoimmun. 2003;20: 183–190. doi:10.1016/S0896-8411(03)00002-7

426. Bhatnagar A, Grover A, Ganguly NK. Superantigen-induced T cell responses in acute rheumatic fever and chronic rheumatic heart disease patients. Clin Exp Immunol. 1999;116: 100. doi:10.1046/J.1365-2249.1999.00853.X

427. Figueroa F, González M, Carrión F, Lobos C, Turner F, Lasagna N, et al. Restriction in the Usage of Variable β Regions in T-cells Infiltrating Valvular Tissue from Rheumatic Heart Disease Patients. J Autoimmun. 2002;19: 233–240. doi:10.1006/jaut.2002.0620

428. Abbott WG, Skinner MA, Voss L, Lennon D, Tan PL, Fraser JD, et al. Repertoire of transcribed peripheral blood T-cell receptor beta chain variable-region genes in acute rheumatic fever. Infect Immun. 1996;64: 2842–5. Available: http://www.ncbi.nlm.nih.gov/pubmed/8698521

429. Davies FJ, Olme C, Lynskey NN, Turner CE, Sriskandan S. Streptococcal superantigen-induced expansion of human tonsil T cells leads to altered T follicular helper cell phenotype, B cell death and reduced immunoglobulin release. Clin Exp Immunol. 2019;197: 83–94. doi:10.1111/cei.13282

430. Dan JM, Havenar-Daughton C, Kendric K, Al-kolla R, Kaushik K, Rosales SL, et al. Recurrent group A Streptococcus tonsillitis is an immunosusceptibility disease involving antibody deficiency and aberrant T FH cells. Sci Transl Med. 2019;11: eaau3776. doi:10.1126/scitranslmed.aau3776

431. Bhatia R, Narula J, Reddy KS, Koicha M, Malaviya AN, Pothineni RB, et al. Lymphocyte subsets in acute rheumatic fever and rheumatic heart disease. Clin Cardiol. 1989;12: 34–38. doi:10.1002/clc.4960120106

432. Faé KC, Kalil J, Toubert A, Guilherme L. Heart infiltrating T cell clones from a rheumatic heart disease patient display a common TCR usage and a degenerate antigen recognition pattern. Mol Immunol. 2004;40: 1129–1135. doi:10.1016/j.molimm.2003.11.007

433. Faé KC, Oshiro SE, Toubert A, Charron D, Kalil J, Guilherme L. How an autoimmune reaction triggered by molecular mimicry between streptococcal M protein and cardiac tissue proteins leads to heart lesions in rheumatic heart disease. J Autoimmun. 2005;24: 101–109. doi:10.1016/J.JAUT.2005.01.007

434. Guilherme L, Dulphy N, Douay C, Nica Coelho V, Cio Cunha-Neto E, Oshiro SE, et al. Molecular evidence for antigen-driven immune responses in cardiac lesions of rheumatic heart disease patients. Int Immunol. 2000;12: 1063–1074.

435. Guilherme L, Cunha-Neto E, Coelho V, Snitcowsky R, Pomerantzeff PMA, Assis

R V., et al. Human Heart–Infiltrating T-Cell Clones From Rheumatic Heart Disease Patients Recognize Both Streptococcal and Cardiac Proteins. Circulation. 1995;92: 415–420. doi:10.1161/01.CIR.92.3.415

436. Ayoub EM, Taranta A, Bartley TD. Effect of Valvular Surgery on Antibody to the Group A Streptococcal Carbohydrate. Circulation. 1974;50: 144–150. Available: http://ahajournals.org

437. Neu N, Rose NR, Beisel KW, Herskowitz A, Gurri-Glass G, Craig SW. Cardiac myosin induces myocarditis in genetically predisposed mice. J Immunol. 1987;139: 3630–3636. Available: http://www.jimmunol.org/

438. Cunningham MW. Cardiac Myosin and the TH1/TH2 Paradigm in Autoimmune Myocarditis. Am J Pathol. 2001;159: 5. doi:10.1016/S0002-9440(10)61665-3

439. Li Y, Heuser JS, Kosanke SD, Hemric M, Cunningham MW. Cryptic Epitope Identified in Rat and Human Cardiac Myosin S2 Region Induces Myocarditis in the Lewis Rat. J Immunol. 2004;172: 3225–3234. doi:10.4049/JIMMUNOL.172.5.3225

440. Pummerer CL, Luze K, Grässl G, Bachmaier K, Offner F, Burrell SK, et al. Identification of cardiac myosin peptides capable of inducing autoimmune myocarditis in BALB/c mice. J Clin Invest. 1996;97: 2057–2062. doi:10.1172/JCI118642

441. Wegmann KW, Zhao W, Griffin AC, Hickey WF. Identification of myocarditogenic peptides derived from cardiac myosin capable of inducing experimental allergic myocarditis in the Lewis rat. The utility of a class II binding motif in selecting self-reactive peptides. J Immunol. 1994;153. Available: http://www.jimmunol.org/content/153/2/892

442. Kodama M, Matsumoto Y, Fujiwara M, Masani F, Izumi T, Shibata A. A novel experimental model of giant cell myocarditis induced in rats by immunization with cardiac myosin fraction. Clin Immunol Immunopathol. 1990;57: 250–262. doi:10.1016/0090-1229(90)90039-S

443. Neu N, Ploier B, Ofner C. Cardiac Myosin-Induced Myocarditis: Heart Autoantibodies Are Not Involved in the Induction of the Disease. 1990;145. Available: http://www.jimmunol.org/

444. Wolfgram LJ, Beisel KW, Rose NR. HEART-SPECIFIC AUTOANTIBODIES FOLLOWING MURINE COXSACKIEVIRUS B3 MYOCARDITIS. J Exp Med. 1985;161: 1112–1121.

445. Tandon R, Sharma M, Chandrashekhar Y, Kotb M, Yacoub MH, Narula J. Revisiting the pathogenesis of rheumatic fever and carditis. Nat Rev Cardiol. 2013;10: 171–177. doi:10.1038/nrcardio.2012.197

446. Dinkla K, Rohde M, Jansen WTM, Kaplan EL, Chhatwal GS, Talay SR. Rheumatic fever-associated Streptococcus pyogenes isolates aggregate collagen. J Clin Invest. 2003;111: 1905–1912. doi:10.1172/JCI17247

447. Dinkla K, Nitsche-Schmitz DP, Barroso V, Reissmann S, Johansson HM, Frick I-M, et al. Identification of a Streptococcal Octapeptide Motif Involved in Acute Rheumatic Fever. J Biol Chem. 2007;282: 18686–18693. doi:10.1074/jbc.M701047200

448. Dinkla K, Talay SR, Mörgelin M, Graham RMA, Rohde M, Nitsche-Schmitz DP, et al. Crucial Role of the CB3-Region of Collagen IV in PARF-Induced Acute Rheumatic Fever. Morty RE, editor. PLoS One. 2009;4: e4666. doi:10.1371/journal.pone.0004666

449. Banerjee T, Mukherjee S, Ghosh S, Biswas M, Dutta S, Pattari S, et al. Clinical Significance of Markers of Collagen Metabolism in Rheumatic Mitral Valve Disease. PLoS One. 2014;9: e90527. doi:10.1371/JOURNAL.PONE.0090527

450. Bisno AL, Brito MO, Collins CM. Molecular basis of group A streptococcal virulence. Lancet Infect Dis. 2003;3: 191–200. doi:10.1016/S1473-3099(03)00576-0

451. Smoot JC, Korgenski EK, Daly JA, Veasy LG, Musser JM. Molecular Analysis of Group A Streptococcus Type emm18 Isolates Temporally Associated with Acute Rheumatic Fever Outbreaks in Salt Lake City, Utah. J Clin Microbiol. 2002;40: 1805–1810. doi:10.1128/JCM.40.5.1805-1810.2002

452. Bisno A. Group A Streptococcal Infections and Acute Rheumatic Fever. N Engl J Med. 1991;325: 783–793.

453. Metzgar D, Zampolli A. The M protein of group A *Streptococcus* is a key virulence factor and a clinically relevant strain identification marker. Virulence. 2011;2: 402–12. doi:10.4161/viru.2.5.16342

454. Shulman ST, Stollerman G, Beall B, Dale JB, Tanz RR. Temporal changes in streptococcal M protein types and the near-disappearance of acute rheumatic fever in the United States. Clin Infect Dis. 2006;42: 441–7. doi:10.1086/499812

455. Ayoub EM, Barrett DJ, Maclaren NK, Krischer JP. Association of class II human histocompatibility leukocyte antigens with rheumatic fever. J Clin Invest. 1986;77: 2019–2026. doi:10.1172/JCI112531

456. Anastasiou-Nana M, Anderson J, Carlquist J, Nanas J. HLA-DR typing and lymphocyte subset evaluation in rheumatic heart disease: a search for immune response factors. Am Heart J. 1986;112: 992–997. doi:10.1016/0002-8703(86)90311-X

457. Rajapakse CN, Halim K, Al-Orainey I, Al-Nozha M, Al-Aska a K. A genetic

marker for rheumatic heart disease. Br Heart J. 1987;58: 659–62. Available: http://www.pubmedcentral.nih.gov/articlerender.fcgi?artid=1277319&tool=pmcen trez&rendertype=abstract

458. Guilherme L, Kohler KF, Postol E, Kalil J, Köhler KF, Postol E, et al. Genes, autoimmunity and pathogenesis of rheumatic heart disease. Ann Pediatr Cardiol. 2011/06/17. 2011;4: 13–21. doi:10.4103/0974-2069.79617

459. Guilherme L, Ramasawmy R, Kalil J. Rheumatic fever and rheumatic heart disease: Genetics and pathogenesis. Scandinavian Journal of Immunology. 2007. pp. 199–207. doi:10.1111/j.1365-3083.2007.01974.x

460. Bryant PA, Robins-Browne R, Carapetis JR, Curtis N. Some of the people, some of the time susceptibility to acute rheumatic fever. Circulation. 2009;119: 742–753. doi:10.1161/CIRCULATIONAHA.108.792135

461. Bouneaud C, Kourilsky P, Bousso P. Impact of Negative Selection on the T Cell Repertoire Reactive to a Self-Peptide. Immunity. 2000;13: 829–840. doi:10.1016/S1074-7613(00)00080-7

462. Zehn D, Bevan MJ. T Cells with Low Avidity for a Tissue-Restricted Antigen Routinely Evade Central and Peripheral Tolerance and Cause Autoimmunity. Immunity. 2006;25: 261–270. doi:10.1016/j.immuni.2006.06.009

463. Friedman SM, Posnett DN, Tumang JR, Crow MK, Cole BC. A potential role for microbial superantigens in the pathogenesis of systemic autoimmune disease. Arthritis Rheum. 1991;34: 468–480. doi:10.1002/art.1780340412

464. Paliard X, West SG, Lafferty JA, Clements JR, Kappler JW, Marrack P, et al. Evidence for the effects of a superantigen in rheumatoid arthritis. Science. 1991;253: 325–9. Available: http://www.ncbi.nlm.nih.gov/htbin-post/Entrez/query?db=m&form=6&dopt=r&uid=1857971

465. White J, Herman A, Pullen AM, Kubo R, Kappler JW, Marrack P. The V beta-specific superantigen staphylococcal enterotoxin B: stimulation of mature T cells and clonal deletion in neonatal mice. Cell. 1989;56: 27-35. Available: http://www.ncbi.nlm.nih.gov/htbin-post/Entrez/query?db=m&form=6&dopt=r&uid=2521300

466. Fujinami RS, Von Herrath MG, Christen U, Whitton JL. Molecular Mimicry, Bystander Activation, or Viral Persistence: Infections and Autoimmune Disease. Clin Microbiol Rev. 2006;19: 80. doi:10.1128/CMR.19.1.80-94.2006

467. Root-Bernstein R, Fairweather D. Unresolved issues in theories of autoimmune disease using myocarditis as a framework. 2015 [cited 4 Nov 2021]. doi:10.1016/j.jtbi.2014.11.022

468. Gorton D, Blyth S, Gorton JG, Govan B, Ketheesan N. An alternative technique

for the induction of autoimmune valvulitis in a rat model of rheumatic heart disease. J Immunol Methods. 2010;355: 80–85. doi:10.1016/J.JIM.2010.02.013

469. Billiau A, Matthys P. Modes of action of Freund's adjuvants in experimental models of autoimmune diseases. J Leukoc Biol. 2001;70: 849–860. Available: http://www.jleukbio.org

470. Cole BC, Griffiths MM. Triggering and exacerbation of autoimmune arthritis by themycoplasma arthritidis superantigen MAM. Arthritis Rheum. 1993;36: 994–1002. doi:10.1002/art.1780360717

471. Schwab JH, Brown RR, Anderle SK, Schlievert PM. Superantigen can reactivate bacterial cell wall-induced arthritis. J Immunol. 1993;150: 4151–4159.

472. Brocke S, Gaur A, Piercy C, Gautam A, Gijbels K, Fathman CG, et al. Induction of relapsing paralysis in experimental autoimmune encephalomyelitis by bacterial superantigen. Nature. 1993;365: 642–644. doi:10.1038/365642a0

473. Schiffenbauer J, Johnson HM, Butfiloski EJ, Wegrzyn L, Soos JM. Staphylococcal enterotoxins can reactivate experimental allergic encephalomyelitis. Proc Natl Acad Sci U S A. 1993;90: 8543–6. Available: http://www.ncbi.nlm.nih.gov/htbin-post/Entrez/query?db=m&form=6&dopt=r&uid=8378329

474. Furukawa F, Tokura Y, Matsushita K, Iwasaki-Inuzuka K, Onagi-Suzuki K, Yagi H, et al. Selective Expansions of T cells Expressing Vβ8 and Vβ13 in Skin Lesions of Patients with Chronic Cutaneous Lupus Erythematosus. J Dermatol. 1996;23: 670–676. doi:10.1111/j.1346-8138.1996.tb02679.x

475. Conrad B, Weidmann E, Trucco G, Rudert WA, Behboo R, Ricordi C, et al. Evidence for superantigen involvement in insulin-dependent diabetes mellitus aetiology. Nature. 1994;371: 351–355. doi:10.1038/371351a0

476. Virtaneva K, Graham MR, Porcella SF, Hoe NP, Su H, Graviss EA, et al. Group A Streptococcus gene expression in humans and cynomolgus macaques with acute pharyngitis. Infect Immun. 2003;71: 2199–2207. doi:10.1128/IAI.71.4.2199-2207.2003

477. GBD 2013 Mortality and Causes of Death Collaborators. Global, regional, and national age–sex specific all-cause and cause-specific mortality for 240 causes of death, 1990–2013: a systematic analysis for the Global Burden of Disease Study 2013. Lancet. 2015;385: 117–171. doi:10.1016/S0140-6736(14)61682-2

Appendices

Appendix 1: Human ethics approval certification

Western Research

Research Ethics

Western University Health Science Research Ethics Board
HSREB Annual Continuing Ethics Approval Notice

Date: June 29, 2016
Principal Investigator: Dr. John McCormick
Department & Institution: Schulich School of Medicine and Dentistry\Microbiology & Immunology, Western University

Review Type: Delegated
HSREB File Number: 1268
Study Title: Molecular architecture of streptococcal superantigen/T cell receptor interactions
Sponsor: Canadian Institutes of Health Research

HSREB Renewal Due Date & HSREB Expiry Date:
Renewal Due -2017/06/30
Expiry Date -2017/07/21

The Western University Health Science Research Ethics Board (HSREB) has reviewed the Continuing Ethics Review (CER) Form and is re-issuing approval for the above noted study.

The Western University HSREB operates in compliance with the Tri-Council Policy Statement Ethical Conduct for Research Involving Humans (TCPS2), the International Conference on Harmonization of Technical Requirements for Registration of Pharmaceuticals for Human Use Guideline for Good Clinical Practice (ICH E6 R1), the Ontario Freedom of Information and Protection of Privacy Act (FIPPA, 1990), the Ontario Personal Health Information Protection Act (PHIPA, 2004), Part 4 of the Natural Health Product Regulations, Health Canada Medical Device Regulations and Part C, Division 5, of the Food and Drug Regulations of Health Canada.

Members of the HSREB who are named as Investigators in research studies do not participate in discussions related to, nor vote on such studies when they are presented to the REB.

The HSREB is registered with the U.S. Department of Health & Human Services under the IRB registration number IRB 00000940.

Ethics Officer, on behalf of Dr. Joseph Gilbert, HSREB Chair

Ethics Officer: Erika Basile ___ Katelyn Harris___ Nicole Kaniki ✓ Grace Kelly ___ Vikki Tran ___ Karen Gopaul ___

Western University, Research, Support Services Bldg., Rm. 5150
London, ON, Canada N6G 1G9 t. 519.661.3036 f. 519.850.2466 www.uwo.ca/research/ethics

Appendix 2: Animal ethic approval certification

Western

2020-041:4:

AUP Number: 2020-041
AUP Title: Streptococcal infections and vaccines
Yearly Renewal Date: 12/01/2022

The **annual renewal** to Animal Use Protocol (AUP) 2020-041 has been approved by the Animal Care Committee (ACC), and will be approved through to the above review date.

Please at this time review your AUP with your research team to ensure full understanding by everyone listed within this AUP.

As per your declaration within this approved AUP, you are obligated to ensure that:

1. This Animal Use Protocol is in compliance with:
   - Western's Senate MAPP 7.12 [PDF]; and
   - Applicable Animal Care Committee policies and procedures.
2. Prior to initiating any study-related activities—as per institutional OH&S policies—all individuals listed within this AUP who will be using or potentially exposed to hazardous materials will have:
   - Completed the appropriate institutional OH&S training;
   - Completed the appropriate facility-level training; and
   - Reviewed related (M)SDS Sheets.

Submitted by: Cristancho, Martha on behalf of the Animal Care Committee

ACC Chair Signature

Dr. Rob Gros,
Animal Care Committee Chair

Animal Care Commitee
The University of Western Ontario
London, Ontario Canada N6A 5C1

Appendix 3: Mouse strains used in this thesis

Strain	Characteristic	Source
C57Bl/6	Inbred black mice	Jackson Laboratories
HLA-DR4/DQ8	C57Bl/6 mice null for endogenous $H2^b$ MHC class II and transgenic for human HLA-DR4 and HLA-DQ8 alleles	McCormick lab breeding colony
HLA-DQ8	C57Bl/6 mice null for endogenous $H2^b$ MHC class II and transgenic for human HLA-DQ8 allele	McCormick lab breeding colony

Appendix 4: Antibodies and dyes used in this thesis

Target	Conjugate	Clone	Purpose	Source
M18	N/A	Polyclonal (Rabbit)	Western blots	ProSci
SpeA	N/A	Polyclonal (Rabbit)	Western blots	ProSci
Rabbit IgG	IRDye800	Polyclonal (Donkey)	Western blots	Rockland
Ly6G	N/A	1A8	Neutrophil depletion	BioXCell
IgG2a	N/A	C1.18.4	Isotype control	BioXCell
Mouse IgG	HRP	Polyclonal (Goat)	IgG titers	Sigma-Aldrich

Appendix 5: Cytokine responses from nasal turbinates of B6$_{HLA}$ mice during infection with *S. pyogenes* MGAS8232 wildtype, Δ*hasA,* and Δ*hasA* +*hasA* strains.
Mice were inoculated with HBSS as sham control (black bars) or infected intranasally with 10^8 CFUs of *S. pyogenes* MGAS8232 wildtype, Δ*hasA,* or Δ*hasA* +*hasA* strains. Mice were sacrificed 48 hours post-infection and cNT homogenates were analyzed for multiple cytokines and chemokines (Th1-type [**A**]; Th2-type cytokines [**B**]; Treg cytokines [**C**]; Th17 cytokines [**D**]; chemokines [**E**]; or growth factors [**F**]). Data represents mean ± SEM of cNT cytokine/chemokine concentrations (pg mL^{-1}) from individual mice ($n \geq 3$ mice per group). Significance was determined by one-way ANOVA with Dunnett's multiple comparison post hoc test (*, $P < 0.05$; **, $P < 0.01$; ***, $P < 0.001$).

A

B

C

D

E

F
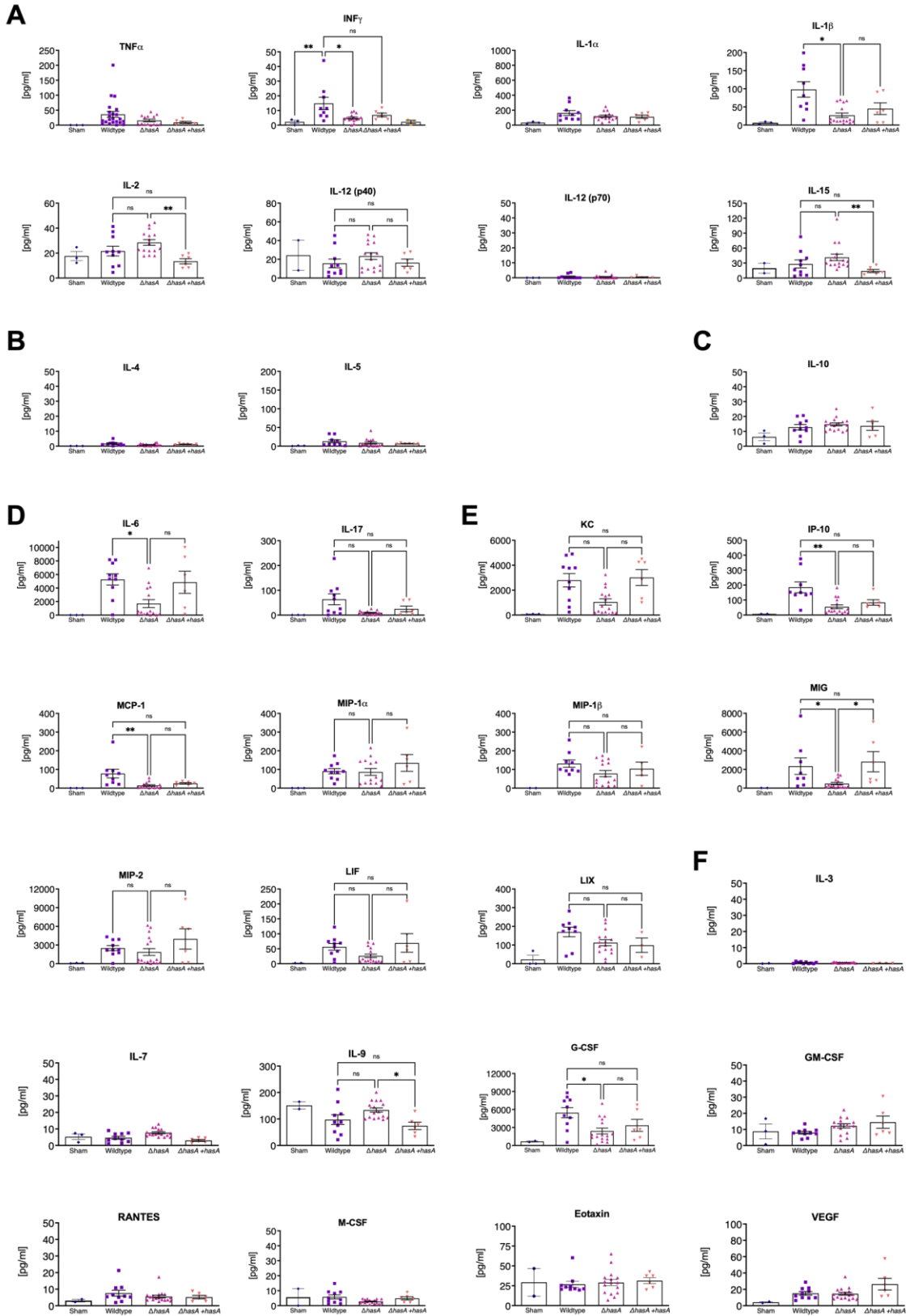
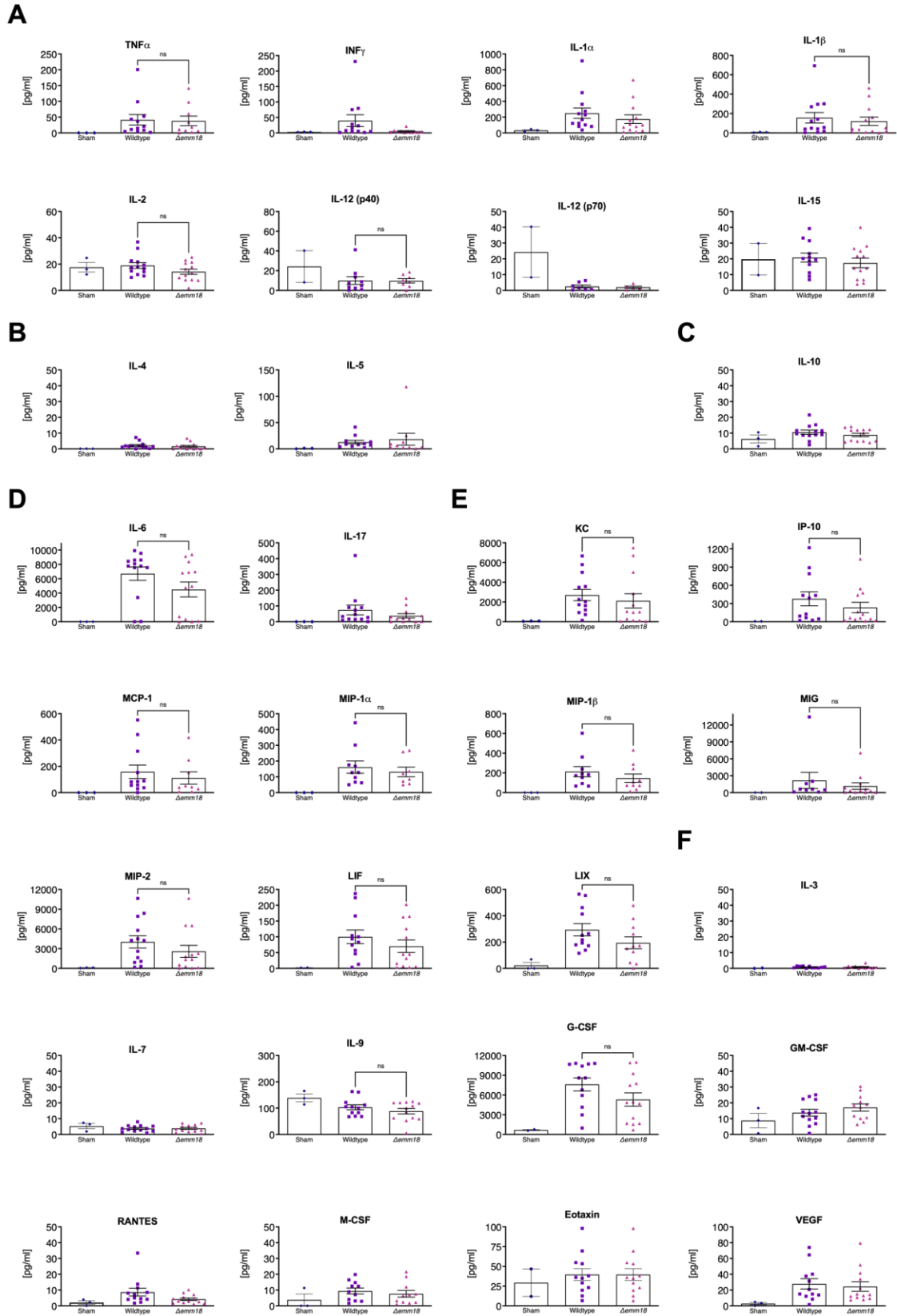**Appendix 6: Cytokine responses from nasal turbinates of B6$_{HLA}$ mice during infection with *S. pyogenes* MGAS8232 wildtype and Δ*emm18* strains**

Mice were inoculated with HBSS as sham control or infected intranasally with 10^8 CFUs of *S. pyogenes* MGAS8232 wildtype or Δ*emm18* strains. Mice were sacrificed 48 hours post-infection and cNT homogenates were analyzed for multiple cytokines and chemokines (Th1-type [**A**]; Th2-type cytokines [**B**]; Treg cytokines [**C**]; Th17 cytokines [**D**]; chemokines [**E**]; or growth factors [**F**]). Data represents mean ± SEM of cNT cytokine/chemokine concentrations (pg mL^{-1}) from individual mice ($n \geq 3$ mice per group). Data was analyzed by one-way ANOVA with Dunnett's multiple comparison post hoc test (data not significant).

Appendix 7: Mice repetitively infected with *S. pyogenes* MGAS8232 do not express increased serum levels of cytokines that indicate damaged cardiomyocytes.

Multiplex cytokine array using endpoint serums of mice repeatedly exposed to biweekly *S. pyogenes* MGAS8232 wildtype and Δ*emm18* nasopharyngeal infections at weeks 10 and 14. Control mice received PBS inoculations. Data points represent mean ± SEM serum cytokine concentrations (pg mL^{-1}) from individual mice ($n \geq 3$ mice per group). Significance was determined by Tukey's two-way ANOVA (*, $P < 0.05$).

A — sCD40L

B — CXCL16

C — Endocan-I

D — Light

E — Oncostatin-M

F — PLGF-2

G — Follistatin

Appendix 8: Cytokine responses from nasal turbinates of B6$_{\text{HLA}}$ mice during infection with *S. pyogenes* MGAS8232 wildtype and Δ*gacI*.

Mice were inoculated with HBSS as sham control or infected intranasally with 10^8 CFUs of *S. pyogenes* MGAS8232 wildtype or Δ*gacI* strains. Mice were sacrificed 48 hours post-infection and cNT homogenates were analyzed for multiple cytokines and chemokines (Th1-type [**A**]; Th2-type cytokines [**B**]; Treg cytokines [**C**]; Th17 cytokines [**D**]; chemokines [**E**]; or growth factors [**F**]). Data represents mean ± SEM cytokine/chemokine concentration (pg mL^{-1}) from individual mice ($n \geq 3$ mice per group). Data was analyzed by one-way ANOVA with Dunnett's multiple comparison post hoc test (data not significant).
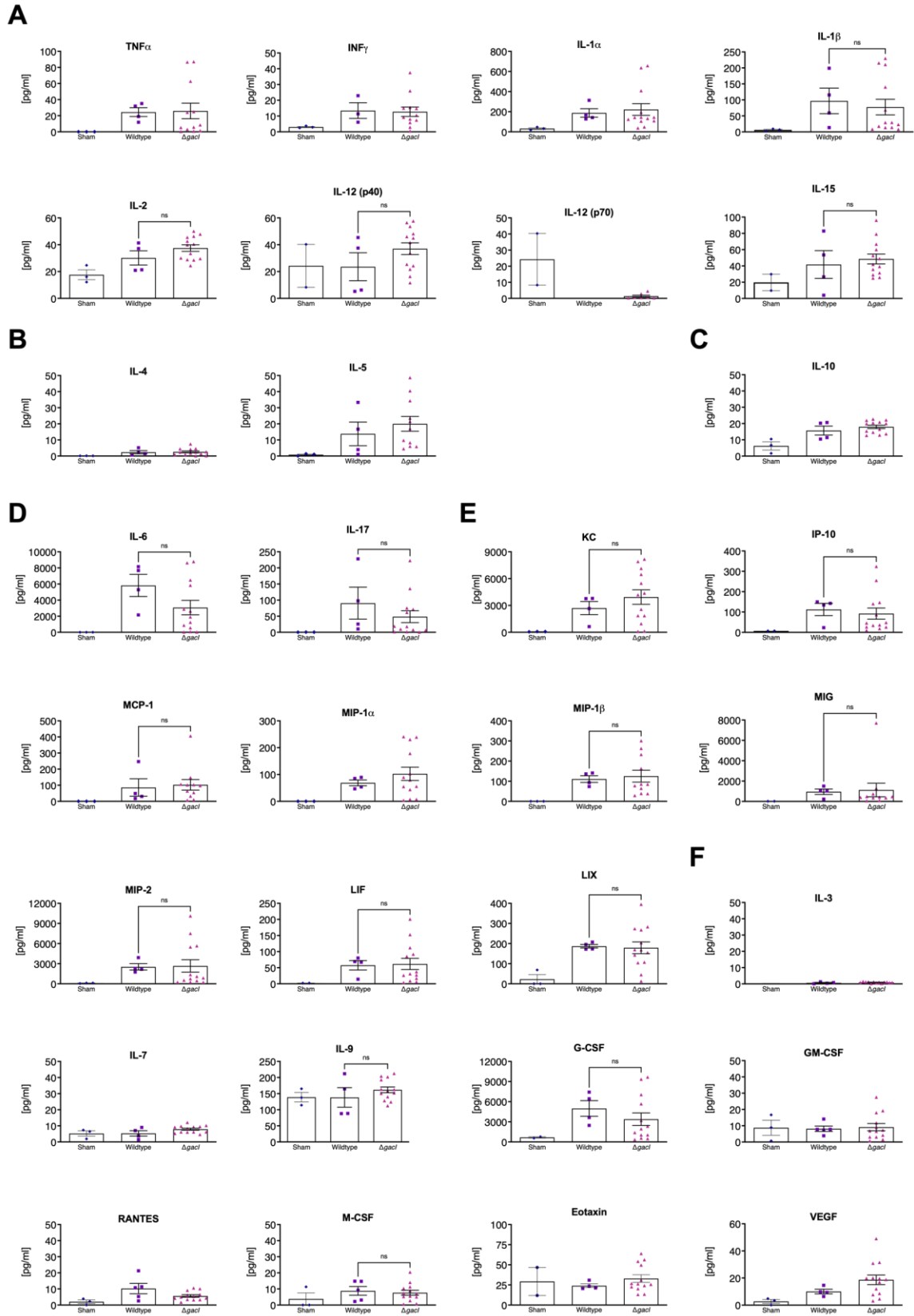
Curriculum Vitae

JACKLYN HURST, BMSc

EDUCATION

Doctor of Philosophy (Ph.D.) Candidate   2016 – Present
Department of Microbiology and Immunology
Western University, London, ON

Bachelor of Medical Sciences (BMSc.)   2012 – 2016
Honors Specialization in Microbiology and Immunology
Western University, London, ON

RESEARCH EXPERIENCE

Ph.D. Candidate Department of Microbiology and Immunology   2016 – Present
Western University, London, ON
Advisor: Dr. John McCormick, PhD

Thesis*: Investigation of S. pyogenes hyaluronic acid capsule and M protein during acute nasopharyngeal and skin infections, as vaccine candidates, and possible drivers of heart dysfunction*

Summer Research Technician, Western University, London, ON   2016
Laboratory of Dr. John McCormick, PhD

Undergraduate Research project, Western University, London, ON   2015 – 2016
Advisor: Dr. John McCormick, PhD

Thesis: *Determining the role of the hyaluronic acid capsule during Streptococcus pyogenes acute nasopharyngeal colonization*

PUBLICATIONS

Hurst J.R., Shannon B.A., Craig H.C., Tuffs S.W., and McCormick J.K. 2022. The Streptococcus pyogenes hyaluronic acid capsule promotes experimental nasal and skin infection by preventing neutrophil-mediated clearance. Submitted.

Hurst J.R., Brouwer S., Walker M.J., and McCormick J.K. 2021. *Streptococcal superantigens and the return of scarlet fever*. PLoS Pathogens. 17(12). Journal Impact Score: 6.823

Hurst, J.R., Kasper, K.J., Sule, A.S., and J. K. McCormick. 2018. *Streptococcal pharyngitis and rheumatic heart disease: the superantigen hypothesis revisited.* Infection Genetics and Evolution. 61:160-175.
Journal Impact Score: 3.342

HONORS AND AWARDS

Oral Presenter 2nd Place Prize ($50)   2020
Infection and Immunity Research Forum, London ON

Queen Elizabeth II Graduate Scholarship in Science and Technology ($15,000)   2020
Western University, London, ON

Dr. RGE Murray Doctoral Student Seminar Award ($500)   2020
Department of Microbiology and Immunology, Western University

Dr. RGE Murray Graduate Scholarship ($10,000)   2019
Department of Microbiology and Immunology, Western University

Dr. Frederick W. Luney Graduate Travel Awards ($1,000/year)   2017 – 2019
Department of Microbiology and Immunology, Western University

Dr. RGE Murray Graduate Scholarship ($10,000)   2017
Department of Microbiology and Immunology, Western University

Dr. Frederick W. Luney Graduate Entrance Award ($3,000)   2016
Department of Microbiology and Immunology, Western University

Robert Hewitt Scholarship of Excellence and C.J. Hewitt Bursary ($1000)   2016
Toromont Caterpillar, Canada

Dean's Honor List   2012–2016
Western University, London, ON

TEACHING EXPERIENCE

Teaching Assistant**,** *MicroImm 3610F*   2021
Undergraduate Microbiology Laboratory Course
Department of Microbiology & Immunology
Western University, London, ON

Undergraduate Thesis Student Supervisor   2018–2021
Western University, London, ON

- Aanchal Rishi, "The role of the cysteine protease SpeB in nasopharyngeal colonization by *Streptococcus pyogenes,*" Graduated June 2021
- Kevin Min, "Superantigens as Vaccine Adjuvants," Graduated June 2020
- Alex Zhou, "The Role of Superantigens in Host Tropism," Graduated June 2019
- Blake Shannon, "*S. pyogenes* Streptolysins and Colonization," Graduated June 2018

Teaching Assistant, *MicroImm 3620G*   2017–2021
Undergraduate Immunology Laboratory Course
Department of Microbiology & Immunology, Western University, London, ON

PRESENTATIONS AND INVITED LECTURES
_____

Poster Presentations

Canadian Society of Microbiologists, (virtual conference)   2021
"The hyaluronic acid capsule expressed on *Streptococcus pyogenes* promotes murine nasopharyngeal and skin infections."

Infection and Immunity Research Forum, London, Ontario, Canada   2019
"The role of *Streptococcus pyogenes* surface virulence factors in colonization and autoimmune disease development."

Canadian Society of Microbiologists, Sherbrooke, Québec, Canada   2019
"The role of *Streptococcus pyogenes* surface virulence factors in nasopharyngeal infection and rheumatic heart disease."

London Health Research Day, London, Ontario, Canada   2019
"The role of *Streptococcus pyogenes* virulence factors in nasopharyngeal infection and rheumatic heart disease."

Infection and Immunity Research Forum, Stratford, Ontario, Canada   2018
"The role of *Streptococcus pyogenes* virulence factors in colonization and rheumatic disease"

Banff Conference of Infectious Disease, Banff, Alberta, Canada   2018
"*Streptococcus pyogenes* virulence factors in murine colonization and disease."

London Health Research Day, London, Ontario, Canada   2018
"*Streptococcus pyogenes* virulence factors in murine colonization and disease."

Infection and Immunity Research Forum, London, Ontario, Canada   2017
"The role of the hyaluronic acid capsule and M18 protein in *Streptococcus pyogenes* colonization and disease."

Canadian Society of Microbiologists, Waterloo, Ontario, Canada   2017

"The role of the hyaluronic acid capsule and M18 protein in *Streptococcus pyogenes* colonization and disease."

London Health Research Day, London, Ontario, Canada   2017
"The role of the hyaluronic acid capsule and M18 protein in *Streptococcus pyogenes* colonization and disease."

Infection and Immunity Research Forum, London, Ontario, Canada   2016
"Determining the role of the hyaluronic acid capsule in *Streptococcus pyogenes* acute nasopharyngeal colonization."

Oral Presentations

Infection and Immunity Research Forum, London, Ontario, Canada   2020
"Echocardiogram confirms cardiac pathology following recurring acute *Streptococcus pyogenes* infection in mice."

Lawson Health Research Institute, London, Ontario, Canada   2017
"The Role of the Hyaluronic Acid Capsule and M18 Protein in *Streptococcus pyogenes* Colonization and Disease."